

**Immune cell carriers and humoral immunity  
in oncolytic virotherapy**

Robert Anthony Berkeley

Submitted in accordance with the requirements  
for the degree of Doctor of Philosophy

The University of Leeds

School of Medicine

March 2018

The candidate confirms that the work submitted is his own and that appropriate credit has been given where reference has been made to the work of others.

This copy has been supplied on the understanding that it is copyright material and that no quotation from the thesis may be published without proper acknowledgement.

The right of Robert Anthony Berkeley to be identified as Author of this work has been asserted by him in accordance with the Copyright, Designs and Patents Act 1988.

# 1. Preface

## 1.1 Acknowledgments

I would like to thank Prof Alan Melcher, Dr Liz Ilett and Dr Fiona Errington-Mais for their guidance throughout this project. Liz, thanks for being a driving force and constant support in the lab and in writing this thesis; I will miss your healthy doses of realism. Alan, for providing your relentless optimism and ideas, even from afar. Thanks to current and prior members of the unique GFKAM – Lynette, Ailsa, Gina, Vicki, Gemma, Louise, Jo, Matt – and to Jenny Reinboth, whose work helped spawn this project.

I appreciate the help of others who together have made this project possible: Prof Richard Vile, Jill Thompson and Tim Kottke at the Mayo Clinic, for *in vivo* studies; Prof Rob Hoeben, Dr Diana van den Wollenberg, Aat Mulder, and Dr Carolina Jost at Leiden for EM visualisation and analysis; Dr Ritika Chauhan, Dr Nik Matthews, Dr James Campbell and Dr Alistair Rust at the ICR for bioinformatics; Georgia Mappa for luminex analysis; Dr Adam Davison and Liz Straszynski for expertise in flow cytometry. I acknowledge funding via a University of Leeds 110 Anniversary Research Scholarship.

Finally, thanks to Vaila and all the family, for love, humour, and patience.

## 1.2 Abstract

Oncolytic viruses (OV) represent an emerging modality in cancer therapy. Antiviral immunity is currently viewed as a barrier to systemic OV efficacy. Approaches have been taken to promote OV activity by attenuating virus-neutralising antibodies (NAb). However, the presence of NAb does not prevent intravenously administered OV, such as reovirus, reaching tumours in patients. Recent evidence suggests that NAb may in fact support virotherapy in mice by facilitating reovirus carriage upon circulating immune cells, principally monocytes.

In this thesis, the applicability of these observations to the human setting is examined, modelling the loading of monocytes with reovirus in virus-immune patients. A novel *in vitro* cell carriage assay was employed, involving clinical trial patient-derived sera, isolated primary human monocytes, and human tumour cell lines. It was discovered that monocytes treated with fully neutralised reovirus reliably delivered the virus to kill melanoma targets. This was transferable across target cell histologies, and applicable to another OV, CVA21. Neutralised reovirus successfully accessed syngeneic melanoma flank tumours in mice.

Prior murine studies suggested a role for surface Fc receptors in facilitating the antibody-dependent enhancement (ADE) of monocyte infection. A major role for Fc receptors in antibody-mediated entry of neutralised reovirus to human monocytes was confirmed. Yet no overall enhancement of virus loading or hand-off was conferred by the presence of NAb, in contrast to existing observations from mouse monocytes.

Transcriptomic and secretory profiling identified discrete variations in the effects of free and neutralised reovirus upon monocyte phenotype. NAb significantly attenuated the monocyte IFN response to reovirus *in vitro*. However, in the presence of monocytes, reo-NAb successfully induced NK cell degranulation and killing of melanoma targets. Therefore this study identifies a mechanism by which, following neutralisation, reovirus may rely on circulating monocytes to gain tumour access, and to initiate oncolytic and/or immune-mediated tumour cell death.

## 1.3 Table of contents

<b>1. Preface</b> .....	<b>i</b>
1.1 Acknowledgments .....	i
1.2 Abstract .....	ii
1.3 Table of contents .....	iii
1.4 Table of figures .....	ix
1.5 List of tables .....	xii
1.6 List of abbreviations .....	xiii
<b>2. Introduction</b> .....	<b>1</b>
2.1 Melanoma .....	1
2.1.1 Burden .....	1
2.1.2 Aetiology .....	2
2.1.3 Treatment .....	4
2.2 Cancer and the immune system .....	8
2.2.1 Anti-tumour immunity .....	8
2.2.2 Immune evasion and suppression .....	13
2.2.3 Emerging immunotherapies .....	16
2.3 Oncolytic viruses .....	21
2.3.1 Background .....	21
2.3.2 Interaction with host cells .....	23
2.3.3 Tropism and engineering .....	25
2.3.4 Mechanisms of OV activity .....	28
2.3.5 Clinical trials .....	31
2.4 Reovirus .....	38

2.4.1	Background.....	38
2.4.2	Structure and replication.....	40
2.4.3	As an oncolytic agent.....	42
2.4.4	Pre-clinical evidence.....	46
2.4.5	Clinical trials.....	48
2.5	Oncolytic viruses and the immune system.....	52
2.5.1	The delivery conundrum.....	52
2.5.2	Anti-tumour or antiviral immunity?.....	54
2.5.3	Modulation of antiviral immunity.....	56
2.5.4	The monocyte as a Trojan horse.....	58
2.5.5	Cell carriers.....	61
2.6	Aims of the project.....	65
<b>3.</b>	<b>Materials &amp; methods.....</b>	<b>66</b>
3.1	Cell culture.....	66
3.1.1	Method.....	66
3.1.2	Cell lines and media.....	66
3.1.3	Cryopreservation.....	67
3.1.4	Preparation of PBMC by density gradient separation.....	67
3.2	Virus.....	67
3.2.1	Use and storage.....	67
3.2.2	UV inactivation of virus.....	67
3.3	Sources of antiviral antibody.....	68
3.3.1	Use and storage.....	68
3.3.2	Neutralisation assay.....	68
3.3.3	Depletion of antibody isotypes from anti-reovirus serum.....	69

3.3.4	Immunoprecipitation of reovirus .....	69
3.3.4.1	Detection of anti-reovirus antibodies in serum.....	69
3.3.4.2	Detection of endogenous reo-NAb complexes in serum.... .....	70
3.4	In vitro hand-off assay .....	70
3.4.1	Standard protocol.....	70
3.4.1.1	Preparation of target cells.....	70
3.4.1.2	Formation of reovirus-antibody complexes .....	70
3.4.1.3	Selection of carrier cells .....	71
3.4.1.4	Carrier cell loading and co-culture .....	71
3.4.2	Adaptations of the hand-off assay.....	72
3.4.2.1	Negative selection of monocytes for electron microscopy . .....	72
3.4.2.2	Selection of CD16 <sup>+</sup> and CD16 <sup>-</sup> populations.....	72
3.4.2.3	Blockade of monocyte virus entry.....	73
3.4.2.4	Target cell killing by monocyte conditioned medium.....	73
3.4.2.5	Blockade of virus transmission by monocytes .....	74
3.4.2.6	Virus loading of monocytes in whole blood.....	74
3.5	Immune cell stimulation assays.....	75
3.5.1	Co-culture of immune cell populations .....	75
3.5.1.1	Virus-loaded monocytes and whole PBMC.....	75
3.5.1.2	Virus-loaded monocytes and NK cells .....	75
3.5.2	Chromium release assay .....	76
3.6	Flow cytometry .....	77
3.6.1	Default antibody staining protocol .....	77
3.6.2	Live-dead viability assay .....	78

3.6.3	Detection of reovirus binding.....	78
3.6.4	Analysis of monocyte phenotype.....	78
3.6.4.1	Monocyte migration .....	79
3.6.5	Degranulation assay .....	79
3.7	Plaque assay .....	80
3.7.1	Protocol.....	80
3.8	Western blotting .....	81
3.8.1	Preparation of samples .....	81
3.8.1.1	Reovirus-infected cell line lysates.....	81
3.8.1.2	Monocyte lysates.....	81
3.8.2	DC assay.....	82
3.8.3	Electrophoresis and blotting.....	82
3.8.3.1	IP of patient-derived serum for reovirus.....	83
3.9	Cytokine analysis .....	83
3.9.1	Luminex .....	83
3.9.2	ELISA.....	83
3.10	Transcriptional analysis .....	84
3.10.1	RNA analysis by qPCR .....	84
3.10.1.1	Virus treatment .....	84
3.10.1.2	RNA processing.....	85
3.10.1.3	qPCR analysis .....	85
3.10.2	RNA analysis by RNAseq .....	86
3.10.2.1	Virus treatment .....	86
3.10.2.2	RNAseq methodology.....	86
3.11	Imaging.....	87
3.11.1	Electron microscopy.....	87

3.11.1.1	Visualisation of reo-NAb complexes by EM .....	87
3.11.1.2	Visualisation of virus-loaded monocytes by EM.....	88
3.11.2	Confocal microscopy .....	89
3.12	In vivo work .....	89
3.12.1	Delivery of reovirus to tumours.....	90
3.12.2	Analysis of therapeutic benefit .....	91
3.13	Statistical analysis .....	91
<b>4.</b>	<b>Formation of reovirus-antibody complexes .....</b>	<b>101</b>
4.1	Introduction.....	101
4.2	Reovirus neutralisation by patient-derived serum.....	102
4.3	Characterisation of specific mediators of neutralisation .....	109
4.4	The interaction of virus with anti-reovirus antibody to form complexes .....	114
4.5	Summary .....	116
<b>5.</b>	<b>Delivery of reovirus for tumour cell oncolysis by primary human monocytes .....</b>	<b>118</b>
5.1	Introduction.....	118
5.2	Susceptibility of melanoma targets to reovirus .....	119
5.3	In vitro hand-off assay .....	123
5.4	Transferability to other OV platforms.....	131
5.5	In vivo effects of reo-NAb complexes .....	135
5.6	Summary .....	143
<b>6.</b>	<b>Interaction of reovirus-antibody complexes with monocyte carrier cells .....</b>	<b>147</b>
6.1	Introduction.....	147

6.2	Imaging reovirus-treated monocytes .....	148
6.3	Mechanism of reo-NAb entry.....	156
6.4	Monocytes as replication factories? .....	165
6.5	Mechanism of reovirus transfer .....	172
6.6	Summary .....	178
<b>7.</b>	<b>Immunological consequences of antibody-bound reovirus on immune populations .....</b>	<b>183</b>
7.1	Introduction.....	183
7.2	Activation of monocyte carrier cells .....	184
7.3	Effects of carriage on transcriptional profile.....	191
7.4	Effects of carriage on secretory profile .....	203
7.5	Functional effects on immune effector populations .....	213
7.6	Summary .....	223
<b>8.</b>	<b>Discussion.....</b>	<b>227</b>
<b>9.</b>	<b>References.....</b>	<b>237</b>

## 1.4 Table of figures

Figure 4.2.1	Western blot for reovirus $\sigma 3$ protein from IP fraction of serum .	105
Figure 4.2.2	Reovirus neutralisation by control or patient-derived sera .....	106
Figure 4.2.3	Reovirus neutralisation by patient-derived sera .....	107
Figure 4.2.4	Influence of heat-labile factors in reovirus neutralisation.....	108
Figure 4.3.1	The reovirus-binding antibody repertoire of patient serum .....	111
Figure 4.3.2	Western blot for serum antibody classes binding to reovirus ...	112
Figure 4.3.3	Serum antibody classes mediating reovirus neutralisation.....	113
Figure 4.4.1	Immunogold labelling of reovirus-bound antibodies from serum .....	115
Figure 5.2.1	Surface expression of JAM-A by Mel-624 cells .....	121
Figure 5.2.2	Susceptibility of melanoma cell lines to reovirus .....	122
Figure 5.3.1	Hand-off assay schematic .....	125
Figure 5.3.2	Selection of monocytes from human healthy donor PBMC .....	126
Figure 5.3.3	Monocyte expression of JAM-A.....	127
Figure 5.3.4	Representative images of outcomes from the hand-off assay..	128
Figure 5.3.5	Quantification of tumour cell killing in the hand-off assay.....	129
Figure 5.3.6	Application of the hand-off assay to other target cell lines .....	130
Figure 5.4.1	Expression of receptors for other OV by Mel-624 cells .....	132
Figure 5.4.2	Susceptibility of melanoma cell lines to selected OV .....	133
Figure 5.4.3	Application of the hand-off assay to other oncolytic viruses.....	134
Figure 5.5.1	Generation of mouse anti-reovirus serum .....	139
Figure 5.5.2	Delivery of replicating virus to melanoma tumours by i.v. administration of reo-NAb complexes formed ex vivo with immune serum .....	140
Figure 5.5.3	Delivery of replicating virus using complexes formed of reovirus- immune serum or monoclonal antibodies .....	141

Figure 5.5.4 Therapeutic benefit of i.v. administration of reo-NAb complexes.....	142
Figure 6.2.1 Immunofluorescence analysis of reovirus-treated monocytes..	152
Figure 6.2.2 Flow cytometry analysis of binding of reovirus or reo-NAb to monocytes .....	153
Figure 6.2.3 Positive staining of reovirus or reo-NAb treated monocytes.....	154
Figure 6.2.4 Immunogold labelling of reovirus or reo-NAb treated monocytes for $\sigma 3$ protein .....	155
Figure 6.3.1 Neutralising patient antibodies favour routing of virus to CD14 <sup>+</sup> cells in whole blood.....	160
Figure 6.3.2 Expression of Fc receptors on primary human monocytes .....	161
Figure 6.3.3 Effect of monocyte Fc receptor blockade upon Mel-624 killing via reo-NAb hand-off.....	162
Figure 6.3.4 Effect of monocyte Fc receptor blockade upon virus loading ...	163
Figure 6.3.5 CD16 <sup>+</sup> monocytes are superior mediators of reo-NAb hand-off .....	164
Figure 6.4.1 Reovirus amplification following reo-NAb hand-off by monocytes .....	168
Figure 6.4.2 Tumour cell killing via hand-off using live or UV-inactivated virus .....	169
Figure 6.4.3 Viral genomes in monocytes following reovirus or reo-NAb loading .....	170
Figure 6.4.4 Replicating virus titre in monocytes following reovirus or reo-NAb loading .....	171
Figure 6.5.1 Ability of conditioned medium from virus-loaded monocytes to kill tumour targets.....	175
Figure 6.5.2 Effect of tumour JAM-A blockade on tumour cell killing via hand-off .....	176
Figure 6.5.3 Tumour cell killing via hand-off in transwell assay format.....	177
Figure 7.2.1 Analysis of treated monocyte phenotype by western blot .....	188

Figure 7.2.2	Analysis of treated monocyte phenotype by flow cytometry .....	189
Figure 7.2.3	Migratory capacity of treated monocytes.....	190
Figure 7.3.1	Volcano plots of differential gene expression by monocytes ....	197
Figure 7.3.2	Clustering and principal component analysis of the treated monocyte transcriptome .....	198
Figure 7.3.3	Induction of a minor gene subset by reo-NAb but not reovirus.	199
Figure 7.3.4	Limited differential expression in reo-NAb treated monocytes .	200
Figure 7.3.5	Enrichment analysis of DE gene sets induced by reo or reo-NAb treatment of monocytes .....	201
Figure 7.3.6	Validation of RNAseq expression analysis by qPCR.....	202
Figure 7.4.1	Transcriptomic analysis of cytokine induction by reovirus and reo-NAb .....	208
Figure 7.4.2	Broad analysis of monocyte 'secretome' by luminex.....	209
Figure 7.4.3	Validation of monocyte-secreted factors by ELISA.....	210
Figure 7.4.4	Induction of cytokine secretion by live and UV-inactivated virus .....	211
Figure 7.4.5	Lack of evidence for an IFN-repressing factor specific to reo-NAb treated monocytes .....	212
Figure 7.5.1	Effect of NK cell co-culture on phenotype of virus-treated monocytes .....	218
Figure 7.5.2	Activation of immune cell populations via virus-loaded monocytes .....	219
Figure 7.5.3	Mechanism of NK cell activation by monocyte-secreted factors .....	220
Figure 7.5.4	Ability of treated monocytes to stimulate NK cell degranulation.....	221
Figure 7.5.5	Ability of treated monocytes to stimulate NK cell-mediated cytotoxicity .....	222

## 1.5 List of tables

Table 1 Cell lines, primary cells and media.....	92
Table 2 Oncolytic viruses employed .....	93
Table 3 Sources of antiviral antibody .....	93
Table 4 Blocking antibodies used in cell culture.....	94
Table 5 Antibodies used in western blotting.....	95
Table 6 Primers used for qPCR .....	96
Table 7 Buffers used for magnetic selection, flow cytometry, western blotting, ELISA, and EM .....	97
Table 8 Antibodies used for flow cytometry .....	99
Table 9 Antibodies used for ELISA .....	100
Table 10 Protein standards used for ELISA.....	100

## 1.6 List of abbreviations

°C	degrees Celsius
$\Delta\Delta C_T$	double-delta threshold cycle method
$\mu\text{Ci}$	microcurie
$\mu\text{g}$	micrograms
$\mu\text{l}$	microlitres
$\mu\text{m}$	micrometres
$\mu\text{M}$	micromolar
$^{51}\text{Cr}$	chromium-51
Ab	antibody
ADCC	antibody-dependent cellular cytotoxicity
ADCP	antibody-dependent cellular phagocytosis
ADE	antibody-dependent enhancement of infection
AF	Alexa Fluor
AML	acute myeloid leukaemia
ANOVA	analysis of variance
APC	antigen-presenting cell
APC (fluorophore)	allophycocyanin
ATP	adenosine triphosphate
BCR	B-cell receptor
BGT	BSA-glycine-Tween-20
bld	below limit of detection
BP	biological process (GO)
BSA	bovine serum albumin
CC	cellular component (GO)
CD	cluster of differentiation

cDNA	complementary DNA
CH <sub>50</sub>	50% haemolytic complement
CLR	C-type lectin receptor
CM	conditioned medium
cm	centimetres
CO <sub>2</sub>	carbon dioxide
con	control
CPA	cyclophosphamide
CPE	cytopathic effect
cpm	counts per minute
CR	complete response
CRUK	Cancer Research UK
CS	control serum
CTL	cytotoxic T-lymphocyte
CTLA-4	cytotoxic T-lymphocyte-associated protein 4
CV	coefficient of variation
CVA21	coxsackievirus A21
d.p.i.	days post-infusion
DAMP	danger-associated molecular pattern
DAPI	4',6-diamidino-2-phenylindole
DC	dendritic cell
DC (assay)	detergent compatible
DE	differentially expressed
df	degrees of freedom
DMEM	Dulbecco's modified Eagle medium
DMSO	dimethyl sulfoxide
DNA	deoxyribonucleic acid
d.p.i.	days post-infusion

ds	double-stranded
DSHB	Developmental Studies Hybridoma Bank
DTIC	dacarbazine
DTT	dithiothreitol
E:T	effector:target
ECHO	enteric cytopathic human orphan
ED <sub>50</sub>	50% effective dose
EDTA	ethylenediaminetetraacetic acid
EGFR	epidermal growth factor receptor
ELISA	enzyme-linked immunosorbent assay
EM	electron microscopy
EMA	European Medicines Agency
ERK	extracellular signal-regulated kinase
F/R (primer)	forward/reverse
Fab	antigen-binding fragment
FACS	fluorescence-activated cell sorting
FC	fold-change
Fc	constant fragment
FCM	filtered conditioned medium
FcRn	neonatal Fc receptor
FCS	foetal calf serum
Fc $\alpha$ R	Fc-alpha receptor
Fc $\gamma$ R	Fc-gamma receptor
FDA	US Food and Drug Administration
FITC	fluorescein isothiocyanate
g	times gravity
GA	glutaraldehyde
GAPDH	glyceraldehyde 3-phosphate dehydrogenase

GFP	green fluorescent protein
GLB	Giordano lysis buffer
GM-CSF	granulocyte-macrophage colony stimulating factor
GO	gene ontology
GTP	guanosine triphosphate
h.p.i.	hours post-infusion
HBSS	Hanks' balanced salt solution
HI	heat-inactivated
HKG	housekeeping gene
HLA	human leukocyte antigen
HNSCC	head and neck squamous cell carcinoma
HPV	human papillomavirus
HRP	horseradish peroxidase
HSP	heat shock protein
HSV	herpes simplex virus
i.p.	intraperitoneal
i.t.	intra-tumour
i.v.	intravenous
ICAM-1	intercellular adhesion molecule 1
ICR	Institute of Cancer Research
IDO-1	indoleamine 2,3-dioxygenase
IF	immunofluorescence
IFN	interferon
IFNAR	interferon-alpha receptor
Ig	immunoglobulin
IL	interleukin
IP	immunoprecipitate
IRF	interferon regulatory factor

ISG	interferon-stimulated gene
ISVP	intermediate subviral particle
JAK	Janus kinase
JAM-A	junctional adhesion molecule A
kDa	kilodalton
KEGG	Kyoto Encyclopaedia of Genes and Genomes
L	litre
LDH	lactate dehydrogenase
LOD	limit of detection
LPS	lipopolysaccharide
MA	microarray
MACS	magnetic-activated cell sorting
MAGE	melanoma-associated antigen
MAPK	mitogen-activated protein kinase
MART	melanoma antigen recognised by T cells
MAVS	mitochondrial antiviral-signalling protein
MCP	monocyte chemotactic protein
MDA5	melanoma differentiation-associated protein 5
MDSC	myeloid-derived suppressor cell
MEK	MAPK/ERK kinase
MF	molecular function (GO)
MFI	median fluorescence intensity
MHC	major histocompatibility complex
MIP	macrophage inflammatory protein
miRNA	micro-RNA
ml	millilitre
MOI	multiplicity of infection
mono	monocyte

MTT	3-(4,5-dimethylthiazol-2-yl)-2,5-diphenyltetrazolium bromide
NAb	neutralising antibody
NCCN	National Comprehensive Cancer Network
nd	not determined
ND <sub>50</sub>	50% neutralising dose
NDV	Newcastle disease virus
NF-κB	nuclear factor kappa-light chain enhancer of activated B cells
NHSBT	National Health Service Blood and Transplant
NICE	National Institute for Health and Care Excellence
NK	natural killer
NLR	NOD-like receptor
nm	nanometre
nM	nanomolar
NOD	nucleotide-binding oligomerization domain
ns	not significant
NTC	no template control
ORR	overall response rate
OS	overall survival
OV	oncolytic virus
P/C	paclitaxel/carboplatin
padj	adjusted p value
PAGE	polyacrylamide gel electrophoresis
PAMP	pattern-associated molecular pattern
PBMC	peripheral blood mononuclear cell
PBS	phosphate-buffered saline
PBST	phosphate-buffered saline, Tween-20
PC	principal component
PCA	principal component analysis

PD-1	programmed death-1
PD-L1	programmed death-ligand 1
PE	phycoerythrin
PerCP	peridinin chlorophyll A protein
PFA	paraformaldehyde
PFS	progression-free survival
pfu	plaque-forming units
pg	picogram
PHEM	PIPES-HEPES-EGTA-MgCl <sub>2</sub>
PKR	protein kinase R
pNPP	p-nitrophenyl phosphate
poly(I:C)	polyinosinic-polycytidylic acid
PR	partial response
PRR	pattern recognition receptor
PS	patient serum
pt	patient
PTA	phosphotungstic acid
qPCR	quantitative polymerase chain reaction
R	Pearson correlation coefficient
RAF	rapidly accelerated fibrosarcoma
RANTES	regulated on activation, normal T cell expressed and secreted
RAS	rat sarcoma
RdRp	RNA-dependent RNA polymerase
reo	reovirus
reo-NAb	reovirus-antibody complex
RIG-I	retinoic acid-inducible gene I
RIPA	radioimmunoprecipitation assay
RLR	RIG-I-like receptor

RNA	ribonucleic acid
RNAseq	RNA sequencing
RPMI	Roswell Park Memorial Institute
RT	room temperature
-RT	no reverse transcriptase
s.c.	subcutaneous
SD	standard deviation
SDS	sodium dodecyl sulphate
SEM	standard error of the mean
ss	single-stranded
STAT	signal transducer and activator of transcription
SV40	simian virus 40
T3D	type 3 Dearing
TAA	tumour-associated antigen
TCID <sub>50</sub>	50% tissue culture infectious dose
TCR	T-cell receptor
TEM	transmission electron microscopy
TGF- $\beta$	transforming growth factor-beta
T <sub>H</sub>	helper T
TK	thymidine kinase
TLR	Toll-like receptor
T <sub>m</sub>	melting temperature
TME	tumour microenvironment
TNF	tumour necrosis factor
TNM	tumour-node-metastasis
TRAF	TNF receptor associated factor
TRAIL	TNF-related apoptosis-inducing ligand
T <sub>reg</sub>	regulatory T

TRIF	TIR domain-containing adaptor protein inducing IFN-beta
TRP	tyrosinase-related protein 2
T-VEC	talimogene laherparepvec
UV	ultraviolet
v/v	volume per volume concentration
VSV	vesicular stomatitis virus
w/v	weight per volume concentration

## **2. Introduction**

### **2.1 Melanoma**

#### **2.1.1 Burden**

The global incidence of melanoma is rising. Over the last three decades, incidence has increased by approximately 3% per year, and nearer 5% per year in the fair-skinned Caucasian population (DeSantis et al., 2014; Ferlay et al., 2015; Guy and Ekwueme, 2011). This rise equates to the probability of a fair-skinned individual developing melanoma rising from 1 in 1,500 in 1935, to 1 in 50 today (Sandru et al., 2014). Cutaneous melanoma, originating in the skin, accounts for well over 90% of all melanoma cases (Chang et al., 1998). Despite representing less than 1% of all cases of skin cancer, melanoma causes the vast majority of deaths.

Although only the 19<sup>th</sup> most prevalent indication worldwide, in 2012 there were an estimated 232,000 new cases of cutaneous melanoma diagnosed, and 55,000 deaths, according to GLOBOCAN data (Ferlay et al., 2015). Globally, the spatial distribution of melanoma varies considerably, according to patterns of exposure to sunlight and racial skin phenotype. Incidence is highest in Australia, where fair-skinned populations experience high exposure to the subtropical sun (Erdmann et al., 2013).

The UK experiences a relatively high burden from melanoma. In 2014, over 15,000 new diagnoses of melanoma were made. Incidence has more than doubled in the past quarter of a century, with melanoma representing 4% of all new cases. This makes melanoma the fifth most common cancer in the UK. Approximately 2,500 deaths occurring in 2014 were due to malignant melanoma, making it the 18<sup>th</sup> most common cause of cancer death in the UK. This discrepancy is due to the high proportion of patients in whom detection and treatment at an early stage permits long-term survival; currently, 90% of melanoma patients survive beyond 5 years ([www.cancerresearchuk.org](http://www.cancerresearchuk.org)). Although UK incidence is expected to continue to rise in the coming decades,

mortality rates are projected to fall by 15% by 2035, largely through improved detection and improved therapeutics (Smittenaar et al., 2016).

Melanoma is more common in men; globally, the male/female ratio is approximately 1.2, although substantial variation exists between continents (Ferlay et al., 2015). Unlike many cancers which are typically rare until later in life, melanoma is increasingly common in younger adults and even adolescents, and has become the leading cause of cancer-related death in subgroups of young adults in some nations (Iannacone et al., 2015; Smittenaar et al., 2016; Weir et al., 2011). In a study evaluating data on melanoma incidence over recent decades from 19 national registries, values for the 25-44 age group were highest in England, with an estimated relative increase of 5.8% per annum (Erdmann et al., 2013). Combined with the aggressive nature of the disease, this unusual age demographic means that the number of years of potential life lost to melanoma is considerable, at an average of 15-20 (Guy and Ekwueme, 2011; Thiam et al., 2016).

### **2.1.2 Aetiology**

Cutaneous melanoma originates from melanocytes, melanin-generating cells derived from the neural crest. Positioned in the basal epidermis, where they comprise 5-10% of the cell population (Cichorek et al., 2013), melanocytes shield keratinocytes from DNA damage induced by ultraviolet radiation (UV) (Abdel-Malek et al., 2010). In performing this protective role, melanocytes are subjected to solar (and artificial) UV wavelengths, which are primarily responsible for their malignant transformation and consequently the genesis of frank melanoma.

Given that the major modifiable risk factor for melanoma is UV exposure, the disease is eminently preventable (Armstrong et al., 1997; Chang et al., 2009). Epidemiological studies demonstrate a robust association between melanoma incidence and temporal and spatial patterns of sun exposure (Elwood and Jopson, 1997). In addition to overall exposure, the number of sunburns appears to be a particularly pertinent risk factor (Dennis et al., 2008). Exposure to

artificial, non-solar UV insult through the use of sunbeds also carries a significantly increased risk of developing melanoma (Gallagher et al., 2005).

Melanocyte transformation is now widely regarded as a multiple-step process. Incoming UV-A or UV-B radiation is absorbed by genomic DNA, generating lesions such as pyrimidine dimers and 6-4 photoproducts (You et al., 2001). These DNA changes can accumulate when the cell's endogenous repair mechanisms, orchestrated by the p53 protein and aided by cell cycle arrest, fail to ameliorate the damage in a prompt and accurate manner. For instance, resolution of pyrimidine dimers by nucleotide excision repair often yields cytosine-to-thymine substitutions, characteristic UV-induced point mutations (Daya-Grosjean and Sarasin, 2005). Mutations in specific proto-oncogenes or tumour suppressor genes can thus become initiating events for oncogenesis, driving uncontrolled replication and thus neoplastic growth.

Unlike the common benign melanocytic nevus, these 'nests' of transformed melanocytes proliferate to form a malignant nevus within the epidermis, termed melanoma *in situ*. This is clinically classified as stage 0 disease under the AJCC 'TNM' staging system, in its 8<sup>th</sup> edition this year (Gershenwald et al., 2017), which includes metrics of tumour thickness and ulceration (T), and spread to regional lymph nodes (N) and distant organs (metastasis, M) (Balch et al., 2009). The proliferating cells penetrate in the vertical plane through the dermal-epidermal junction and subsequently the dermis, and potentially cause ulceration; these lesions are progressively classified as stage I and II melanoma.

The progression to more advanced disease requires melanoma cells to acquire a migratory phenotype and to transit away from the initial neoplastic site. Thus stage III melanoma is broadly characterised by the malignant colonization of adjacent tissues and/or lymph nodes. Stage IV disease represents metastatic melanoma, in which malignant cells have spread to distant lymph nodes or organ sites – most often the liver, lungs, bone and brain (Tas, 2012).

The staging of melanoma at diagnosis is the key determinant of outcome. Along with the molecular factors of lactate dehydrogenase (LDH) level and mitotic index, the anatomical TNM metrics included in the staging system are pivotal

prognostic factors (Crowson et al., 2006). The presence of metastasis is undoubtedly the strongest of these; while 5-year survival for the whole melanoma patient population exceeds 90%, this drops to approximately 16% in those with stage IV melanoma (DeSantis et al., 2014). Consequently, early detection and treatment of local disease is a priority.

### **2.1.3 Treatment**

The stage of melanoma diagnosed largely dictates the course of treatment. Surgical excision of the primary tumour proves curative in most cases of the less advanced stages of melanoma; this can be supplemented with lymphadenectomy to address lower levels of nodal disease. It is in the later stages of melanoma that available treatments are considerably less effective, forming a clear unmet need.

These patients, and in particular those with stage IV melanoma, typically require systemic treatment. Cytotoxic chemotherapy, mostly reliant on dacarbazine (DTIC), yields a response rate – that is, the proportion of patients experiencing a substantial reduction in tumour volume – of approximately 10%, with complete responses in below 5% (Eigentler et al., 2003; Mandarà et al., 2006).

Chemotherapy, even in combination, has failed to generate a proven survival benefit in randomised phase III trials (Lui et al., 2007). Nevertheless, despite these poor response rates over more than two decades, DTIC – along with interleukin (IL)-2 – remained standard treatment as late as 2008 (Wilson and Schuchter, 2016). Temozolomide, another DNA alkylating agent often used in the treatment of brain metastases, exhibits similar response rates to DTIC (Middleton et al., 2000).

Conventional single-agent chemotherapy regimens are now widely relegated to the second- or third-line setting, or discarded altogether, in favour of novel therapeutic approaches emerging over the past decade. Clinical strategies have now undergone a fundamental shift with the advent of targeted agents and immunotherapies.

As an indication, melanoma was not a major focus of research until around 2002. It was at this point that the Cancer Genome Project identified the presence of oncogenic mutations in the *BRAF* (rapidly accelerated fibrosarcoma kinase B) gene in over 50% of melanoma cases (Davies et al., 2002). The BRAF protein, a serine-threonine kinase, is a key link in the RAS/MAPK (rat sarcoma/mitogen-activated protein kinase) signalling cascade underlying cellular patterns of differentiation and proliferation (Pearson et al., 2001). Since then, research into the dysregulation of the MAPK pathway has made melanoma one of the most heavily studied tumour types.

Activating mutations in the MAPK pathway are key to melanomagenesis (Cohen et al., 2002; Hocker et al., 2008; Wellbrock and Arozarena, 2016). In sum, mutations within this cascade – typically in *NRAS* or *BRAF* – are present in around 90% of melanomas. Notably, mutations in *BRAF* are also common in benign melanocytic nevi, suggesting that activation of BRAF is insufficient for transformation in isolation, but may represent an important contributory step in this direction (Pollock et al., 2003).

Over 90% of activating mutations in the *BRAF* gene in melanoma comprise a single nucleotide change encoding for the substitution of glutamine at codon 600 for valine (V600E), while around 5% result in substitution by lysine (V600K) (Klinac et al., 2013; Platz et al., 2008). These mutations promote the constitutive activation of BRAF, and ultimately downstream molecular sequelae leading to unchecked proliferation, invasive capacity, avoidance of apoptosis and even immune evasion, all hallmarks of a malignant cell population (Maurer et al., 2011). The isolation of these mutations exposed BRAF as a principal target for therapeutic inhibition.

Sorafenib, the first-generation BRAF inhibitor, showed promise in Phase I and II trial with response rates over 30% against melanoma. Its eventual failure in both pre-treated and treatment-naïve patients with advanced melanoma in confirmatory Phase III trial stimulated the development of more specific and potent inhibitors (Eggermont and Robert, 2011). The first of these, vemurafenib, demonstrated superior efficacy versus sorafenib and DTIC (Chapman et al., 2011; Young et al., 2012) and in light of the unprecedented outcomes subsequently gained regulatory approval for V600E-mutant advanced

melanoma in 2011 and 2012 (Dias et al., 2013; Kim et al., 2014). Other BRAF inhibitors such as dabrafenib have since been approved in these patients (Hauschild et al., 2012).

The MEK (MAPK kinase)-ERK (extracellular signal-related kinase) pathway represents a group of effectors immediately downstream of RAS. As with MAPK blockade, the inhibition of MEK using trametinib is effective against V600-mutant melanoma (Flaherty et al., 2012). These small molecule inhibitors against BRAF and MEK generate impressive speed and scale of response, heightened when deployed together (Flaherty et al., 2012). Yet the majority of patients relapse within a year with BRAF inhibitor-resistant disease, even when these agents are used in combination (Larkin et al., 2014; Long et al., 2015). Thus although targeted inhibitors can achieve an initial rapid benefit, durable responses are limited to small minority and come at the expense of considerable toxicity (Sznol et al., 2017).

Since 2008, immunotherapy agents have commanded an ever-increasing share of the market in melanoma therapy. Although the majority of these drugs are new, the first immunotherapy agent in widespread use was the T cell stimulant IL-2, originally deployed successfully against melanoma in 1984 (Rosenberg et al., 1985). This first melanoma patient – and many since – have experienced long-term remission through its use (Agarwala, 2009; Rosenberg, 2014). The durability of response and distinctive patterns of toxicity observed with immunotherapies such as IL-2 are products of their broader *modus operandi*, which is discussed below.

Following the robust success of IL-2 in a very small subset of patients, further waves of immunotherapy agents have made incremental progress in improving prognosis for melanoma patients: first interferon (IFN), then more recently a cadre of ‘checkpoint inhibitor’ antibodies including ipilimumab and subsequently pembrolizumab and nivolumab (Blumenthal and Pazdur, 2017). While IFN and IL-2 often elicit tumour responses, they generally fail to enhance overall survival versus chemotherapy (Ives et al., 2007). By contrast, checkpoint inhibitor therapy is revolutionising outcomes: while only around 12% of advanced melanoma patients are alive 3 years after commencing DTIC (Maio et al., 2015), this figure expands to over 50% in pembrolizumab- or nivolumab-treated

populations, according to most recent reports (Robert et al., 2017; Wolchok et al., 2017).

Checkpoint inhibitors and targeted drugs have rapidly surpassed their predecessors as standard of care in melanoma. In the UK, according to NICE guidelines, surgical excision of the primary tumour remains default treatment for local disease (stages 0, I and II). The biopsy of sentinel lymph nodes is common for more invasive primary lesions. 'Loco-regional' or locally advanced (stage III) melanoma is managed by additional lymphadenectomy (Essner et al., 1999). While the use of adjuvant (post-surgical) radiotherapy, IFN or ipilimumab is now commonplace (Eggermont et al., 2016), the use of newer checkpoint inhibitors in the adjuvant and neo-adjuvant (pre-surgical) settings appears inevitable in efforts to evade progression to stage IV (Rozeman et al., 2017; Weber et al., 2017).

In patients with systemic dissemination of melanoma, a wide range of treatment options are now approved for use. In *BRAF*-mutant patients, genetics dictate the use of targeted agents against BRAF and MEK; checkpoint inhibitor use is indicated regardless of BRAF status (Larkin et al., 2015b; Schachter et al., 2017). An avalanche of ongoing studies seek to address the superiority of targeted agents or checkpoint inhibitors in the *BRAF*-mutant setting, emerging immunotherapies, the optimal sequencing of existing agents, and the delicate balance between toxicity and efficacy in combination regimens.

## 2.2 Cancer and the immune system

### 2.2.1 Anti-tumour immunity

It is increasingly well recognised that the immune system plays a dual role in the development of cancer, with elements that can quash or encourage neoplastic growth. Our knowledge of the involvement of the immune system in both the genesis and potential treatment of cancer has not always been so secure. The first evidence for the relevance of immunity came from disparate anecdotal reports, associating acute infection with the onset of spontaneous tumour regression (Hopton Cann et al., 2002). The infecting agents implicated were diverse, and included bacterial, viral, fungal and protozoan organisms (Rohdenburg, 1918). This phenomenon was even observed in the disease course of Peregrine Laziosi, the patron saint of cancer patients, in whom rejection of a tibial tumour appeared to be triggered by severe infection (Jackson, 1974).

Although not yet formally examined, these reports encouraged some the more innovative 19<sup>th</sup>-century physicians to actively promote sepsis in the peri- or post-surgical period, which did yield apparent delays in tumour recurrence (reviewed in Jessy, 2011; Thiery, 1909). Such spontaneous regression events subsequently inspired what might today be called basic immunotherapies (Coley, 1891). Around the turn of the century, the American surgical pioneer William Coley employed a ‘vaccine’ comprising inactivated bacterial strains – now known as ‘Coley’s toxins’ – to treat cancer lesions, with some evidence of regression in sarcoma and lymphoma (Coley, 1910, 1928). However, with the rise of chemo- and radiotherapies, and the increasing importance placed on surgical asepsis in general, such approaches fell from favour during the 20<sup>th</sup> century.

Further observational studies broadly corroborate the link between cancer and the immune system. The prevalence of cancer is higher in immunodeficient mice (Shankaran et al., 2001). This is mirrored somewhat in humans; for instance, those prescribed immunosuppressive agents following solid organ

transplant are at higher risk of cancer (Euvrard et al., 2003; London et al., 1995). Similarly, the compromised immune system of HIV-positive patients yields a higher incidence of cancers such as Kaposi's sarcoma (Rabkin et al., 1991). Collectively, these reports are indicative of a clinically meaningful association between a competent and active immune system and the prevention of cancer.

There have been a number of attempts to justify these observations with a functional model for immune involvement in cancer. It has long been recognised that the immune system exists primarily as a surveillance system for pathogens. This dogma was manifested as the 'self/non-self model' (Burnet and Fenner, 1949). The dominance of this model subsequently presented a major obstacle to the rationale behind the burgeoning field of cancer immunology. The model, based on the endogenous ('self') or exogenous ('non-self') source of material, is well suited to account for the evolved role for the immune system against pathogens. It is less well suited to addressing its role against cancer, which originates from healthy endogenous cells and is genetically similar. Wouldn't cancer be subject to the same evolved constraints preventing immune assault on 'self' tissues?

A subsequent attempt to crystallise our understanding of the immune system gave rise to the 'danger model' (Matzinger, 1994, 2002). Largely a critique of the self/non-self model, this approach identifies 'alarm' signals from endogenous or exogenous tissue, including cellular proteins such as heat-shock proteins (HSP) and interferon  $\alpha$  (IFN- $\alpha$ ), as requirements for immune activation. While the danger model accounts well for various modes of cell death in which these factors are implicated, its proposition that tumours do not elicit immune responses (Matzinger, 1998) has subsequently been dismantled by comprehensive evidence for anti-tumour immunity, often in response to specific molecular modifications rather than overt damage (Dunn et al., 2006). So how are immune effectors able to detect aberrant malignant cells?

It was around the time of Coley that the pioneering German physician Paul Ehrlich suggested that host defences actively suppress neoplastic cell growth (Ehrlich, 1909). It was over half a century later that this belief was reinforced by systematic evidence and formal theory. The 'immune surveillance model'

proposed by Frank MacFarlane Burnet was predicated upon novel antigens which “provoke an effective immunological reaction with regression of the tumour” (Burnet, 1970). The model was based upon the rejection of tumour tissue – but not normal tissue – in syngeneic transplants, and thus the implication of tumour-specific antigens.

Indeed, Burnet’s concept was to be substantiated by the first identification of a human tumour-specific antigen, melanoma antigen 1 (MAGE-A1), recognised by cognate T cells (van der Bruggen et al., 1991). The idea of immunity against a tumour-specific antigen constitutes a violation of the self/non-self model; cancer cells are of course self-derived, but due to their (often causative) mutations they are genetically aberrant, a state termed ‘altered self’ (Medzhitov and Janeway, 2002). Further, the immune surveillance model is supported by the increased incidence of cancer in mouse models deficient in specific aspects of immunity, particularly those centred around the activity of T cells (Brennan et al., 2010; Smyth et al., 1999).

T cells are CD3<sup>+</sup> lymphocytes derived from the thymus, which are essential mediators of tumour surveillance. The genetic deletion of activatory T cell populations renders mice acutely susceptible to cancer, while their artificial depletion promotes progression (Andreasson et al., 2010; Haines et al., 2006; Knocke et al., 2016). The successful use of adoptive T cell transfer as a therapy for metastatic melanoma patients demonstrates the potency of this cell population (Rosenberg et al., 2011). T cells are pivotal in the ability of the immune system to respond flexibly to temporal changes in exogenous pathogens and other immune stimuli – the cell-mediated aspect of the adaptive immune response. Naïve T cells, once briefed or ‘primed’ against a particular antigen, can mount a rapid and specific response upon subsequent exposure, and thus can carry ‘immunological memory’.

Antigens linked with tumours, some of which are tumour-specific, are more broadly known as tumour-associated antigens (TAA). Those that are indeed tumour-specific are commonly neoantigens arising directly from mutations. While many of the most common melanoma ‘driver’ mutations in genes such as *NRAS* appear to yield poorly immunogenic antigens, other ‘passenger’ mutations in genes such as *CDK4* also occur which enable this type of TAA to

account for often the majority of tumour-targeted T cells (Lennerz et al., 2005; Linard et al., 2002). Other TAA are more subtle in their violation of immune surveillance mechanisms. For instance, germ cell antigens result from the expression of transcripts that are present in germline tissues but are usually silenced in adult somatic cells, unless reactivated; these include the well-known cancer/testis antigens MAGE-A1 (van der Bruggen et al., 1991) and NY-ESO-1 (Chen et al., 1997).

The differentiation antigens, such as TRP-1 and MART-1, are present on normal melanocytes as well as melanoma cells, and this lack of cancer specificity means that these TAA enjoy a degree of immune tolerance (Coulie et al., 1994; Wang et al., 1995). However, the observation of T cell responses to such peptides in patients suggests that such tolerance is not insurmountable (Kawakami et al., 1994). The onset of skin depigmentation (vitiligo) is attributed to responses against differentiation antigens, and is a positive prognostic marker (Yee et al., 2000). Similarly, other shared antigens are expressed to a significantly higher level in melanoma cells versus untransformed melanocytes, potentially enabling an antigen-specific response in the event that this exceeds the threshold required for T cell recognition (Fisk et al., 1995).

For primed T cell responses to antigen to occur, the offending antigen must be processed and constituent epitopes presented appropriately to the T cell receptor (TCR). The major type of antigen-presenting cell (APC) responsible for this process is the dendritic cell (DC), a key linker of innate and adaptive immunity. After taking up and degrading antigen, DC supply epitopes to T cells by their presentation on major histocompatibility complex (MHC) molecules, to which the antigen-specific TCR can bind. Classically, CD8<sup>+</sup> cytolytic T lymphocytes (CTL) recognise epitopes loaded on MHC class I, while the CD4<sup>+</sup> helper T cells recognise those on MHC class II.

Ligation of the cognate TCR, supplemented by a second signal between APC co-stimulatory molecules and T cell CD28 (Lafferty and Cunningham, 1975), stimulates the conversion of naïve T cells into effectors and induces clonal expansion. On encountering cells expressing antigen, effector CTL can then launch an assault in order to induce apoptotic cell death, either through the release of cytolytic granules containing proteolytic granzymes and perforin, or

through the contact-dependent engagement of death receptors such as Fas on the cell surface. Upon stimulation, CD4<sup>+</sup> T cells can differentiate into two types of effector helper cells, termed T<sub>H</sub>1 and T<sub>H</sub>2, which facilitate the activation of CTL and macrophages, or antibody-producing B cells, respectively. T<sub>H</sub>1 cells therefore promote cell-mediated immunity, while T<sub>H</sub>2 cells support the humoral arm of the adaptive immune response.

Adaptive immunity therefore enables us to keep pace with the 'moving target' of a genetically unstable tumour, but takes time to react. The innate immune system is indispensable as the first line of defence, not only against exogenous pathogens but also endogenous malignant cells. It includes a battery of 'response-ready' effectors, which include DC, neutrophils, macrophages, natural killer (NK) and NKT cells. These generally respond to evolutionarily conserved features of pathogens; for instance, the pattern recognition receptors (PRR) expressed by DC and macrophages enable them to react to foreign nucleic acid and protein motifs, by cytokine secretion or phagocytosis. With the help of humoral immune elements, they are also able to bring these functions to bear upon tumour cells through complement- or antibody-dependent cytotoxicity (ADCC) and phagocytosis (ADCP).

It is NK cells, lymphocytes expressing CD56 but no CD3, that are best equipped to respond immediately to challenge with a transformed cell. Tumours seek to avoid the adaptive immune response by downregulating MHC-I and minimizing exposure of TAA. This so-called 'missing self' causes insufficient binding to inhibitory receptors on the NK cell surface (Ljunggren and Kärre, 1985). Aided by simultaneous ligation of stress ligands, this triggers cytolytic activity via similar mechanisms to T cells, and the secretion of stimulatory factors such as IFN- $\gamma$  which support T cell activation. MHC-I loss is observed in melanoma (Garrido et al., 2012), and therapeutic strategies aimed at targeting this and other aspects of NK-mediated anti-tumour immunity have been deployed with some success (reviewed in Hölsken et al., 2015).

### 2.2.2 Immune evasion and suppression

The tumour stroma includes all the non-malignant cells of the tumour, such as immune cells, fibroblasts, components of the vasculature, and elements of the extracellular matrix, and frequently comprises over 50% of the cells within a solid tumour (Wu et al., 2016). Over the entire course of the initiation and progression of a tumour, its malignant cells are involved in intimate cross-talk with these cells. Tumour cells can corrupt and elicit the support of the immune system in order to aid tumour persistence and growth. This immunosuppressive capacity is a key hallmark of cancer (Hanahan and Weinberg, 2011).

Only recently has the ability of cancer to evade immunity been modelled in significant detail. Building upon the framework of the broad theory of immune surveillance, the 'cancer immunoediting' model describes discrete stages which are defined by the state of the dynamic bidirectional relationship between transformed cells and their stromal neighbours (Dunn et al., 2006). The model provides molecular rationale for clinical phenomena, such as stochastic periods of tumour dormancy and growth, and tumour progression in spite of functional immune effectors (Croci et al., 2007).

The three 'E's' of immunoediting are as follows. In the 'elimination' phase, the immune system is readily able to ablate the most immunogenic tumour cells, such as those with high levels of surface tumour antigen expression. Those variants that are less immunogenic, by virtue of genetic instability within the heterogenous tumour, are not so readily recognised and can persist and proliferate. This process of editing yields a state of 'equilibrium' – continued division of some clonal subpopulations is balanced by clearance of others, giving the impression of dormancy. Prolonged dormancy gradually promotes immunosuppressive changes in the tumour microenvironment, and these permit the renewed progression of overt cancer, or 'escape'.

A variety of cell populations and the factors they secrete are implicated in tumour immune evasion. Regulatory T cells ( $T_{reg}$ ) are foremost amongst these. In normal physiology,  $T_{reg}$  are key in maintaining the balance of immunity and tolerance to 'self' to avoid destructive autoimmunity.  $T_{reg}$  are commonly induced from helper T cells by secreted factors such as transforming growth factor  $\beta$

(TGF- $\beta$ ) derived from macrophages and other cell types in the tumour milieu (Chen et al., 2003); they are also drawn there by chemokines released from tumour cells (Curiel et al., 2004). The T<sub>reg</sub> population in the tumour, which is more concentrated and more suppressive than elsewhere (Miracco et al., 2007; Yokokawa et al., 2008), limits immune activation in various ways. These broadly involve the surface expression or short-range secretion of molecules which suppress (or even kill) APC and T cells with activatory potential (reviewed in Sakaguchi et al., 2009). The depletion of T<sub>reg</sub> enhances the rejection of murine melanoma and prolongs survival (Nizar et al., 2010) while T<sub>reg</sub> infiltration – and particularly the ratio of CD8<sup>+</sup> T to regulatory T cells – represents a meaningful prognostic factor in melanoma patients (Knol et al., 2011; Miracco et al., 2007).

In addition to lymphocytes, myeloid immune cells also comprise a numerically and functionally significant proportion of a tumour mass. Many of these, derived from the monocyte population circulating in blood, will be DC and pro-inflammatory ('M1') macrophages with anti-tumour functionality. However, the exposure of other monocytic cells to soluble factors such as TGF- $\beta$ , or granulocyte-macrophage colony stimulating factor (GM-CSF) and IL-4, promotes the development of myeloid-derived suppressor cells (MDSC) and 'M2' macrophages respectively.

MDSC quash T cell responses by the expression of arginase 1 (Arg-1) and inducible nitric oxide synthase (iNOS). L-arginine, an amino acid required for T cell proliferation and TCR expression, is degraded by these molecules – in the case of iNOS, into nitric oxide, which dampens T cell activity (Bronte and Zanovello, 2005). MDSC are of functional relevance to the extent that their numbers are inversely correlated with survival in melanoma patients (Weide et al., 2014). Meanwhile, tumour-associated macrophages (TAM), which typically represent a significant minority of cells in the tumour mass, are commonly of the alternatively activated, M2-polarized phenotype. After being guided towards this phenotype by tumour-derived factors, M2 macrophages actively contribute towards the immunosuppressive tumour microenvironment by secreting TGF- $\beta$ , IL-1 $\beta$ , IFN- $\gamma$  and other cytokines, which promote angiogenesis and invasion (Gehrke et al., 2014; Sica et al., 2006; Tanese et al., 2015). Consequently, M2

macrophages progressively accumulate throughout melanoma progression, and are associated with poor outcomes (Falleni et al., 2017).

Transformed cells themselves boast a variety of traits which enable their evasion of immune clearance. Arguably more influential than the suppression of a cell's functionality is its ablation. Melanoma cells commonly display some resistance to apoptosis by their downregulation of death receptors such as Fas and TRAIL-R, or upstream effectors including caspase-8, which are central to its induction (reviewed in Hersey et al., 2006). Moreover, cancer cells are capable of 'counter-attack' against infiltrating immune cells. Their expression of Fas ligand (FasL) can induce apoptosis in neighbouring T cells, thereby contributing to the establishment of poorly regulated, 'immune-privileged' niches where tumours can grow unchecked (Strand et al., 1996).

Although it does provide an opportunity for NK cells, the progressive loss of melanoma MHC-I expression to impair antigen presentation provides a virtual 'invisibility cloak' against T cell recognition, and is a prime example of immunoediting in action (del Campo et al., 2014; Rees and Mian, 1999). Similarly, tumour cells commonly lack the co-stimulatory molecules CD80 and CD86; by permitting TCR engagement without the necessary 'signal 2', they foster a state of tolerance or anergy in antigen-specific T cells (Staveley-O'Carroll et al., 1998).

However, it appears to be the active expression of immunosuppressive molecules by malignant cells that is particularly influential in driving immune evasion. At present, the most clinically relevant example of this phenomenon involves the expression of programmed death ligands PD-L1 and PD-L2, which bind to their receptor PD-1 on tumour-infiltrating lymphocytes. In effector T cells, PD-1 ligation provides a powerful 'off' signal, preventing cytolytic activity, cytokine release, proliferation and even T cell survival (Dong et al., 2002; 2016). The chronic exposure of melanoma-specific CTL to tumour antigen upregulates PD-1, making them more sensitive to PD-1 ligands and promoting a state of T cell exhaustion (Ahmadzadeh et al., 2009). The PD-1 axis represents one of an increasing number of 'immune checkpoints' limiting anti-tumour immune programs which are the subject of intense therapeutic development.

### 2.2.3 Emerging immunotherapies

Conventional approaches to cancer therapy, dominated by chemo- and radiotherapy, are associated with poor outcomes and substantial toxicity. These modalities have attributes which work with and against the immune system. Although radiotherapy boasts a well-described immune-mediated abscopal effect, it also has long-term lymphotoxic effects (Campbell et al., 1976). While cytotoxic chemotherapy can promote the cytolytic potential of CD8<sup>+</sup> T cells, it too yields T cell immunodeficiency (Mackall, 1999). Even the surgeon's scalpel is immunosuppressive (Kadosawa and Watabe, 2015).

The success of this century's immuno-oncology agents is reliant upon a different approach: harnessing the patient's own immune system against the tumour. The commitment of the field to this paradigm is encapsulated in increasingly complex models, the latest being the 'cancer immunogram' framework designed to address all known immune facets of a target lesion (Blank et al., 2016).

As an indication, melanoma has become the 'poster child' for immunotherapy for a number of reasons. Firstly, melanoma is intrinsically resistant to chemo- and radiotherapy (Pawlik and Sondak, 2003). This likely encouraged investigators to pursue other therapeutic avenues; even, cynically, for the opportunity to test against less effective comparators. Melanoma also has a reputation for being a tumour type with perhaps the highest immunogenicity, or potential to induce an immune response. It demonstrates a uniquely high somatic mutation rate and neoantigen burden, a product of its UV-linked aetiology (Berger et al., 2012; Rajasagi et al., 2014). Multiple melanoma-associated antigens have been found to be clinically relevant (Barrow et al., 2006), and lymphocytic tumour infiltration is a positive prognostic factor (Oble et al., 2009), both implicating T cell activity in the disease course. The tendency of melanoma lesions to undergo spontaneous regression is also suggestive of an undercurrent of anti-tumour immunity (Printz, 2001).

The first robust clinical evidence of success in targeting melanoma immunologically was manifested in the durable remissions observed in response to toxic doses of IL-2 (Rosenberg, 2014). This formed proof of

principle for immune – and particularly T cell – activation as a viable therapeutic strategy. Subsequently, the use of adjuvant interferon to promote the immune-mediated clearance of residual and micro-metastatic disease after resection was based on the same broad rationale. Albeit more sophisticated, newer vaccination strategies using immunostimulatory peptides or DC also fall under this premise.

The oncology market is increasingly inundated with a class of molecules termed immune checkpoint inhibitors (ICI). These agents target natural molecular ‘checkpoints’ designed to limit immune activation and prevent damaging autoimmunity. The two checkpoint molecules most successfully targeted to date are cytotoxic T-lymphocyte antigen-4 (CTLA-4) and programmed cell death protein 1 (PD-1), both present on T cell populations. Predominantly on CD4<sup>+</sup> helper T cells but also T<sub>reg</sub>, CTLA-4 mimics and is able to outcompete CD28 for their common ligands CD80 and CD86, present on APC (Yokosuka et al., 2010). While it was thought that this allows CTLA-4 to replace stimulatory CD28 signalling with its own inhibitory signalling, it is now considered that it functions primarily on T<sub>reg</sub> by regulating the access of CD28 to their shared ligands (Walker and Sansom, 2015). This process retards the ability of APC to promote activation of T cells during antigen presentation in the periphery.

A similar mechanism underlies the PD-1 checkpoint operating at the tumour site. The ligation of T cell PD-1 by PD-L1/2 largely present on malignant cells also dampens T cell stimulation; this pro-tumour checkpoint therefore functions more directly by preventing the elimination of ligand-expressing tumour cells themselves. Consequently both CTLA-4 and PD-1 proteins supply inhibitory signals to specific T cells at two key points of antigen exposure: during presentation in the periphery, and subsequent recognition within the tumour bed (reviewed in Pardoll, 2012).

Antibodies designed to block these molecular interactions and revitalise anti-tumour T cell activity have entered the clinical arena in the past decade. The first-in-class CTLA-4 inhibitor ipilimumab was the first checkpoint inhibitor to reach the clinic, gaining regulatory approval for metastatic melanoma in 2011 (Cameron et al., 2011). Although response rates to ipilimumab were higher than with cytotoxic chemotherapy at around 20%, its real superiority was in the

durability of these responses (Hodi et al., 2010; Specenier, 2016). Subsequently ipilimumab was approved for use in the adjuvant setting for high-risk stage III melanoma in light of its benefit in regression-free and overall survival (Eggermont et al., 2016).

The newer anti-PD-1 checkpoint inhibitors nivolumab and pembrolizumab exhibit even greater activity than ipilimumab, with overall response rates typically around 30-35% (Robert et al., 2015b; Topalian et al., 2012; Wolchok et al., 2017). The CheckMate-066, -067 and -037 trials demonstrated the superiority of nivolumab to chemotherapy and to ipilimumab respectively, both in pre-treated and treatment-naïve patients, and triggered its approval (Larkin et al., 2015a; Robert et al., 2015a; Weber et al., 2016; Wolchok et al., 2017). Similarly, the efficacy shown by pembrolizumab in the KEYNOTE-002 and -006 studies brought about its approval in metastatic melanoma in second-line in 2014, and subsequently as a first-line agent in 2015 (Barone et al., 2017; Chuk et al., 2017; Robert et al., 2015b). Both of these agents are now listed as preferred first-line therapies for advanced melanoma in the latest US NCCN guidelines (National Comprehensive Cancer Network, 2017). The PD-1 inhibitors increasingly dominate the treatment of advanced melanoma, comprising 23% of the market share in 2015, projected to rise to 51% by 2025 (Decision Resources Group, 2017).

The efficacy of checkpoint inhibitors appears to be reliant upon a number of factors, including the total mutational load or neoantigen burden, across indications and specifically in melanoma (Le et al., 2015; McGranahan et al., 2016; Van Allen et al., 2015). Other factors include inflammatory gene signatures (Jamieson and Maker, 2017; McGranahan et al., 2016). These elements may however represent general prognostic factors of survival rather than specific *predictive* factors for response to checkpoint inhibitor therapy (Hugo et al., 2016). Highly relevant in the context of PD-1 inhibitor therapy is the PD-L1 protein itself, which is overexpressed in melanoma (Hino et al., 2010; Oba et al., 2014). PD-L1 expression level is not only prognostic but is also predictive of response to PD-1 inhibitor therapy (Abdel-Rahman, 2016; Topalian et al., 2012; Weber et al., 2013). This and various other metrics are ultimately likely to contribute towards a multifactorial algorithm, like the recent 'cancer

immunogram' (Blank et al., 2016), used to predict the subsets of patients likely to respond to these agents. These would fall alongside existing tools such as testing for BRAF/MEK mutations, and for tumour PD-L1 status, which is already an important marker for anti-PD-1 patient selection.

As it is often the testing ground for these agents, melanoma is an excellent prism through which to anticipate the future landscape of cancer immunotherapy. With the avalanche of trials underway and in development, this landscape is constantly evolving. In the short-term, the most significant change appears likely to be the spread of combination immunotherapy. The combination of ipilimumab and nivolumab, which markedly elevates both efficacy and toxicity, has already gained NICE approval in advanced melanoma (Postow et al., 2015; Wise, 2016; Wolchok et al., 2017). The publication of long-term survival outcomes in melanoma will soon guide the uptake of combination immunotherapy in other indications. Other ongoing trials examine the combination of checkpoint inhibitors and tyrosine kinase inhibitors in suitable patient subgroups, with the optimal sequencing of combination agents an area of particular focus.

In addition to combining agents which are already approved for use as monotherapy, the field will also expand through the addition of novel agents, the majority of which appear likely to be immunotherapies. As well as the now well (but not completely) understood CTLA-4 and PD-1 axes, other immune targets are under intense scrutiny. Foremost amongst these are other inhibitory checkpoints such as LAG-3 and TIM-3 (Anderson et al., 2016); others are stimulatory T cell molecules such as OX40, which may be exploited using ligand-mimicking agonists, rather than antagonistic antibodies (Linch et al., 2015). This new wave of T cell modulators carries great momentum as it speeds through clinical trial. Other agents target tumour metabolism: epacadostat, an agent inhibiting the generation of the T cell suppressor kynurenine from tryptophan by the IDO-1 enzyme, demonstrates impressive efficacy with combination anti-PD-1 (Hamid et al., 2017). Indeed, the potential of these agents to synergise with immune checkpoint blockade is now of enormous therapeutic relevance.

The combination of checkpoint inhibitors is feasible, and is achieving unprecedented response rates; particularly when used early in the treatment pathway, but also against advanced disease (Rozeman et al., 2017; Wolchok et al., 2017). Although half of advanced melanoma patients still die within four years of commencing combination treatment (Wolchok et al., 2017), the remaining cohort demonstrate durable responses, as signified by a plateau in the survival curve, and can increasingly be termed 'cured' (McDermott et al., 2013). Incremental gains are being made in 'chasing the tail' of this curve (Harris et al., 2016), whilst trying to evade the punishing toxicities associated with combination checkpoint blockade. Enter the oncolytic virus: an emerging immunotherapy modality with the potential to contribute to this pursuit.

## 2.3 Oncolytic viruses

### 2.3.1 Background

Various naturally occurring viruses show an intrinsic preference towards entry into, and replication within, transformed cells, as a direct consequence of their aberrant phenotype. Their ability to destroy the architecture of malignant cells affords these viruses the term *oncolytic*, or 'cancer bursting'. This historical terminology is somewhat restrictive in describing the true mechanism of action of many viruses in clinical testing, but it has hitherto been adopted as a 'one size fits all' label for viruses with anti-cancer activity.

Oncolytic viruses (OV) hold advantages over traditional modalities. In a field which increasingly aims to avoid the toxicities often seen with more indiscriminate agents such as cytotoxic chemotherapies, the tumour selectivity inherent to OV represents their defining trait. True cancer-selective activity also opens the door to the targeted delivery of other anti-cancer agents which can be encoded within an OV vector. The amplification of a replicating OV within the tumour itself should theoretically enable a lower amount of virus to be administered to the body, giving a good therapeutic index. Lastly, OV have the ability to reverse the immune suppression characteristic of the tumour microenvironment by promoting inflammatory activity, and to prime a long-lasting immune response to the tumour.

As with many therapeutic agents, the oncolytic properties of some viruses were first noted using anecdotal evidence. Dating back into the 19<sup>th</sup> century, historical reports typically describe the regression of tumours coinciding with environmental infection with pathogens now identified as viruses. One heavily cited report associated the remission of leukaemia with a presumed influenza infection (Dock, 1904). Along with some solid neoplasms including melanoma (Pack, 1950), these accounts most commonly involved short-lived remissions of haematological cancers (Dock, 1904; Pelner et al., 1958), with the lymphotropic measles virus particularly heavily implicated (Bierman et al., 1953; Taqi et al., 1981). These case reports later led clinicians to conduct primitive, often

unethical clinical trials involving the transfer of crude bodily fluids as therapeutic material (Hoster et al., 1949). Although severe virus-induced pathology and death was reported in some patients, benefit was observed in others. In a series of pioneering human studies in the US, Southam and Moore spearheaded the use of West Nile virus isolates against various malignancies, yielding both fatal neurotoxicities and tumour regressions (Southam and Moore, 1952).

Around the same time, the advent of human cell culture systems enabled viruses to be propagated *ex vivo*, triggering rapid progress in virology research, then centred around vaccine development (Sanford et al., 1948; Weller et al., 1949). Indeed, vaccines themselves were already starting to be tested against human malignancies (Higgins and Pack, 1951). The cytopathic properties of various viruses *in vitro* were quickly noted. Simultaneously, following on from observations of the anti-neoplastic potential of vaccinia virus some decades earlier, viruses began to be tested more formally in new animal models of cancer (Levaditi and Nicolau, 1922). In a landmark paper of 1949, Moore showed that a complete remission of murine sarcoma – and subsequently other neoplasms – could be induced by Russian Far East encephalitis virus (Moore, 1949, 1951). Such observations served to spawn broad interest in the field of virotherapy for cancer, with a variety of human and non-human pathogens scrutinised. Although it soon became clear that tumour regression in an animal model was no guarantee of success in humans, animal testing was quickly adopted as a prerequisite for clinical testing (Moore, 1952).

The screening of potential OV was conducted on a large scale, with the emphasis firmly on safety as well as efficacy in light of the outcomes from the first experimental trials. A cadre of more favourable candidate viruses emerged, many of which remain in study today. For instance, having shown preclinical promise, one adenovirus was employed against cervical carcinoma; while it showed limited toxicity and some local tumour activity, virus treatment failed to improve survival (Georgiades et al., 1959). Contrastingly, a later (erratic and non-controlled) trial of the mumps virus in various malignancies produced remarkable results, with responses observed in nearly half of patients (Asada, 1974). However, the use of such non-attenuated human viruses drew ethical concern and, combined with the uninspiring impact made on survival in the

majority of trials using naturally occurring viruses (Kelly and Russell, 2007), this allowed the OV as a modality to fall temporarily from favour in the 1970s and 1980s.

### **2.3.2 Interaction with host cells**

In the absence of malignant transformation, normal cells boast a number of conserved mechanisms for the clearance of viruses, their obligate intracellular pathogens. These comprise signalling cascades which lie dormant until their activation by viral PAMP. PAMP, such as viral nucleic acid or protein and envelope motifs, engage host cell PRR stationed within the cell and on the surface. Engagement of the major PRR, namely Toll-like receptors (TLR) and RIG-I-like receptors (RLR), triggers signalling via a multitude of intracellular adaptor and hub proteins which influence antiviral gene transcription. The TLR-activated myeloid differentiation primary response protein MYD88 promotes the expression of pro-inflammatory cytokines via nuclear factor  $\kappa$ -B (NF- $\kappa$ B) (Hemmi et al., 2002). Simultaneously, adaptors such as TNF-associated factor 3 (TRAF3) stimulate interferon response factors IRF3 and IRF7 to increase the expression of type I IFN (Oganesyan et al., 2006).

The IFN proteins typically secreted from a cell as a consequence of viral detection influence neighbouring cells locoregionally and can even act in an autocrine manner. By binding IFN receptors at the surface, they mobilise a second wave of innate signalling which reinforces the antiviral state. The pathways involving proteins of the Janus kinase and signal transducer and activator of transcription (JAK-STAT) families are integral to this second wave, triggering transcriptional programs collectively termed IFN-stimulated genes (ISG). Control is further asserted at a translational level by the IFN-responsive protein kinase R (PKR). PKR itself identifies intracellular viral motifs like double-stranded (ds)RNA and, via autophosphorylation, halts protein synthesis in order to restrict the generation of viral progeny. These comprise the major molecular mediators of antiviral defence in untransformed cells.

To a greater or lesser extent, many naturally occurring viruses, by definition OV, boast a heightened ability to kill cancer cells. This is a consequence of the OV

being able to exploit molecular changes intrinsic to transformed cells which confer a shared phenotype, as follows. Firstly, cell entry – to access the transcriptional machinery the virus requires. Broadly, OV are able to enter both transformed and untransformed cells alike, as many viruses have evolved to co-opt receptors that are common to many target cells. For instance, depending on their natural tropism, many use the adhesion molecules present on leukocytes and epithelial cells to gain entry. Reovirus hijacks junctional adhesion molecule A (JAM-A; gene *F11R*), while intercellular adhesion molecule 1 (ICAM-1; gene *CD54*) is the major receptor used by group A Coxsackieviruses and others (Barton et al., 2001; Shafren et al., 1997). Nevertheless, the aberrant expression of virus receptors by transformed cells can sometimes provide OV with an entry advantage. The CD46 protein exploited for measles virus entry is overexpressed in various cancer types (Anderson et al., 2004). The receptors which contribute towards the neurotropism of type 1 herpes simplex virus (HSV-1), herpesvirus entry mediator (HVEM) and nectin-1, are also abundant on carcinoma and melanoma cells (Farassati et al., 2001; Yu et al., 2005).

The selective advantage that OV hold for cancer cells is more typically due to abnormal elements within the cell which support viral replication: so-called 'post-entry tumour specificity'. These generally involve corrupted intracellular signalling pathways which promote malignant traits while simultaneously increasing vulnerability to viral threats. Perhaps the most universal example is the dampening or total loss of IFN signalling. Cancer cells either restrict their own generation of IFN, or restrict the effect of 'incoming' IFN by limiting IFN receptor expression or signalling cascade activity. These acquired defects in IFN signalling are useful in that they can facilitate the evasion of anti-tumour immunity, limit apoptotic signalling through the p53 protein, and release the 'brake' on proliferation that IFN signalling can impose (Balkwill et al., 1978; Bidwell et al., 2012; Hasthorpe et al., 1997) – all changes that serve the viral life cycle too.

Aside from IFN modulation, transformed cells exhibit other changes in growth and survival pathways which benefit OV. The constitutive activation of AKT, a protein kinase commonly dysregulated in human malignancies, can confer susceptibility to myxoma virus (Testa and Bellacosa, 2001; Wang et al., 2006).

Similarly, oncogenic mutations in the *KRAS* and *NRAS* genes have been linked to OV susceptibility. Activation of the Ras pathway, and in particular the pro-proliferative repression of PKR, has long been considered a major determinant of reovirus replication (Shmulevitz et al., 2005; Strong et al., 1998). Despite the serendipitous gain of some cancer-selectivity through the parallel natural evolution of both malignant cells and viruses, this often provided insufficient anti-cancer activity, or excessive off-target toxicity, in clinical practice. Thus, the field turned to genetic engineering to tip the balance in the oncologist's favour.

### **2.3.3 Tropism and engineering**

The whole cancer cell phenotype is aberrant. Intriguingly, a number of the characteristics which comprise this anomalous phenotype, many elegantly described by Hanahan and Weinberg as 'hallmarks of cancer', are mirrored in cells undergoing viral infection (Hanahan and Weinberg, 2011). Of course, these two phenotypes can be considered as one and the same in the context of cellular transformation induced by a virus with oncogenic potential, such as human papillomavirus (HPV). Indeed, these similarities provided the basis for the use of viral genes such as the large T antigen of SV40 to study transformation (Sullivan et al., 2000).

However, leaving aside multicellular processes such as metastatic 'behaviour', malignant traits at the single-cell level have correlates in cells infected with replicative, non-oncogenic viruses as well, even though the factors underlying these two phenotypes are so different (Seymour and Fisher, 2016). For instance, a resistance to cell death (particularly via apoptosis) is a cancer hallmark that is common to virus-infected cells (Thomson, 2001). The vested interest that viruses have in avoiding immune detection means that infected cells display characteristics of immune evasion like those of cancer cells (Iannello et al., 2006). Viruses can also subvert the cell cycle machinery so critical to neoplastic growth in order to facilitate replication (Bagga and Bouchard, 2014). These and other similarities between the two phenotypes provide an opportunity for OV that can be capitalised upon by genetic engineering.

A number of viruses do have a natural suitability or tropism for certain types of cell, some of them malignant. For instance, the tropism of human immunodeficiency virus (HIV) for T cell subpopulations, on account of CD4 being its major receptor, has provoked its use in targeting T cell leukaemias (Jeeninga et al., 2006). In the era before genetic manipulation, our mode of 're-engineering' a virus was primitive, being limited to adapting a viral strain to a particular cell type, typically by repeated passaging. This concept of 'evolutionary engineering' appeared to hold value: in Moore's translational work, passaging the encephalitis virus through sarcoma cells endowed it with greater lytic ability (Moore, 1952). However, clinical use of these early OV was plagued by an inability to limit toxicity, particularly of neurotropic viruses to the brain; the status of live OV as the causative agents of potentially severe pathology was not to be forgotten.

It took all of three decades since genetic engineering was proposed as a solution to this trade-off (Southam, 1960) for the technology to reach its advent in the 1990s. Molecular advances enabled the modification of OV in order to enhance their safety and efficacy profiles, creating 'second-generation' viruses. The main change has involved better selectivity through attenuation; that is, deleting genes in order to limit activity in healthy cells, but not to the extent of crippling replication in malignant cells. The parallels between the attributes of virus-infected and cancer cells, and our increasing ability to tailor the virus genome, provided the opportunity to create more tumour-specific viruses. By engineering viruses without the ability to induce typical 'virus-infected' cell hallmarks, such agents rely on the presence of these traits in cancer cells alone – a strategy named *phenotypic complementation*.

The first effective example of this novel process saw Martuza successfully treat human glioma xenografts by intracranial injection of HSV bearing a deleted thymidine kinase (TK) gene (Martuza et al., 1991). The virus demonstrated cancer-selective activity without inducing encephalitis, based on the enhanced TK activity seen in cancer cells versus non-transformed cells (Hengstschläger et al., 1994). The same paradigm was exploited in the design of the adenovirus Onyx-015, the first OV in phase I trials in 1996. Onyx-015 harbours an ablation in the gene which otherwise permits the inactivation of cellular p53, leaving the

virus reliant on the inactive p53 often present in cancer cells (Heise et al., 1997). Although the mechanism of selectivity was subsequently questioned (Kirn, 2001), Onyx-015 demonstrated good tumour selectivity and formed the basis for the adenovirus termed H101, which was the first virus to be licensed as a modern cancer therapy upon its approval alongside chemotherapy for head and neck cancer in China (Lu et al., 2004; Xia et al., 2004).

A variety of strategies have been employed in trying to reap maximal benefit from our ever-improving ability to genetically modify OV. As with Onyx-015 and H101, adenovirus backbones provide the typical OV constructs (Alemany, 2007). The re-engineered adenovirus CV706 was designed to replicate under the control of a promoter driven by prostate-specific antigen (PSA), most highly secreted by prostate cancer cells, yielding a tissue-specific OV which has reached clinical trial (DeWeese et al., 2001; Hardcastle et al., 2007). A similar strategy involves the use of an OV promoter responsive to conditions common among tumours, such as hypoxia (Post et al., 2007). Newer constructs target the expression of OV based on specific microRNA (miRNA) which are dysregulated in cancer cells or their often immunosuppressive stromal neighbours (Kumar et al., 2007; V. Jennings, personal communication).

Moving 'backwards' a step out of the cell interior, other viruses generated to date have been targeted towards specific cancer types by equipping them with the capacity to bind certain receptors, such as CD46 (Takagi-Kimura et al., 2013), or receptor families such as  $\alpha_v\beta$  integrins (Dmitriev et al., 1998; Lal and Raffel, 2017), overexpressed on tumour cells themselves or its vascular endothelium. They can even be targeted towards other viral antigens, such as proteins of the HPV virus implicated in the aetiology of head and neck cancer (LaRocca et al., 2016). Other investigators have adopted translational approaches for viruses already in clinical testing, by encoding imaging markers within OV to track spread and persistence (Dispenzieri et al., 2017).

A natural extension of these strategies involves 'arming' OV by encoding pro-therapeutic proteins that are only expressed during productive infection of the viral target cell. The possibilities are enormous: immune modulators such as miRNA, immunostimulatory cytokines including the pro-apoptotic tumour necrosis factor (TNF), and even checkpoint inhibitor antibodies (Dias et al.,

2012; Hirvinen et al., 2015). To further their stimulation of the tumour-specific response, OV have also been engineered with pre-defined TAA or entire cDNA libraries (Kottke et al., 2011b; Pulido et al., 2012).

Some 'third-generation' OV, providing combination therapy within one agent, have already breached the clinical market. The most clinically successful agent to date is talimogene laherparepvec (T-VEC), a modified type-1 HSV construct. T-VEC bears the genetic deletion of *ICP34.5*, which minimises neurovirulence by limiting antagonism of PKR, and deletion of *ICP47*, which enhances antigen presentation to T cells via MHC. T-VEC is also armed with a human GM-CSF cassette in order to promote the anti-tumour activity of local APC, acting as an *in situ* tumour vaccine (Liu et al., 2003; Senzer et al., 2009).

Molecular engineering is indeed a powerful tool for the translational virotherapist. However, it would be wise to remember the inherent traits of OV that have brought the field to this point. The safety profiles of unmodified OV are truly remarkable, and represent a product of the prolonged co-existence of virus and host. Compared to this stable relationship, the introduction of a genetically modified agent offers risk. Even with extensive precautions, there remains the potential for rapid evolution or recombination, as well as unforeseen immune interactions (Lehrman, 1999), with engineered viral vectors. Even in the absence of modification, many viruses – reovirus included – display powerful natural oncolytic properties which have been essential to bringing the field to its current state. To paraphrase a popular 1990s hit – for oncolytic virologists, it is surely advisable to never forget where you've come here from.

#### **2.3.4 Mechanisms of OV activity**

The mechanisms by which OV generate anti-cancer effects *in vivo* remain far from comprehensively understood. In part, this is due to the sheer diversity of tumour types targeted and viruses used, plus our evolving ability to manipulate the viral genome to optimise its activity.

Historically, OV were considered therapeutic agents by virtue of their intrinsic ability to lyse infected cells; hence their 'oncolytic' tag. Changes to cellular morphology prior to and during lytic death underlie the characteristic cytopathic effect and monolayer destruction observed due to OV infection *in vitro*. The lytic potential of an OV in commandeering the cell as a virus factory is dependent primarily on entry, via cell surface receptors, and replication, via the viral replication machinery and its interface with host cell antiviral responses. Many viruses contain components which modulate the timing or execution of cell death; a well-understood example is the delay of apoptosis by adenovirus, vaccinia, and other viruses, to facilitate generation of viral progeny (Dobbelstein and Shenk, 1996; Han et al., 1996). The subsequently released viral load is able to infect neighbouring cells, a process ideally repeated in order to consume the whole tumour mass.

While the process of lysis or 'bursting' would appear likely to be indiscriminate and uniform among viruses, modes of OV-induced cell death are many and varied. Some OV stimulate the somewhat controlled process of apoptosis, and some trigger necroptosis, necrosis or autophagic cell death (reviewed in De Munck et al., 2017). Although one often predominates, the profound impact that OV have upon multiple aspects of cellular physiology means that they seldom inflict only one mode of death (reviewed in Guo et al., 2014). Every virus is different, and the type of death – if it occurs – is reliant on host, virus and cell type.

While progeny virus is ostensibly the main element released from an OV-infected cell upon death, a degree of the intracellular material is also exposed to nearby cells, by its ectopic display on the cell membrane or its egress into the extracellular milieu. As far as the immune system is concerned, the relevant components are cytokines, DAMP, PAMP, and TAA. In the 'classical', non-immunogenic version of apoptosis, cellular integrity is maintained, limiting the spread of these components. By contrast, in necrosis and pyroptosis this is commonly compromised, allowing DAMP, PAMP and TAA release.

Immunogenic modes of apoptosis also permit DAMP release and their exposure on the cell surface. Such characteristics have earned these three latter modes the collective term of *immunogenic cell death* (ICD). In the field of oncolytic

virotherapy, this terminology reflects a realisation that rather than being an end in itself, the death of virus-infected cells may be merely one step towards the ultimate clearance of a tumour.

OV are a particularly attractive modality for overturning the chronic immunosuppressive state found in the TME. During infection and OV-induced death, cells release a characteristic array of pro-inflammatory cytokines and chemokines – commonly TNF, CCL5/RANTES, IL-12, CCL3/4 (MIP-1 $\alpha/\beta$ ), numerous IFN molecules, and others – which can influence both innate and adaptive immunity. DAMP, typically heat-shock proteins (HSP), calreticulin, uric acid and ATP, also have this capacity. Specifically, these encourage the recruitment and maturation of APC, and consequently facilitate the activation and expansion of antigen-specific T cell clones. This process is aided by the release of antigens from dying cells, whether they be tumour-associated (TAA) or viral, both of which can prime T cells to elicit adaptive responses upon subsequent exposure in the context of infected, live tumour cells potentially expressing both types of antigen. Indeed, increases in both virus- and tumour antigen-specific T cells have been noted following virotherapy (Diaz et al., 2007; Li et al., 2017; Zamarin et al., 2014). Cytokine-activated T cells within the TME are also capable of eliminating uninfected or antigen-poor ‘bystander’ tumour cells via the release of cytolytic granules (Spiotto et al., 2004).

Alongside these effects on adaptive effectors, it should be noted that OV are potent stimulators of innate immunity. While DC are the prototypical APC, they also modulate innate cells, being able to communicate bidirectionally with and activate NK cells against tumour targets following reovirus infection (Errington et al., 2008a; Prestwich et al., 2009a). The capacity to stimulate NK-mediated tumour cell killing appears to be an attribute shared by a diverse range of OV (Bhat and Rommelaere, 2013; Ogbomo et al., 2013). This is supported by the broad ability of OV to trigger the influx of immune cells to tumour sites via PAMP and cytokines, contributing towards turning an immunologically ‘cold’ tumour ‘hot’ (Benencia et al., 2005; Diaz et al., 2007). Indeed, in the context of systemic GM-CSF administration, the efficacy of reovirus appears highly reliant upon two innate immune effectors: monocytes and NK cells (Ilett et al., 2014).

The process of replicative cell death formed the presumed mechanism of action for the clinical efficacy of OV and underpinned the rationale for their use. However, it emerged through the transition from cell culture assays to *in vivo* studies that the ‘oncolytic’ label is restrictive. The mechanism of action is not limited to OV replication, but includes – and in many cases may even be reliant on – engagement of the immune system and the initiation of a broader anti-tumour immune response. Hints that this is the case have emerged from the lack of efficacy observed in immunodeficient mice, when compared to immunocompetent animals (Kirn and Thorne, 2009; Miller and Fraser, 2000; Qiao et al., 2008b). The ability of OV to mediate regression of oncolysis-resistant tumour types *in vivo* provides further corroborative evidence (Prestwich et al., 2009b). Thus the contribution of the – particularly adaptive – immune response towards OV therapy was soon clear (Melcher et al., 2011; Prestwich et al., 2009b; Sobol et al., 2011).

The importance of the pro-inflammatory, ‘immune adjuvant’ activity of OV has since been proven throughout their collective clinical trajectory (Andtbacka et al., 2016; Ribas et al., 2017). This is encapsulated by the popularity of GM-CSF, itself an independent clinical agent (Lawson et al., 2010), as a viral transgene (Heo et al., 2013; Hu et al., 2006; Kanerva et al., 2013). Arming OV in this way aims to augment their intrinsic immunostimulatory ability. The position of the GM-CSF-expressing herpes virus T-VEC as the most advanced OV in the clinical arena supports the use of engineering to fine-tune our growing arsenal of viruses, and provides a validation of the OV as a true immunotherapy agent.

### **2.3.5 Clinical trials**

Driven by the momentum gained by the field after interest was revived in the 1990s, OV swiftly progressed into formal clinical testing. Not long after Martuza’s successful use of an oncolytic HSV-1 derivative against glioma xenografts, similar results were obtained with the recombinant adenovirus Onyx-015 (Heise et al., 1997) which subsequently entered phase I testing in 1996. The virus was administered to patients with recurrent, refractory

squamous cell carcinoma of the head and neck (HNSCC), with a single intratumoural bolus given as monotherapy (Ganly et al., 2000). With the highest dose tested of  $10^{11}$  plaque-forming units (pfu) being well tolerated, Onyx-015 progressed to phase II evaluation, showing modest anti-tumour activity as monotherapy and potentially synergistic efficacy when combined with cytotoxic chemotherapy as shown by a response rate of 65% (Khuri et al., 2000; Nemunaitis et al., 2001).

Development of Onyx-015 stalled when, for corporate reasons, its ongoing highly-anticipated phase III trial was abandoned: an unfortunate event that many – probably wrongly – interpreted as a failure of the agent itself (Jia and Kling, 2006). Yet the highly related adenovirus H101 was subsequently tested in a randomised phase III trial for nasopharyngeal carcinoma, alongside platinum-based chemotherapy. With the chemotherapy-alone arm yielding responses in 40% of patients, the combination of H101 plus chemotherapy generated a 79% response rate (Xia et al., 2004). This statistically significant improvement triggered the approval of H101 in this setting in China (Garber, 2006).

However, H101 was not the first virus to gain regulatory approval as a virotherapeutic for cancer. An unmodified ECHO virus termed Rigvir has held approval for the treatment of melanoma in Latvia since 2004, founded on dubious activity in the adjuvant setting for resectable disease (Doniņa et al., 2015). However, without a rigorous level of clinical trial evidence, Rigvir has not gained acceptance outside Eastern Europe. Until the recent emergence of T-VEC, global oncology markets have remained without access to a proven, established viral therapy for melanoma.

As for many immunotherapies, melanoma has represented a major clinical ‘testing ground’ for prospective OV. This is in part due to its status as an immunogenic tumour type, which in the more advanced stages has a particularly poor prognosis, leaving a pool of patients standing to gain substantially from a novel immunotherapy modality. Alongside carcinoma of the head and neck, primary cutaneous melanoma is also an anatomically accessible lesion. Tumour access is relevant in that, to date, the majority of OV in clinical testing have been administered directly into the tumour bed, rather than being given systemically. With early-phase trials in this new field being

focused on safety, the intratumoural injection route has proven attractive in aiming to limit adverse events. The relative merits of local and systemic therapy are the subject of ongoing scrutiny, as will be discussed later.

The major viral platforms under clinical investigation as oncolytic agents in melanoma are as follows. The double-stranded (ds)RNA reovirus type 3 Dearing and single-stranded (ss)RNA Coxsackievirus serotype A21 – marketed as Reolysin<sup>®</sup> and Cavatak<sup>®</sup> respectively – have both completed phase II trials in advanced melanoma (Andtbacka et al., 2015a; Galanis et al., 2012). These non-enveloped viral strains are unmodified, not generally being associated with major human disease, and represent the most clinically advanced wild-type OV candidates. Other well-known viruses that have required modification include OV derived from the dsDNA vaccinia virus by attenuation, such as JX-594 (Hwang et al., 2011). Similarly, the highly amenable nature of the adenoviral dsDNA genome has enabled a band of variously retargeted, armed and conditionally replicative oncolytic adenovirus constructs to reach human melanoma patients (Larson et al., 2015; Linette et al., 2013).

As a human pathogen, the dsDNA backbone of type 1 HSV is one that has been heavily re-engineered in the 25 years since the pivotal Martuza study. As described above, the removal of the TK gene has been superseded by more complex attenuation measures to avoid neurotoxicity, and the virus' natural immunogenicity augmented with stimulatory factors such as GM-CSF. HSV1716 (Seprehvir<sup>®</sup>), derived from the 17+ strain with a single attenuating deletion in *ICP34.5*, was one of the first wave of oncolytic HSV to show activity *in vitro*, and subsequently demonstrated safety and signs of efficacy in phase I melanoma trial (MacKie et al., 2001). The HF10 virus is derived from a different HSV-1 strain and is attenuated by disruption to the protein transport factor UL56; this too has more recently progressed from preclinical to clinical evaluation, first as monotherapy in phase I and then in combination with ipilimumab in phase II trial for melanoma (Andtbacka et al., 2017; Ferris et al., 2014).

Between the initial testing of HSV1716 and the recent emergence of HF10, one HSV construct has blazed a trail for OV through the clinical landscape. T-VEC is a JS1-derived virus with an attenuating deletion in *ICP34.5* and the

immunostimulatory deletion of *ICP47* and addition of human GM-CSF. Preclinical data indicated potent lytic efficacy against various cell lines, including melanoma, which successfully translated into efficacy *in vivo* when the virus was given intratumourally (Liu et al., 2003). T-VEC, then known as OncoVEX<sup>GM-CSF</sup>, therefore entered phase I testing, being administered to patients with various malignancies that were amenable to intralesional injection, including melanoma (Hu et al., 2006). A regimen in which a low dose of virus was administered prior to the larger therapeutic doses as a safety precaution was quickly adopted. T-VEC was well tolerated and, although no responses were generated according to standard response criteria, demonstrated signs of efficacy, including visible flattening of tumours and necrotic areas associated with virus by histology.

In 2005, T-VEC was thus taken forward into phase II trial in a cohort of 50 melanoma patients with either unresectable local disease or metastases at pre-specified sites (NCT00289016; Senzer et al., 2009). In this largely pre-treated population, the virus was given every three weeks and obtained an objective response rate (ORR) of 26%. Particularly promising was that 8 of 13 responders gained complete responses (CR), the majority being durable over time, and that efficacy was shown in both injected and non-injected (including visceral) lesions. 52% of patients were alive beyond 2 years, highly suggestive of a benefit to overall survival (OS).

With a good safety profile and a strong evidence of efficacy, the OPTiM phase III study (NCT00769704) opened in 2009. This trial recruited 436 treatment-naïve or pre-treated patients with stage IIIb-IV melanoma, who were randomised 2:1 to receive intratumoural T-VEC or subcutaneous GM-CSF. In this larger group, the virus was again well tolerated, with the most common high-grade toxicity being cellulitis in only 2.1% of patients. The trial successfully met its primary endpoint of durable response rate for T-VEC (16% vs 2%,  $p < 0.0001$ ), and similar to phase II, registered an ORR of 26% (CR 11%) versus 6% (CR 1%) (Andtbacka et al., 2015b; Andtbacka et al., 2016). Responses were noted in injected (64%) as well as non-injected (34%) and visceral (15%) lesions, suggestive of an abscopal effect sufficient to underpin a degree of

systemic anti-tumour immunity. Median OS in the T-VEC arm was 23.3 months, versus 18.9 months for GM-CSF ( $p = 0.051$ ).

Despite this statistical miss on extending OS, the first-in-class OV T-VEC was approved by the US Food and Drug Administration (FDA) for recurrent melanoma in 2015; a landmark regulatory milestone for the field (Greig, 2016). It was subsequently approved in Europe in 2016, after an exploratory sub-analysis of the earlier-stage III/IVM1a population demonstrated its superiority in overall (40.5% vs 2.3%) and durable (25.2% vs 1.2%) response rates, and OS (median 41.1 vs 21.5 months) (Harrington et al., 2016). A recent phase IIIb study confirms that the post-approval use of T-VEC outside of the clinical trial setting is safe, despite its extra challenges in handling and administration (Chesney et al., 2018; Harrington et al., 2017).

With the clinical performance of T-VEC noted, it is clear from the multitude of earlier-phase trials that, across indications, the ability of OV to induce tumour regression and prolong survival when used alone is limited. Response rates in metastatic melanoma are typically 25% at best, compared to approaching 40% for anti-PD-1 agents. Collectively however, OV safety profiles are very good, making them excellent candidates for combination therapy. Further, during preclinical development, various OV showed a propensity to synergise with other established modalities. Chemo-, radio- and targeted therapies can sensitise tumour cells to OV killing, via the upregulation of receptors and the enhancement of antigen presentation or apoptosis (Dai et al., 2014; Kaneno et al., 2011; Zurakowski and Wodarz, 2007). For instance, reovirus synergises with cytotoxic chemotherapy in melanoma and other tumour types (Heinemann et al., 2011; Pandha et al., 2009), both in murine models and potentially in cancer patients (Karapanagiotou et al., 2012). In a phase I/II trial for advanced HNSCC, 82% of patients obtained a response to the combination of T-VEC with chemoradiotherapy (Harrington et al., 2010a).

That OV can combine effectively with traditional modalities has been known for some time. The potential for OV to enhance the already impressive efficacy of checkpoint inhibitors is an altogether more exciting prospect. OV appear to have a shared capacity to promote lymphocyte infiltration into tumours and to liberate TAA; this suggests they are ideal agents to partner with checkpoint

inhibitors, which are incapable of reversing immune tolerance to tumours without the presence of lymphocytes and tumour-reactive antigens (reviewed in Robert, 2017; Tumei et al., 2014). The relatively novel use of dual checkpoint inhibitors in melanoma has resulted in unprecedented benefits in response rate and survival, but their overlapping toxicity profiles cause tolerability issues. In advanced melanoma patients receiving first-line nivolumab and ipilimumab, the majority experienced grade 3-4 toxicities (Larkin et al., 2015a) – surely an unpalatable rate for routine practice. By contrast, checkpoint inhibitors and OV are separate modalities with different modes of action, and thus far appear to be far better tolerated.

T-VEC is in trial with each of the three major checkpoint inhibitors to date. In the first of these, the combination of T-VEC plus ipilimumab recently reached its phase II primary endpoint in melanoma, more than doubling ORR (39% vs 18%) over ipilimumab alone without significantly increasing the incidence of severe toxicities (Chesney et al., 2017). Another phase II study, combining T-VEC with nivolumab in order to interrogate the OV's mechanism of action, has recently been opened (NCT02978625).

The third of these is MASTERKEY-265 (NCT02263508), a phase Ib/III trial of T-VEC plus pembrolizumab in treatment-naïve advanced melanoma patients. Results from the phase Ib part have recently been updated, showing a confirmed ORR of 62% and CR rate of 33% (Long et al., 2016; Ribas et al., 2017). These data compare favourably with the published ORR from phase III trials of pembrolizumab (42%) or T-VEC (26%) alone (Andtbacka et al., 2015b; Robert et al., 2017). It should however be noted that differences in the study populations prevent the direct comparison of these trials; in particular the fact that the combination trial involved injectable and therefore earlier-stage disease compared to the entire advanced melanoma population. Nevertheless, these measures of efficacy, allied with an associated IFN- $\gamma$  signature and T-cell infiltration, represent the most promising yet for the OV-checkpoint combination. If borne out in the phase III part, such data may enable it to threaten the existing combination regimen.

Even more encouragingly, it is not only T-VEC which is meriting inclusion in combination trials, but a wide variety of OV. Alongside ipilimumab, its cousin

HF10 has now demonstrated encouraging efficacy in a phase II patient group with even more advanced melanoma than in OPTiM (37% stage IV), extending median progression-free survival (PFS) to 22 months versus a landmark of 6 months with ipilimumab alone (Andtbacka et al., 2017). Although the field is increasingly comfortable with HSV-derived oncolytics, the candidates do not stop there. Adenovirus constructs are currently under investigation with nivolumab for carcinoma (Harb et al., 2016) and with pembrolizumab for melanoma (NCT03003676). JX-594 is being combined with ipilimumab in phase I testing across indications (NCT02977156).

In addition to these numerous re-engineered OV, a select few naturally occurring viruses are quietly progressing into similar trials. CVA21 is the first wild-type virus to do so, being combined with ipilimumab in a phase I trial for advanced melanoma (Curti et al., 2017). A virus on the brink of doing so is reovirus.

## 2.4 Reovirus

### 2.4.1 Background

The virus now generically known as reovirus was first isolated from an aboriginal Australian child in 1951. It was termed hepato-encephalomyelitis virus, on account of the symptoms elicited on its administration to mice (Stanley et al., 1953, 1954), and categorised as ECHO (enteric cytopathic human orphan) virus 10. This being a time of rapid change in virology, the virus was promptly renamed *reovirus* (respiratory enteric orphan) due to its host cell tropism and lack of association with human disease (Sabin, 1959; Stanley, 1961).

The isolate currently in testing as a cancer therapeutic is the serotype 3 Dearing strain of mammalian orthoreovirus, belonging to the *Orthoreovirus* genus, and to the *Reoviridae* family, which also includes the more well-known rotavirus. Each of the three serotypes of the mammalian orthoreovirus have a prototype strain: type 1 Lang, type 2 Jones, and type 3 Dearing (Ramos-Alvarez and Sabin, 1954). Reoviruses are found across kingdoms, having found hosts in mammals, fish, birds and plants. Among mammals, the mammalian reoviruses infect a broad spectrum of host species, and this promiscuity is thought to enable some infection events to be zoonotic (Lelli et al., 2016; Steyer et al., 2013).

Although there are discrepancies in its effects between human and murine systems, the pathogenesis of reovirus in newborn mice has made it a useful experimental model of virus-host interaction and spread. Following initial infection in the gut mucosa, the virus spreads via the bloodstream and lymphatic system to the central nervous system and other organs (Forrest and Dermody, 2003). In immunodeficient mice, reovirus infection leads to fatal myocarditis (Sherry et al., 1993).

Consistent with its taxonomy, reovirus type 3 Dearing (hereafter reovirus) is typically isolated from the human gastrointestinal and upper respiratory tracts, and is found in the faecal material of both healthy and symptomatic individuals

(Ramos-Alvarez and Sabin, 1954, 1958). Upon transmission by the faecal-oral route, natural infection first involves the attack of epithelial cells in the ileum, which can precipitate diarrhoea and vomiting. Similarly, infection of the respiratory tract can lead to symptoms of the common cold. However, in most individuals, reovirus infection is considered to proceed asymptotically, in line with its historical designation as an orphan virus. The deliberate intranasal inoculation of healthy volunteers with reovirus yielded symptoms in only a third (Rosen et al., 1963).

The literature does contain sporadic reports of severe pathology associated with reovirus infection, particularly in infants and the immunocompromised. Reovirus has been associated with conditions consistent with its main tissue tropism, such as gastroenteritis, acute respiratory disease and pneumonia (Chua et al., 2007; Steyer et al., 2013; Tillotson and Lerner, 1967), others such as encephalitis and meningitis which indicate its neurotropic ability (Ouattara et al., 2011; Tyler et al., 2004), and still others with a less apparent aetiology, including hepatitis and biliary atresia (Morecki et al., 1982; Richardson et al., 1994). For some, although causative roles for reovirus have not been exhaustively proven, corroborative evidence is provided by mouse studies (Wilson et al., 1994). Most recently, reovirus has been implicated in coeliac disease by promoting the  $T_H1$  response, an association that bodes well for the virus as an immunotherapy (Bouziat et al., 2017).

Reovirus is ubiquitous in the environment, particularly in stagnant water and raw sewage (Matsuura et al., 1988). A multitude of studies, spanning temporal and geographical boundaries, have been conducted into reovirus exposure, indicating that global seroprevalence for reovirus among adults is commonly above 50%, and typically closer to 100% (Lerner et al., 1962; Minuk et al., 1985, 1987; Pal and Agarwal, 1968; Selb and Weber, 1994; Stanley, 1974). At birth, passive immunity stands at around 75% and diminishes quickly in the first few years of life. Exposure in childhood is frequent, with around 50% of 5-year-olds seropositive (Leers and Rozee, 1966; Tai et al., 2005). Multiple peaks of seroprevalence have been observed throughout adulthood, indicative of re-infection (Berger and Brody, 1967).

Serum immunoglobulin G (IgG) is the major class of neutralising antibody, as corroborated by the transfer of maternal immunity; in line with mucosal exposure, IgA are also elicited, but decay more rapidly (Selb and Weber, 1994). The innate immune response to reovirus does not appear to be serotype-specific, as antiviral antibodies are cross-reactive between serotypes (Virgin and Tyler, 1991). However, unlike humoral responses, cell-mediated responses to type 1 Lang and type 3 Dearing vary qualitatively, indicating that they bear immunologically relevant structural differences. Due to the frequency of infection, it not yet clear whether cellular immunity confers protection across serotypes (Douville et al., 2008).

#### **2.4.2 Structure and replication**

The identification of the reovirus genome as a dsRNA structure was made in the 1960s, marking the first description of dsRNA in any biological system (Gomatos and Tamm, 1963). It is therefore a Group III virus, with the genome comprising 10 segments of dsRNA (Shatkin et al., 1968), which are classified as large (L1-3), medium (M1-3) or small (S1-4). These segments give rise to viral proteins respectively termed  $\lambda$ ,  $\mu$  and  $\sigma$ . The segmented RNA backbone makes reovirus relatively difficult to modify genetically, partly due to its lower genetic stability. Recently, a reverse genetics approach has made this possible (Mohamed et al., 2015), and small transgenes including reporter constructs have been inserted (Kemp et al., 2016; van den Wollenberg et al., 2015), suggesting that the oncoytic potency of reovirus could be enhanced in future.

The 10 gene segments of reovirus encode for 8 structural proteins –  $\lambda$ 1-3,  $\mu$ 1-2, and  $\sigma$ 1-3 – which contribute towards the structure of the mature virion, and the non-structural proteins  $\mu$ NS and  $\sigma$ NS, which facilitate the intracellular viral replication cycle (Chandran et al., 2001). The assembled virion is non-enveloped, 80 nm in diameter, and is formed of an icosahedral outer capsid and inner core. The three reovirus serotypes are defined by their antibody neutralisation and haemagglutination activity, and differ in their tropism *in vivo*. There is a high degree of genetic similarity between types 1-3, with approximately 90-98% of their identity being conserved (Gaillard and Joklik,

1982). The exception is in the highly type-specific S1 gene, encoding the  $\sigma$ 1 attachment protein in the outer capsid, which has undergone significant evolutionary divergence (Cashdollar et al., 1985).

It is via the  $\sigma$ 1 protein that reovirus is able to initiate the process of target cell entry. This process occurs over multiple steps, with the first being a low-affinity 'tethering' event between the carbohydrate-binding domain of  $\sigma$ 1 and cell-surface sialic acid (Barton et al., 2001a; Chappell et al., 2000). This use of surface carbohydrates, a trait shared by many viruses, is important for reovirus infection *in vivo* (Barton et al., 2003; Olofsson and Bergström, 2005).

Subsequently,  $\sigma$ 1 engages JAM-A, the canonical reovirus receptor from the immunoglobulin superfamily. This high-affinity interaction is also essential for viral spread *in vivo* (Antar et al., 2009; Barton et al., 2001b). The substantial effect on reovirus infectivity and oncolysis mediated by the mutation of  $\sigma$ 1 highlights its critical role in cell binding (Shmulevitz et al., 2012).

Following sialic acid tethering and JAM-A binding, reovirus gains entry to the cell interior by receptor-mediated endocytosis.  $\beta$ 1 integrins on the cell surface are subverted by the binding of the viral  $\lambda$ 2 protein, and trigger internalisation; this integrin-binding strategy appears to be highly conserved between reovirus and adenovirus (Stehle and Dermody, 2004). Within the endosome, the viral particle undergoes acid-dependent proteolysis and well-defined conformational changes. The entry intermediate, known as an intermediate (or infectious) subviral particle (ISVP), is characterised by the loss of the prominent outer capsid protein  $\sigma$ 3 and cleavage of  $\mu$ 1 (Ebert et al., 2002).

This proteolytic uncoating, principally by cathepsins, is critical for the eventual penetration of the endosomal membrane by  $\mu$ 1. Indeed, if reovirus uncoating occurs extracellularly, ISVP can gain entry independent of surface receptors (Borsa et al., 1979). It is considered that acid-dependent proteases in the respiratory tract and intestinal environment may facilitate epithelial infection through this mechanism (Bass et al., 1990; Golden and Schiff, 2005).

Immediately prior to endosomal escape, ISVP become ISVP\* as a result of conformational changes and autocleavage of  $\mu$ 1 into  $\mu$ 1N, triggering pore formation in the endocytic membrane (Chandran et al., 2002). This permits the

delivery of the transcriptionally active reovirus core, lacking  $\sigma 1$ , into the cytosol of the host cell (Nibert et al., 2005; Odegard et al., 2004).

Aside from the very earliest phase of transcription, which occurs while still an ISVP, the replication of the reovirus genome is entirely cytoplasmic. The core contains the transferases and the catalytic RNA-dependent RNA polymerase (RdRp, encoded by  $\lambda 3$ ) necessary to conduct RNA synthesis. Capped, positive-sense ssRNA is thus generated and serves both as mRNA for the translation of reovirus proteins, and also as the template for the regeneration of nascent dsRNA genomes by conservative replication (Li et al., 1980). Transcription and translation occur in cytoplasmic inclusions; viral 'factories', nucleated by non-structural proteins, which oversee the two processes (Fields et al., 1971; Kobayashi et al., 2006). The assortment and packaging of the segmented genome into individual virions is highly accurate and appears to occur concomitantly with RNA synthesis, by a presumably sophisticated yet largely undefined mechanism (Antczak and Joklik, 1992; McDonald and Patton, 2011). Although viral egress can be non-cytolytic in the absence of transformation, release of progeny virus is typically lytic, particularly in permissive, transformed cell lines (Connolly et al., 2001; Lai et al., 2013).

### **2.4.3 As an oncolytic agent**

The basis for the success of reovirus as an oncolytic agent has been the subject of decades of research, and at times, dispute. It began in the virology lab of Patrick Lee, with a series of discoveries that – as is so often the case – were serendipitous in their origin (Thagard, 2002). As part of an investigation into the role of cell-surface sialic acid in facilitating reovirus binding, an association was revealed between a cell's permissivity to reovirus and its epidermal growth factor receptor (EGFR) status (Strong et al., 1993; Tang et al., 1993). It emerged through transfection with the *v-erb* oncogene that the critical factor was not the receptor itself but the activation of downstream signal transduction cascades (Strong and Lee, 1996). Transfection of cells with constitutively active elements of the Ras pathway, a group of small GTP-binding

proteins regulating cell fate and growth, enabled it to be specifically implicated (Strong et al., 1998).

By showing that reovirus infection can be established by inhibiting the phosphorylation of the dsRNA sensor PKR, precluding its ability to inhibit protein synthesis, it was determined that Ras activation may promote susceptibility via PKR (Strong et al., 1998). The absence of PKR phosphorylation in Ras-transformed cells suggested that they, unlike wild-type cells, are unable to prevent viral replication by halting the formation of the translation initiation complex (de Haro et al., 1996). This is corroborated by reports finding no enhancement in viral attachment, entry, or initial transcription in Ras-transformed cells (Norman et al., 2004). Indeed, the dysregulation of PKR is implicated in malignant transformation, given it can function as a tumour suppressor by promoting the apoptosis of aberrant cells via IFN (Barber et al., 1995; Donzé et al., 1999). The reovirus  $\sigma 3$  protein is capable of stimulating translation by binding PKR directly, providing further evidence for its potential involvement in susceptibility (Yue and Shatkin, 1997).

Consequently, what started as a hunt for a reovirus receptor actually crystallised a link between corrupted intracellular signalling and reovirus activity. However, the potential impact of this series of studies in the context of cancer was only realised by Lee in 1995 (Thagard, 2002). This was nearly 20 years after the original link was made between reovirus and oncolysis, in the absence of a molecular basis. The ability of reovirus to exert cytotoxic effects on transformed cell lines, and the predisposition of cells to infection by transformation with the viral SV40 T antigen, was first reported in the 1970s (Duncan et al., 1978; Hashiro et al., 1977). Further, these findings were translated into *in vivo* models, with reovirus successfully generating anti-tumour responses against mouse lung tumours (Theiss et al., 1978).

Despite these early reports, it was only after the virologist Lee published his studies on the underlying mechanism that interest in reovirus as a cancer therapeutic began in earnest. In a pivotal 1998 paper, one intratumoural injection of the virus was found to induce responses in the majority of immunodeficient mice bearing human glioma xenografts, and efficacy was also shown in immunocompetent animals (Coffey, 1998). The link between reovirus

and cellular Ras status was strengthened by observations that tumour cell susceptibility could be influenced by modulating Ras and its downstream effectors using short-hairpin (sh)RNA or small-molecule inhibitors (Norman et al., 2004; Smakman et al., 2005).

Across cancer types, Ras mutations are highly prevalent – present in nearly 20% on average, with a range of 1-63% (Prior et al., 2012) – and this does not take into account activating mutations elsewhere in the Ras cascade. Consequently there would appear to be a strong rationale to underpin the oncolytic capacity of reovirus. This is relevant even in the non-malignant context, where it has been suggested that the basal level of Ras activity in the highly proliferative ileal epithelium may be sufficient to permit replication (Shmulevitz et al., 2005). Cellular permissivity to other viruses, such as HSV, is also influenced by activation in the Ras pathway, and specifically its effector MEK, which can directly suppress PKR (Farassati et al., 2001; Veerapong et al., 2007).

Although the Ras-PKR axis would appear to provide a neat explanation, the true molecular mediator of reovirus susceptibility has been the subject of debate. Doubt has been cast by the susceptibility of cells with wild-type Ras status, and the ability of a minority of tumour cells to survive virus treatment *in vitro* in spite of Ras transformation (Kim et al., 2007; Smakman et al., 2006). The absence of a correlation between total or phospho-PKR and either Ras expression or cell death contradicts previous studies (Song et al., 2009), and is corroborated by a lack of association between oncolysis and EGFR signalling (Twigger et al., 2012). Ras may therefore modulate susceptibility via other steps in the replication cycle, such as virion uncoating, infectivity of progeny, and induction of cell death (Shmulevitz et al., 2009).

The diverse effects of Ras transformation on multiple elements of cellular homeostasis and signalling – and therefore many aspects of the virus-cell interaction – have made this issue a complex one. There is a gathering acceptance that reovirus susceptibility is multifactorial: dependent on more than Ras status alone. It is also increasingly apparent that viral replication and cell death are not inextricably linked; Ras activation appears not to underlie replication but instead a sensitivity to apoptosis, and apoptosis can occur

independently of replication (Connolly et al., 2001; Smakman et al., 2005). Thus, a more careful examination of both replication and death appears essential to a precise judgement upon the true basis for the cancer-selective activity of reovirus.

Reovirus was originally considered to operate predominantly by apoptosis (reviewed in Clarke et al., 2005). The apoptotic signalling often displayed by infected cells includes the generation of IFN and acute activation of the NF- $\kappa$ B hub, either through detection of cytoplasmic dsRNA by PKR, RIG-I and MDA5, or of the  $\sigma$ 1 and  $\mu$ 1 proteins upon receptor engagement or membrane penetration (Connolly et al., 2001; Deb et al., 2001). A study in which cells were transfected with Fc receptors to enable antibody-bound reovirus to enter independently of JAM-A and sialic acid demonstrated that the canonical mode of entry is not key for apoptosis to occur (Danthi et al., 2006). In response to NF- $\kappa$ B and IRF3, inflammatory cytokines such as TRAIL are secreted, bind to surface death receptors, and trigger mitochondrial Smac/Bid signalling and pro-apoptotic activation of caspase-3 and -7 (Clarke et al., 2000; Kominsky et al., 2002). While IFN are potent promoters of cell death, it appears that IFN may be dispensable for reovirus-induced apoptosis, which may explain the ability of infected, IFN-deficient tumour cells to undergo apoptosis (Knowlton et al., 2012; Kominsky et al., 2002).

However, blockade of apoptotic caspases does not entirely abrogate reovirus-induced cell death *in vitro*, suggesting that other modes of cell death contribute (Berger and Danthi, 2013). In particular, necroptotic cell death has been observed in reovirus-infected cells. This does appear to be contingent on type I IFN, elicited not only by the exogenous dsRNA of the infecting virion, but also the subsequent wave of RNA synthesis within the cell (Berger et al., 2017). Additionally, like many viruses, reovirus is capable of triggering autophagy as a consequence of acute endoplasmic reticulum stress (Thirukkumaran et al., 2013). While certain types of cell death are broadly common between reovirus and other OV, it is increasingly apparent that the molecular intricacies within each mode can vary significantly, with novel OV-mediated subtypes of cell death now emerging (Weigert et al., 2017). Thus, as for any OV, both the

category of reovirus-induced death and its finer details are exquisitely linked to the phenotype of the target cell and the attributes of the incoming virus.

#### **2.4.4 Pre-clinical evidence**

Although the mechanism by which reovirus exerts cytotoxic effects has been the subject of some debate, the fact that it can reliably do so against malignant targets remains largely unquestioned. Following the observations of Hashiro, reovirus has demonstrated oncolytic activity in cells derived from the vast majority of the major solid tumour types *in vitro*, including lung, breast, ovarian, prostate, colorectal, pancreatic, glioma, melanoma, and head and neck carcinoma (Adair et al., 2013; Errington et al., 2008b; Hirasawa et al., 2002; Norman et al., 2002; Sei et al., 2009; Thirukkumaran et al., 2010; Twigger et al., 2012). Reovirus also shows promise in haematological models, such as multiple myeloma and both lymphoid and myeloid leukaemias (Hall et al., 2012; Parrish et al., 2015; Thirukkumaran et al., 2012). Of these, melanoma models have served as perhaps the most common testing ground.

Despite the evidence for the involvement of PKR dysfunction in cellular susceptibility to reovirus, in melanoma cells it does appear that PKR is functional in the detection of intracellular virus. Via the degradation of I- $\kappa$ B, autophosphorylated PKR is able to stimulate the NF- $\kappa$ B-mediated production of the inflammatory cytokines IL-1, -6 and -8, CCL3/4 (MIP-1 $\alpha/\beta$ ), CCL5/RANTES, and the chemokine CXCL10 (also known as IP-10) (Errington et al., 2008b; Steele et al., 2011). These cyto- and chemokines not only serve as chemoattractants for immune cells, but also stimulate the priming ability of DC and bystander killing by lytic NK cells *in vitro*. APC such as DC are also activated by direct infection with reovirus via PRR, whereupon they mature and secrete soluble factors which elicit innate tumour cell killing by both NK and T cells. This is corroborated by the anti-tumour activity shown by human PBMC cultured with reovirus (Errington et al., 2008a; Prestwich et al., 2008a). The innate immune killing by NK cells in the context of PBMC is highly reliant on type I IFN, secreted principally by DC and CD14<sup>+</sup> monocytes in response to virus (Adair et al., 2013; Parrish et al., 2015).

When first used as a cancer therapeutic *in vivo*, reovirus was delivered directly into tumour lesions (Coffey, 1998). Reovirus administered by the intratumoural (i.t.) route is able to induce the regression of established subcutaneous B16 melanoma tumours, and significantly extends survival in immunocompetent mice (Qiao et al., 2008a). The virus primes a tumour-specific T<sub>H</sub>1 response mediated by CD8<sup>+</sup> T cells (Prestwich et al., 2008a), which along with NK cells mediates anti-tumour activity (Rajani et al., 2016). The therapeutic outcome to i.t. reovirus is also influenced by other arms of T cell immunity. Locally administered reovirus can also promote the accumulation of T<sub>reg</sub> to the detriment of therapy (Clements et al., 2015; Rajani et al., 2016). The induction of a melanoma-specific T<sub>H</sub>17 response, in a dual-OV 'prime-boost' regimen, augments existing T<sub>H</sub>1 responses to i.t. reovirus (Ilett et al., 2017).

As part of a strategy aiming to treat inaccessible and metastatic cancer deposits, the systemic delivery of reovirus has been investigated. In the context of intravenously (i.v.)-administered reovirus, the contribution of immune cells to efficacy is even more critical. Indeed, although administered reovirus gains access to tumours, its ability to purge reovirus-resistant B16ova tumour cells *in vitro* and *in vivo* – but not in immunodeficient animals – demonstrates that, unlike immune-mediated killing, oncolysis is not essential for therapy (Prestwich et al., 2009b). Given alone, the impact of i.v. reovirus upon tumour growth is often somewhat limited in comparison to i.t. injection. As this has long been associated with the generation of antiviral antibodies in circulation, i.v. reovirus has been combined with cyclophosphamide with a view to maximising the virus titre reaching tumour beds (Qiao et al., 2008b). While this approach was associated with elevated systemic toxicity, some enhancement of reovirus efficacy against subcutaneous B16 melanoma was observed.

In the past, systemic reovirus has been co-administered with a variety of agents in pre-clinical models, such as chemotherapy compounds and inhibitors of angiogenesis (Kottke et al., 2010, 2011a). More recently, the virus has been combined successfully with immunostimulatory agents, in order to capitalise upon its inherent traits as an immune adjuvant. As will be discussed later, based on the carriage of virus by circulating lymphocytes, i.v. reovirus therapy has been potentiated by pre-conditioning the host with GM-CSF, to expand

immune effector populations (Ilett et al., 2014). The efficacy of GM-CSF/reovirus is reliant on innate populations: monocytes and NK cells. Most recently, i.v. reovirus has shown promising efficacy in combination with checkpoint inhibitors. Murine models of myeloma, glioma and melanoma suggest that the two modalities operate by complementary mechanisms, and together induce highly durable tumour responses (Ilett et al., 2017; Kelly et al., 2018; Samson et al., 2018).

#### **2.4.5 Clinical trials**

Reovirus type 3 Dearing is the subject of one of the largest clinical trial programmes in oncolytic virotherapy. Aside from CVA21, it is the only unmodified virus in late-phase clinical development, being the first to reach phase III trial, and its clinical grade formulation is marketed as Reolysin® (generic name pelareorep) by Oncolytics Biotech (Calgary, Canada). The virus is listed in 22 trials identified on *clinicaltrials.gov*, although the number is believed to be over 30 based on additional others not listed. As of 2018, reovirus holds orphan drug status from the FDA for glioma, ovarian, pancreatic, peritoneal and gastric cancers, and from the EMA for ovarian and pancreatic cancer.

The first-in-man phase I study of reovirus as a cancer therapy, REO-001, enrolled 19 patients with accessible, advanced malignancies, who were treated intralesionally with ascending doses of the virus. No dose-limiting toxicities were observed, all being grade 2 or below, with the most common being nausea, headache or vomiting in 50-80% of patients (Morris et al., 2013). Tumour responses were also apparent in 37%. Based on this, and its promising safety profile in animal models, reovirus progressed quickly into trials of systemic treatment. Intravenous delivery was first tested in REO-004, in which 18 patients with advanced solid tumours received virus doses of up to  $3 \times 10^{10}$  TCID<sub>50</sub> without identifying a maximum tolerated dose, or dose-limiting toxicity. In fact, only two patients experienced grade 2 events, even when multiple doses were given on successive days (Gollamudi et al., 2010). When corroborated by other phase I trials (Vidal et al., 2008; White et al., 2008), these results

demonstrated that, when delivered by infusion as a very large, non-physiological bolus, the unmodified reovirus is remarkably well tolerated.

Reovirus has now undergone further evaluation in phase I and II clinical trials across a range of indications. Historically, the tumours most heavily targeted within the reovirus programme have been melanoma, myeloma and glioma (Forsyth et al., 2008; Galanis et al., 2012; Sborov et al., 2014), although trials have also taken place in pancreatic, lung, breast, colorectal, prostate, and head and neck cancers (Bernstein et al., 2017; Karnad et al., 2011; Noonan et al., 2016; Ocean et al., 2013; Samson et al., 2018; Villalona-Calero et al., 2016). Initial trials deployed reovirus as a monotherapy, with the majority of these by i.v. administration. With safety largely established in the almost total absence of serious adverse events (Gong et al., 2016), a small number of phase II trials were conducted, with equivocal outcomes.

In REO-014, 52 patients with sarcoma lung metastases were treated i.v. with five daily doses of  $3 \times 10^{10}$  TCID<sub>50</sub> reovirus every four weeks. Depending on the data source, disease control was achieved in 34-43% of patients, and in some for as long as 22 months (Gong et al., 2016; Mita et al., 2009). The first phase II study of reovirus in melanoma employed the same dosing schedule. None of the 21 patients registered responses by pre-defined criteria, precluding a positive conclusion or expansion of the trial. 29% of patients did however exhibit stabilisation of disease, and reovirus was detected in 2/13 metastasis biopsies, with one patient experiencing extensive necrosis in two lesions (Galanis et al., 2012). The low degree of efficacy may have been linked to the paucity of BRAF mutations in the trial cohort (2 of 13 tested), and the presence of prior systemic therapy in the vast majority.

As a result of the generally disappointing outcomes from such phase II trials, the virus is no longer under active investigation as a monotherapy. No monotherapy trials of reovirus are currently open on [clinicaltrials.gov](http://clinicaltrials.gov), and Oncolytics Biotech is instead developing the virus along three combination programmes ([www.oncolyticsbiotech.com](http://www.oncolyticsbiotech.com)). Indeed, reovirus has been combined with a wide variety of agents over the past decade. Based on its ability to synergise with ionising radiation in culture and in murine models (Twigger et al., 2008), the combination of reovirus with radiotherapy has been

tested further, demonstrating tolerability in phase I and a promising disease control rate of 93% in a small phase II trial (Harrington et al., 2010b; Saunders et al., 2009).

By far the more extensive line of enquiry has been the combination of reovirus with standard chemotherapy agents, including platinum-based compounds, taxanes, gemcitabine and cyclophosphamide. Similar to the effects observed with radiotherapy, reovirus readily synergises with chemotherapy *in vitro* and in murine models of melanoma and prostate cancer (Heinemann et al., 2011; Pandha et al., 2009). Minimal exacerbation of the side effects of chemotherapy was noted in phase I combination testing (Comins et al., 2010; Karapanagiotou et al., 2012; Lolkema et al., 2011). The addition of reovirus to dual paclitaxel/carboplatin (P/C) chemotherapy has been the most heavily studied combination. In REO-020, reovirus plus P/C provided signs of efficacy in melanoma, with responses observed in 21% (Mahalingam et al., 2017a). Two phase II trials for non-small cell lung cancer have tested this combination, identifying objective responses in 48% of patients with squamous cell carcinomas (Mita et al., 2013) and 31% of patients with Ras-activated carcinomas (Villalona-Calero et al., 2016) in REO-021 and REO-016 respectively. Allied with a median OS of 13.1 months, this compares favourably to a historical rate of approximately 20% with P/C alone (O'Byrne et al., 2011). The inclusion of randomised control groups in these trials would have enabled a formal comparison to be made.

A subsequent, larger phase II trial of reovirus plus pemetrexed or docetaxel in lung cancer (IND-211) did include comparator arms, and although exploratory analyses hinted at potential benefit for patients with mutations in EGFR or p53, the addition of reovirus failed to improve PFS or OS (Morris et al., 2016). Similarly, the addition of reovirus to paclitaxel failed to improve therapy in gynaecological cancer patients (Cohn et al., 2017). Thus, even in combination, the results of efficacy-based trials with reovirus have not been universally positive. The only phase III trial conducted to date, REO-018, was a randomised, double-blind trial of P/C with or without reovirus in HNSCC. The virus was given by i.v. infusion at a dose of  $3 \times 10^{10}$  TCID<sub>50</sub> on days 1-5 every four weeks, alongside standard-of-care P/C. As reported on the Oncolytics

Biotech website (but not published), the interim trial results were positive: in 118 evaluable patients with locoregional disease, reovirus extended median PFS from 48 to 95 days, and significantly enhanced OS, using censoring for subsequent therapies. In fact, the study was curtailed, converted from a phase III to a large phase II trial, and no analysis of the pre-defined endpoints published, leaving the results unconvincing.

These mixed results have made the therapeutic potential of reovirus a topic of debate. It is accurate to state that i.v. reovirus has often shown very modest activity, particularly as monotherapy (Galanis et al., 2012). However, it has also demonstrated promising efficacy, sometimes in much the same patient population, and reliably gains access to tumour lesions when given systemically (Adair et al., 2012; Samson et al., 2018). It is important to note that, like many immunotherapies, reovirus shows potential to extend overall survival in the presence of limited PFS benefit; this phenomenon has been observed in IND-213, a recent phase II trial involving combination with paclitaxel in metastatic breast cancer, which will likely spawn the next phase III study (Bernstein et al., 2017).

With the virtues of chemotherapy combinations accepted, it is trials adding reovirus (and its fellow OV) to other immunotherapies that appear destined for the most success. Somewhat similar to T-VEC, combining reovirus with anti-PD-1 inhibitors elicits powerful anti-tumour responses in animal models (Rajani et al., 2016; Samson et al., 2018) and is currently under investigation for pancreatic cancer in the REO-024 trial (Mahalingam et al., 2017b). Another trial with translational support that has been planned, REO Melanoma GM-CSF (NCT03282188), is designed to mobilise not only cellular effectors but also humoral immunity in the cause of tumour clearance. It is surely by innovating, and maximising our ability to harness the immune system, that the best outcomes for patients will be found.

## 2.5 Oncolytic viruses and the immune system

### 2.5.1 The delivery conundrum

Outside the therapeutic setting, a natural viral infection typically involves small-scale virus exposure, either by venous puncture or (as for reovirus) contact at the mucous membranes of the gut and respiratory tract. The administration of a large OV bolus differs primarily in scale – the number of virus particles involved – but also in the compartments exposed to virus, meaning that virotherapy must operate under a very different set of pharmacokinetic considerations. It is currently unclear how best to administer an OV to obtain the optimal therapeutic response while prioritising patient safety. The route designed to maximise efficacy based on the historical rationale in which oncolysis is paramount may vary from that designed to facilitate immune-mediated tumour clearance.

The only robustly approved OV as of 2018, T-VEC and to a lesser extent H101, are administered by direct injection into the lesion (i.t.). Intuitively, delivery of virus directly into tumour beds would appear to be the most capable of maximising virus titre in tumour tissue, while circumventing off-target toxicity in normal cells. It does not appear that i.t. T-VEC injection leads to substantial viraemia, although it remains possible that a delayed viraemia may occur secondary to explosive amplification within the tumour (Ott and Hodi, 2016). OV administered i.t., including T-VEC and JX-594, can elicit regression of non-injected lesions in the absence of viraemia, indicative of abscopal effects mediated by the immune system (Andtbacka et al., 2016; Park et al., 2008).

However, the degree of systemic anti-tumour immunity generated by i.t. OV may be sub-maximal. Responses to T-VEC were observed in 15% of visceral metastases, compared to 64% of injected lesions (Andtbacka et al., 2015b). Further, and perhaps more important, the use of i.t. administration immediately restricts the range of tumour types and anatomical sites that can be targeted to those that are readily accessible through the skin, or can be safely targeted using ultrasound guidance (Chang et al., 2012). A range of other administration routes have been tested for OV delivery: ovarian cancer has been targeted with

intraperitoneal measles virus (Galanis et al., 2010), mesothelioma by intrapleural HSV1716 (Danson et al., 2017), and bladder cancer by intravesical adenovirus (Burke et al., 2012). Although they may prove marginally more practical than i.t. delivery, these modes of administration are utilised against local or regionally disseminated disease, limited to specific cancer types, and are anatomy-dependent.

Compared to local delivery, the systemic administration of virus into the bloodstream would appear to have the greatest potential to access disseminated tumour cells within the vascular system or distant organs. This is of clinical importance given that metastasis is estimated to be the cause of 90% of cancer-related deaths (Mehlen and Puisieux, 2006). Oral intake, by far the most commonly used and convenient route of systemic drug administration, appears the least suited to OV therapy given the need for virus to gain tumour access, and the ability of the gastrointestinal system to inactivate virus.

Vascular injection is therefore the preferred method of systemic delivery, being only mildly more impractical and invasive than taking a pill, and far less so than most locoregional administration routes which demand significant clinical support.

An exploration of the course taken by an i.v.-administered OV reveals the numerous anatomical challenges required for the virus to persist and generate therapy. Once dumped in the bloodstream, the OV bolus is immediately diluted. Complement and any antiviral antibodies rapidly opsonise the virus, while the virus also interacts with the cellular components of blood. Virions that remain free must evade the reticulo-endothelial system in the liver and spleen. To access tumour cells outside the vasculature, free or cell-associated virus must take advantage of the high permeability of tumour capillaries (Fang et al., 2011) to extravasate, and subsequently negotiate the aberrant tumour matrix to reach its target population. Therefore circulatory pharmacokinetics, virus clearance, and practical barriers to viral egress must all be considered. Tailoring the dosing and scheduling of i.v. delivery over time has allowed us to maximise circulating levels of virus and mitigate against the occasionally significant flu-like side effects (Calvo et al., 2014; Small et al., 2006).

Critically, recent translational studies reliably demonstrate that the nucleic acid and proteins of OV (such as reovirus) can be identified in patient tumour samples after i.v. administration (Adair et al., 2012; Samson et al., 2018), and that systemic therapy is capable of generating the long-lasting remission of widespread disease (Russell et al., 2014).

### **2.5.2 Anti-tumour or antiviral immunity?**

The viraemic state established immediately after i.v. delivery allows an OV to provoke inflammatory effects upon cells in peripheral blood. These agents are immune adjuvants; recognition of viral motifs by PRR engages functional antiviral signalling within immune cells, characterised by IRF3/7 and NF- $\kappa$ B activation and synthesis of pro-inflammatory cytokines and IFN, which are consistently upregulated in the serum of reovirus-treated patients (Samson et al., 2018; White et al., 2008). These soluble factors are known for their ability to promote the maturation of APC, and the activation of NK and T cells, as evidenced by the upregulation of CD69 on patient NK cells (El-Sherbiny et al., 2015).

These initial inflammatory processes are classical innate responses to a viral pathogen, and in the absence of a subsequent adaptive component are not inherently classified as 'anti-tumour' or 'antiviral'. They become so as a result of adaptive events. This is particularly well demonstrated in the humoral response to virus, characterised by massive production of virus-binding immunoglobulins. The key event is the recognition of virus-specific epitopes by immature B lymphocytes, triggering their maturation into antibody-secreting plasma cells. The process is reinforced by activated helper T cell signalling (Mari et al., 2013) and the direct influence of type I IFN (Braun et al., 2002), both of which are induced by virus. The corresponding process on the side of cellular immunity is the generation of virus-specific CTL, designed to identify and kill infected cells.

While such 'antiviral' responses are evolutionarily designed as strategies to combat the invading pathogen alone, it is increasingly clear that they are fundamental to the efficacy of OV because of their overlap with 'anti-tumour' processes. The activation and recruitment of immune cells out of the

vasculature is normally involved in the resolution of infection in the lymphatic system. Lymphocyte extravasation is also routinely observed following administration of OV (Ribas et al., 2017). In a recent phase I study of i.v. reovirus, 48-72 hours after infusion there was an increase in transcripts of the pro-recruitment chemokines CCL3/4 (MIP-1 $\alpha/\beta$ ) in tumour RNA, and in the expression of the adhesion molecule ICAM-1 by T cells (Samson et al., 2018). Along with CD68<sup>+</sup> myeloid cells, tumours of reovirus-treated versus control patients appeared to contain a higher number of CD8<sup>+</sup> T cells, whose presence is strongly associated with superior outcomes (Gooden et al., 2011). Collectively the evidence suggests that, as immune adjuvants, OV promote leukocyte infiltration into tumours and thus support tumour immune surveillance. Immune responses to virus that have anti-tumour effects are also elicited by OV within the tumour itself. For instance, it is not just cytotoxic T cells reactive to tumour antigen (liberated by oncolysis) that may kill other tumour cells. CD8<sup>+</sup> T cells specific for virus antigen may also be able to recognise and kill infected cells that express such antigens, even before oncolysis can take place. Similarly, the recognition of virus-infected tumour cells by CD4<sup>+</sup> T cells promotes their activation of DC by secretion of IFN- $\gamma$ , or of CD8<sup>+</sup> T cells via secretion of IL-2 or ligation of CD40. As both malignant transformation and viral infection promote downregulation of MHC molecules, an OV-infected tumour cell may have sufficiently low MHC-I to evade T cell recognition and killing. However, as a result, this increases the risk of NK cell-mediated cytolysis. Consequently, even if an OV does not itself induce cell death, it may subvert antiviral responses to deliver anti-tumour effects.

Compared to the cell-mediated response to OV, humoral immunity would appear less well suited to being harnessed against a tumour. Because of the size of the typical therapeutic OV infusion ( $10^9$ - $10^{10}$  pfu), B cell mobilisation and antibody production occurs rapidly and on an enormous scale. From a not-insubstantial baseline, anti-reovirus antibody titre following infusion commonly increases ~1,000-fold (Adair et al., 2012). Antibody generation is greater in response to i.v. than i.t. injection, and is dose-dependent (White et al., 2008). In the context of natural reovirus infection, systemic antibody generation is fundamentally protective (Sherry et al., 1993). Virus clearance is normal in mice

lacking CD8<sup>+</sup> T cells, but is significantly delayed in B cell-deficient mice (Barkon et al., 1996). Protection is predominantly attributed to the ability of neutralising antibodies (NAb), mainly IgG, to impair viral binding and entry into target cells.

### 2.5.3 Modulation of antiviral immunity

Correspondingly, in the context of virotherapy, there is evidence from studies using reovirus (Qiao et al., 2008b) and other OV (Chen et al., 2000; Tsai et al., 2004) that circulating antiviral antibodies can impair viral persistence and spread to tumours. This is relevant even for seronegative individuals as, unless therapy can be obtained by a 'one-shot cure' (Russell et al., 2014), NAb arise prior to subsequent cycles of OV. Regardless, most individuals are seropositive for reovirus, making NAb an unavoidable factor in i.v. therapy.

Consequently, with the view that NAb are universally detrimental to OV, various strategies have been adopted to suppress the influence of antiviral immunity. Perhaps the simplest is the use of animal pathogens such as Newcastle disease virus (NDV) and vesicular stomatitis virus (VSV), which combine the ability to replicate in human tumour cells with low seroprevalence. The use of multiple virus serotypes or even entirely different viruses should in theory allow the virus delivered second to evade the antibody response to the first. This approach is particularly applicable to adenovirus, given that over 50 serotypes that infect humans are available (Bangari and Mittal, 2006). As measles virus only has one serotype, a variation on the 'serotype switching' strategy has been devised by creating chimaeric viruses with mutated or homotypic envelope glycoproteins, which permit evasion of NAb (Lech et al., 2014; Miest et al., 2011).

For reovirus, the range of NAb evasion strategies is more limited. Within the mammalian *Orthoreoviridae*, only three distinct serotypes exist, and NAb appear cross-reactive between the three (Virgin and Tyler, 1991). Interestingly, the possibility of using avian reoviruses as OV has recently been raised as a solution (Kozak et al., 2017). Similarly, although mutations in surface proteins can be made (Shmulevitz et al., 2012), the limited pliability of the reovirus

genome has largely prevented the generation of variants capable of evading antibody detection.

As a result, efforts to circumvent humoral immunity in aid of reovirus have centred around the use of immunosuppressive chemotherapy, particularly cyclophosphamide (CPA). CPA is an alkylating agent which at low doses can deplete  $T_{reg}$  and at higher doses can kill or profoundly suppress the effector functions of all lymphocytes, including the production of antibody by B cells (Hurd and Giuliano, 1975; Varkila and Hurme, 1983). In preclinical models, CPA successfully curtails the antibody response and facilitates the persistence and delivery of OV including reovirus, measles virus and HSV (Ikeda et al., 1999; Peng et al., 2013; Qiao et al., 2008b). CPA and other chemotherapy agents have been used alongside i.v. reovirus in clinical trials; some focusing on the antineoplastic effects of both (Comins et al., 2010), and others explicitly using chemotherapy as a modulator of anti-OV NAb. These trials were able to show attenuation of anti-reovirus NAb by chemotherapy (Karapanagiotou et al., 2012; Lolkema et al., 2011), with the exception of one phase I trial employing CPA as a bolus (Roulstone et al., 2015).

It is difficult to draw solid conclusions from these trials as to the potential therapeutic benefit of NAb suppression for reovirus therapy, due to their small scale and lack of comparator groups, and the fact that chemotherapy may contribute to anti-tumour efficacy aside from its effect on NAb levels. In fact, across OV, pre-clinical and clinical evidence that circulating NAb entirely precludes viral efficacy is weak. After i.v. infusion of adenovirus, which also has a high seropositivity rate, tumour antigen-specific immune responses were generated regardless of patient NAb status (Morse et al., 2013). Similarly, the efficacy of oncolytic HSV is not lost in NAb-bearing animals, and NAb titre does not appear to predict response in patients (Markert et al., 2014).

Early pre-clinical studies of the *in vivo* potential of reovirus indicated no difference in tumour regression between reovirus-naïve and -immune mice (Coffey, 1998). Indeed, the enhancement of reovirus therapy by chemotherapy in murine melanoma was shown to be independent of NAb titre (Pandha et al., 2009). In patients, reovirus persists in the bloodstream of seropositive individuals after i.v. infusion, often in association with immune cells (Adair et al.,

2012; Roulstone et al., 2015). Moreover, in spite of NAb, reovirus gains access to tumour beds. In the recent REO-013 Brain trial, after a single viral infusion, evidence of reovirus was found in 6 of 9 brain tumours by IHC and 9 of 9 tumours by electron microscopy (Samson et al., 2018). In its predecessor REO-013, reovirus protein was found in 9 of 10 colorectal liver metastases by IHC (Adair et al., 2012). In REO-020, it was in patients exhibiting some of the highest NAb titres that reovirus was successfully detected (Galanis et al., 2012). Thus it would seem that the elimination of circulating NAb is not essential for effective viral delivery. NAb also play an important role in controlling toxicity. In mice with NAb ablated by CPA, reovirus replication in the heart and other organs results in lethality, mirroring observations in B cell-deficient mice (Qiao et al., 2008b). Although not severe, the identification of occasional hepatic and cardiac toxicities in trials combining reovirus with chemotherapy emphasise the importance of NAb in systemic virotherapy (Lolkema et al., 2011). It is also important to note that immunosuppressive agents such as CPA dampen cell-mediated immunity (Varkila and Hurme, 1983), and may therefore compromise the development of anti-tumour immunity which is critical to long-term therapeutic benefit (Prestwich et al., 2009b).

#### **2.5.4 The monocyte as a Trojan horse**

Of the cell types in peripheral blood, the monocyte population is key in the context of viral infection. Monocytes represent a cell subset that originate from myeloid precursors in the bone marrow during haematopoiesis (Hettinger et al., 2013). They enter the bloodstream where they comprise roughly 10% of the nucleated cells, and undergo constant turnover, with a short half-life of 1-5 days (Haller Hasskamp et al., 2005). Three sub-populations have recently been defined, based on expression of the lipopolysaccharide receptor and classical monocyte marker CD14, and the Fc receptor CD16 / FcγR III (Wong et al., 2011). Along with CD14 itself which is activated by bacterial motifs, monocytes express a variety of PRR, including RLR and a number of TLR, consistent with their remit as mediators of innate pathogen surveillance. Circulating monocytes act as a reservoir: upon receiving the appropriate (often inflammatory) signals,

they begin the process of differentiation towards the myeloid-derived DC or macrophage lineage, and extravasate in order to traffic to lymph nodes (typically DC) or to become tissue-resident macrophages. Broadly, while the macrophage is characterised by its phagocytic capacity and the DC by antigen presentation, their precursor monocyte retains both abilities (Cros et al., 2010; Kim and Braciale, 2009).

Among human PBMC, the monocyte is the primary cell type targeted by many viruses, both oncolytic and otherwise (Esolen et al., 1993; Hou et al., 2012; Kou et al., 2008). *Ex vivo*, adenovirus associates rapidly with blood monocytes (Lyons et al., 2006). Using a representative panel including VSV, influenza and vaccinia viruses, between 50-100% of monocytes were infected *in vitro*, versus 0-25% in all other major PBMC subsets (Hou et al., 2012). In this study, viral infection of monocytes provided a potent stimulus for differentiation to DC, which were then able to prime an antiviral T cell response. VSV exerts similar phenotypic effects (Tomczyk et al., 2018). Thus it has been proposed that the readily infectable nature of the myeloid phagocytes in blood represents an evolutionary strategy, in that by allowing cellular entry and often abortive or limited viral replication, they promote inflammatory signalling and differentiation that actually facilitates the immune response (Yewdell and Brooke, 2012).

Evidence suggests that the interaction between human blood monocytes and reovirus may be similarly dynamic. Monocytes are major producers of IFN- $\alpha$  on recognition of viral motifs, as evidenced by their vigorous response to the dsRNA analogue poly(I:C) (Hansmann et al., 2008). A significant elevation in IFN- $\alpha$  is observed in patient serum obtained two days after a single i.v. infusion of reovirus (Samson et al., 2018). Further, reovirus-induced monocyte production of IFN- $\alpha$  is vital in driving killing of tumour cell targets by patient-derived NK cells (Adair et al., 2013; El-Sherbiny et al., 2015; Parrish et al., 2015). However, in mice, i.v. administration of reovirus has also been implicated in the accumulation of suppressive myeloid cells in tumours, suggesting that the interaction of the myeloid compartment as a whole may be more complex than anticipated (Clements et al., 2015).

Like other cells of the innate immune system, monocytes are endowed with Fc receptors – proteins typically at the cell surface which, among other functions,

enable their interaction with and response to opsonised pathogens. Fc receptors bind to the Fc domain of their corresponding immunoglobulin subclasses: Fc $\alpha$ R for IgA, Fc $\epsilon$ R for IgE, and multiple Fc $\gamma$ R for IgG. In doing so, Fc receptors link humoral and cellular immunity, by enabling cells to respond to antibody-tagged material. For instance, the degranulation of mast cells and basophils in the allergic response is mediated by the ligation of Fc $\epsilon$ R by IgE-opsonised allergen (Rivera et al., 2008). Specific Fc $\gamma$ R isoforms allow NK cells to recognise IgG-opsonised cells prior to killing by ADCC (Srivastava et al., 2013).

There are multiple Fc $\gamma$ R isoforms in humans, encoded by *FCGR1* (CD64, Fc $\gamma$ R I), *FCGR2A-C* (CD32, Fc $\gamma$ R IIa-c) and *FCGR3A/B* (CD16, Fc $\gamma$ R IIIa-b) respectively (Guilliams et al., 2014). The neonatal Fc receptor (FcRn) is an additional molecule responsible for recycling IgG. Most Fc $\gamma$ R have activatory functions, such as the NK cell-expressed Fc $\gamma$ R IIIa, while the Fc $\gamma$ R IIb present on B cells and most other leukocytes acts as an important inhibitory checkpoint (Nimmerjahn and Ravetch, 2008). Fc $\gamma$ R signalling is triggered by their spatial clustering upon binding of aggregated IgG, which signals opsonised material or 'immune complexes'; the exception being Fc $\gamma$ R I, whose higher binding affinity allows it to be stimulated by monomeric IgG. Activating motifs in the Fc $\gamma$ R-associated  $\gamma$ -chain instigate intracellular phosphorylation cascades, and these elicit effector functions which are cell type-specific. The response of myeloid cells is characterised by inflammatory cytokine release and phagocytosis of the immune complex, ostensibly leading to its degradation and the presentation of antigen (Amigorena and Bonnerot, 1999).

This same process designed to facilitate pathogen clearance is simultaneously implicated in a phenomenon that promotes virus persistence, termed *antibody-dependent enhancement* (ADE). Viewed from a viral perspective, if it can evade subsequent degradation, antibody binding and uptake via Fc receptors (or complement receptors) theoretically provides an increased number of host cells in which to propagate. The ability of monocytes to permit ADE was first identified in the context of dengue virus infection, which has become a prototypical example. During acute dengue infection either *ex vivo* or in the *in vivo* scenario, human monocytes are principal viral targets and display an

activated phenotype (Durbin et al., 2008; Kou et al., 2008). The presence of anti-dengue antibodies at a defined titre actively promotes the infection of monocytes, which amplify the virus and precipitate more severe disease (Sun et al., 2011; Tsai et al., 2014). Recently FcγR IIIa (*FCGR3A*) was specifically identified as the causative Fc receptor (Wang et al., 2017). Far from being an *in vitro* process, epidemiological studies demonstrate that this paradoxical phenomenon is one of real clinical relevance (Katzelnick et al., 2017) and even questions the safety of antiviral vaccines which elevate antibody levels (Ferguson et al., 2016).

ADE has clinically significant consequences in the context of a natural viral infection, begging the question: wouldn't the influence of ADE be proportionately greater on the outcome of a massive, non-physiological infusion of virus? There appears no fundamental reason why ADE should not be applicable to a virotherapy scenario. In addition to dengue, the relevance of ADE has been demonstrated in diverse virus types, from the highly pathogenic blood-borne Ebola to seasonal respiratory viruses (reviewed in Taylor et al., 2015). This includes viruses with oncolytic properties, such as Coxsackievirus (Hober et al., 2001). Indeed, by conjugation to a non-neutralising anti-VSV antibody, the ability of oncolytic VSV to infect myeloid cells and extend the survival of tumour-bearing mice when given i.v. can be increased (Eisenstein et al., 2013). The amenability of reovirus to antibody-dependent cell entry outside the oncolytic context has been assessed in two studies, which have shown that the virus is capable of infecting Fc receptor-transfected cells (Danthi et al., 2006) and mouse macrophages (Burstin et al., 1983) via the binding of antibody. This raises the possibility that human monocytes may remain able to be infected even in the presence of anti-reovirus antibody.

### **2.5.5 Cell carriers**

Concern over the detrimental effect of antibodies and complement on the persistence of OV in the bloodstream spawned the concept of using cellular chaperones to deliver virus to tumours. This is regarded as a natural strategy, which is well matched to the aim of delivering viruses systemically to gain

maximum therapeutic benefit. The overarching rationale is that these so-called 'cell carriers' will shield the viral payload from antiviral effectors, and will home to tumour beds in order to deliver it. The ability of the carrier to amplify virus on the way to the tumour, and to exert its own anti-tumour effects once there, are viewed as a potential bonus. A wide repertoire of immune and non-immune cell types have been shown to be capable of OV carriage. Tumour cells themselves have been courted as carriers, on the basis that they may be best able to amplify virus and to stimulate anti-tumour immunity (Guo et al., 2010; Liu et al., 2010; Power et al., 2007). The tumour-homing ability of progenitor cells, particularly neural and mesenchymal stem cells, is a particularly attractive property that appears to facilitate the delivery of their adenovirus cargo to brain tumours (García-Castro et al., 2010; Tyler et al., 2009).

Immune cells are another population with excellent tumour trafficking potential, and offer the potential advantage of generating anti-tumour effects once there: two traits that OV carriage may itself promote. A plethora of immune populations have been tested as carriers. These are typically autologous cells that are loaded with virus *ex vivo* prior to i.v. infusion. T cells represent an attractive option given their ability to become tumour-specific and contribute to therapy. VSV has been successfully delivered to murine melanoma metastases by association with T cells, providing therapy that was superior to either unloaded T cells or VSV alone (Qiao et al., 2008a; Qiao et al., 2008c). Similarly, cytokine-induced killer cells, a heterogenous NK/T cell population, have been used as carriers to deliver both adenovirus (Yang et al., 2012) and vaccinia virus (Thorne et al., 2006) and yield tumour regression in mice.

These effector cell populations are poorly phagocytic, if at all, and typically allow virus to ride on, rather than within, the carrier cell. By contrast, myeloid cells are far more amenable to internalisation, which may offer increased viral protection. They are also capable of 'regurgitating' internalised antigen intact, on demand (Le Roux et al., 2012). Myeloid cells evaluated as OV carriers include MDSC, which deliver VSV cargo to tumours following systemic administration and simultaneously acquire a more 'M1' phenotype which promotes tumour killing (Eisenstein et al., 2013). Similarly, human monocyte-derived macrophages serve as hosts for vaccinia virus dissemination (Byrd et al., 2014), and are

capable of conveying adenovirus to inhibit the growth of murine prostate tumours (Muthana et al., 2011, 2013). Human monocytes themselves have been used for the carriage of measles virus to human ovarian and myeloma xenografts, which prolongs mouse survival (Iankov et al., 2007; Peng et al., 2009). With the exception of vaccinia (Byrd et al., 2014), this group of cells appears to resist large-scale amplification of their OV cargo – in contrast to murine myeloid DC and monocytes (Ilett et al., 2014, 2009) – although abortive or low-level replication is commonly observed.

When administered i.v., reovirus associates with a number of immune cell populations in blood. In patient blood sampled during a single therapeutic infusion, reovirus RNA was detected on monocytes, NK cells, B cells and granulocytes (Samson et al., 2018). Indeed, replication-competent reovirus associates with PBMC in patients known to be seropositive for the virus (Adair et al., 2012; Roulstone et al., 2015). These observations have given rise to strategies aiming to use PBMC as reovirus carriers, based on the hypothesis that they may allow the virus to evade neutralisation. Human PBMC were found to be capable of reovirus ‘hitch-hiking’, and its subsequent delivery to kill colorectal tumour targets *in vitro*, in the presence of neutralising serum, supplemented by their ability to trigger tumour cell lysis by patient-derived NK cells (Adair et al., 2013). A subsequent study used a heterogeneous population of lymphokine-activated killer cells and DC to demonstrate similar results against ovarian targets (Jennings et al., 2014).

Having found that *ex vivo*-loaded murine DC are able to deliver reovirus for the clearance of disseminated melanoma (Ilett et al., 2009), it was demonstrated that, in the presence of neutralising serum, human monocyte-derived DC internalise the virus and deliver it to kill melanoma targets (Ilett et al., 2011). As the therapeutic use of cells virus-loaded *ex vivo* is expensive and requires complex regulatory oversight, a new approach of ‘*in vivo* loading’ was developed, predicated on the use of circulating monocytes as potential carriers. In mice with previous exposure to reovirus – like most human adults – i.v. reovirus associates predominantly with the myeloid (CD11b<sup>+</sup>) fraction, consistent with a role for monocytes as primary viral targets (Ilett et al., 2014). Hence a treatment schedule was designed in which intraperitoneal GM-CSF

was administered in order to mobilise this pool in circulation, prior to i.v. reovirus infusion. GM-CSF pre-conditioning successfully increased both myeloid cell trafficking and viral delivery to B16 melanoma tumours (Ilett et al., 2014). The resulting regression of tumours and extension of survival was shown to be dependent on both the myeloid and NK cell fractions.

Most significantly, the therapeutic value of the GM-CSF/reovirus combination was only observed in mice pre-immunised to the virus, but not in reovirus-naïve mice. There also appeared to be a role for Fc receptors, given that Fc receptor blockade abrogated the killing of melanoma targets *in vitro* (Ilett et al., 2014). Viewed together, and in light of the capacity of monocytes to take up immune complexes, these data suggested a model in which systemically administered reovirus is rapidly bound by antibody and via Fc receptors gains access to circulating monocytes, which deliver the virus to tumour sites and initiate oncolytic and/or immune-mediated killing.

If proven, this hypothesis represents a highly novel way in which antiviral immunity may potentiate anti-tumour efficacy of OV. It is consistent with burgeoning data using other OV, where pre-immunity to NDV enhances therapy in mice (Ricca et al., 2016), and has prompted the prospective evaluation of reovirus pre-immunisation as a therapeutic element, alongside the GM-CSF/reovirus regimen, in clinical trial for melanoma (NCT03282188). It is not yet clear whether anti-OV immunity can offer anti-tumour benefit in humans.

## 2.6 Aims of the project

This study aimed to investigate the hypothesis that primary human monocytes can permit the carriage of antibody-neutralised reovirus, and ultimately generate melanoma cell killing *in vitro* and *in vivo*.

The specific elements of this multi-faceted 'hitch-hiking' process to be examined were:

- i. The formation of reovirus-antibody (reo-NAb) complexes within patient-derived, reovirus-treated serum
- ii. The ability of monocytes to carry and deliver reo-NAb for melanoma cell oncolysis in a novel *in vitro* assay
- iii. The molecular mediators enabling monocytes to interact with reo-NAb cargo
- iv. The impact of reo-NAb carriage upon monocyte phenotype
- v. The capacity of reo-NAb to generate immune-mediated tumour cell killing
- vi. The therapeutic benefit of reo-NAb in a mouse model of melanoma

## **3. Materials & methods**

### **3.1 Cell culture**

#### **3.1.1 Method**

Cell cultures were maintained in a Sanyo CO<sub>2</sub> incubator (Sanyo, Loughborough, UK) at 37°C in a humidified atmosphere of 5% CO<sub>2</sub> in air. Cells were manipulated under aseptic conditions using Nuaire (Plymouth, UK) Class II biological safety cabinets, Pipetman pipettes (Gilson; from Anachem, Bedfordshire, UK) and Pipetboy pipette guns (Integra, Berkshire, UK). Cabinets were cleaned before and after use with 2% (w/v) Virkon (Thermo Fisher, Loughborough, UK) and 70% (v/v) ethanol (Sigma, Dorset, UK). Cells were cultured in vented plastic tissue culture flasks (25, 75 or 150 cm<sup>2</sup>) or well plates (Corning, High Wycombe, UK). Adherent cell lines were passaged near confluence twice per week, first by washing with phosphate-buffered saline (PBS) (Sigma), then adding a 1X solution of trypsin-EDTA (Sigma) in Hanks' balanced salt solution (HBSS) (Sigma) to detach. Cells were centrifuged in an Eppendorf 5810R centrifuge (Eppendorf, Leicestershire, UK), at 400 g for 5 minutes at room temperature (RT), unless stated otherwise. Cells were harvested and washed using 15 ml or 50 ml sterile plastic Falcon tubes (Corning) or 25 ml plastic universal tubes (SLS, Nottingham, UK). A Nikon Eclipse TS100 microscope (Nikon, Kingston upon Thames, UK) was used to view cells, which were counted using a Neubauer chamber (Marienfeld, supplied by Thermo Fisher) following staining with 0.2% (v/v) trypan blue (Thermo). Light microscopy images were obtained using a Nikon DS-Fi1 camera. Cells were regularly tested for the presence of mycoplasma using Mycoalert (Lonza, Slough, UK) and were confirmed to be free from contamination.

#### **3.1.2 Cell lines and media**

Cell lines and primary cells were cultured in Dulbecco's modified Eagle's medium (DMEM) or Roswell Park Memorial Institute (RPMI)-1640 (Sigma); this was supplemented with 10% (v/v) foetal calf serum (FCS) (Life Technologies, Thermo Fisher) which had been heat-inactivated at 56°C for 30 minutes. The cells and media used are shown in Table 1.

### **3.1.3 Cryopreservation**

Cells were suspended in freezing medium (FCS + 10% (v/v) dimethyl sulphoxide (DMSO) (Merck, Nottingham, UK)) and 1 ml aliquots added to cryovials (Nunc, Thermo Fisher) which were frozen at  $-80^{\circ}\text{C}$  prior to transfer to liquid nitrogen storage the following day. Cells were recovered by rapid thawing of aliquots at  $37^{\circ}\text{C}$ , addition of excess fresh medium, centrifugation and transfer into tissue culture flasks in further fresh medium.

### **3.1.4 Preparation of PBMC by density gradient separation**

Human peripheral blood leukapheresis products (cones) were collected from healthy blood donors, who were all recruited locally through the NHS Blood and Transplant Service in Leeds (NHSBT). Cones were rested overnight, then diluted in an equal volume of HBSS and layered gently on to Lymphoprep (Axis-Shield, Dundee, UK) in a 50 ml tube at a 2:1 ratio. Tubes were centrifuged at 800 g for 25 minutes at RT, and the mononuclear cell (PBMC) layer harvested with a Pasteur pipette. PBMC were washed with 50 ml HBSS, centrifuged (400 g, 10 minutes), then washed again and centrifuged (300 g, 5 minutes). Cells were counted prior to further selection of immune cell populations.

## **3.2 Virus**

### **3.2.1 Use and storage**

All virus stocks were stored in PBS at  $4^{\circ}\text{C}$  (for up to 3 weeks) or at  $-80^{\circ}\text{C}$  (for long-term storage). Virus stock sources, titres, and susceptible cell lines for plaque assay and neutralisation assay are shown in Table 2.

### **3.2.2 UV inactivation of virus**

To render virions incompetent of replication, 100  $\mu\text{l}$  aliquots of virus in a 96-well plate were irradiated with UV-C ( $\lambda = 254 \text{ nm}$ ) for 2 minutes, using a Stratalinker

UV 1800 (Stratagene, Cambridge, UK) to give a 500 mJ dose. Virus was confirmed to be non-replicative by plaque assay (section 3.7).

### **3.3 Sources of antiviral antibody**

#### **3.3.1 Use and storage**

Serum was obtained with ethical approval and consent from patients enrolled in clinical trials: for reovirus, the REO-013 Brain trial (ISRCTN70443973); for CVA21, the STORM trial (NCT02043665). For REO-013 Brain, ethical approval was obtained through NHS REC, via NRES Committee Yorkshire & The Humber – Leeds East (reference number 12/YH/0402). The REC granted an extension to ethical approval for the study of patient samples (reference number 18/LO/0080).

Blood was taken one to six weeks following the final intravenous (i.v.) infusion of virus and allowed to clot in red-topped Vacutainer tubes (BD, Berkshire, UK). Serum was obtained by centrifugation (800 g, 10 minutes) and stored at  $-80^{\circ}\text{C}$  until use. For this study, ten serum samples were available from six individual REO-013 Brain trial patients, and five serum samples from four individual STORM trial patients. Serum was limited, with approximately 5 ml of each sample available.

Pleural fluid from patients treated with repeat intrapleural HSV1716 (trial NCT01721018) was provided by Joe Conner (Virttu Biologics) with whom a Material Transfer Agreement is in place. Pleural fluid was collected one to six weeks following the virus infusion, passed through a  $0.22\ \mu\text{m}$  filter (Merck) and stored at  $-80^{\circ}\text{C}$  until use. Three pleural fluid samples (approximately 3 ml each) were available for use.

Serum (for reovirus and CVA21) and pleural fluid (for HSV1716) were used as shown in Table 3.

#### **3.3.2 Neutralisation assay**

The neutralising capacity of the three antibody sources listed in Table 3 was tested on virus-susceptible cell lines by a modified neutralisation assay protocol (Yang et al., 2004). Halving dilutions of serum or pleural fluid were made in

DMEM-10 and 100  $\mu$ l added to sub-confluent monolayers of susceptible cells (see Table 2) in a 96-well plate. Virus was diluted in serum-free DMEM to achieve MOI 0.05 (reovirus and CVA21) or MOI 1 (HSV1716), unless stated, in a final volume of 200  $\mu$ l per well. Control wells without virus were included for all plates to exclude the possibility that the sera or pleural fluid were cytotoxic. After 72 hours, 20  $\mu$ l of the tetrazolium dye MTT was added to each well. After a further 4 hours, the medium was removed and replaced with 150  $\mu$ l DMSO to solubilise formazan crystals (5 minutes), after which a Multiskan EX microplate reader (Thermo Fisher) was used to assess optical density at  $\lambda = 540$  nm. Readings were used to infer metabolic activity and thus viability of the treated cell population. Cell viability was calculated by normalising values to wells free from virus or serum/pleural fluid in each case.

To assess the involvement of heat-labile factors in serum neutralisation of reovirus, patient sera were incubated in a 56°C water bath for 30 minutes in order to inactivate complement. Inactivated and non-inactivated sera were immediately assayed for neutralising capacity as above.

### **3.3.3 Depletion of antibody isotypes from anti-reovirus serum**

To determine the contribution of specific immunoglobulin classes to reovirus neutralisation, individual classes were depleted using agarose bead-conjugated antibodies specifically targeting the human  $\gamma$ - or  $\alpha$ -chain (Sigma). Serum from reovirus-treated patients was diluted 1:1 in PBS and incubated with bead-conjugated antibodies for 90 minutes at RT, on an SRT9 tube roller (Stuart, Staffordshire, UK). Depleted samples were obtained by centrifuging to remove beads (3,000 g, 15 seconds) and harvesting the supernatant. Antibody depletion was confirmed by enzyme-linked immunosorbent assay (ELISA) using human IgG/IgA ELISA kits (Mabtech, via 2B Scientific, Oxfordshire, UK) (section 3.9.2) and the effect of depletion assessed by neutralisation assay (section 3.3.2).

### **3.3.4 Immunoprecipitation of reovirus**

#### **3.3.4.1 Detection of anti-reovirus antibodies in serum**

Reovirus was added to anti-reovirus patient serum at a 1:5 (v/v) ratio, i.e. 1  $\mu$ l serum per  $10^6$  pfu, and incubated at 37°C for 3 hours. Screw-cap 1.5 ml

Eppendorf tubes were first blocked with 3% (w/v) bovine serum albumin (BSA) for 1 hour at 4°C, prior to the addition of reovirus-antibody samples. Pre-washed protein A resin beads (GenScript, via 2B Scientific) in excess were mixed with samples and allowed to bind for 2 hours at 4°C on an SB3 rotator (Stuart). Samples were centrifuged (400 g, 2 minutes) and washed four times in 0.1% (v/v) Triton-X in PBS, then boiled (95°C, 5 minutes) in loading buffer (Table 7) to dissociate IgG from beads, and centrifuged (13,200 g, 2 minutes) using an Eppendorf 5415D microcentrifuge to yield supernatant for analysis.

#### **3.3.4.2 Detection of endogenous reo-NAb complexes in serum**

Serum samples, taken 24 hours following i.v. virus infusion, were directly combined with protein A beads, and centrifuged, washed, boiled and purified antibodies harvested as above.

### **3.4 *In vitro* hand-off assay**

#### **3.4.1 Standard protocol**

##### **3.4.1.1 Preparation of target cells**

Confluent flasks of target cells (as stated) were trypsinised (section 3.1.1) and counted. Cell density was adjusted to  $1.5 \times 10^5$  cells/ml in DMEM-10, and 2 ml added to each well of a 6-well plate. After 24 hours, any floating cells were removed by replacing medium with fresh DMEM-10, and treatments added as below.

##### **3.4.1.2 Formation of reovirus-antibody complexes**

To form reovirus-antibody complexes (reo-NAb), reovirus was combined with patient serum at a ratio known to be neutralising by neutralisation assay on L929 cells (section 3.3.2) and by the absence of cell death in target cells treated directly with reo-NAb, by flow cytometry (section 3.6.2). Neutralisation was also confirmed for complexes formed by CVA21 and HSV1716 (Table 3). In all

cases, virus was incubated with serum/pleural fluid for 2-3 hours at 37°C prior to loading on to carrier cells.

#### **3.4.1.3 Selection of carrier cells**

PBMC were isolated from leukapheresis cones (section 3.1.4). CD14<sup>+</sup> monocytes were isolated from PBMC by positive selection with anti-CD14 microbeads (Miltenyi, Surrey, UK): PBMC were re-suspended in 20 µl MACS buffer (Table 7) per 10<sup>7</sup> cells, and incubated with 5 µl anti-CD14 microbeads per 10<sup>7</sup> cells at 4°C for 15 minutes. Cells were washed in excess cold MACS buffer and pelleted (300 g, 5 minutes), then re-suspended in 40 µl MACS buffer per 10<sup>7</sup> cells and added to pre-rinsed LS columns within a QuadroMACS separator (Miltenyi). Columns were washed three times with 3 ml cold MACS buffer, and CD14<sup>+</sup> cells eluted in 5 ml MACS buffer per column. These were counted and washed in excess cold HBSS, then 2 x 10<sup>6</sup> (in 500 µl, unless otherwise stated) transferred to individual universal tubes. Purity of positively-selected monocytes was confirmed by flow cytometry (section 3.6.1).

#### **3.4.1.4 Carrier cell loading and co-culture**

Treatments (virus, NAb or the combination) were added to monocytes as described, mixed, and tubes returned to 4°C for 2-3 hours to permit adsorption. Cells were then washed in 10 ml PBS and pelleted three times (300 g, 5 minutes). Cell pellets were re-suspended first by flicking, and then gently triturating in 500-750 µl RPMI-10. If to be analysed by plaque assay, a set volume of monocyte cell suspension was routinely set aside from all conditions and stored at -80°C. The remaining cell suspension was then added to wells containing pre-seeded target cells (section 3.4.1.1) and co-cultured at 37°C for 72 hours, unless stated otherwise. Target cell viability was subsequently analysed by flow cytometry (section 3.6.2).

### **3.4.2 Adaptations of the hand-off assay**

#### **3.4.2.1 Negative selection of monocytes for electron microscopy**

Due to interference from uptake of anti-CD14 microbeads in electron microscopy (EM) images, monocyte cells for EM analysis were negatively selected using the Human Pan Monocyte Isolation Kit (Miltenyi) as per the manufacturer's instructions. Briefly, after isolation of PBMC (section 3.1.4), cells were suspended with 40  $\mu$ l MACS buffer, 10  $\mu$ l FcR blocking reagent, and 10  $\mu$ l Biotin-Antibody Cocktail per  $10^7$  cells respectively, and incubated at 4°C for 5 minutes. Subsequently, anti-biotin microbeads (20  $\mu$ l per  $10^7$  cells) and MACS buffer (30  $\mu$ l per  $10^7$  cells) were added, and cells further incubated at 4°C for 10 minutes.

Labelled non-monocytes were then depleted from PBMC by magnetic separation. Cell suspension was added to pre-rinsed LS columns and washed three times with 3 ml MACS buffer, the flow-through (enriched monocytes) being collected. Purity of the enriched fraction was confirmed by flow cytometry (section 3.6.4).

#### **3.4.2.2 Selection of CD16<sup>+</sup> and CD16<sup>-</sup> populations**

Isolation of monocyte subsets from PBMC according to differential CD16 expression was performed based on a previously described method (Frankenberger et al., 2012).

CD16<sup>+</sup> monocytes were isolated from  $4 \times 10^8$  PBMC per donor using the CD16<sup>+</sup> Monocyte Isolation Kit (Miltenyi). To deplete CD16<sup>+</sup> non-monocytes, PBMC were first incubated with 400  $\mu$ l of FcR Blocking Reagent and Non-Monocyte Depletion Cocktail (Miltenyi) respectively in 1.2 ml MACS buffer (hereafter 'buffer') at 4°C for 15 minutes. Cells were washed in excess buffer and centrifuged (300 g, 5 minutes). The pellet was re-suspended in 3 ml buffer and added to pre-rinsed LS columns. Columns were washed twice with 2 ml buffer, retaining the flow-through. Subsequently, CD16<sup>+</sup> monocytes were positively selected from the enriched PBMC. Cells were pelleted, re-suspended in 2 ml buffer, and incubated with 400  $\mu$ l anti-CD16 microbeads at 4°C for 15 minutes. After washing in excess buffer and centrifuging (300 g, 5 minutes), cells were re-suspended in 3 ml buffer and added to fresh pre-rinsed LS columns. Three 3 ml washes were performed with buffer, and positively selected CD16<sup>+</sup>

monocytes eluted in 5 ml buffer per column. These were counted and rested overnight at  $2 \times 10^6$  per ml in RPMI-10 to allow beads to dissociate from the receptor. Cells were gently mechanically re-suspended in medium using cell scrapers (Falcon, Thermo Fisher), washed in HBSS and re-counted prior to virus loading as described.

CD16<sup>-</sup> monocytes were isolated from  $1 \times 10^8$  PBMC per donor. First, CD16<sup>+</sup> cells were depleted using anti-CD16 microbeads: PBMC were incubated with 200  $\mu$ l anti-CD16 microbeads in 1 ml buffer (4°C, 15 minutes), then washed in excess buffer, centrifuged (300 g, 5 minutes), re-suspended in 1.5 ml buffer and added to pre-rinsed LS columns. Columns were washed three times with 2 ml buffer, and flow-through retained. These CD16<sup>-</sup> enriched PBMC were pelleted (300 g, 5 minutes), re-suspended in 1 ml buffer and incubated with 200  $\mu$ l anti-CD14 microbeads (4°C, 15 minutes). After washing with excess buffer and centrifuging (300 g, 5 minutes) cells were transferred to LS columns in 1.5 ml buffer. Three 2 ml washes were performed prior to elution of magnetically labelled CD14<sup>+</sup> monocytes. As for the CD16<sup>+</sup> population, cells were rested overnight at  $2 \times 10^6$  cells per ml in RPMI-10, then re-suspended, washed in HBSS and re-counted prior to virus loading.

#### **3.4.2.3 Blockade of monocyte virus entry**

For assays in which specific monocyte receptors were targeted, carrier cells in a total volume of 150  $\mu$ l were pre-treated with blocking agents at 10 or 100  $\mu$ g/ml as stated at 4°C for 45 minutes. These blocking agents (Table 4) remained present during subsequent incubation with virus/antibody cargo. Washing and co-culture with targets was then performed as described (section 3.4.1.4).

#### **3.4.2.4 Target cell killing by monocyte conditioned medium**

After loading with reovirus or reo-NAb at MOI 10 and washing, monocytes were either directly added to Mel-624 target cells, or resuspended at  $1 \times 10^6$  per ml in RPMI-10 and cultured in 6-well plate format for 48 hours. The resulting medium was aspirated and centrifuged to remove cells (400 g, 5 minutes) to yield conditioned medium (CM). Filtered CM (FCM) was generated by passing CM through OptiScale-25 Viresolve NFP filters (Merck). Flow cytometry was then used as described (section 3.6.2) to analyse the killing of Mel-624 cells after 72

hours, by either loaded monocytes, or CM or FCM derived from an equivalent number of loaded monocytes.

#### **3.4.2.5 Blockade of virus transmission by monocytes**

To assess the involvement of JAM-A, the JAM-A-expressing Mel-624 line was used, being seeded the day before treatment at  $1.5 \times 10^5$  cells per well (12-well plate format). Prior to the addition of loaded monocytes, targets were incubated with an azide-free preparation of the J10.4 antibody against JAM-A (Santa Cruz), or isotype, at 10  $\mu$ g per well in DMEM-10. After a 30-minute incubation at 37°C, loaded and washed carrier cells (section 3.4.1.4) were added for 90 hours and co-cultures processed as described (section 3.6.2).

To assess the involvement of cell-cell contact, a 24-well transwell system was used (Corning). Mel-624 cells were seeded in the well base the day before treatment at  $0.6 \times 10^5$  cells per well. Monocytes loaded at MOI 5 (or reovirus or reo-NAb alone) were added to the well insert in a volume of 150  $\mu$ l RPMI-10. For 'no transwell' conditions, a standard 24-well plate was used. After a 90-hour incubation, co-cultures were processed as described (section 3.6.2).

#### **3.4.2.6 Virus loading of monocytes in whole blood**

Blood was taken from healthy donors by venepuncture, and collected in purple-topped Vacutainer tubes containing EDTA (BD). 9 ml blood was supplemented with 500  $\mu$ l patient-derived serum prior to the addition of  $90 \times 10^6$  pfu reovirus (MOI 10 based on  $1 \times 10^6$  PBMC per ml blood). Tubes were incubated at 37°C for 30 minutes with occasional agitation. Density gradient separation with Lymphoprep was then used to obtain PBMC. Myeloid cells were selected as before using anti-CD14 microbeads. Both the CD14-selected and -depleted fractions were collected, washed in HBSS and analysed by plaque assay on L929 targets (section 3.7).

## **3.5 Immune cell stimulation assays**

### **3.5.1 Co-culture of immune cell populations**

#### **3.5.1.1 Virus-loaded monocytes and whole PBMC**

To broadly assess the influence of virus-loaded monocytes on other human PBMC, monocytes were first selected and loaded with antibody, virus or reo-NAb complexes at MOI 10 for 3 hours at 4°C as described above (section 3.4.1.4). After washing with PBS, monocytes were re-suspended in RPMI-10 and counted.  $2.5 \times 10^6$  cells were either cultured alone in 3 ml RPMI-10 in 6-well plates, or added to  $12.5 \times 10^6$  autologous CD14<sup>-</sup> PBMC (i.e. at a physiological 1:5 ratio) in a total of 15 ml RPMI-10 in 75cm<sup>2</sup> flasks. Cells were cultured for 40 hours at 37°C.

Medium was then aspirated and centrifuged (300 g, 5 minutes) to obtain cell-free supernatants, which were stored at -20°C prior to cytokine analysis. Plates/flasks were scraped and flushed with PBS to harvest adherent cells, which were combined with pelleted cells from suspension. Cells were centrifuged again, re-suspended in FACS buffer (Table 7) and  $2 \times 10^5$  cells added to each FACS tube; the cells were stained with antibodies as below (Table 8).

#### **3.5.1.2 Virus-loaded monocytes and NK cells**

##### **3.5.1.2.1 Stimulation of monocytes by NK cells**

Monocytes were first positively selected from PBMC according to CD14 expression (section 3.4.1.3), and the depleted fraction then used for the negative selection of NK cells using the human NK cell isolation kit (Miltenyi). After loading with NAb, reovirus or reo-NAb (MOI 10), monocytes were washed with PBS and cultured at a 2:1 monocyte:NK ratio in RPMI-10 for 48 hours. Cells were then harvested and stained with PE-conjugated antibodies against activation markers as indicated, in addition to FITC CD11b (Biolegend, London, UK), and processed by flow cytometry (section 3.6).

### 3.5.1.2.2 Stimulation of NK cells by monocytes

To assess NK cell activation and the specific monocyte-generated factors involved, monocytes loaded with reovirus or reo-NAb at MOI 5 (section 3.4.1.4) were cultured overnight (16 hours) at  $2 \times 10^6$  cells/ml in RPMI-10. Cells were collected by scraping and flushing with medium, then centrifuged (300 g, 5 minutes) to obtain conditioned medium (CM). CM was passed through OptiScale-25 Viresolve NFP filters (Merck) to generate filtered CM (FCM).

Prior to the addition of CM/FCM,  $1.5 \times 10^6$  autologous PBMC were added to each well of a 12-well plate in 1 ml RPMI-10. Receptor blocking antibodies (Table 4) were added to target PBMC at stated concentrations. After 30 minutes at 37°C, CM or FCM was added to wells at a 1:2 (v/v) ratio, and incubated for 48 hours. Cells were harvested, washed in FACS buffer, and NK cell activation quantified by PerCP CD69 staining on the PE CD3<sup>-</sup>, FITC CD56<sup>+</sup> population (section 3.6).

### 3.5.1.2.3 NK cell cytotoxicity

To assess the ability of virus-loaded monocytes to stimulate NK cell-mediated killing of tumour cell targets, monocytes were first loaded with patient serum, reovirus or reo-NAb at MOI 10 (section 3.4.1.4). Autologous NK cells were obtained from PBMC using a negative isolation kit (Miltenyi) according to the manufacturer's instructions.  $2.5 \times 10^6$  NK cells were then cultured with or without  $1 \times 10^6$  loaded monocytes in 2 ml RPMI-10. Alternatively, NK cells were treated directly with the same agents used to treat monocytes, at the same dose. After 40 hours at 37°C, cells were harvested for analysis of NK cell cytotoxicity by chromium assay (section 3.5.2) and expression of CD107 as a degranulation marker (section 3.6.5).

## 3.5.2 Chromium release assay

Cell line targets were trypsinised, and  $1 \times 10^6$  cells transferred to 50 ml Falcon tubes and centrifuged (300 g, 5 minutes). The supernatant was discarded and 100 µCi of <sup>51</sup>Cr (Amersham Biosciences, Buckinghamshire, UK) added. Cells were labelled for 1 hour at 37°C, and subsequently washed three times with excess PBS to remove unbound <sup>51</sup>Cr. Labelled tumour cell targets were re-

suspended in RPMI-10 and 5,000 added to each well of a round-bottom 96-well plate.

Treated effector NK cells (section 3.5.1.2.3) were harvested from culture, counted and added to target cells at effector:target (E:T) ratios ranging from 20:1 ( $1 \times 10^5$  NK cells) to 2.5:1 ( $1.25 \times 10^4$  NK cells) in a total of 200  $\mu$ l fresh RPMI-10. For each target, spontaneous  $^{51}\text{Cr}$  release was determined from wells containing 5,000 target cells alone, and maximum release from wells containing 5,000 targets in RPMI-10 plus 1% (v/v) Triton X-100. E:T co-cultures were incubated at 37°C for 4 hours to allow NK cell cytotoxicity to proceed, after which the cells were pelleted (300 g, 5 minutes). 50  $\mu$ l supernatant was transferred to 96-well scintillant LumaPlates (Perkin Elmer, Buckinghamshire, UK) and allowed to dry overnight. Chromium release as counts per minute (cpm) was detected using the Wallac 1450 MicroBeta TriLux scintillation counter. The degree of target cell killing was assessed by the formula

$$\% \text{ killing} = 100 * \frac{\text{test cpm} - \text{spont. cpm}}{\text{max. cpm} - \text{spont. cpm}}$$

## 3.6 Flow cytometry

### 3.6.1 Default antibody staining protocol

For routine analysis, cells from culture were transferred to FACS tubes (Corning), washed once in 2 ml FACS buffer, centrifuged (300 g, 5 minutes) and the supernatant discarded. Tubes were flicked to re-suspend cells in the residual volume, and antibodies added (Table 8) and incubated for 30 minutes at 4°C in the dark. Cells were then washed in FACS buffer, centrifuged and the supernatant removed prior to fixing cells in 300  $\mu$ l PBS + 1% (w/v) paraformaldehyde (PFA) (hereafter 1% PFA/PBS). These were stored wrapped in foil at 4°C for up to 3 days, until data were acquired and analysed using the Attune® Acoustic Focusing flow cytometer and Attune software (v. 2.1.0) (Life Technologies).

Where antibody staining was used to assess expression of surface markers, the median fluorescence intensity (MFI) of the protein of interest was subtracted from that of the appropriate isotype control antibody as standard. In all cases, at least 30,000 events were recorded in the gate analysed.

### 3.6.2 Live-dead viability assay

All cells (both adherent and non-adherent) were harvested from culture plates, transferred to numbered plastic FACS tubes (Falcon) and washed with 2 ml PBS. After centrifuging (400 g, 5 minutes) and discarding supernatant, the cell pellet was washed once in 2 ml PBS and centrifuged. The supernatant was discarded, and tubes gently flicked to re-suspend cells in the residual volume. To assess viability, cells were then stained using the LIVE/DEAD® Fixable Red Dead Cell Stain (Thermo) at 1 µl stain in 1 ml PBS per tube (4°C, 30 minutes, in the dark). Tubes were then centrifuged, washed in 2 ml PBS and centrifuged again, prior to fixing cells with 300 µl of 1% PFA/PBS.

For the default use of the Mel-624 cell line in hand-off assays, the smaller monocyte and larger Mel-624 populations - both alive and dead - could be readily discriminated by size and granularity, necessitating no further gating strategy. Where other cell lines were used as targets, a gate was drawn around the entire cell population; myeloid carrier cell number was quantified by staining with CD11b FITC antibody (Biolegend) and this subtracted from the total 'live' population in order to generate a target cell-specific assessment of viability.

### 3.6.3 Detection of reovirus binding

Freshly isolated monocytes were pulsed with patient serum, virus or reo-NAb (MOI 50) as above (section 3.4.1.4), then washed twice with PBS and once with FACS buffer. Cells were distributed between FACS tubes and stained with 1 µg of primary antibody against reovirus  $\sigma 3$  (Developmental Studies Hybridoma Bank (DSHB), Iowa, USA) or human IgG (Thermo) for 30 minutes at 4°C. After washing with FACS buffer, 0.2 µg of fluorophore-conjugated secondary antibody against mouse or rabbit IgG was added (30 minutes, 4°C). Cells were subsequently washed and fixed with 300 µl of 1% PFA/PBS, prior to acquisition.

### 3.6.4 Analysis of monocyte phenotype

Freshly isolated monocytes were pulsed with patient serum, virus or reo-NAb (MOI 10), then washed three times with excess PBS. Cells were resuspended in RPMI-10 at  $1 \times 10^6$  per ml and cultured in 6-well plate format for 48 hours.

Wells were scraped to ensure that suspended and adherent cells were harvested into FACS tubes. Cells were washed in FACS buffer, stained with antibodies as indicated, and fixed in 1% PFA/PBS prior to acquisition.

#### **3.6.4.1 Monocyte migration**

To assess the ability of reovirus to stimulate monocyte migration, monocytes were first loaded with reovirus or reo-NAb (MOI 5) and cultured overnight (16 hours) at  $2 \times 10^6$  cells/ml in RPMI-10. Cells were collected by scraping and flushing with medium, and  $2 \times 10^5$  cells added to the upper 'insert' of a 24-well transwell system with 5  $\mu$ m pore size (Corning). The lower chamber of the well contained either fresh RPMI-10 medium or  $1 \times 10^5$  Mel-624 cells which had already been *in situ* for 48 hours in order to create a chemoattractant gradient. Transwell plates were returned to 37°C for 5 hours to permit monocyte migration. The lower face of the transwell membrane was then flushed twice with medium from the chamber. This medium was collected and stained with 2  $\mu$ l CD11b FITC antibody to detect the number of monocytes present in the lower chamber by flow cytometry.

#### **3.6.5 Degranulation assay**

Alongside the  $^{51}\text{Cr}$  killing assay, CD107 expression was employed as a complementary marker for NK cell degranulation. To co-cultures of NK cells and treated monocytes (section 3.5.1.2.3),  $2 \times 10^5$  target cells were added and incubated for 1 hour at 37°C in lidded FACS tubes (Falcon). Cells were then stained by incubation with 100  $\mu$ l RPMI containing 2.5  $\mu$ g brefeldin A (Biolegend), PerCP CD3, PE CD56, and FITC CD107a and CD107b antibodies (4 hours, 37°C). After washing with 2 ml FACS buffer, cells were centrifuged, the supernatant removed, and cells fixed in 1% PFA/PBS. The degree of NK cell degranulation was determined by the proportion of CD56<sup>+</sup> cells staining positively for FITC CD107a/b.

### 3.7 Plaque assay

The same general protocol was employed for the titration of virus stocks and the quantification of viral load in cell culture samples. For the determination of reovirus stock titre, the new batch was thawed and small aliquots made and returned to  $-80^{\circ}\text{C}$ ; one aliquot was thawed and used to calculate the titre for that batch.

For the quantification of viral load in infected cells, cell suspension samples at  $-80^{\circ}\text{C}$  were rapidly thawed in a  $37^{\circ}\text{C}$  water bath and subjected to two further rounds of freeze-thaw (5 minutes each) using a methanol-dry ice bath, to lyse cells. After the third thaw, samples were vortexed vigorously for 10 seconds to liberate virus, and cell debris removed by centrifugation (500 g, 2 minutes). Where cell-free supernatants were analysed, additional freeze-thaw cycles were not performed.

#### 3.7.1 Protocol

Reovirus-susceptible L929 cells were seeded in 6-well plates at  $5 \times 10^5$  cells per well in 2 ml DMEM-10. These were allowed to adhere for 24 hours. Serial dilutions of the reovirus stock or virus-containing samples from culture were created in serum-free DMEM in a 96-well plate. Medium was removed from near-confluent L929 cells, and 100  $\mu\text{l}$  of serially diluted reovirus added drop-wise directly on to the monolayer in each well, followed by 500  $\mu\text{l}$  of serum-free DMEM. Plates were tilted to mix, and incubated at  $37^{\circ}\text{C}$  for 2.5 hours to allow virus adsorption. The inoculum was subsequently removed and cells covered with 2 ml of overlay solution, which was made from two parts DMEM-10 to one part 1.6% (w/v) carboxy-methylcellulose (CMC). Plates were returned to  $37^{\circ}\text{C}$  incubators for 72-96 hours to permit plaque formation. The overlay was then tipped away, and the cells rinsed with 2 ml PBS and fixed with 500  $\mu\text{l}$  of 1% PFA/PBS for 10 minutes at RT. PFA was tipped away and replaced by 750  $\mu\text{l}$  of stain solution, containing 1% (w/v) methylene blue (Sigma) in 50% (v/v) ethanol. After 3 minutes, the stain solution was washed away with running water and plates dried prior to manually counting plaques. The mean plaque number was obtained from duplicate wells, and titre was calculated by the formula

$$\text{pfu/ml} = \frac{\# \text{ plaques}}{0.1 * \text{ dilution factor}}$$

## **3.8 Western blotting**

### **3.8.1 Preparation of samples**

#### **3.8.1.1 Reovirus-infected cell line lysates**

In order to probe for antibodies against reovirus, lysates were made from reovirus-infected Mel-624 and L929 cell lines. First, these cells were seeded from culture into 10 cm<sup>2</sup> tissue culture dishes (Corning) at  $2 \times 10^6$  cells per dish in 12 ml DMEM-10. After 24 hours, cells were treated with either reovirus (MOI 10) or PBS as a control. After a further 24 hours, medium was removed, and cells harvested by scraping in 1 ml cold PBS. These were pelleted in a 1.5 ml Eppendorf tube (400 g, 5 minutes) and the pellet re-suspended in 200  $\mu$ l cold Giordano lysis buffer (GLB) (Table 7) (van den Wollenberg et al., 2008) supplemented with 5  $\mu$ l Complete protease inhibitors (Roche, Welwyn Garden City, UK). Samples were left on ice for 15 minutes, then centrifuged (14,000 g, 4°C, 15 minutes). The lysed cell supernatant was harvested and stored at -80°C.

#### **3.8.1.2 Monocyte lysates**

$1 \times 10^7$  CD14-selected monocytes (section 3.4.1.3) were pulsed with stated treatments (MOI 10) for 2-3 hours at 4°C. Following two washes in 10 ml PBS, cells were transferred into 5 ml RPMI-10 and cultured in T25 flasks at 37°C. After 24 hours, attached cells were gently released by scraping, and cells pelleted (400 g, 5 minutes) and washed in excess cold PBS. The resulting pellet was repeatedly triturated in 200  $\mu$ l radioimmunoprecipitation assay (RIPA) buffer (Table 7) supplemented with protease inhibitors as above, on ice for 30 minutes. Cell debris was removed by centrifugation (14,000 g, 4°C, 15 minutes) and the supernatant aspirated for analysis. Protein levels were subsequently assessed and equalised by DC assay.

### 3.8.2 DC assay

The protein concentration in lysates was determined by the colorimetric DC Protein Assay (Bio-Rad, Hertfordshire, UK) according to manufacturer's instructions. Briefly, samples (diluted 1:1) were dispensed into triplicate wells of a 96-well plate, and mixed with 25  $\mu$ l of solution A' and 200  $\mu$ l of solution B. After incubation for 15 minutes at RT, protein concentration was quantified according to optical density at  $\lambda = 620$  nm using a Multiskan EX plate reader (Thermo). Sample concentrations were subsequently equalised by the addition of further GLB or RIPA buffer as appropriate, supplemented with protease inhibitors.

### 3.8.3 Electrophoresis and blotting

100  $\mu$ l of lysate was added to 100  $\mu$ l of 2X SDS-PAGE loading buffer (Table 7). Immediately prior to loading, the reducing agent dithiothreitol (DTT) was added to a final concentration of 2 mM, and samples boiled in a heat block (95°C, 5 minutes).

Samples (15-20  $\mu$ g protein per lane) were loaded on to standard 10% SDS-polyacrylamide gels alongside the PageRuler Plus molecular weight marker (Thermo). In some blots, as a control for antibody specificity, ChromPure human IgG (Jackson ImmunoResearch, Cambridgeshire, UK) was prepared in loading buffer as above and used at 1  $\mu$ g per lane. Gels were run at 120 V in running buffer (Table 7) for 2 hours to separate proteins by size. Proteins were then transferred to nitrocellulose membrane (Bio-Rad) in transfer buffer (Table 7) at 25 V for 2.5 hours. Membranes were blocked for 1 hour in PBS + 0.1% (v/v) Tween-20 (Sigma) (PBST), supplemented with 5% (w/v) non-fat skim milk powder (Sigma). Membranes were then probed, using primary antibody or serum as described (Table 5) in 5% milk/PBST (overnight incubation at 4°C). After three 5-minute washes in PBST, membranes were incubated with an HRP-conjugated secondary antibody, diluted as described (Table 8) in 5% milk/PBST (1 hour, RT). After a further three washes, blots were visualised with the chemiluminescent SuperSignal West Pico substrate (Thermo) on a Gel Doc XR system using Image Lab software (Bio-Rad). ImageJ software (NIH) was used for densitometry analysis.

### 3.8.3.1 IP of patient-derived serum for reovirus

After immunoprecipitation of patient antibodies using protein A beads (section 3.3.4), the protein concentration of samples was determined and adjusted, and gels run, as above. After transfer to nitrocellulose and blocking, membranes were incubated overnight with the 4F2 antibody against reovirus  $\sigma 3$  (DSHB) at 1:200 in 1% (w/v) milk/PBST. Three PBST washes were performed prior to a 1-hour incubation with an HRP-conjugated secondary antibody against mouse IgG (Sigma) at 1:5,000 in 0.1% (w/v) milk/PBST. After a further three washes, antibody binding was assessed as above by chemiluminescence.

## 3.9 Cytokine analysis

### 3.9.1 Luminex

The secreted factors in cell culture were broadly analysed using a magnetic bead-based kit. Cells and debris were removed from supernatants by centrifugation (400 g, 5 minutes) and stored at  $-20^{\circ}\text{C}$ .

Multiple analytes were investigated from the same samples using the Bio-Plex Pro human cytokine 21-plex and 27-plex immunoassay kits (Bio-Rad) according to manufacturer's instructions. Fluorescence intensity values were obtained using the Bio-Plex 100 machine (Bio-Rad), corrected for background signal and converted to cytokine concentrations (pg/ml). Values above the standard range were either extrapolated from the standard curve or assigned the maximal standard value, as appropriate. For the purposes of calculating fold-change over mock-treated samples, readings below 5 pg/ml were assigned a value of 5 pg/ml to mark the lower limit of detection.

### 3.9.2 ELISA

Culture medium was rendered cell-free by centrifugation (400 g, 5 minutes) and the supernatant stored at  $-20^{\circ}\text{C}$  prior to analysis by enzyme-linked immunosorbent assay (ELISA).

Flat-bottomed 96-well Maxisorp plates (Nunc) were first coated with capture antibodies against specific protein targets – at optimised concentrations in 100

$\mu$ l PBS or coating buffer (Table 7) as stated (Table 9) – overnight at 4°C. Plates were washed three times with 200  $\mu$ l per well PBST (PBS + 0.05% (v/v) Tween-20) using a Skanwasher 300 machine, and 200  $\mu$ l of ELISA blocking solution (PBS + 10% (v/v) FCS) added for 2 hours at RT. After three further washes in PBST, 100  $\mu$ l of supernatant (or standard as per Table 10, diluted in RPMI-10) was added to triplicate wells, and incubated overnight at 4°C. Wells were washed six times in PBST, and 100  $\mu$ l of biotinylated detection antibodies (Table 9), diluted in blocking solution, added for 2 hours at RT. After a further six washes in PBST, 100  $\mu$ l of Extravidin alkaline phosphatase conjugate (Sigma) was added to each well, diluted at 1:5,000 in PBST, and left at RT for 1 hour. Plates were then washed three times in PBST and three times in double-distilled water (ddH<sub>2</sub>O). Sigmafast pNPP substrate solution (Sigma) was pre-prepared in water according to manufacturer's instructions, and added at 100  $\mu$ l per well. Plates were incubated at RT in the dark for up to one hour to permit the development of signal, prior to reading optical density at  $\lambda = 405$  nm with the Multiskan EX plate reader.

### **3.10 Transcriptional analysis**

#### **3.10.1 RNA analysis by qPCR**

##### **3.10.1.1 Virus treatment**

PBMC were isolated from fresh leukocyte cones (section 3.1.4) and monocytes selected (section 3.4.1.3) exactly as described for the hand-off assay, for three healthy donors. After washing in HBSS, 3 x 10<sup>7</sup> monocytes were added to universal tubes, and treated with MOI 3 (9 x 10<sup>7</sup> pfu) reovirus or reo-NAb (section 3.4.1.2) with or without prior UV inactivation of virus (section 3.2.2). Cells were incubated (4°C, 2-3 h) and washed as in the hand-off assay (section 3.4.1.4). The washed cell pellet was thoroughly re-suspended in 15 ml RPMI-10, and 5 ml of cell suspension added to each of three T25 flasks, which were left in 37°C incubators for the stated time.

To harvest cells, flasks were gently scraped and medium flushed to re-suspend both adherent and floating cells. The cell suspension was transferred to 15 ml falcon tubes and cells pelleted (400 g, 5 minutes); the supernatant was saved at -20°C for analysis by ELISA. Cells were subsequently re-suspended in 1 ml

PBS, transferred to Eppendorf tubes, and centrifuged (400 g, 5 minutes). After aspirating the PBS, the resulting pellet was stored at  $-80^{\circ}\text{C}$  prior to processing.

### 3.10.1.2 RNA processing

RNA was extracted from treated cells using the RNeasy mini kit (Qiagen, Manchester, UK) according to manufacturer's instructions. Briefly, frozen cell pellets were first thawed and immediately re-suspended in buffer RLT. Cells were lysed and homogenised using QIAshredder spin columns (Qiagen). RNA was purified using RNeasy spin columns by sequential ethanol precipitation, column binding, washing, and RNA elution in nuclease-free water (Ambion, Thermo Fisher). A Nanodrop ND-1000 spectrophotometer (Thermo Fisher) was used to quantify RNA concentration and quality. A total of  $0.5\ \mu\text{g}$  RNA was taken forward for cDNA synthesis using the SuperScript IV first-strand system (Thermo Fisher). cDNA was generated according to manufacturer's instructions, using random hexamer primers ( $50\ \text{ng}$  per reaction) in a reaction volume of  $20\ \mu\text{l}$ . Controls without reverse transcriptase ( $-RT$ ) controls were included in all experiments to control for the presence of genomic DNA in cDNA preparations.

### 3.10.1.3 qPCR analysis

The expression of specific RNA sequences was determined by interrogating cDNA with gene-specific primers via SYBR Green chemistry. Primers (Table 6) were designed using Primer BLAST (NCBI) according to the following criteria: must span exon-exon junction<sup>1</sup>; primer length 18-30 bases; GC content 35-65%; preferred amplicon size 70-150 bases; range of F/R primer melting temperatures ( $T_m$ )  $< 3^{\circ}\text{C}$ . Specificity for the target gene and absence of self-complementarity and secondary structure were confirmed. Primers were ordered from IDT and on arrival, were re-suspended at  $100\ \mu\text{M}$  in nuclease-free water and stored at  $-20^{\circ}\text{C}$  until use.

For each gene, a master mix was made, containing 2X SYBR Green master mix (Applied Biosystems, Thermo Fisher), and gene-specific forward and reverse primers at a final concentration of  $0.5\ \mu\text{M}$  each.  $18\ \mu\text{l}$  of the master mix was transferred into each well of a MicroAmp Optical 96-well reaction plate (Applied

---

<sup>1</sup> The IFNA1 mRNA is monocistronic, therefore exon junctions could not be considered for this gene. As such, this IFNA1 primer pair cannot discriminate between gDNA and cDNA.

Biosystems, Thermo Fisher). 10% (i.e. 2  $\mu$ l) of the final cDNA product was then added to triplicate wells. In all experiments, water was also used in place of cDNA to act as a 'no template' control (NTC). Plates were briefly centrifuged to ensure that the entire volume was combined, and then sealed using Optical adhesive film (Applied Biosystems).

Analysis was conducted using the ABI 7500 real-time system (Applied Biosystems, Thermo Fisher). 35 cycles were performed, with denaturation step at 95°C (15 seconds) and annealing/extension at 2°C below the lowest primer  $T_m$ . The  $T_m$  selected for multiple-gene plates was the lowest of the range, and genes to be compared were always included on the same plate. Quantification was subsequently performed using the  $\Delta\Delta C_T$  method against a housekeeping gene. For human monocytes, reovirus *S4* (for  $\sigma 3$  protein) (Adair et al., 2012) was compared to the  $\beta$ -actin gene *ACTB*, and cytokines compared to the *YWHAZ* (14-3-3  $\zeta \delta$ ) gene (Vandesompele et al., 2002). In murine tumours, the mouse *GAPDH* gene was used as a comparator for reovirus *S4* copies.

### **3.10.2 RNA analysis by RNAseq**

#### **3.10.2.1 Virus treatment**

PBMC isolation (section 3.1.4) and monocyte selection (section 3.4.1.3) were performed as previously described, from three healthy donors. After washing in HBSS,  $5 \times 10^6$  monocytes were added to universal tubes, and treated with MOI 10 ( $5 \times 10^7$  pfu) reovirus or reo-NAb. After adsorption (4°C, 2-3 hours), cells were washed three times in PBS and re-suspended in 5 ml RPMI-10, then transferred to T25 flasks to incubate (37°C, 24 hours). Flasks were scraped and cells flushed in medium and transferred to 15 ml falcon tubes. After centrifugation (400 g, 5 minutes), pellets were stored at -80°C.

#### **3.10.2.2 RNAseq methodology**

RNA was extracted from the cell pellets as described above for qPCR analysis (section 3.10.1.2) and stored at -80°C. RNA was then transported on dry ice to the Tumour Profiling Unit staff at the Institute for Cancer Research (ICR) in London. Here, samples were subject to DNase I clean-up prior to quality control with Qubit (Thermo Fisher) and Bioanalyzer (Agilent, Shropshire, UK) platforms. mRNA libraries were prepared from each sample using the NEBNext Ultra

Directional RNA library prep kit (New England BioLabs, Hitchin, UK). Libraries were subsequently sequenced using the HiSeq 2500 system (Illumina, Essex, UK) with single-end 50 base pair (SE50) reads, to generate 20-25 million total reads. Fastq files were subsequently analysed in R using the DEseq2 package (Bioconductor). Here, raw count data between groups were normalised to correct for library size and RNA composition bias, then interrogated to generate differential gene expression data. DE genes were identified by statistical significance based on  $\text{padj} < 0.1$ , i.e. Wald test  $p$  value with adjustment for multiple comparisons (Benjamini and Hochberg, 1995).

Significant assistance with transcriptomic profiling and analysis was provided by Nik Matthews, Ritika Chauhan and James Campbell at the ICR.

### **3.11 Imaging**

#### **3.11.1 Electron microscopy**

Imaging of virus or virus-loaded cells was performed by individuals in the group of Prof. Rob Hoeben, and Electron Microscopy staff at the Leiden University Medical Center, including Diana van den Wollenberg, Carolina Jost and Aat Mulder.

##### **3.11.1.1 Visualisation of reo-NAb complexes by EM**

Reovirus stock was added drop-wise to Veco 100-mesh copper grids (Electron Microscopy Sciences, Hatfield, PA, USA) and allowed to attach (RT, 5 minutes). Grids were washed four times in PBS (2 minutes each), prior to incubation with patient serum or control serum, diluted 1:10 in PBS (RT, 90 minutes). After four further washes in PBS, grids were incubated with protein A-conjugated 10 nm gold particles (1:300 in PBS + 1% v/v BSA) (in-house) for 30 minutes at RT. Further washes in PBS (4 x 2 minutes) and ddH<sub>2</sub>O (4 x 1 minute) were performed. Grids were then fixed for 1 hour with 1.5% (v/v) glutaraldehyde (GA) in 0.1 M sodium cacodylate. After further washes in ddH<sub>2</sub>O (4 x 1 minute), grids were negatively stained with 1% (w/v) phosphotungstic acid (PTA) for 30 seconds, then blotted and air-dried. Grids were then visualised using an FEI Tecnai TWIN microscope at 120 kV (magnification 52,000 X).

### 3.11.1.2 Visualisation of virus-loaded monocytes by EM

Negatively selected monocytes (section 3.4.2.1) were pulsed with virus as described (section 3.4.1.4) at MOI 50 (4°C, 3 hours). Monocytes were subsequently washed twice with 15 ml ice-cold PBS and centrifuged (400 g, 5 minutes). 700 µl RPMI-10 was added, and cells allowed to rest at RT for 10 minutes to permit internalisation, prior to addition of 700 µl double-strength fixative – giving final concentrations of 2% (v/v) PFA and 0.2% (v/v) GA in 0.1 M PHEM buffer (Table 7). After centrifuging (300 g, 3 minutes), the supernatant was aspirated and pellets gently re-suspended in 1 ml storage buffer (0.5% w/v PFA in 0.1 M PHEM) and kept at 4°C prior to processing.

For morphological analysis, cell pellets were rinsed in 0.1 M sodium cacodylate buffer (Table 7), then post-fixed with osmium tetroxide solution (1% (w/v) in 0.1 M cacodylate buffer) on ice for 1 hour. Cells were rinsed again and resuspended in 2% (w/v) agar. After solidification, 0.5 – 1 mm<sup>3</sup> blocks were cut and dehydrated using an ascending ethanol series. Blocks were then transferred from 100% ethanol to propylene oxide, and subsequently infiltrated with ascending ratios of LX-112 Epon resin (Ladd Industries, Kettering, OH, USA) to propylene oxide (1 hour each). After 1 hour in pure Epon, fresh Epon was added and polymerised at 70°C for 48 hours. 80 nm sections were made on an Ultracut S microtome (Leica) and visualised with an FEI Tecnai TWIN microscope at 120 kV.

For immunogold labelling, cell pellets were first embedded in 12% (w/v) gelatin in PBS, and 0.5 mm<sup>3</sup> cubes infiltrated with 2.3 M sucrose in PBS for 30 minutes. Cells were then plunge-frozen in liquid nitrogen. 70 nm sections were made using a diamond knife and the Ultracut/FCS machine (Leica, Milton Keynes, UK) at –110°C. Sections were collected on mesh-100 grids and washed with PBS (3 x 4 minutes) and 50 mM glycine in PBS (3 x 4 minutes) to block aldehyde groups. Primary antibody (DSHB mouse anti-σ3 4F2, or isotype control) was added as stated in BSA-PBS (1% w/v) for 1 hour, and grids washed in PBS-glycine (3 x 4 minutes). Anti-mouse secondary antibody was added at 1:200 in BSA-PBS for 1 hour, and grids washed (3 x 4 minutes). Protein A-conjugated 10 nm gold particles were then added at 1:300 in BSA-PBS for 30 minutes. Finally grids were washed with PBS and then ddH<sub>2</sub>O prior to contrasting with uranyl acetate (0.3% (w/v) in 2% (w/v) methylcellulose) on

ice for 5 minutes. Grids were dried in air, prior to visualisation with an FEI Tecnai TWIN microscope (Thermo Fisher) at 120 kV.

### 3.11.2 Confocal microscopy

Monocytes were harvested from fresh PBMC (section 3.4.1.3) and seeded on sterile poly-D-lysine coated coverslips in 24-well plates (Corning) at  $6.5 \times 10^4$  cells per well in 0.5 ml RPMI-10. Cells were allowed to adhere overnight, then chilled and pulsed with reovirus (MOI 2,000) in serum-free RPMI. Virus was allowed to adsorb for 1 hour at 4°C, followed by 2 hours at 37°C; the inoculum was then removed and cells washed once with excess PBS. Fresh RPMI-10 was added, and cells incubated at 37°C as stated prior to washing with PBS and fixing with 4% (w/v) PFA (20 minutes, RT). Fixative was quenched with 0.1 M glycine in PBS, and cells washed three times with PBS. Cells were permeabilised with 0.5% (v/v) Triton X-100 in PBS for 5 minutes, and blocked for 10 minutes with PBS-BGT (0.5% w/v BSA, 0.1% w/v glycine, 0.05% v/v Tween-20).

To stain for reovirus, cells were incubated in the dark with the mouse 4F2 antibody against  $\sigma 3$  (1:200 in PBS-BGT) for 1 hour at RT. After three washes with PBS-BGT, a cocktail of secondary antibodies was added in PBS-BGT: anti-mouse Alexa Fluor 488 (1:500), phalloidin-Alexa Fluor 647 (1:100) and DAPI (1:10,000) (all Thermo Fisher). After a further hour at RT, three PBS-BGT washes were performed and coverslips mounted on slides using 10  $\mu$ l Mowiol (Sigma). Labelled cells were visualised using the A1R confocal laser microscope (Nikon).

### 3.12 In vivo work

All animal experiments carried out at the University of Leeds were approved by the local Animal Welfare and Ethical Review Body and under appropriate Home Office licence (project licence PFD4C5062); those conducted at the Mayo Clinic were approved by the Institutional Animal Care and Use Committee.

Reo-NAb complexes to be employed *in vivo* were formulated using serum obtained from reovirus-immunised mice. These mice (female C57BL/6, 6-12 weeks of age) were given two intraperitoneal (i.p.) doses of reovirus at  $2 \times 10^7$

pfu in 100  $\mu$ l PBS, one week apart. One week after the second dose, mice were sacrificed under terminal anaesthesia and blood obtained by cardiac puncture. After clotting, blood was centrifuged at 800 g for 10 minutes, and serum collected. The neutralising capacity of serum was established as detailed above (section 3.3.2) and neutralising ratios of serum to virus determined. *Ex vivo*-formed complexes were then generated by incubating serum with virus for at least 3 hours (37°C) prior to administration as below.

In a follow-up experiment, a comparison was made between reo-NAb complexes formed using serum from immune mice, and those formed artificially using monoclonal antibodies against reovirus epitopes (DSHB). All complexes used were confirmed as neutralised by standard L929 neutralisation assays. The NAb used for comparison were either G5 alone, or a mAb 'combo' of G5, 10F6, 8H6, 10C1 and 10G10 (directed against epitopes on either  $\sigma$ 1,  $\mu$ 1 or  $\sigma$ 3), all at equal  $\mu$ g doses.

### 3.12.1 Delivery of reovirus to tumours

Female C57BL/6 mice at 6-8 weeks of age (reovirus-naïve) were obtained from Charles River Laboratories. Flank tumours were seeded by sub-cutaneous (s.c.) injection of  $2 \times 10^5$  or  $5 \times 10^5$  B16-F10 melanoma cells, suspended in 100  $\mu$ l PBS. After seven days, mice (3-4 per group) were given three consecutive daily doses of 300 ng recombinant mouse GM-CSF (Peprotech) or PBS by i.p. injection. Subsequently on days 10 and 11, reo-NAb complexes (or PBS) were administered i.v. at a dose of  $2 \times 10^7$  or  $5 \times 10^7$  pfu in a total of 100  $\mu$ l PBS. All mice were sacrificed by cervical dislocation three days after the second infusion, and tumours harvested immediately.

Tumour virus burden was analysed by both plaque assay and qPCR. For plaque assay, tumours were mechanically homogenised in PBS, and the cells in suspension lysed by three freeze-thaw cycles. The functional reovirus titre in these samples was analysed by standard plaque assay on L929 cells (section 3.7). Separately, for RNA analysis, tumour explants were mechanically homogenised in buffer RLT (Qiagen) supplemented with  $\beta$ -mercaptoethanol (to denature RNases). Samples were further homogenised using QIAshredder columns, and RNA extracted from lysates using the RNeasy kit. 1  $\mu$ g total RNA was used for cDNA synthesis and qPCR analysis as described above (section 3.10.1). The number of reovirus *S4* gene copies was compared to mouse *GAPDH* as a housekeeping gene.

### 3.12.2 Analysis of therapeutic benefit

The reovirus-sensitive murine B16tk model was used to maximise detection of therapeutic benefit, and for consistency with a substantiated model (Rajani et al., 2016). Mice were not formally randomised according to tumour burden since tumours were too small to be easily seen prior to therapy. Blinding was not performed as insufficient personnel were available to conduct the process.

Based on detecting an effect size observed in a similar prior experiment with 90% power (at  $\alpha = 0.05$ ), a group size of 8 mice was selected using the G\*power programme (<http://www.gpower.hhu.de/en.html>). Female C57BL/6 mice at 8-10 weeks of age were first pre-immunised with  $2 \times 10^7$  pfu UV-inactivated reovirus ('immune') or PBS ('naïve'). After 11 days, mice were subjected to s.c. flank implantation with  $5 \times 10^5$  B16tk melanoma cells, in 50  $\mu$ l PBS.

After three days, mice were given three daily i.p. doses of 300 ng recombinant mouse GM-CSF (Peprotech, London, UK). On the following two days, PBS, free reovirus or reo-NAb complexes (made using serum) were administered i.v. at a dose of  $1.5 \times 10^7$  pfu in a total of 100  $\mu$ l. Tumours were measured manually three times per week, and mice euthanised when tumour diameter reached 1.5 cm in any direction, or upon tumour ulceration or appearance of clinical symptoms.

### 3.13 Statistical analysis

Data were analysed using GraphPad Prism software. Significance was evaluated using Student's t-test, one-way or two-way ANOVA as appropriate, with  $p < 0.05$  considered significant. Kaplan-Meier curves were assessed by Log-rank test. Where multiple comparisons were performed, corrections were made to adjust for type 1 error; typically using the Holm-Šídák method (t-test) or Dunnett's multiple comparisons test (ANOVA).

<b>Cell type</b>	<b>Origin</b>	<b>Medium</b>	<b>Source</b>
Mel-624	human melanoma	DMEM + 10% (v/v) FCS (DMEM-10)	CRUK
SKmel-28	human melanoma	DMEM-10	CRUK
HCT116	human colorectal carcinoma	DMEM-10	CRUK
Panc-1	human pancreatic carcinoma	DMEM-10	n/a
SU.8686	human pancreatic ductal carcinoma (metastasis)	DMEM-10	ATCC
SKOV3	human ovarian adenocarcinoma	DMEM-10	CRUK
PC3	human prostate adenocarcinoma (metastasis)	RPMI + 10% (v/v) FCS (RPMI-10)	n/a
L929	mouse fibrosarcoma	DMEM-10	ATCC
Vero	African green monkey kidney	DMEM-10	ATCC
B16tk	mouse melanoma	DMEM-10	Richard Vile, Mayo Clinic
B16-F10	mouse melanoma	DMEM-10	ATCC
Primary monocyte cells	healthy donor PBMC	RPMI-10	leukocyte cones (NHSBT)

**Table 1: Cell lines, primary cells and media**

<b>Virus (trade name)</b>	<b>Subtype</b>	<b>Stock titre (pfu/ml)</b>	<b>Source</b>	<b>Susceptible cell line</b>
Reovirus (REOLYSIN)	Orthoreovirus type 3 Dearing	2–5 x 10 <sup>9</sup> (batches titred individually)	Oncolytics Biotech	L929
CVA21 (CAVATAK)	Coxsackievirus type A 21	5 x 10 <sup>8</sup>	Viralytics	SKmel-28
HSV1716 (SEPREHVIR)	Herpes simplex virus type I (ICP34.5 null)	1 x 10 <sup>9</sup>	Virttu Biologics	Vero

**Table 2: Oncolytic viruses employed**

<b>Virus</b>	<b>Antibody source</b>	<b>Source</b>	<b>Treatment regime</b>	<b>Period post last infusion</b>
Reovirus	Serum	In-house (REO-013 Brain trial ISRCTN70443973)	i.v. reovirus - 1 dose of 10 <sup>10</sup> TCID <sub>50</sub> *	2-6 weeks
CVA21	Serum	In-house (STORM trial NCT02043665)	i.v. CVA21 - 3 ascending doses, 1 x 10 <sup>8</sup> – 1 x 10 <sup>9</sup> TCID <sub>50</sub>	3 weeks
HSV1716	Pleural fluid	Virttu Biologics (trial NCT01721018)	intrapleural HSV1716 - 4 doses of 1 x 10 <sup>7</sup> IU	2-6 weeks

**Table 3: Sources of antiviral antibody**

\* 1 x 10<sup>10</sup> TCID<sub>50</sub> is equivalent to 7 x 10<sup>9</sup> pfu (Davis et al., 1972).

Target	Clone	Host / isotype	Type	Stock conc.	Supplier
isotype IgG1 $\kappa$	107.3	mouse IgG1	whole antibody	1 mg/ml	BD
CD64 (Fc $\gamma$ R I)	10.1	mouse IgG1	F(ab') <sub>2</sub> fragment	1 mg/ml	Ancell
CD32 (Fc $\gamma$ R II)	7.3	mouse IgG1	F(ab') <sub>2</sub> fragment	1 mg/ml	Ancell
CD16 (Fc $\gamma$ R III)	3G8	mouse IgG1	F(ab') <sub>2</sub> fragment	1 mg/ml	Ancell
CD89 (Fc $\alpha$ R)	REA234	human - recombinant	whole antibody	1 mg/ml	Miltenyi
isotype IgG1 $\kappa$	MOPC-21	mouse IgG1	whole antibody	1 mg/ml	Biologend
JAM-A	J10.4	mouse IgG1	whole antibody	2 mg/ml	Santa Cruz
CXCR3	G025H7	mouse IgG1	whole antibody	1 mg/ml	Biologend
IFNAR2	MMHAR-2	mouse IgG2a	whole antibody	0.5 mg/ml	PBL

**Table 4: Blocking antibodies used in cell culture**

Target	Clone	Host	Concentration	Supplier
reovirus $\sigma 3$	4F2	mouse	1:200	DSHB
GAPDH	14C10	rabbit	1:1,000	CST
NF- $\kappa$ B p50	H-119	rabbit	1:200	Santa Cruz
RIG-I	D14G6	rabbit	1:500	CST
PKR	13/PKR	mouse	1:200	BD
anti-human IgG / IgA / IgM (HRP)	(secondary)	goat	1:5,000	Thermo
anti-mouse IgG (HRP)	(secondary)	sheep	1:5,000	Sigma
anti-rabbit IgG (HRP)	(secondary)	goat	1:1,000	CST

**Table 5: Antibodies used in western blotting**

Target (gene, if terms differ)	F/R	Sequence (5' – 3')	T <sub>m</sub> (°C)	Product size (bp)
reovirus $\sigma 3$ <i>S4</i>	F	GGGCTGCACATTACCACTGA	59.3	300
	R	CTCCTCGCAATACAACCTCGT	56.0	
CXCL10	F	TCCAGTCTCAGCACCATGAA	56.0	84
	R	AGGTACTCCTTGAATGCCACT	55.8	
IFNA1* (monocistr.)	F	AGGAGGAAGGAATAACATCTGGT	55.3	106
	R	GCAGGGGTGAGAGTCTTTGA	56.8	
MCP-1 <i>CCL2</i>	F	GATGCAATCAATGCCCCAGT	56.1	114
	R	AGCTTCTTTGGGACACTTGC	55.8	
IL-8 <i>CXCL8</i>	F	CACCGGAAGGAACCATCTCA	56.8	109
	R	GGCAAACTGCACCTTCACA	56.5	
EF1A <i>EEF1A1</i>	F	GATTACAGGGACATCCTAGGCTG	57.0	195
	R	TATCTCTCCTGGCTGTAGGGTGG	57.7	
YWHAZ	F	CCTTGCTTCTAGGAGATAAAAAGAA	52.7	134
	R	CTCCTTGCTCAGTTACAGACTTC	55.0	
GAPDH (mouse)	F	ACTGAGCAAGAGAGGCCCTA	57.7	80
	R	TATGGGGGTCTGGGATGGAA	57.7	

**Table 6: Primers used for qPCR**

Human, unless stated otherwise.

MACS buffer	PBS + FCS (1% v/v) + EDTA (20 mM)
FACS buffer	PBS + FCS (1% v/v) + sodium azide (0.1% w/v)
RIPA buffer	Tris (50 mM, pH 8.0) + sodium chloride (150 mM) + EDTA (5 mM) + Triton X-100 (1% v/v) + sodium deoxycholate (0.5% w/v) + SDS (0.1% w/v)
Giordano lysis buffer (GLB)	Tris (50 mM, pH 7.4) + sodium chloride (250 mM) + EDTA (5 mM) + Triton X-100 (0.1% w/v)
SDS-PAGE loading buffer (2x)	Tris (100 mM, pH 6.8) + SDS (4% w/v) + bromophenol blue (0.2% w/v) + glycerol (20% v/v)  DTT added to samples before use, to final concentration of 100 mM
SDS-PAGE running buffer (1x)	Tris (25 mM) + glycine (250 mM) + SDS (0.1% w/v)
SDS-PAGE transfer buffer (1x)	Tris (12 mM) + glycine (96 mM)
ELISA coating buffer (1x)	NaHCO <sub>3</sub> (100 mM) - pH 8.2
PHEM buffer (0.1 M)	PIPES (60 mM) + HEPES (25 mM) + MgCl <sub>2</sub> (2 mM) + EGTA (10 mM) - pH 7.4

**Table 7: Buffers used for magnetic selection, flow cytometry, western blotting, ELISA, and EM**

Target	Fluorophore	Clone	Host	Volume	Supplier
isotype controls	PE	MOPC-21	mouse IgG1	5 µl	BD
	PE	G155-178	mouse IgG2a	5 µl	BD
	PE	MPC-11	mouse IgG2b	5 µl	BD
	PerCP	MOPC-31C	mouse IgG1	5 µl	BD
	APC	11711	mouse IgG1	5 µl	R&D
CD3	PE	HIT3a	mouse IgG2a	5 µl	BD
	PerCP	SK7	mouse IgG1	5 µl	BD
CD4	FITC	RPA-T4	mouse IgG1	5 µl	BD
CD8	FITC	RPA-T8	mouse IgG1	5 µl	BD
CD11b	FITC	ICRF44	mouse IgG1	3 µl	Biolegend
CD14	PE	M5E2	mouse IgG2a	5 µl	BD
CD16	FITC	B73.1	mouse IgG1	5 µl	BD
CD32	PE	2E1	mouse IgG2a	5 µl	Miltenyi
CD54	PE	LB-2	mouse IgG2b	5 µl	BD
CD55	PE	IA10	mouse IgG2a	5 µl	BD
CD56	FITC	NCAM16.2	mouse IgG2b	3 µl	BD
	PE	AF12-7H3	mouse IgG1	5 µl	Miltenyi
CD64	FITC	10.1.1	mouse IgG1	5 µl	Miltenyi
CD69	PE	FN50	mouse IgG1	5 µl	BD
	PerCP	L78	mouse IgG1	5 µl	BD
CD80	PE	L307.4	mouse IgG1	5 µl	BD
CD86	PE	FUN-1	mouse IgG1	5 µl	BD
CD89	unconjugated	REA234	recombinant human IgG1	5 µl	Miltenyi
CD107a	FITC	H4A3	mouse IgG1	5 µl	BD
CD107b	FITC	H4B4	mouse IgG1	5 µl	BD
CD111	PE	R1.302	mouse IgG1	5 µl	Miltenyi

CD112	PE	R2.525	mouse IgG1	5 $\mu$ l	BD
CD317	PE	26F8	mouse IgG1	5 $\mu$ l	Thermo
HLA-ABC	PE	G46-2.6	mouse IgG1	5 $\mu$ l	BD
HLA-DR	PE	G46-6	mouse IgG2a	5 $\mu$ l	BD
HVEM	APC	94801	mouse IgG1	5 $\mu$ l	R&D
JAM-A	PE	1H2A9	mouse IgG2b	5 $\mu$ l	Santa Cruz
reovirus $\sigma$ 3	unconjugated	4F2	mouse	50 $\mu$ l	DSHB
human IgG (H&L)	unconjugated	-	rabbit polyclonal	5 $\mu$ l	Thermo
mouse IgG	FITC	-	goat polyclonal	0.5 $\mu$ l	BD
rabbit IgG (H&L)	AF-594	-	goat polyclonal - F(ab') <sub>2</sub>	0.1 $\mu$ l	Thermo
human IgG	PE	-	goat polyclonal	5 $\mu$ l	Bio-Rad

**Table 8: Antibodies used for flow cytometry**

Target	Antibody	Dilution	Diluent	Host	Supplier
CXCL10	capture	1:180	PBS	mouse	R&D Systems
	detection	1:180		goat	
IL-29	capture	1:180	PBS	mouse	R&D Systems
	detection	1:180		goat	
CCL5/ RANTES	capture	1:250	coating buffer	mouse	R&D Systems
	detection	1:500		goat	
TRAIL	capture	1:180	PBS	mouse	R&D Systems
	detection	1:180		goat	
IFN- $\alpha$	capture	1:250	PBS	mouse	Mabtech
	detection	1:1,000		mouse	
TNF	capture	1:1,000	coating buffer	mouse	BD
	detection	1:1,000		mouse	

**Table 9: Antibodies used for ELISA**

Target	Standard range	Supplier
CXCL10	2,000 – 15.6 pg/ml	R&D Systems
IL-29	4,000 – 31.3 pg/ml	R&D Systems
CCL5/RANTES	1,000 – 7.8 pg/ml	R&D Systems
TRAIL	1,500 – 11.7 pg/ml	R&D Systems
IFN- $\alpha$	5,000 – 39.1 pg/ml	Peprtech
TNF	2,000 – 15.6 pg/ml	R&D Systems

**Table 10: Protein standards used for ELISA**

## 4. Formation of reovirus-antibody complexes

### 4.1 Introduction

Independent of the use of the type 3 Dearing strain as a clinical agent, reovirus types 1-3 are ubiquitous, naturally-occurring strains in the environment (Lee and Jeong, 2004; Spinner and Di Giovanni, 2001). Further, while it has only sporadic association with significant clinical disease, humans are routinely exposed to the virus at the mucosal interface of the gastrointestinal and respiratory tracts. Consequently, seropositivity for reovirus in the general population is considerable. Infection commonly occurs in childhood, with approximately half of five-year-olds showing seroconversion (Leers and Rozee, 1966; Pal and Agarwal, 1968; Selb and Weber, 1994; Tai et al., 2005). Exposure increases with age, with 60-100% of older adults showing serological evidence (Lerner et al., 1962; Minuk et al., 1987, 1985; Selb and Weber, 1994).

A number of early-phase clinical trials have involved the administration of OV as a large intravenous (i.v.) bolus. Seen in the context of a pre-existing low-level immunity to the virus, these therapeutic infusions represent a re-exposure to abundant viral antigens and result in a large-scale anamnestic response. This is characterised by the rapid generation of antiviral antibodies in circulation at very high titre (Vidal et al., 2008; White et al., 2008).

Antibodies are considered a key component of the evolutionarily conserved humoral response, which cannot discriminate therapeutic from pathogenic viruses. Antibody production arises upon the presentation of viral antigen to B cells via specific immunoglobulin receptors. The synthesised antibodies function principally by binding directly to pathogens and – in the case of viruses – frustrating their binding, uptake and/or uncoating during the infection process. The resulting reduction in viral infectivity is termed neutralisation. Separately, although some antibodies may be non-neutralising based on direct infectivity, they may retain other protective functions; opsonising antibodies may be able to trigger more complex immune effector functions such as antibody-dependent cellular cytotoxicity (ADCC) or phagocytosis (ADCP).

## 4.2 Reovirus neutralisation by patient-derived serum

Prior to assessing any immunomodulatory effects of anti-reovirus antibodies, the neutralising capacity and class of reovirus-specific antibodies in cancer patients was characterised. In order to do this, serum samples were obtained from patients enrolled in the REO-013 Brain trial. These patients received i.v. reovirus as monotherapy, 3 to 17 days prior to surgical resection of primary brain tumours or metastases in the brain (Samson et al., 2018). Reovirus was administered as a single dose of  $1 \times 10^{10}$  TCID<sub>50</sub> (i.e.  $7 \times 10^9$  pfu (Davis et al., 1972)) each, and blood samples taken within two months of the infusion. Some were taken around the time of surgery (approximately 1-2 weeks post-infusion), while others were taken during the following month. Patient-derived serum (hereafter PS) was obtained by allowing the blood sample to clot, followed by centrifugation and harvest of the cell-free fraction.

Initially, the presence of reovirus-binding immunoglobulins (Ig) in PS was confirmed. As an *in vitro* model of i.v. reovirus infusion, PS – or control serum (CS) taken from untreated healthy donors – was combined with virus at a ratio of  $10^6$  pfu per 1  $\mu$ l serum and incubated at 37°C for 3 hours. The virus-serum suspension was subsequently incubated with beads conjugated to protein A, which binds to human IgG1, IgG2, IgG4, IgA and IgM, but not IgG3. The beads were used in order to immunoprecipitate (IP) antibodies and their binding partners, which were subsequently interrogated for reovirus by SDS-PAGE and western blot. The presence of virus-binding antibodies in PS was confirmed by positive identification of the reovirus  $\sigma 3$  protein in the IP fraction from PS but not CS (Figure 4.2.1a). When virus alone (i.e. without serum) was incubated with beads, no signal was detected, indicating that reovirus does not bind to the beads.

Following the detection of *ex vivo*-formed reo-NAb, the possibility of detecting reo-NAb in circulation shortly after i.v. administration of virus was assessed. Serum obtained from reo-treated patients 24 hours post-infusion (PS-24hpi) was not combined with further virus *in vitro*, but was directly subjected to purification with protein A beads. The IP fraction was subjected to SDS-PAGE and western blot. While a band corresponding to reovirus  $\sigma 3$  was detected in the positive control, such a band was absent in IP samples from PS-24hpi, even with lengthy membrane exposure (Figure 4.2.1b). This indicates that reo-NAb complexes are either absent or at a level below the limit of detection in patient serum one day after i.v. virus administration.

Having confirmed the binding of patient serum antibodies to the reovirus particle, in order to prove their neutralising capacity a colorimetric viability assay was employed (MTT assay) (Mosmann, 1983). Briefly, this involves testing halving dilutions of sera for their ability to prevent reovirus infection of L929 mouse fibroblasts, which are acutely sensitive to reovirus. After a 48-hour incubation, viability of the treated cell population can be inferred from their metabolic activity.

First, serum samples from two reovirus-treated patients were compared to serum samples from two healthy controls. As shown in Figure 4.2.2, PS demonstrated considerably higher neutralising capacity compared to CS – evidenced by the right-shift of the neutralisation curve. The  $ND_{50}$  values, an illustration of neutralising capacity, indicate that PS exceeds CS by approximately 100-fold in this regard.

Six patient serum samples taken at various times following infusion were then compared. Notably, the sera obtained from patients shortly (1-3 weeks) after their last virus infusion appeared more neutralising than those obtained after 5 or 6 weeks (Figure 4.2.3). Indeed, serum 1 & 4 and 2 & 6 respectively were actually taken at different time points from the same patient, which illustrates the drop-off in anti-reovirus NAb in the weeks following administration.

Alongside the antibody compartment, the other pivotal component of humoral immune surveillance is the complement system. Elements of the complement network have various antimicrobial functions: from their ability to directly lyse or neutralise viruses (Spear et al., 1993; Sullivan et al., 1998), to their role as a 'danger signal' heralding innate clearance processes such as complement-dependent cytotoxicity (Terajima et al., 2011). Indeed, in some circumstances, complement is crucial in bridging innate and adaptive immunity during the antiviral response (Da Costa et al., 1999; Kopf et al., 2002). Further, in the context of an oncolytic virus, complement inhibition was recently shown to substantially diminish neutralisation of the enveloped vaccinia virus in a range of *in vitro* and animal models (Evgin et al., 2015).

This paper suggested that complement also plays a significant role in the neutralisation of reovirus. Therefore, after confirming the presence of complement activity in patient serum samples using a haemolytic  $CH_{50}$  assay (data not shown), this concept was investigated; a basic assay was used, predicated upon the heat-labile nature of complement, in which patient serum was heat-inactivated (HI) at 56°C for 30 minutes prior to analysis by neutralisation assay. Figure 4.2.4 shows that HI-serum demonstrated equivalent

neutralising capacity to otherwise untreated serum, suggesting that heat-labile factors such as complement are not fundamental to reovirus neutralisation *in vitro*.

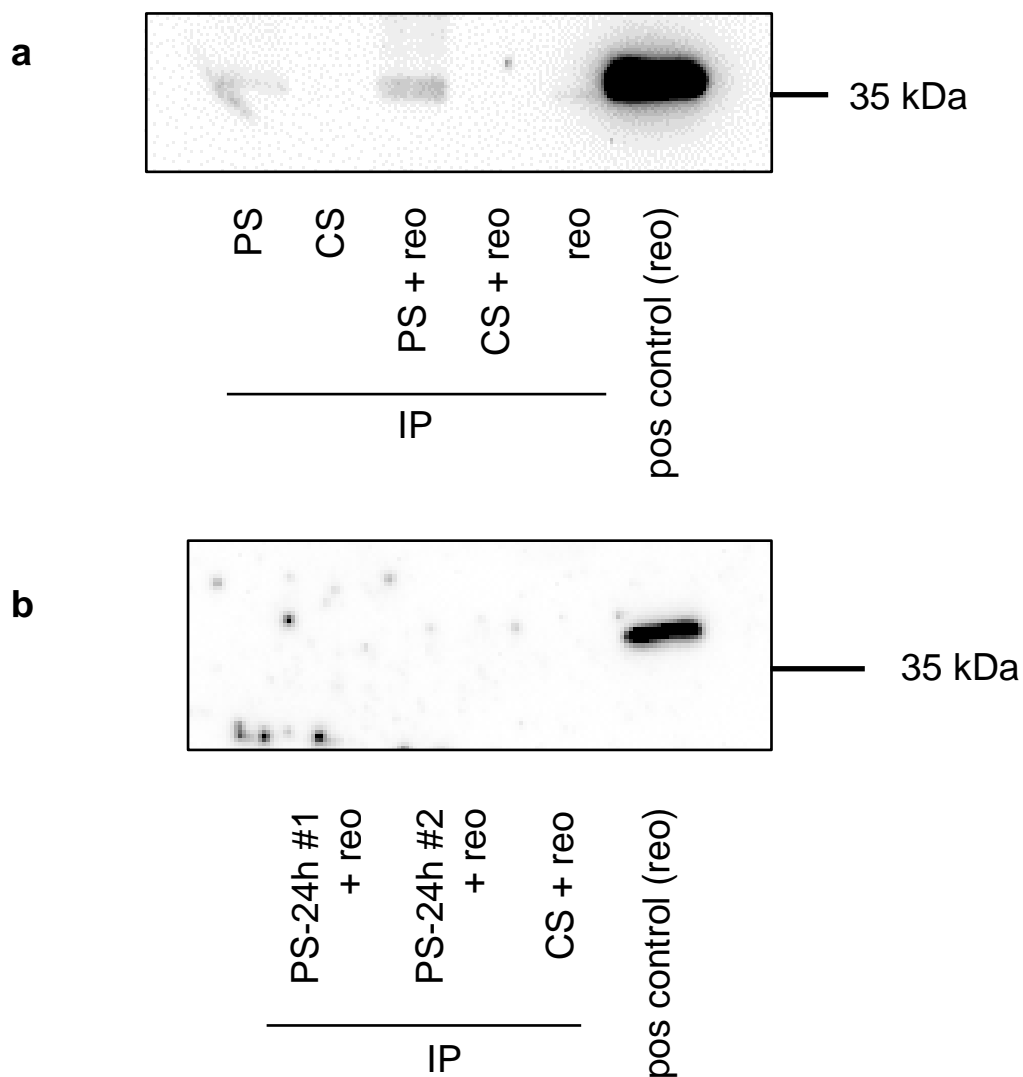
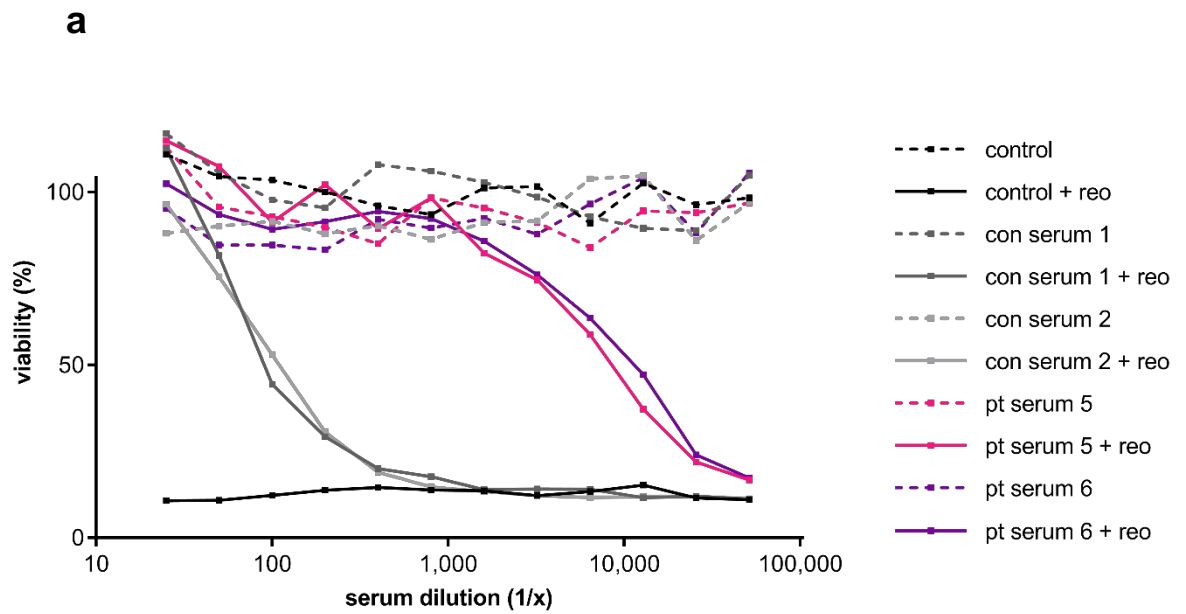


**Figure 4.2.1 Western blot for reovirus  $\sigma 3$  protein from IP fraction of serum**

(a) 20  $\mu$ l of patient (PS) or control serum (CS) was mixed with  $20 \times 10^6$  pfu exogenous reovirus (+ reo), and then antibodies immunoprecipitated (IP) using protein A-beads. Equal amounts of protein (20  $\mu$ g) from IP fractions were then subjected to SDS-PAGE, transferred to nitrocellulose, and probed for exogenous reovirus  $\sigma 3$ . Neat reovirus (no IP), added directly to the gel after boiling, was used directly as a positive control (far right lane).

(b) Two patient sera taken 24 h.p.i. (#1 and #2) or control serum (CS) were directly combined with protein A-beads to IP the antibody fraction, prior to SDS-PAGE, transfer, and blotting as above. Both blots shown are representative of two replicate assays.



**b**

Condition	ND <sub>50</sub> (1/x)
con serum 1	92.6
con serum 2	113.2
pt serum 5	8,940.9
pt serum 6	11,954.4

**Figure 4.2.2 Reovirus neutralisation by control or patient-derived sera**

100  $\mu$ l of halving dilutions of control (con) or patient (pt) sera (1/25 - 1/51,200) or DMEM-10 (control) were added to  $2.5 \times 10^4$  L929 target cells in advance of the addition of reovirus at MOI 0.05. **(a)** Cell viability was determined by MTT assay after incubating for 48 hours. **(b)** 50% neutralising dose calculations were made by interpolating between points in (a). The assay was performed twice.

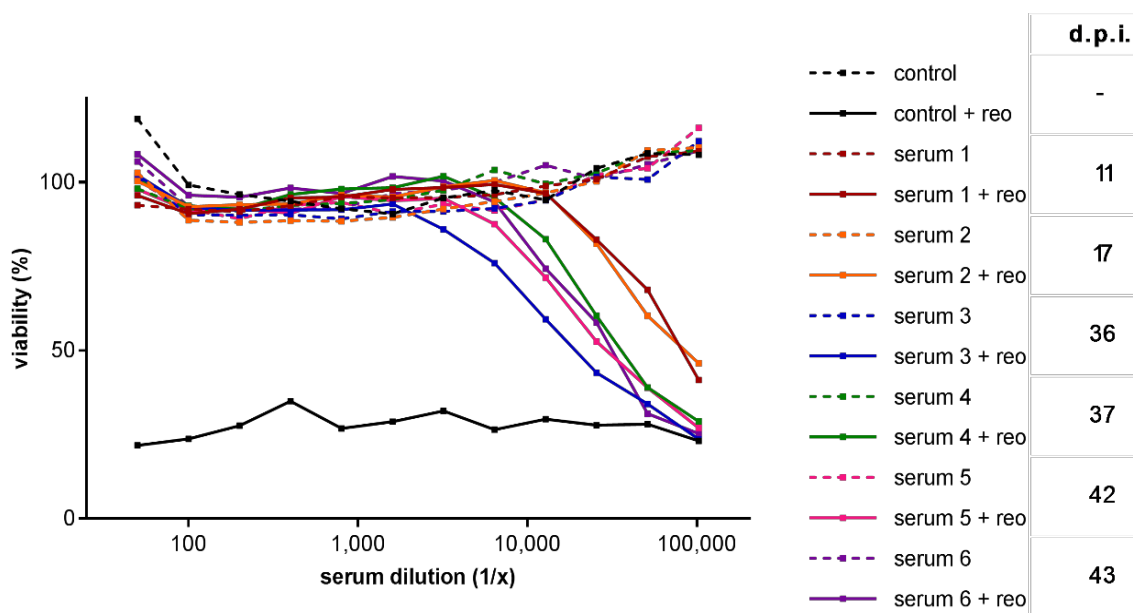


**Figure 4.2.3 Reovirus neutralisation by patient-derived sera**

100  $\mu$ l of halving dilutions of various patient sera (1/50 - 1/102,400) or DMEM-10 (control) were added to  $2.5 \times 10^4$  L929 target cells in advance of the addition of reovirus at MOI 0.05. Cell viability was determined by MTT assay after incubating for 48 hours. The time between patients' therapeutic dose of virus and the time serum was obtained is referred to as days post-infusion (d.p.i.). Paired samples (same patient, different time points) are samples 1 & 4 and 2 & 6. The assay was performed twice.

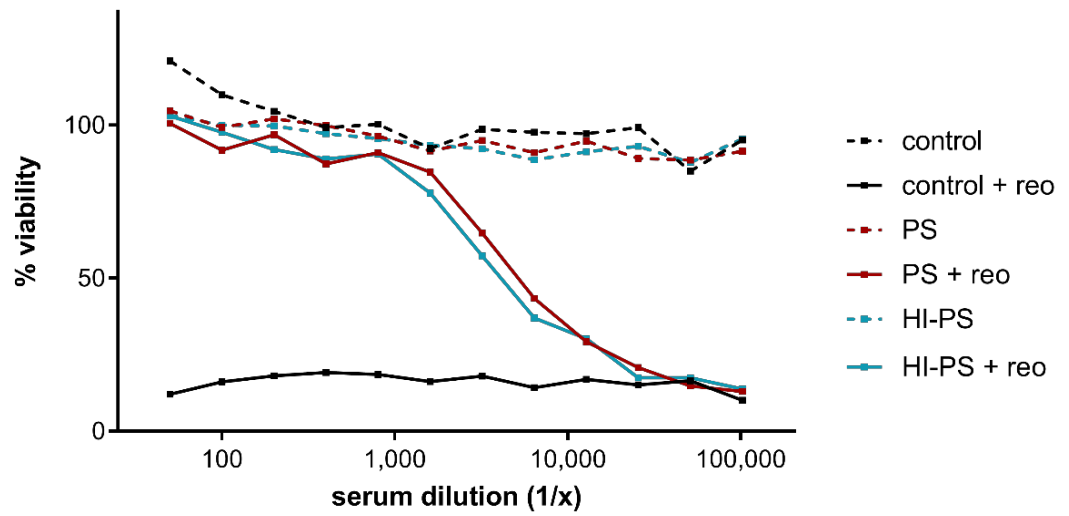


**Figure 4.2.4 Influence of heat-labile factors in reovirus neutralisation**

Patient serum was either heat-inactivated at 56°C for 30 minutes (HI-PS) or not (PS); halving dilutions were made in DMEM-10 and 100 µl added to wells containing  $2.5 \times 10^4$  L929 target cells. Reovirus was added in a further 100 µl of DMEM to an MOI of 0.05. After 48 h incubation at 37°C, cell viability was determined by MTT assay as previously described. Plot is representative of two patient sera.

### 4.3 Characterisation of specific mediators of neutralisation

The previous data indicated the importance of circulating antiviral antibodies to reovirus neutralisation *in vitro*. Next, further insight into the breadth of the humoral response to reovirus in these patients – both in terms of the virus proteins detected and the types of antibody involved – was obtained.

The B-cell antigen receptor (BCR) is a cell-surface immunoglobulin (Ig) which confers antigen specificity on B cells. Only antigens which are able to bind the BCR with sufficient affinity are capable of stimulating B cell proliferation and differentiation, and concomitant antibody production. This tight specificity means that the viral proteome recognised by serum Ig can provide an informative guide as to the antigens ‘visible’ to circulating immune cells.

An unorthodox approach was taken to analysing the antibody repertoire present in patient-derived serum. First, lysates were made from mock- or reovirus-infected mouse and human cell lines. After separation of the protein content of lysates by electrophoresis and transfer to nitrocellulose membranes, PS was employed as a primary antibody to probe the blot. The serum antibodies recognising reovirus proteins were then detected using a secondary antibody against human IgG. As shown in Figure 4.3.1a, a variety of proteins are identified in reovirus-infected – but not uninfected – lysates, indicating that these are indeed virus-specific. No proteins were detected when CS was used instead, demonstrating the abundance of antiviral antibodies in patient blood (data not shown).

Based on molecular weight, the individual bands match well with individual members of the reovirus proteome, with structural proteins of the  $\mu$  and  $\sigma$  families most strongly represented. Although it appears that the  $\mu 1/\mu 1c$  protein attracts the largest antibody response, given that the stoichiometry of proteins in the reovirus virion (and thus on the blot) is not equal, it is not possible to draw accurate conclusions as to the ‘most immunogenic’ proteins (Coombs, 1998). Interestingly it appears that  $\sigma 3$ , at 41 kDa the smallest of the 10 proteins in T3D and a major element of the capsid, is not detected by PS in this assay, with the two bands nearby probably corresponding to  $\sigma 1$  (49 kDa) and  $\sigma 2$  (47 kDa). It was confirmed that the protein itself was present on the blot using the specific monoclonal antibody 4F2 (Figure 4.3.1b). This raises the intriguing prospect that patients do not generate antibodies against  $\sigma 3$ . However, perhaps more likely is the explanation that this assay was insufficiently sensitive to detect

them, or that such antibodies may recognise conformational epitopes on  $\sigma 3$  that are eliminated in the context of a denaturing western blot.

To more accurately identify the specific molecular players in the neutralisation process, the involvement of different antibody classes was examined. IgG is the predominant class present in serum (~ 80%), with only IgA (~ 15%) also present to any significant degree (Gonzalez-Quintela et al., 2008). Although rapidly generated, the IgM pentamer is less common (~ 5%) and has a shorter half-life than IgG due to constant IgG salvage by the neonatal Fc receptor, FcRn (Kim et al., 2007). The monomeric IgG is thought to play the major role in neutralising pathogens in circulation, whereas IgA – dimeric in secretions and monomeric in blood – is largely secretory and thus typically operates at the mucosa (Delacroix et al., 1982). Further, IgG is the main class induced during an anamnestic response (Godfrey et al., 1969; McDermott et al., 1990); relevant given that patients had likely been previously exposed to reovirus. Consequently it was hypothesised that IgG will represent the primary neutralising source over the other classes.

To obtain a qualitative assessment of the presence of antiviral Ig classes in patient serum, the existing western blot approach was modified with secondary antibodies restricted to human IgG, IgA or IgM. These revealed the presence of anti-reovirus IgG and IgA, while IgM was not detected (Figure 4.3.2). Exposure times were kept low to avoid potential non-specific background. To confirm antibody class specificity, pure human IgG was run on the same blots; only the secondary antibody against IgG (and not IgA) reacted in this lane, indicating that antiviral IgA are indeed present in PS.

Following this preliminary assay, a more quantitative measure of class contribution to neutralisation was required. This was evaluated by depleting IgG and IgA from PS by targeting their class-specific heavy chains. PS was incubated with agarose-conjugated antibodies targeting the  $\gamma$ - or  $\alpha$ -chain, and then centrifuged. Depletion was confirmed by ELISA, with levels of IgG or IgA respectively below the detection limit of the assay (data not shown). The neutralising capacity of depleted and intact serum samples were compared by the MTT assay previously described. As expected, extraction of IgG considerably reduces neutralisation, with IgA depletion exerting a more minor effect (Figure 4.3.3). Dual IgG/A depletion almost entirely abrogated neutralisation. Thus, as expected, reovirus neutralisation is a predominantly IgG-mediated phenomenon, yet IgA does appear to contribute.

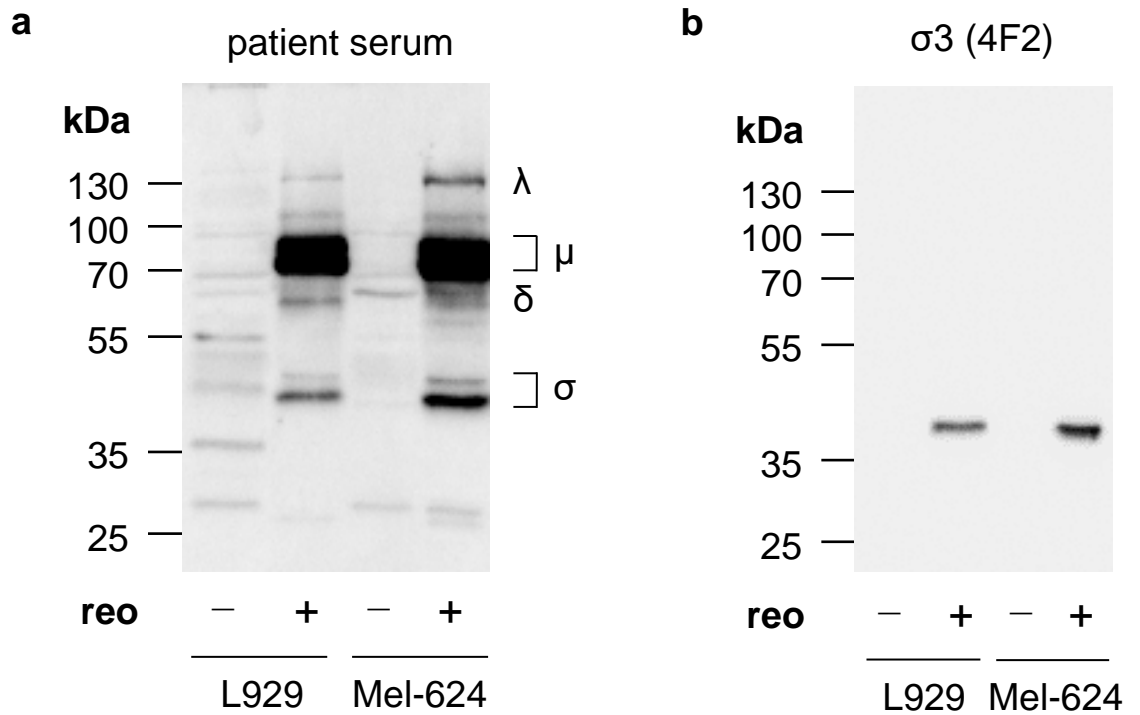


**Figure 4.3.1 The reovirus-binding antibody repertoire of patient serum**

Lysates from mock or reovirus-infected L929 or Mel-624 cells were analysed by SDS-PAGE and western blot, with protein concentrations equalised.

(a) Membranes were probed with patient serum (1:200) and a secondary antibody against human IgG (1:5,000). The reovirus proteins bound by patient serum antibodies are indicated. Blots are representative of four patient sera.

(b) Membranes were probed with the 4F2 antibody against reovirus  $\sigma$ 3 (1:200) and a secondary antibody against mouse IgG (1:5,000).

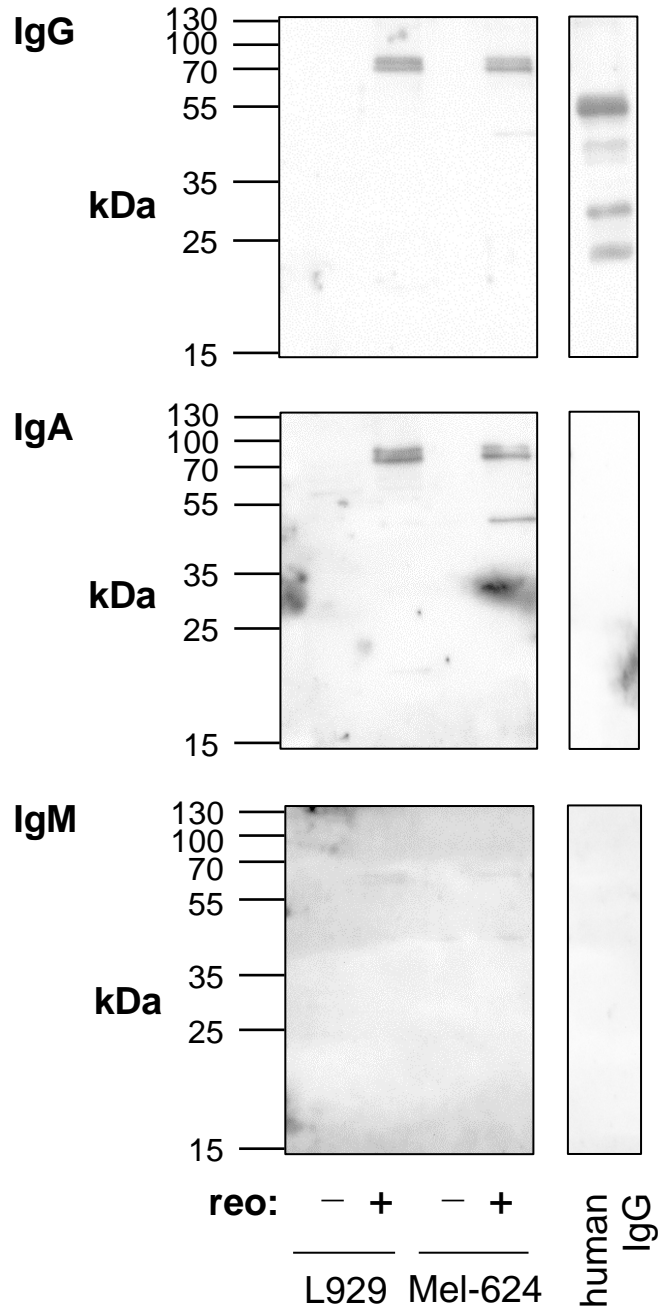


**Figure 4.3.2 Western blot for serum antibody classes binding to reovirus**

Mock or reovirus-infected lysates were interrogated as before, using patient serum as a primary antibody (1:200). Blots were then probed with secondary antibodies against human IgG, IgA or IgM (1:25,000) as indicated. Blot exposures were equal. Human IgG was also included in one lane to confirm the specificity of secondary antibodies to Ig classes. Blots shown were produced using the same serum sample, and are representative of three patient sera.

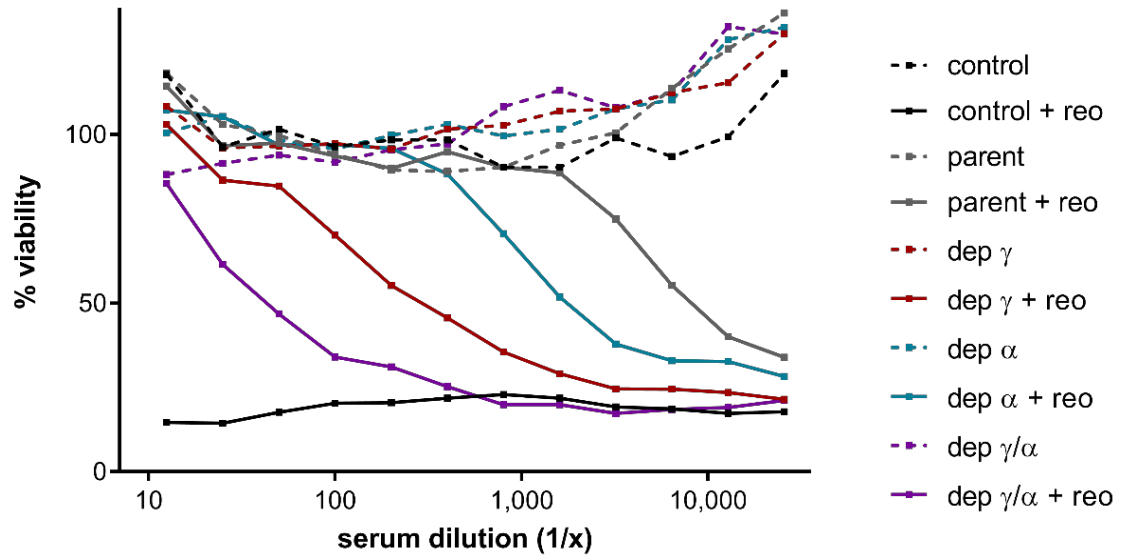


**Figure 4.3.3 Serum antibody classes mediating reovirus neutralisation**

IgG or IgA were specifically depleted from patient serum using agarose-conjugated antibodies against the  $\gamma$ - or  $\alpha$ -chain of IgG or IgA respectively, or both (dep  $\gamma/\alpha$ ). Depleted (or intact) sera were serially diluted and tested for neutralising capacity against reovirus on L929 targets.

#### 4.4 The interaction of virus with anti-reovirus antibody to form complexes

Having demonstrated that Ig in serum was able to bind to and neutralise reovirus, a visual representation of this interaction was obtained using electron microscopy (EM). Virus was allowed to adhere to EM grids, which were incubated with PS or CS and then labelled with protein A-gold. A higher proportion of virions were gold-labelled when pre-incubated with PS (76%) as opposed to CS (40%) (Figure 4.4.1a). This difference was found to be statistically significant at  $p < 0.01$  by  $\chi^2$  test ( $\chi^2 = 92.9$ , cut-off 6.6 where  $df = 1$ ). This demonstrates the extensive binding of PS neutralising antibodies (NAb) to the virion, hereafter termed a reovirus-neutralising antibody (reo-NAb) complex, as depicted in the representative micrographs (Figure 4.4.1b). The lower degree of labelling with CS present is consistent with the presence of residual NAb in the wider population.

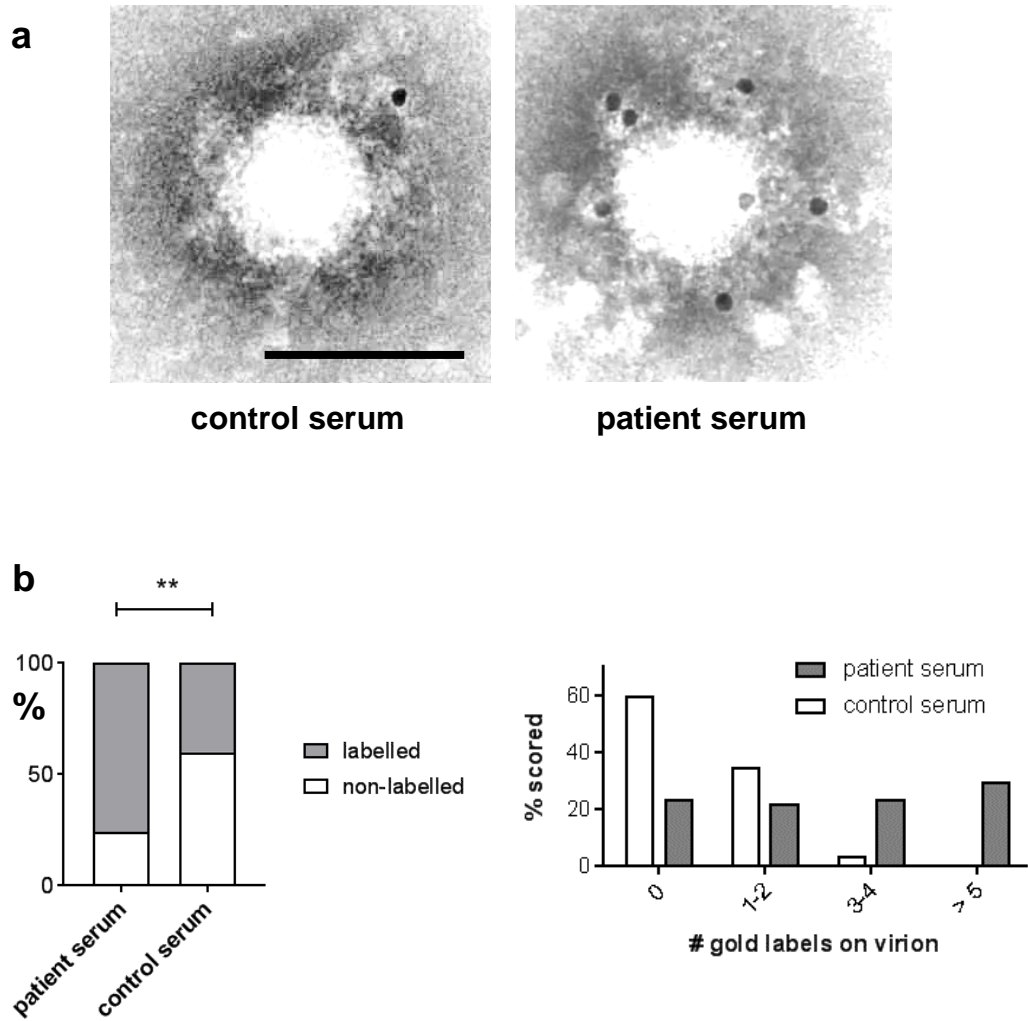


**Figure 4.4.1 Immunogold labelling of reovirus-bound antibodies from serum**

Reovirus was bound to copper grids prior to incubation with CS or PS, and subsequent labelling with protein A-gold (10 nm). Preparations were fixed and negatively stained with PTA, then visualised at 52,000 X magnification by TEM. (a) Representative micrographs of labelled virions (large white area), demonstrating typical gold labelling patterns (small dark circles). Scale bar = 100 nm.

(b) Quantification of the percentage of virions labelled, or the number of gold labels on individual virions.  $n > 340$  virions for each condition.

\*\* indicates significance at  $p = 0.01$  by  $\chi^2$  test (df = 1).

## 4.5 Summary

Intravenous delivery of an oncolytic virus represents not only the optimal means of accessing disseminated neoplastic tissue, but also likely the most practical way of stimulating a systemic response from the immune system. However, this route of infusion is often eschewed in favour of more local methods given the many 'hurdles' to viral persistence present in the vasculature; one prominent obstacle being neutralising antibodies (NAb).

Anti-reovirus antibodies in patient serum are highly neutralising *in vitro*. Based on the highest serum dilution at which 50% of susceptible cells remain viable, the neutralising capacity of patient serum is considerably higher than that of a representative control sample, and is consistent with the 100- to 1,000-fold increase in NAb titre observed in previous reovirus trials (White et al., 2008).

There was no evidence for the involvement of the complement system in reovirus neutralisation, with heat-inactivation of serum generating no overt effect. While supporting previous data indicating no role for complement in reovirus neutralisation in ascites (Jennings et al., 2014), this contradicts a recent study in which an inhibitor of the complement C3 molecule was shown to significantly preclude reovirus neutralisation in plasma (Evgin et al., 2015). The basis for this disparity is unclear. This study employed a different strategy of disabling complement (HI vs inhibitor) and output method (MTT assay vs plaque assay), and used serum rather than anticoagulant-treated plasma; all of which could interfere with the outcome.

Comparison of six different serum samples, including two sets of paired samples, yields an insight into the temporal variation in patient NAb titre. Peak titre appears to occur within 1-3 weeks of infusion, with NAb levels diminishing somewhat beyond five weeks. This reflects the findings of existing trials, wherein maximal titres are reached within two weeks (Gollamudi et al., 2010; White et al., 2008). Although no pre-treatment samples were available, this rapid generation of NAb upon infusion resembles a secondary response, supporting the notion that these specific patients had experienced prior exposure to the virus.

The anamnestic response is dominated by high-affinity IgG, and it was hypothesised that this antibody class would form the chief defence against the virus. Western blot analysis revealed the presence of reovirus-specific IgG and IgA in patient serum. IgM was not detected; a more sensitive method such as

an indirect ELISA (Selb and Weber, 1994; Tai et al., 2005) would be required to conclusively prove its absence.

As expected, IgG was found to play the most substantial role in neutralisation, albeit with a significant auxiliary role for IgA. This is consistent with the conclusion inferred from epidemiological studies that reovirus infection stimulates a specific IgA response that is not long-lived (Selb and Weber, 1994). Further, with any prior reovirus exposure in these patients presumably at the respiratory or gut mucosa, memory B cells in circulation are more likely to be IgA-secreting. These may represent a cell pool primed – upon i.v. reovirus – to differentiate into IgA-secreting plasma cells, thus generating a serum antibody reaction somewhat polarised towards IgA. Nevertheless this bispecific antibody response to the virus is of relevance when considering the ability of reo-NAb to interact with certain immune populations.

As seroprevalence for reovirus is common, in most individuals any i.v.-administered virus will encounter low-level NAb. This was recapitulated using a crude *in vitro* model, in order to make a visual and functional assessment of the proteins binding the virus. It was hypothesised that, in contrast to controls, patients treated with a massive, non-physiological dose of virus will develop a ‘hyper-immune’ NAb response. Electron microscopy demonstrated that patient-derived serum does indeed boast an enriched quota of virus-binding antibodies. The presence of these antibodies is further evidenced by their ability to immunoprecipitate reovirus when added exogenously. These assays substantiate the concept of a ‘reo-NAb’ immune complex.

Interestingly, it was not possible to detect endogenous reo-NAb in patient serum by the same immunoprecipitation method. While this may be due to insufficient assay sensitivity, it appears that levels of free reovirus in serum do decline sharply after administration. In the serum of most patients in the REO-013 trial – the precursor to REO-013 Brain – the viral genome could not be detected more than 24 hours beyond infusion (Adair et al., 2012). Virus can however be retrieved from blood mononuclear cells after i.v. infusion in both mice and humans (Adair et al., 2012; Ilett et al., 2014), a finding influential to the ‘virus hitch-hiking’ tenet discussed later.

In summary, this chapter confirms the potent neutralising capacity of serum from reovirus-treated patients. IgG and IgA readily coat the surface of the virion, forming a reo-NAb complex. The influence of these reo-NAb complexes on immune and cancer cells is the topic of the following chapters.

## 5. Delivery of reovirus for tumour cell oncolysis by primary human monocytes

### 5.1 Introduction

The field of oncolytic virotherapy is predicated upon the ability of some viruses to specifically infect, replicate in and kill malignant cells, whilst leaving other cells unharmed. This viral tropism is reliant on exploiting the aberrant pathways underpinning the enhanced survival and growth of a cancer cell.

The selectivity of reovirus for transformed cells was first demonstrated four decades ago (Duncan et al., 1978; Hashiro et al., 1977), and the virus has represented a leading clinical candidate ever since the resurgence of the field in the 1990s. Reovirus demonstrates cytopathic activity against a broad array of tumour cell types, both *in vitro* and in pre-clinical animal models. Consequently the virus has been deployed in an international clinical development programme spanning over ten indications, with one phase III trial conducted ([www.oncolyticsbiotech.com](http://www.oncolyticsbiotech.com)).

Initial phase I trials were based on intratumoural delivery of reovirus, but this has since been supplanted by intravenous (i.v.) administration as the preferred approach to treating disseminated, metastatic disease. Although a highly practical approach, systemic delivery does present its own barriers to effective virotherapy. Many of these are unique to the vasculature: the humoral immune system for example is a highly evolved pathogen surveillance system, seemingly at odds with even a 'benign' virus.

Loading virus on to 'carrier' immune cells represents one approach to evading complement and NAb as defensive mediators (Ilett et al., 2009; Jennings et al., 2014). For instance, reovirus can be successfully delivered to tumours by loading dendritic cells (DC) or T cells *ex vivo*, even in the context of pre-existing antiviral immunity (Ilett et al., 2011, 2009). This is consistent with the findings of the translational REO-013 trial, in which systemically delivered virus accessed colorectal liver metastases despite NAb at baseline (Adair et al., 2012).

Reovirus was associated with circulating immune cells but not found in plasma, indicating that while virus is swiftly neutralised in serum, a substantial fraction is conveyed to tumours by blood cell 'hitch-hiking'. Reovirus also accessed brain tumours following a single i.v. infusion in REO-013 Brain trial patients, from

whom reovirus-immune serum was obtained for this study (Samson et al., 2018).

Consequently, the potentially costly and impractical *ex vivo* loading approach has been adapted in order to investigate the concept of loading carrier cells with virus *in vivo*. As systemically delivered reovirus in mice associates primarily with the myeloid fraction (Ilett et al., 2014), this compartment was targeted for expansion using the cytokine granulocyte macrophage colony-stimulating factor (GM-CSF). Mobilising the myeloid CD11b<sup>+</sup> population prior to i.v. reovirus administration translated into effective virotherapy in a B16 melanoma model (Ilett et al., 2014). Alongside NK cells, monocytes were essential for therapy. Crucially, the efficacy of this pre-conditioning regime was only manifested in mice that had been pre-immunised with reovirus and thus carried significant antiviral NAb titres, consistent with a pro-therapeutic role for NAb.

It was intended to translate these findings into the human setting, employing patient-derived sera and primary human monocytes to model systemic reovirus treatment for melanoma *in vitro*.

## 5.2 Susceptibility of melanoma targets to reovirus

Historically, metastatic melanoma treatments have been of extremely limited efficacy and prognoses poor. Conventional chemotherapy is gradually being surpassed by targeted and immunotherapy agents giving improved frequency and duration of response, with OV an emerging modality. The typical mutation status (MAPK pathway activation) of melanoma makes it an excellent target for direct lysis by reovirus in particular; its neopitope burden, and thus immunogenicity, render it vulnerable to subsequent elimination by effector T cells.

The potential for lytic elimination of melanoma cells by reovirus was first examined. Flow cytometry was used to confirm that JAM-A, the cognate receptor for reovirus, is abundantly expressed on the surface of resting melanoma cells, using Mel-624 as a representative cell line and the JAM-A clone 1H2A9 (Table 8) (Figure 5.2.1).

The susceptibility of two well-characterised melanoma cell lines to reovirus was subsequently evaluated. The virus was added to sub-confluent cultures of Mel-624 or SKmel-28 melanoma cells at a multiplicity of infection (MOI) ranging from

$10^{-5}$  to  $10^1$  plaque-forming units (pfu) per cell. Cytotoxicity was evaluated after 48 or 72 hours by the MTT viability assay described previously (section 3.3.2).

Reovirus exhibits similar cytotoxicity profiles against both cell lines tested (Figure 5.2.2). After 72 hours, the virus completely eradicates viable cells when added at MOI 0.1, and even at MOI 0.001 is able to reduce viability to approximately half that of mock-treated cells.

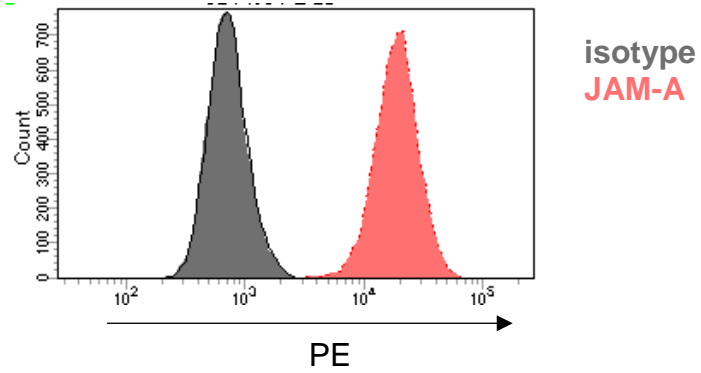


**Figure 5.2.1 Surface expression of JAM-A by Mel-624 cells**

Mel-624 cell monolayers were harvested and stained with PE-conjugated antibodies against the reovirus receptor JAM-A, or a PE-conjugated isotype control. Cells were then washed and fixed, and PE staining analysed by flow cytometry. Histogram is representative of two repeats.

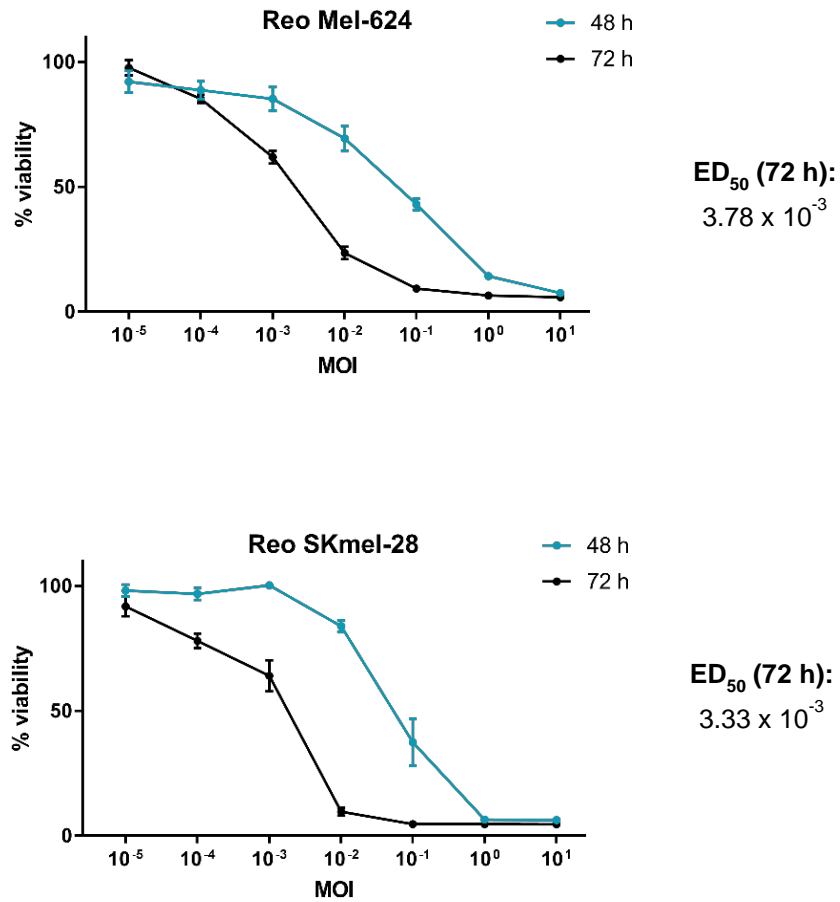


**Figure 5.2.2 Susceptibility of melanoma cell lines to reovirus**

Subconfluent monolayers of Mel-624 and SKmel-28 cell lines were treated with reovirus at stated MOIs for 48 or 72 hours. Cell viability was calculated by MTT assay and normalised to untreated controls at 100%. Values were obtained from four technical replicate wells for each condition.

ED<sub>50</sub> = the MOI at which cell viability is 50% after 72 hours in culture.

### 5.3 *In vitro* hand-off assay

Having confirmed its cytotoxic potential against human melanoma cell lines, reovirus was further investigated in the context of immune cell carriers. This same virus was employed previously to describe the ability of murine myeloid cells to convey virus to tumours in the presence of NAb; thus the aim was to use the sera from reovirus-treated patients (PS) described previously (section 4.2) to replicate this in a human model. To this end, an *in vitro* assay was developed in which the ability of human monocytes to convey free or neutralised reovirus to tumour cells was investigated.

As depicted in Figure 5.3.1, reovirus was first combined with PS such that the virus would be fully neutralised (reo-NAb). The neutralising ratio of PS to virus was determined for each serum by MTT assay (section 3.3.2). Neutralisation was allowed to proceed for 2-3 hours at 37°C. Freshly isolated primary human monocytes were then pulsed with an equivalent dose of either free virus (reo) or PS-neutralised virus (reo-NAb) for 2-3 hours at 4°C, to allow the inoculum to adsorb. Monocytes were thoroughly washed in PBS to remove unbound virus, then co-cultured with Mel-624 target cells to permit viral hand-off and killing. In parallel, reovirus or reo-NAb were added directly to targets, to act as controls for viral killing and viral neutralisation respectively. After 72 hours in culture, targets were harvested and viability assessed by flow cytometry.

The primary human monocytes in this assay were obtained from peripheral blood mononuclear cells (PBMC) of normal donors, by positive selection. Leukapheresis cones from blood donors were rested overnight prior to density gradient separation in order to obtain PBMC. Magnetic beads were then used to positively select the CD14-expressing monocyte fraction. As shown by representative flow cytometry plots using the anti-CD14 clone M5E2 (Table 8), the CD14<sup>+</sup> population comprising ~ 15-20% of live PBMC is consequently enriched to over 90% (Figure 5.3.2a and 5.3.2b). Few monocytes – as identified by CD14 expression, or size and granularity – are omitted by selection, with only ~ 1% of the depleted fraction staining for CD14 (Figure 5.3.2c). CD14 selection was found to yield improved purity over CD11b selection (data not shown).

The expression of the reovirus entry receptor JAM-A on the monocyte surface was confirmed by flow cytometry staining (Figure 5.3.3). This suggests that monocytes may be capable of the binding and internalisation of free reovirus, as previously described for human myeloid-derived DC (Ilett et al., 2011).

Light microscopy images provide an illustration of the results of the *in vitro* hand-off assay (Figure 5.3.4). In the absence of cell or virus treatment, Mel-624 cells form a dense adherent monolayer in the base of the well. At an MOI of 10, free reovirus obliterates this monolayer, leaving cells detached and ostensibly dead after 72 hours. By contrast, cells treated with reo-NAb exhibit no overt signs of viral infection or compromised viability. This remains the case even after 144 hours (data not shown).

In co-culture wells containing both targets and non-loaded monocytes, Mel-624 monolayer integrity appears totally unaffected, indicating that in the absence of cargo primary human monocytes do not (either via phagocytosis or soluble factors) directly kill human melanoma cell lines. When pulsed with reovirus however, monocytes appear very capable of delivering virus to destroy target cells. Similarly, although a minority of targets appear to remain, monocytes pulsed with reo-NAb also generate extensive killing after 72 hours in co-culture.

A more quantitative assessment of the relative potency of direct or monocyte-loaded reovirus or reo-NAb was gained by live-dead staining (Figure 5.3.5). For each condition, an equal input dose was used, and ten-fold dilutions of virus tested. As expected, direct addition of free virus proves the most cytotoxic treatment; at MOI 0.01 (per Mel-624 cell), over half of the target cell population are dead after 72 hours, consistent with the susceptibility data (Figure 5.2.1). In light of this sensitivity, the total absence of killing by any reo-NAb dose strongly indicates that patient serum does indeed abrogate direct infection of tumour cell targets by reovirus.

Co-culture of Mel-624 with reo-loaded monocytes proves only slightly less potent than direct reo, with the vast majority of cells eliminated at an input MOI 1 or above. Crucially, monocytes loaded with reo-NAb can also yield extensive target cell killing, albeit at higher virus doses than those required for free virus.

In order to demonstrate the wider applicability of the neutralised virus hand-off paradigm, a range of other epithelial tumour cell lines were selected – one for each of four tumour tissue origins – and used in place of Mel-624 cells as targets. After a 72-hour incubation, as for Mel-624, all four lines demonstrated increased target cell death upon culture with reo-NAb loaded monocytes compared to reo-NAb alone (Figure 5.3.6). Although this increase was less substantial in the newly tested lines, it reached statistical significance in four of the five. The other cell line, Panc-1, exhibited wider variability in viability at baseline. This illustrates that the delivery of pre-neutralised reovirus by monocytes is not melanoma-specific.

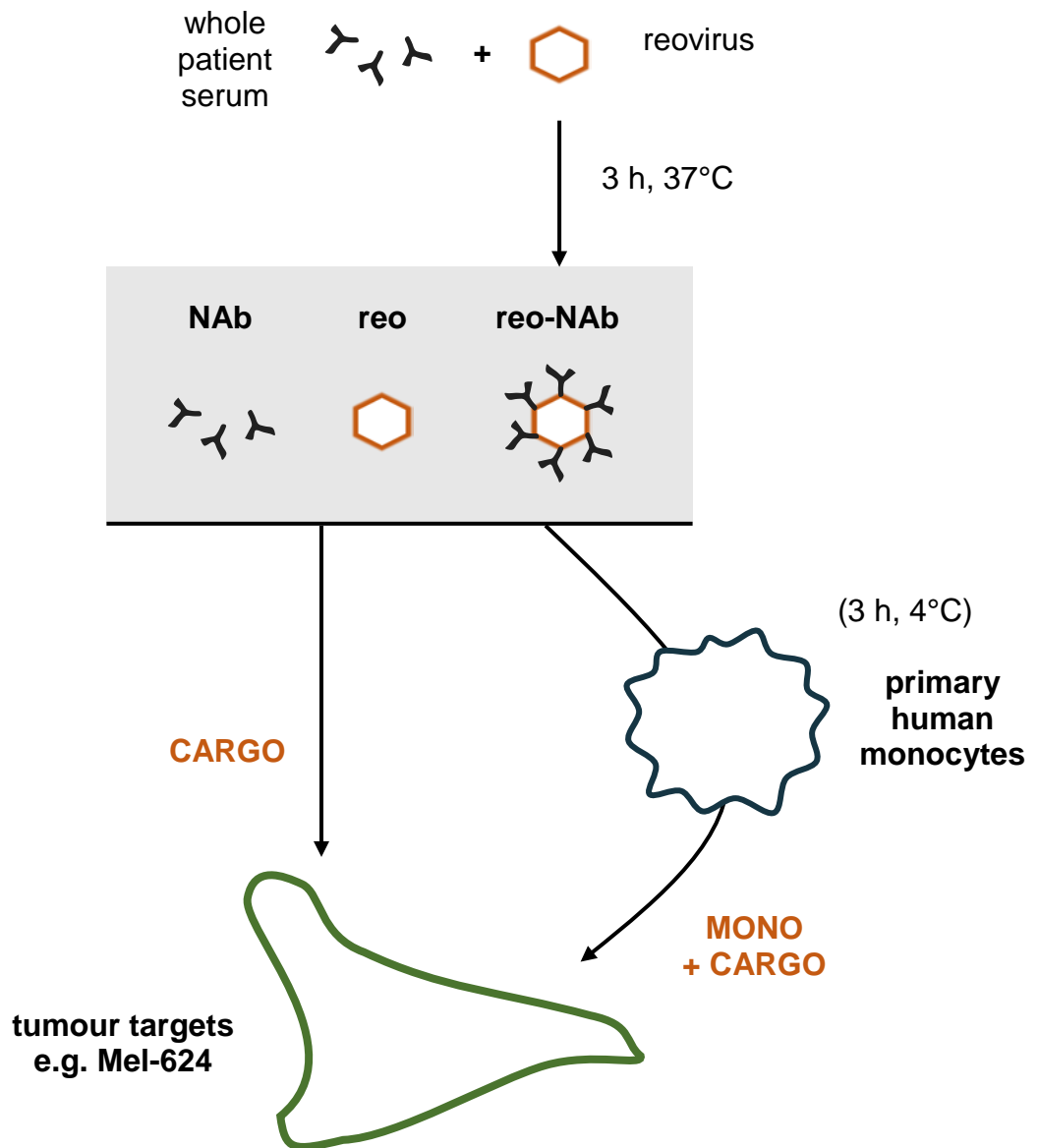


**Figure 5.3.1 Hand-off assay schematic**

First, as per section 3.4.1.2, reovirus was combined with a neutralising dose of patient serum (NAb) and incubated at 37°C for 3 hours to form reo-NAb complexes. These, or other types of cargo (NAb or reovirus alone; grey box) were then pulsed on to primary human monocytes at 4°C for 3 hours, prior to washing and then co-culture of 'loaded' monocytes (mono + cargo) with tumour cell targets. In separate wells, tumour cells were cultured with the same doses of 'cargo' directly. Viability of the target cell population was analysed after 72 hours by flow cytometry.

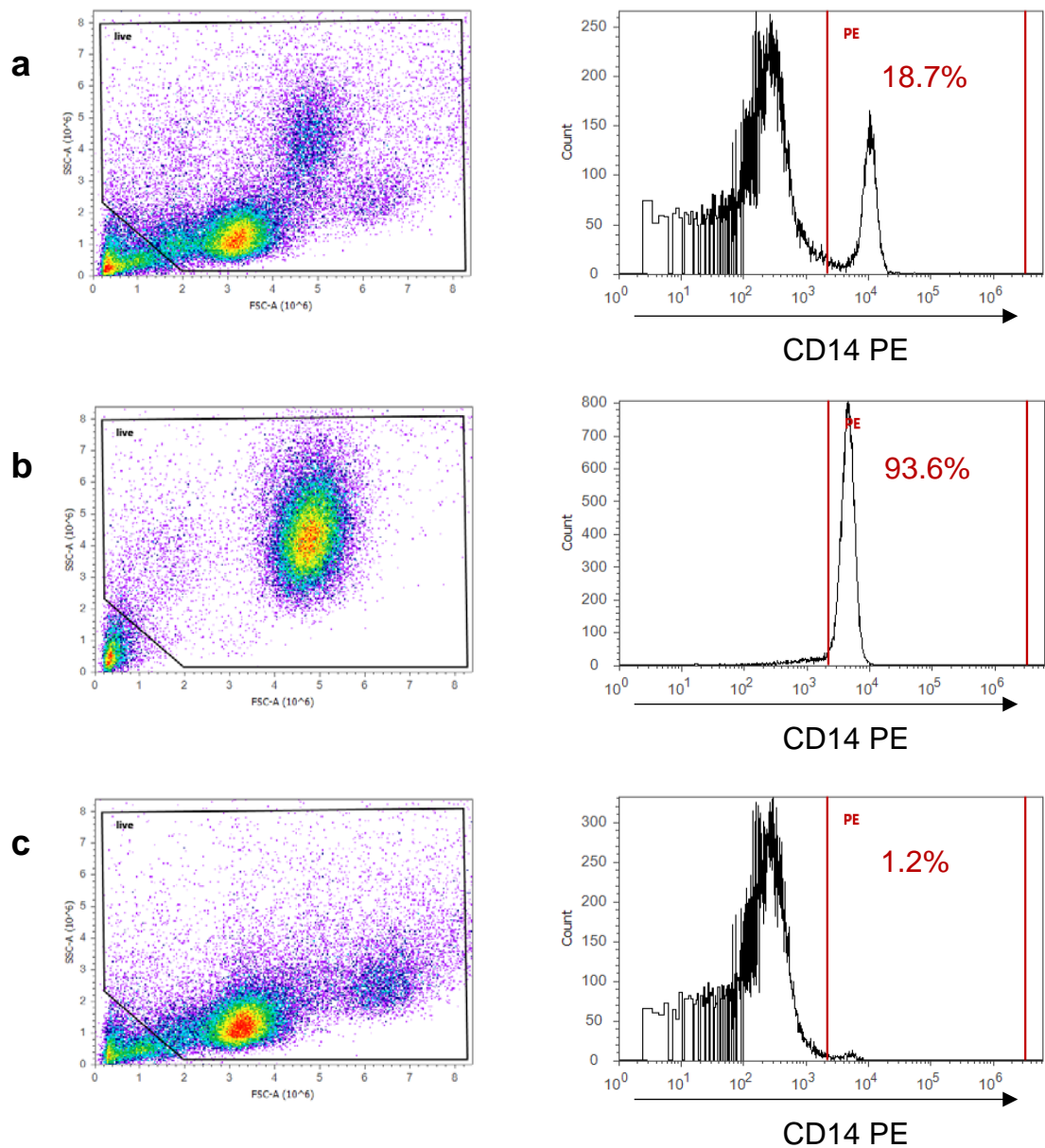


**Figure 5.3.2 Selection of monocytes from human healthy donor PBMC**

Following isolation from whole blood, human PBMC were incubated with anti-CD14 microbeads and a magnetic column used to select microbead-bound cells. Beads were permitted to dissociate overnight prior to staining with a PE-conjugated antibody against human CD14, or isotype control, and flow cytometry analysis.

Whole PBMC (**a**), CD14-selected (**b**), and CD14-depleted (**c**) fractions of PBMC are shown. Monocytes are readily distinguished from lymphocytes by scatter plots (left) as well as CD14 expression (right). The lower threshold of the CD14-positive gate was set at the upper limit of isotype staining.

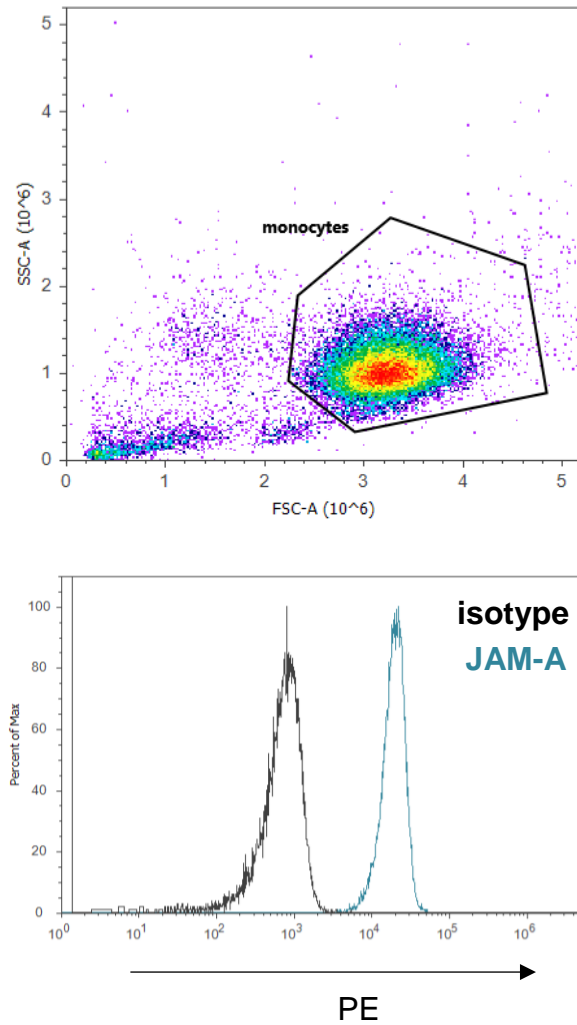


**Figure 5.3.3 Monocyte expression of JAM-A**

Following CD14 selection, cells were stained with PE-conjugated antibody against human JAM-A (blue) or isotype control (grey), washed and fixed with PFA. Gating on monocytes by forward/side scatter, marker expression was determined based on PE signal. Plots are representative of two repeats.

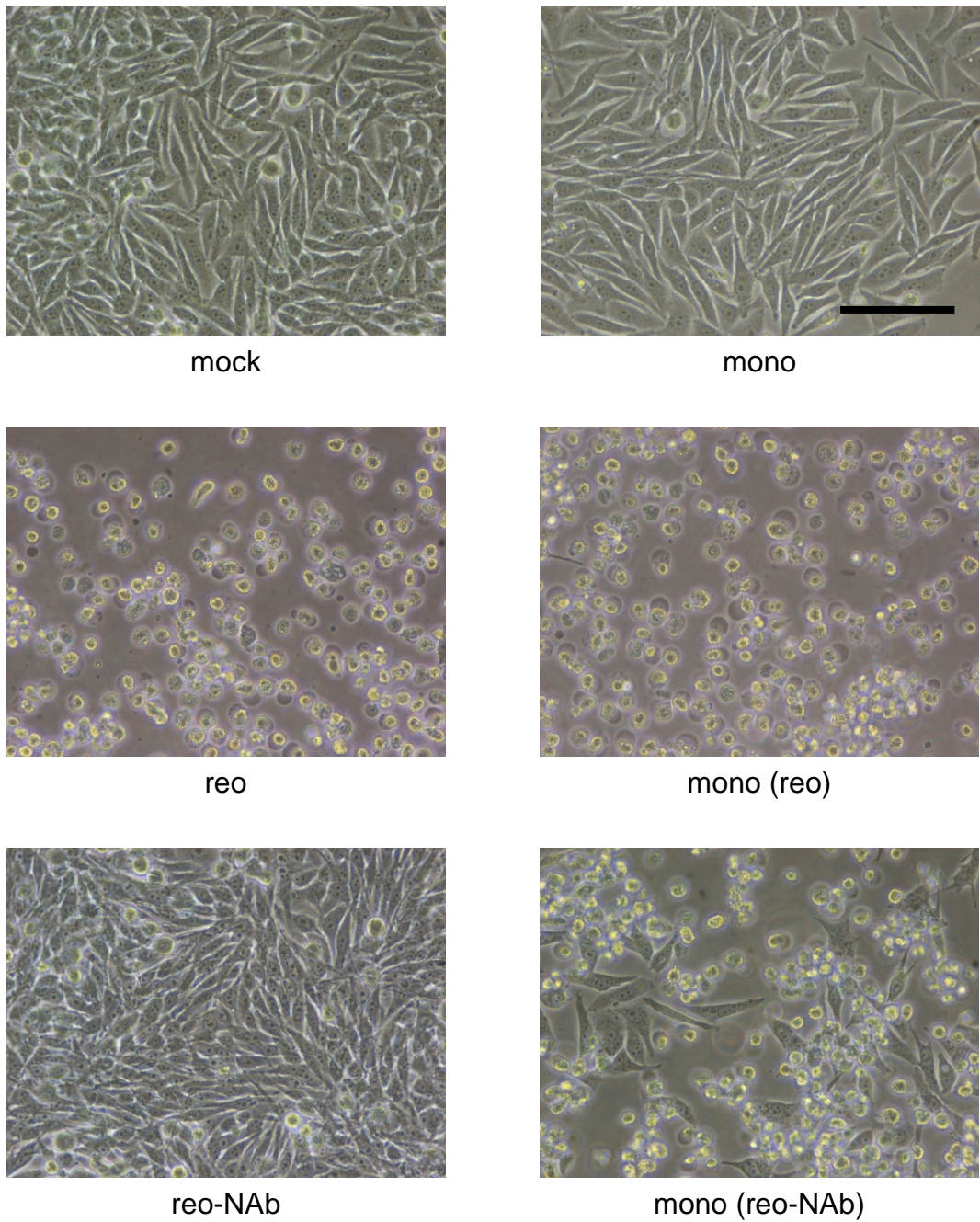


**Figure 5.3.4 Representative images of outcomes from the hand-off assay**

Prior to flow cytometry analysis after 72 hours, light microscopy images were taken of the tumour cell cultures. In this case, the input dose of reovirus used was MOI 10 with respect to Mel-624 cell number. This dose of reovirus or reo-NAb complexes was added either to monocytes (mono) for hand-off, or directly to tumour cells. Compromised cell viability can be clearly observed by cell rounding and detachment. Images are representative of at least five identical experiments in which images were taken. Scale bar = 100  $\mu\text{m}$ .

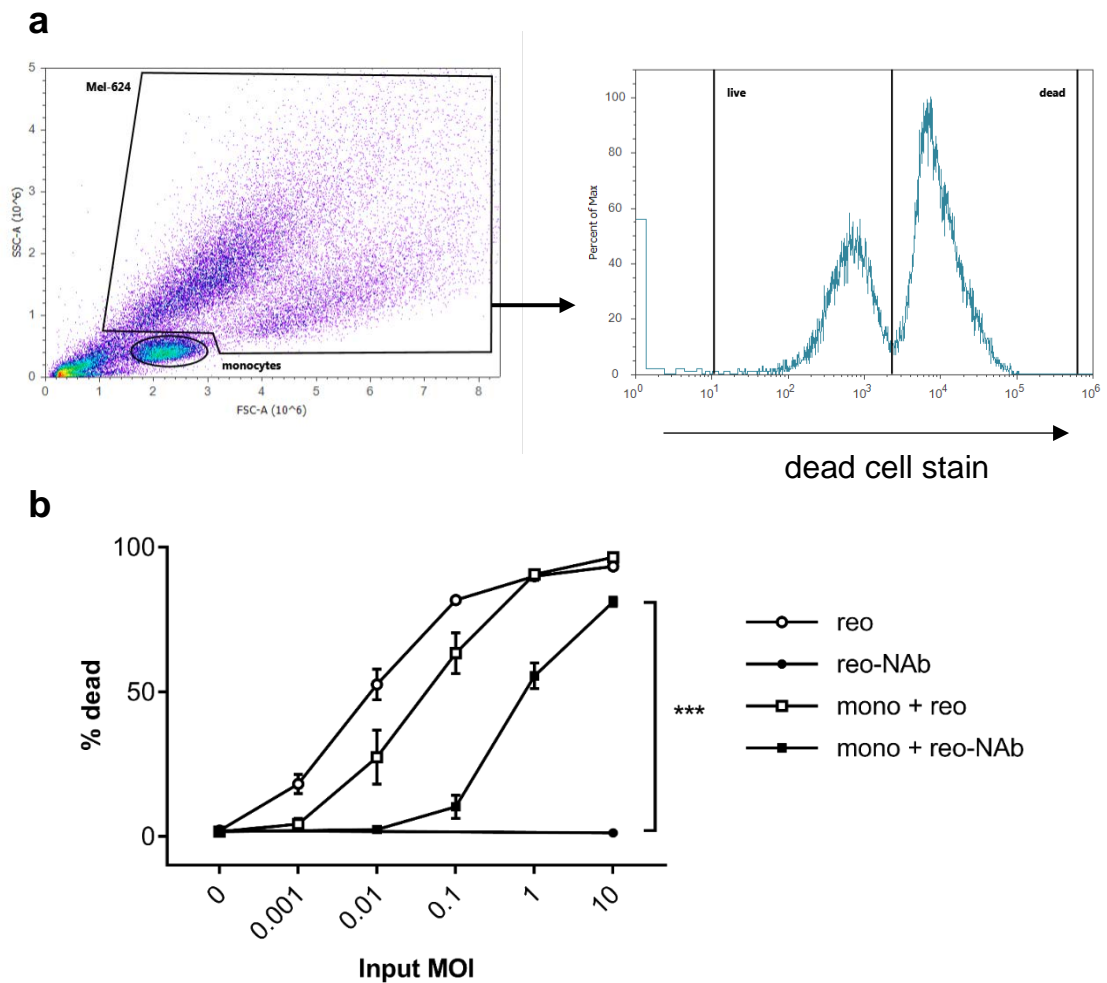


**Figure 5.3.5 Quantification of tumour cell killing in the hand-off assay**

After 72 hours in culture, all cells were harvested from wells and incubated with a fluorophore-tagged dead cell stain prior to analysis by flow cytometry.

Melanoma cells were identified by their greater size and granularity than monocytes (**a**). The proportion of these cells staining positively was determined to be the dead cell fraction, which was quantified for each condition (**b**).

The 'input MOI' of virus was with respect to the starting Mel-624 cell number.

MOI 0 refers to mock treatment for both the direct treatments (circles) and monocyte co-culture conditions (squares) respectively. Data showing the absence of killing by direct addition of serum, or untreated or serum-treated monocytes, are not shown for brevity.

Mean values  $\pm$  SEM from three independent experiments, each using a different serum sample and monocyte donor.

\*\*\*  $p < 0.001$  by Student's t-test, at MOI 10.

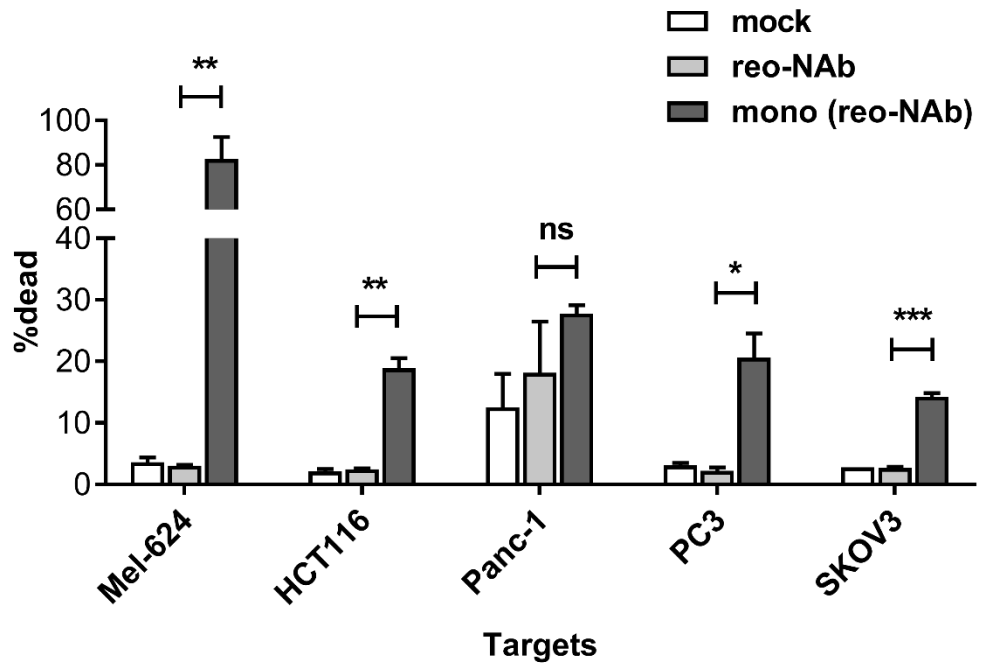


**Figure 5.3.6 Application of the hand-off assay to other target cell lines**

Target cells were treated with medium (clear bars), reo-NAb complexes (light grey bars) or reo-NAb loaded monocytes (dark grey bars), and cell viability assessed by flow cytometry after 72 hours.

Mean values  $\pm$  SEM are shown from at least three independent experiments. *ns* = not significant; \* $p < 0.05$ , \*\* $p < 0.01$ , and \*\*\* $p < 0.001$  respectively by Student's t-test.

## 5.4 Transferability to other OV platforms

Having demonstrated its relevance to various solid tumour types, the hand-off assay was next extended to other virus agents to assess its applicability in the wider OV arena. Two other well-characterised OV in clinical development were selected for comparison to reovirus: coxsackievirus A21 (CVA21), a positive-sense single-stranded RNA virus; and herpes simplex virus 1716 (HSV1716), a modified double-stranded DNA virus.

First, as for reovirus, the capacity of these agents to exert cytotoxic effects upon melanoma cells was confirmed. The expression of the cognate viral receptors by Mel-624 cells was determined by flow cytometry staining, using fluorophore-conjugated antibodies (Table 8). As shown in Figure 5.4.1, this representative melanoma cell line expresses high levels of surface CD54 / CD55 (for CVA21), and high CD111, moderate HVEM, and negligible CD112 (for HSV1716).

In line with these observations, melanoma cell lines are readily killed upon treatment with either CVA21 or, to a lesser degree, with HSV1716. Using the same colorimetric assay as above (Figure 5.2.2), Mel-624 or SKmel-28 cells were treated with tenfold-diluted CVA21 or HSV1716, and viability assessed after 48 or 72 hours following addition of MTT (Figure 5.4.2). After 72 hours, a dose of approximately 0.0001 pfu per cell CVA21 is sufficient to reduce viability by half. In contrast, although viability is compromised by addition of HSV1716, cell death proceeds much more slowly, with over 1 pfu per cell required to reduce viability by half after 72 hours.

These two OV were then compared to reovirus in terms of their efficacy in the hand-off assay. As for reo, this required the prior addition of a neutralising dose of patient-derived anti-CVA21 serum or anti-HSV1716 pleural fluid to form virus-antibody complexes. These complexes were either added directly to Mel-624 targets at MOI 10, or the same dose added to monocytes, prior to co-culture for 72 hours as before. As shown in Figure 5.4.3, direct addition of complexes yielded no Mel-624 cell death over baseline, confirming viral neutralisation in each case. When conveyed by monocytes, CVA21 complexes induced significant killing comparable to reovirus complexes, yet HSV1716 complexes generated no appreciable cell death (reo  $p = 0.0038$ , CVA  $p = 0.0008$ , HSV  $p = 0.292$  respectively by Student's t-test). This remained the case when the co-culture was allowed to proceed for 144 hours (data not shown).

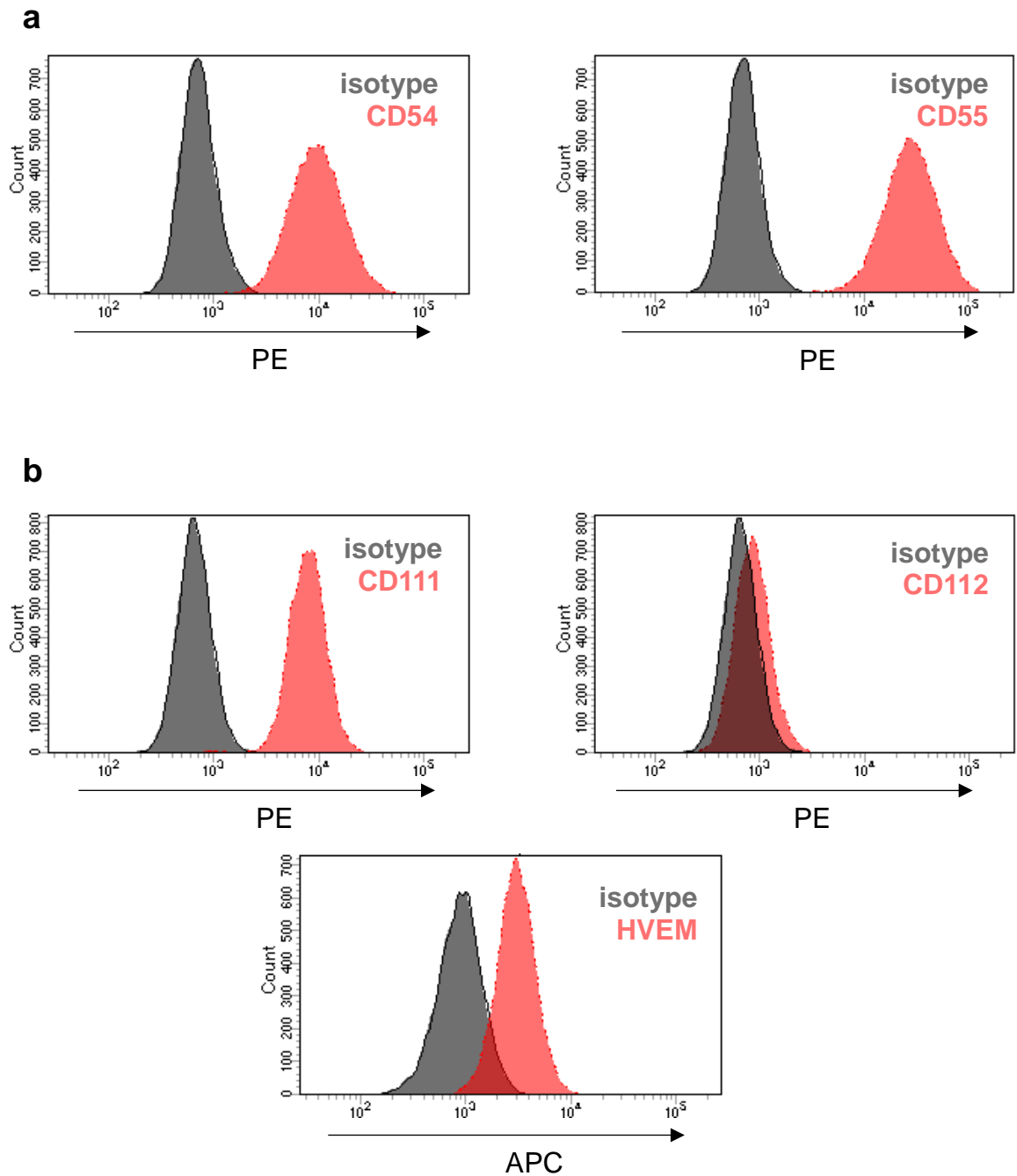


**Figure 5.4.1 Expression of receptors for other OV by Mel-624 cells**

Mel-624 cells were obtained from cell culture and stained with PE- or APC-conjugated antibodies against (a) the CVA21 receptors CD54 and CD55, or (b) the HSV1716 receptors CD111, CD112 and HVEM (red), or matched isotype control (grey). Receptor expression was determined by flow cytometry.

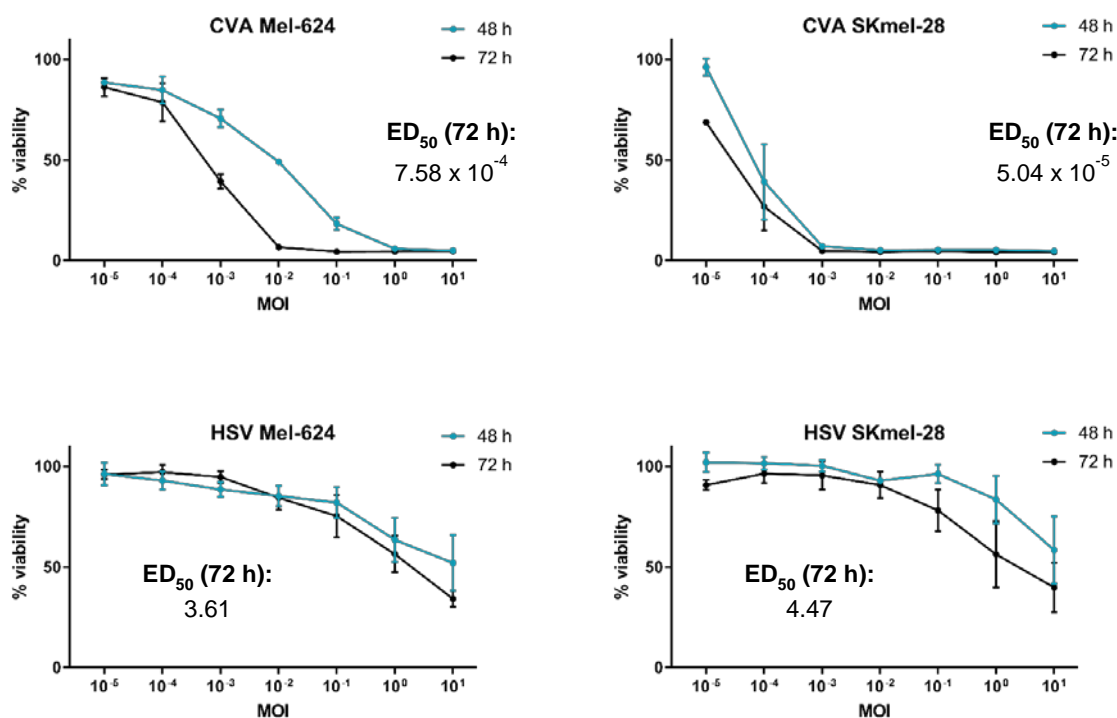


**Figure 5.4.2 Susceptibility of melanoma cell lines to selected OV**

Subconfluent monolayers of Mel-624 and SKmel-28 cell lines were treated with OV at stated MOI for 48 or 72 hours. Cell viability was calculated by MTT assay and normalised to untreated controls at 100%. Values were obtained from four technical replicate wells for each condition.

ED<sub>50</sub> = the MOI at which cell viability is 50% after 72 hours in culture.

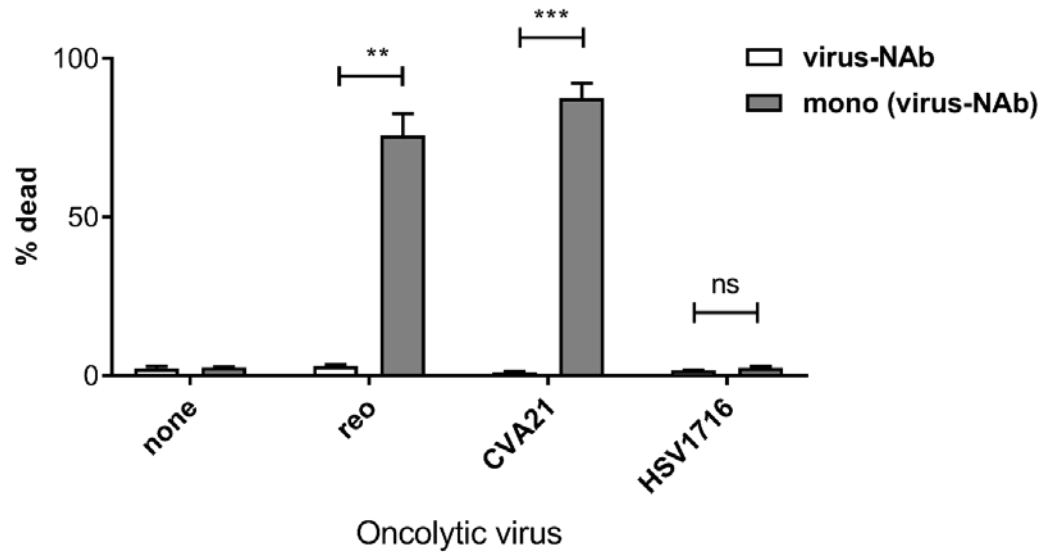


**Figure 5.4.3 Application of the hand-off assay to other oncolytic viruses**

Virus-neutralising antibody complexes (virus-NAb) were formed using matched OV and patient-derived NAb sources (serum or pleural fluid). These were added directly to Mel-624 targets (clear bars), or pulsed on to monocytes prior to washing and co-culture with targets (grey bars) for 72 hours. Mel-624 viability was assessed by flow cytometry.

Mean values  $\pm$  SEM are shown from at least three independent experiments. *ns* = not significant ; \*\* $p < 0.01$ , \*\*\* $p < 0.001$  by Student's t-test.

## 5.5 *In vivo* effects of reo-NAb complexes

The efficacy of systemic reovirus, partnered by GM-CSF, as a therapy for murine melanoma is enhanced by the presence of NAb which bind reovirus in circulation (Ilett et al., 2014). It was intended to replicate the formation of these *in situ*-formed complexes *ex vivo*, prior to administration, in order to formally demonstrate their efficacy.

In order to assess the capacity of neutralised reovirus to access and destroy tumour tissue *in vivo*, it was necessary to generate mouse serum bearing anti-reovirus antibodies. 6- to 8-week old mice were immunised i.p. with  $2 \times 10^7$  pfu live reovirus on days 0 and 7. On day 14 mice were culled, and serum collected from pooled clotted blood as described for patient blood (section 3.3.1).

As previously, the neutralising capacity of mouse serum against reovirus was assessed by MTT viability assay using halving serial dilutions (Figure 5.5.1). As illustrated by the gap between the untreated and anti-reovirus curves, the increase in reovirus neutralising capacity (by  $ND_{50}$ ) is 160-fold in this mouse cohort. Using this information, specific ratios of serum to virus were tested on L929 cells (data not shown), and only those confirmed to be fully neutralised used in subsequent *in vivo* experiments.

The hypothesis that *ex vivo*-neutralised virus remains able to access tumours in mice was next investigated. This was conducted in C57BL/6 mice using the well-characterised and aggressive syngeneic B16-F10 melanoma model. The schematic is shown in Figure 5.5.2a. 6- to 8-week old reovirus-naïve mice were given a s.c. injection of  $2 \times 10^5$  B16-F10 cells, and tumours allowed to establish over seven days. Three i.p. injections of 300 ng GM-CSF (or PBS as control) were administered over three days, to mobilise the myeloid compartment. Mice then received two i.v. injections of reo-NAb, at a low dose (containing  $2 \times 10^7$  pfu) or a high dose ( $5 \times 10^7$  pfu), and were sacrificed three days later.

Tumours were harvested immediately and processed for the presence of reovirus by two methods: qPCR, to detect viral genomes, and plaque assay, to detect functional virions. The accurate quantitation of reovirus RNA in tumour tissue required normalisation to mouse *GAPDH* as a housekeeping gene, using the  $\Delta\Delta C_T$  method. A mean number of copies of the reovirus *S4* gene per cell (see Adair et al., 2012) was calculated within each group, and standardised to the group given a low reovirus dose (without prior GM-CSF).

This revealed that, compared to the 'low reo' dose, the high dose produced a minimal increase in tumour-borne reovirus copies; by contrast, GM-CSF pre-conditioning appears to substantially boost the number of copies reaching the tumour (Figure 5.5.2b). Unfortunately, it was not possible to judge the significance of these findings, as it was necessary to generate individual mean values for each group at an early stage of data processing.

The same tumour samples were homogenised and analysed by standard plaque assay on L929 targets to determine the access of functional pfu to the tumour bed. The number of pfu was corrected according to both the total tumour weight and the volume of lysate derived from the sample, in order to estimate the total pfu in the tumour (assuming homogeneity). The data suggest that in the region of  $1 \times 10^5$  pfu were present in each tumour (Figure 5.5.2c). There appears to be a slight increase in tumour viral load in the high dose and the GM-CSF pre-conditioning groups, which is not significant due to high variation between mice.

Having established that neutralised reovirus can access melanoma lesions when given systemically, it was aimed to assess to what extent this process is influenced by the nature of the NAb present on the virus surface. It was hypothesised that using artificial NAb may reproduce the findings observed with whole mouse serum. This was investigated using monoclonal antibodies against a number of different epitopes on the reovirus  $\sigma 3$ ,  $\sigma 1$  and  $\mu 1$  capsid proteins. Two different reo-NAb complexes were made with these 'artificial NAb'. Reovirus was combined with either a sole, highly neutralising anti- $\sigma 1$  antibody G5, or a mixture comprising a combination of five monoclonal Ab with varying neutralising ability, all in equal proportions, termed 'combo' (Tyler et al., 1993). Both of these formulations were confirmed to be neutralised on reovirus-sensitive L929 targets (data not shown).

These two artificial reo-NAb complexes were tested against the reo-NAb prepared with immune mouse serum, based on the virus load reaching the tumour. The schedule is shown in Figure 5.5.3a. Reovirus-naïve mice (3-4 per group) bearing seven-day established B16-F10 tumours were given three doses of GM-CSF as before (300 ng i.p.) over three days, followed by two daily doses of reo-NAb complexes ( $5 \times 10^7$  pfu); the type of reo-NAb administered to each mouse group is detailed in Figure 5.5.3b. Mice were sacrificed three days later, and tumour viral load assessed by plaque assay.

In comparison to the group with the highest titre from the previous experiment – group C, receiving GM-CSF and reo-NAb complexes containing virus-immune

serum – the groups receiving ‘artificial’ reo-NAb complexes appear to show higher titres (Figure 5.5.3c). The increase in titre between groups C (serum) and E (mAb combo) is statistically significant ( $p = 0.045$  by one-way ANOVA). The increase observed in group D (mAb G5) over group C does not reach significance ( $p = 0.218$ ). These results suggest that a more ‘pure’ solution of NAb may be more capable of accessing the tumour than serum, which contains other factors such as complement that can destroy virus in transit. The trend seen between the ‘combo’ and ‘G5’ conditions is indicative of a benefit from the polyclonal as opposed to monoclonal opsonisation of virus in circulation, although this requires further investigation.

These studies in virus delivery demonstrate that intravenously administered, fully neutralised reovirus can access well-established melanoma lesions in mice, at doses that appear sufficient to yield clinical value. In order to assess the therapeutic benefit of antibody-neutralised reovirus, a further experiment was conducted to measure efficacy in terms of tumour burden and survival. Here, the comparison was made between administering reo-NAb complexes formed *ex vivo* (from mouse serum) to virus-naïve mice, and administering free reovirus to virus-immune mice, thus forming reo-NAb complexes *in situ*. It was hypothesised that as the free reovirus would be rapidly neutralised in the circulation of immune mice, the therapeutic impact in these two groups would be similar; any differences might be attributable to the insufficiency of exogenous NAb to replicate elements of the virus-immune state.

A schematic of the experiment is shown (Figure 5.5.4a). Mice (8 per group) were either pre-immunised i.v. with  $2 \times 10^7$  pfu UV-inactivated reovirus (‘immune’) or PBS (‘naïve’), and NAb allowed to accumulate for 11 days, consistent with the timing of peak NAb titre in mice and patients (Adair et al., 2012; Ilett et al., 2014). Flank tumour implantation was then performed using the reovirus-sensitive B16tk cell line ( $5 \times 10^5$  cells s.c. in 50  $\mu$ l PBS). Mice bearing these three-day established tumours were administered three doses of i.p. GM-CSF as above, prior to two  $1.5 \times 10^7$  pfu ‘live virus’ doses of either free reovirus (immune animals) or reo-NAb complexes (naïve animals).

Data on the progression of tumour growth are displayed in Figure 5.5.4b. The curves representing tumour volumes in both virus-treated groups separate early from the control group, showing a numerical trend for slower tumour growth. However, at no time point do these differences reach statistical significance, as determined by unpaired Student’s t-test (values shown in inset), so it cannot be judged that these treatments significantly retard tumour growth in this instance.

Notably, the main causal 'limiting factor' in this outcome appears to be variation in the control group. No significant difference in tumour volumes was observed between the two reovirus groups.

Figure 5.5.4c shows the Kaplan-Meier survival curves for the three groups tested. All mice in the control group were sacrificed by day 17 after implantation. The virus treatment groups showed no survival benefit over control, as assessed by Log-rank test (data not shown). A substantial number of mice needed to be sacrificed due to tumour ulceration rather than size, which was likely a large confounding factor in the analysis.

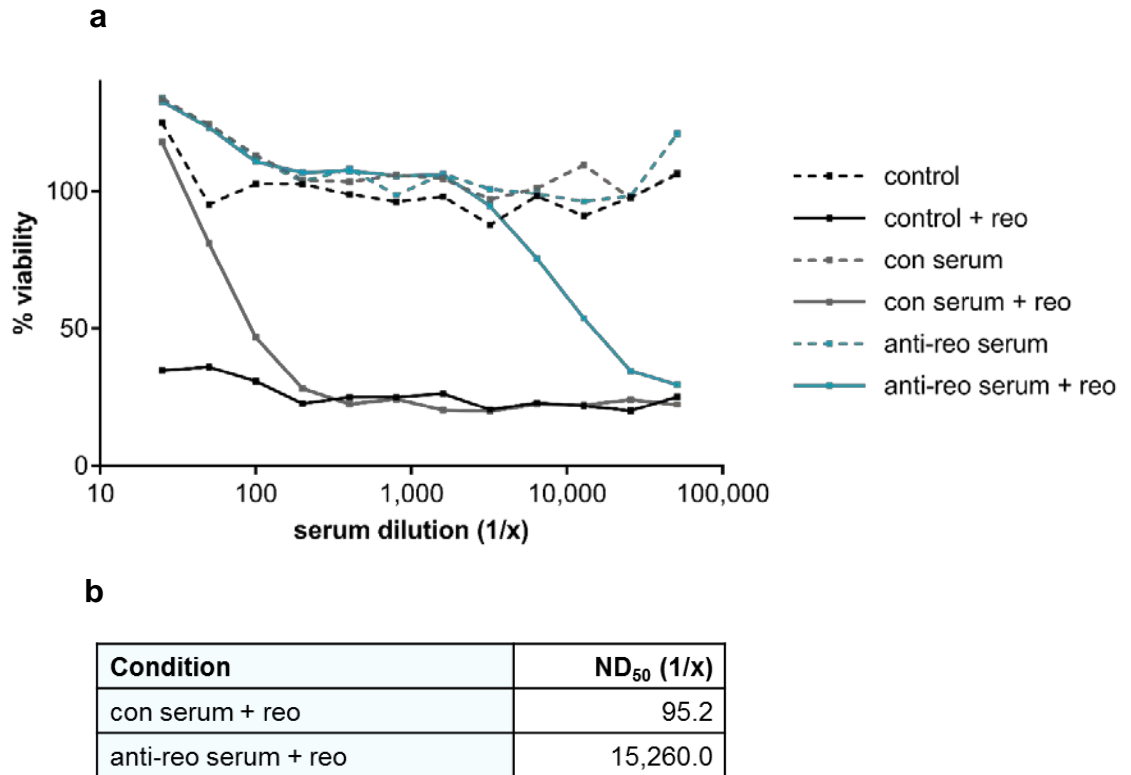


**Figure 5.5.1 Generation of mouse anti-reovirus serum**

6- to 8-week old C57BL/6 mice were twice immunised with i.p. reovirus (reo) or PBS as control (con), then blood was collected and serum obtained. **(a)** Serial dilutions of serum were tested by neutralisation assay against reovirus (MOI 0.05) for 48 hours on L929 cells. **(b)** 50% neutralizing dose values were calculated by interpolating between values in (a).







## 5.6 Summary

Although 5-year survival rates for melanoma as a whole exceed 90%, the prognosis for patients with advanced metastatic disease has been dismal (DeSantis et al., 2014). Prior to the current decade, therapies with the ability to improve this outlook have proven elusive. However, the approval of targeted drugs such as vemurafenib, and immunotherapy agents including checkpoint inhibitors, have fundamentally altered the treatment landscape. Now other emerging classes are adding to the weaponry of immunotherapy, led by adoptive cell therapy and OV.

In a limited sense, some OV may be viewed as targeted therapies in that they are able to infect not just transformed cells but subsets with specific activating mutations – the tropism of reovirus for Ras-transformed cells being one example. Melanoma is at least theoretically an attractive target for reovirus based on the prevalence of activating mutations in the Ras/MAPK pathway, with BRAF mutations in 40-70% and NRAS mutations 15-30% (Dhomen and Marais, 2009). A constellation of *in vitro* studies described an association between reovirus infection and signalling downstream of EGFR (Strong et al., 1993; Strong and Lee, 1996), and more specifically by putative Ras-mediated inhibition of protein kinase R (PKR), which is otherwise pivotal in the clearance of virus from the cytoplasm (Bischoff and Samuel, 1989; Coffey et al., 1998; Imani and Jacobs, 1988; Norman et al., 2004; Strong et al., 1998). The targeting of PKR has also been associated with the cancer-selective tropism of vaccinia virus and an attenuated herpes simplex virus (Parato et al., 2012; Poppers et al., 2000).

The evidence for a causal connection between the Ras pathway and reovirus permissivity has however been questioned by studies demonstrating Ras-independent oncolysis in a range of cell lines (Song et al., 2009; Twigger et al., 2012). Nevertheless there remain defined aspects of reovirus permissivity that are augmented by Ras-transformation, including virus uncoating and progeny infectivity (Shmulevitz et al., 2010). Therefore there remains support for the deployment of reovirus against specific tumour types harbouring Ras pathway activation such as melanoma.

Two well-characterised cell lines expressing the common V600E BRAF mutation, Mel-624 and SKmel-28, were tested for susceptibility to three genetically diverse yet clinically relevant OV: reovirus (dsRNA), CVA21 (positive-strand ssRNA) and HSV1716 (dsDNA). Both cell lines were highly

susceptible to reovirus, as previously described (Errington et al., 2008b). The even higher degree of susceptibility to CVA21 was not surprising given the known efficacy of this virus in the melanoma setting, both *in vitro* and *in vivo* (Andtbacka et al., 2015a; Shafren et al., 2004). Equivalent doses of HSV1716 killed melanoma targets less quickly than other OV; the virus demonstrating lower potency than was shown previously against another melanoma cell line (Randazzo et al., 1997).

The presence of cognate receptors for the two most lytic viruses tested was confirmed: both JAM-A for reovirus (Maginnis et al., 2006) and CD54 and CD55 for CVA21 (Shafren et al., 1997) are richly expressed at the Mel-624 cell surface. These data provide a likely basis for cell susceptibility and are consistent with the tendency for transformed cells to overexpress these receptors (Shafren et al., 2004; Zhang et al., 2013).

The expression of surface receptors for type 1 herpes simplex virus was more variable, which may to some extent explain the comparatively limited cytotoxicity of HSV1716 towards the melanoma cell lines tested. This may also be attributed to other intrinsic differences between HSV1716 and the two RNA viruses, such as its larger and more complex genome, which can result in slower replication or lower toxicity.

Using these melanoma cells as targets, the ability of human myeloid cells to deliver neutralised reovirus to kill tumour cells *in vitro* was illustrated. This assay provides a human correlate of previous studies in which mouse-derived myeloid cells were shown capable of delivering reo-NAb complexes to murine melanoma targets. In the reovirus-immune mouse, myeloid cells are a major sink for systemically administered virus (Ilett et al., 2014). Human monocytes were employed here based on their abundance in blood, and thus provision for use as virus carriers (Ginhoux and Jung, 2014).

Selection of monocytes (at a physiological ratio of 1 in 6 PBMC) was achieved, and found to be highly sensitive and specific. In co-culture assays, these are difficult to distinguish visually from dead target cells, but can be readily discriminated by flow cytometry, enabling killing of tumour cells to be assessed specifically. The direct cytotoxicity of reovirus is almost entirely replicated by reo-loaded monocytes – suggesting that – if all killing is virus-mediated – monocytes are well-suited to reovirus carriage. This is substantiated by their expression of JAM-A and sialic acid (Malergue et al., 1998; Stamatou et al., 2004), and previous evidence of reovirus hand-off to tumour cells by human myeloid cells (Ilett et al., 2011).

Given that replication-competent virus is retained by PBMC despite the presence of NAb in reovirus-treated patients (Adair et al., 2012; Roulstone et al., 2015), myeloid cells could represent an important reservoir for virus in circulation. In this study, reovirus that is otherwise fully neutralised by antibody can be delivered to kill targets by monocytes – indicating that these cells can not only bind and release virus in this form, but can also liberate it from antibody neutralisation.

That this mode of virus carriage can also kill targets of other tumour types indicates that the ‘hitch-hiking’ paradigm may be a more widely applicable one. Similarly, the delivery of serum-neutralised reovirus can be faithfully replicated with CVA21, indicating that this phenomenon could prove more broadly relevant in the OV field. However, data suggesting that HSV1716 cannot productively hitch-hike in the same way suggests that specific aspects of virus physiology may determine applicability, such as the influence of a glycoprotein envelope on the initial binding of antibody. A further investigation of this finding would also need to consider the far inferior cytotoxicity of HSV1716 towards melanoma cell lines, as this, rather than a mechanistic, qualitative explanation, may constitute the major reason.

Building on previous evidence for the efficacy of GM-CSF pre-conditioning plus reovirus in virus-immune animals (Ilett et al., 2014), it was hypothesised that upon the systemic administration of virus, reo-NAb complexes form *in situ* which can be bound by myeloid cells and conveyed to the melanoma tumour bed to mediate therapy. The formation of reo-NAb complexes *ex vivo* prior to i.v. infusion into naïve animals represents a correlate of this approach, designed to confirm the therapeutic potential of neutralised virus. Serum-neutralised virus accessed tumours in all mice tested, as shown convincingly by the presence of viral genomes and replicating virus in tumour homogenates. This is a strong indication that reovirus is able to escape from the vasculature and reach neoplastic sites, despite – or even via – NAb binding. The increase in tumour viral load observed upon the substitution of immune serum for a ‘pure’ solution of artificial monoclonal antibodies suggests that other factors in serum aside from NAb, such as complement, may exert antiviral effects upon reovirus.

The presence of virus was associated with a non-significant trend towards a reduction in tumour volumes in animals pre-conditioned with GM-CSF prior to reo-NAb therapy, when compared to the control group. This numerical trend did not translate into meaningful clinical benefit, in that no significant improvement in survival was detected over mock-treated mice. Thus it was not possible to

replicate the therapeutic benefit observed in virus-immune mice, where the incoming virus encounters NAb *in situ* instead of *ex vivo* (Ilett et al., 2014). However, based on this prior evidence and the observed trend in tumour growth, it can be speculated that there may be superior efficacy observed upon use of reovirus in pre-immune animals as opposed to reo-NAb in immune animals. If this proves the case, it is likely underpinned by the global presence of NAb able to support anti-tumour processes such as ADCC at the tumour site – consistent with a role for both monocytes and NK cells in therapy (Ilett et al., 2014).

The human-derived *in vitro* and murine *in vivo* data in this chapter substantiate the stated model: in pre-immune patients, i.v. reovirus rapidly binds to NAb, and is subsequently able to hitch-hike in or on myeloid cells to the tumour site, where it has the potential to induce both oncolysis and anti-tumour immune effects.

## 6. Interaction of reovirus-antibody complexes with monocyte carrier cells

### 6.1 Introduction

Along with immune molecules such as antibodies and complement, immune cells represent a major arm of the apparent 'barriers' to intravenously administered virus, being an evolutionarily conserved surveillance system for viral and bacterial defence. These cells are equipped with a range of tools for interacting with pathogens, ultimately designed to promote recognition and clearance. But what if – in the context of a 'friendly', oncolytic virus – these cells could be exploited in order to promote viral persistence, rather than elimination?

The concept of using cell carriers to deliver a viral payload to the tumour bed is not a novel one in the context of virotherapy. This stems from the observation that systemically administered virus does not exist freely in circulation for long (Ilett et al., 2014; Willmon et al., 2009) – in patient blood, OV is readily found associated with the immune cell fraction (Adair et al., 2012; Roulstone et al., 2015). Further, in the non-oncolytic context of HIV transmission, the transfer of virus between unwitting 'carrier' DC and 'target' CD4<sup>+</sup> T cells in secondary lymphoid organs is a well-described phenomenon (Geijtenbeek et al., 2000).

Early enquiries into the use of cell carriers deployed T cells as vehicles for retroviruses and rhabdoviruses, among others (Cole et al., 2005; Kottke et al., 2008; Qiao et al., 2008c), with the rationale that tumour antigen-specific T cells might permit exquisite specificity of OV targeting. In the last decade, a desire to optimise viral loading and persistence, tumour homing, immune evasion and viral delivery has led to the testing of various candidate carrier cell types, including tumour cells themselves (Power et al., 2007), activated T and NK cells (Jennings et al., 2014; Yang et al., 2012), and stem cells (Ahmed et al., 2011; Mader et al., 2009).

More recently, antigen-presenting cell types (APC) have been examined as putative carriers. These typically share the ability to bind and internalise virus, and to traffic to lymph nodes and tumour sites, offering the possibility of engendering a broader anti-tumour response once there via co-operation with infiltrating T cells. The fact that APC are unusually prone to viral infection (Hou et al., 2012) and, simultaneously, commonly well poised to direct antiviral

immune responses is surely no coincidence (Yewdell and Brooke, 2012). More likely is that viruses evolve to infect these cell types – or perhaps the other way around – in a high-stakes game of bluff. By becoming a willing host at the cellular level, the APC can ultimately succeed by co-ordinating forces against the virus on a broader scale. In the context of OV however, it is hoped that the antiviral response is either sufficiently delayed to deliver a viral payload, or is outweighed by a gathering inflammatory response against tumour antigens.

To date, various myeloid cells, predominantly DC and macrophages, have been deployed as vehicles for OV including reovirus, measles virus, vaccinia virus and adenovirus (Byrd et al., 2014; Iankov et al., 2007; Ilett et al., 2011; Jennings et al., 2014; Muthana et al., 2013; Peng et al., 2009). As their common precursor, the blood monocyte therefore represents a cell abundant in the circulation which may be readily targeted by OV. While the original cell carriage paradigm sought to sequester virus and evade NAb, this chapter aims to examine the mechanism by which human monocytes can interact with, internalise, and deliver infectious virus following its neutralisation by patient-derived antibody.

## 6.2 Imaging reovirus-treated monocytes

The initial binding, and (in many cases) uptake of an OV by a cell is a prerequisite for cell carriage. In keeping with their remit as pathogen sensors, lymphocytes express a wide repertoire of virus receptor molecules. Human PBMC such as monocytes express high levels of surface JAM-A; this commonly operates in extravasation, but in this context functions as the cognate receptor for reovirus, readily enabling the virus to bind (Adair et al., 2013). Both T cells and DC are capable of reovirus carriage; while T cells permit ‘surface’ carriage, DC allow internalisation of the virus, which can ‘shield’ it from antibody neutralisation (Ilett et al., 2011, 2009).

Further to their ability to convey otherwise neutralised reovirus to kill melanoma cell targets *in vitro*, primary human monocytes were assessed by a variety of methods to better comprehend their interaction with both free reovirus and reo-NAb complexes. Immunofluorescence (IF) microscopy has the capacity to visually localise sub-cellular components with sensitivity and precision, and has become a powerful tool for virus quantification and trafficking. Thus,

confirmation of the binding of virus to the monocyte surface using IF was first sought.

Monocytes on glass coverslips were pulsed with reovirus (MOI 2,000) at 4°C for 1 hour, then incubated at 37°C for 2 hours to allow the internalisation process to begin. The cells were then fixed using PFA, washed, and permeabilised with Triton X-100 prior to IF staining. Cells were stained for the reovirus  $\sigma 3$  protein (clone 4F2, Alexa Fluor 488), the F-actin cytoskeleton (phalloidin Alexa Fluor 647) and the nucleus (DAPI), and visualised on a confocal laser scanning microscope.

Figure 6.2.1 provides an illustration of the immunofluorescence images obtained. Although as phagocytic cells monocytes are known to be cytoplasm-rich, in these artificial conditions there is limited cytoplasm visible around the nucleus, as represented by diffuse F-actin staining. Using actin to delineate the outer margin of the cell, abundant green signal indicates the binding of a substantial number of reovirus particles to the cell membrane (Figure 6.2.1a). Further, by using Z-stacks to interrogate multiple planes within the same cell, individual reovirus-positive 'pockets', likely inbound endosomal compartments, can be identified (Figure 6.2.1b).

However, the reliance of IF on antibody labelling means that reo-NAb, in which the virus capsid is coated in antibody, is rendered undetectable by this method. Consequently, alternative methods of assessing the binding of both reovirus and reo-NAb were pursued.

While IF can provide reasonable spatial resolution on individual cells, other methods such as flow cytometry are capable of providing quantitative information on a much larger cell population by virtue of its high throughput. Monocytes were thus treated with reo-NAb, or an equivalent dose of either NAb or reovirus alone (MOI 50), prior to staining for the reovirus  $\sigma 3$  protein (FITC) or for human IgG (Alexa Fluor 594). Cells were then washed, fixed in PFA and analysed by flow cytometry. As shown in Figure 6.2.2a, only monocytes treated with free reovirus demonstrated positive staining for reovirus  $\sigma 3$  (28.09% of the viable cell population). The viral component of reo-NAb could not be detected by  $\sigma 3$  staining. However, while no human IgG was detected on monocytes when treated with NAb alone, over 10% of monocytes stained exhibited a signal for human IgG following treatment with reo-NAb (Figure 6.2.2b).

With this evidence of direct adhesion of reo-NAb to the monocyte surface, a more detailed insight into this binding event at the ultrastructural level was sought using electron microscopy (EM). Initial attempts to assess the interaction

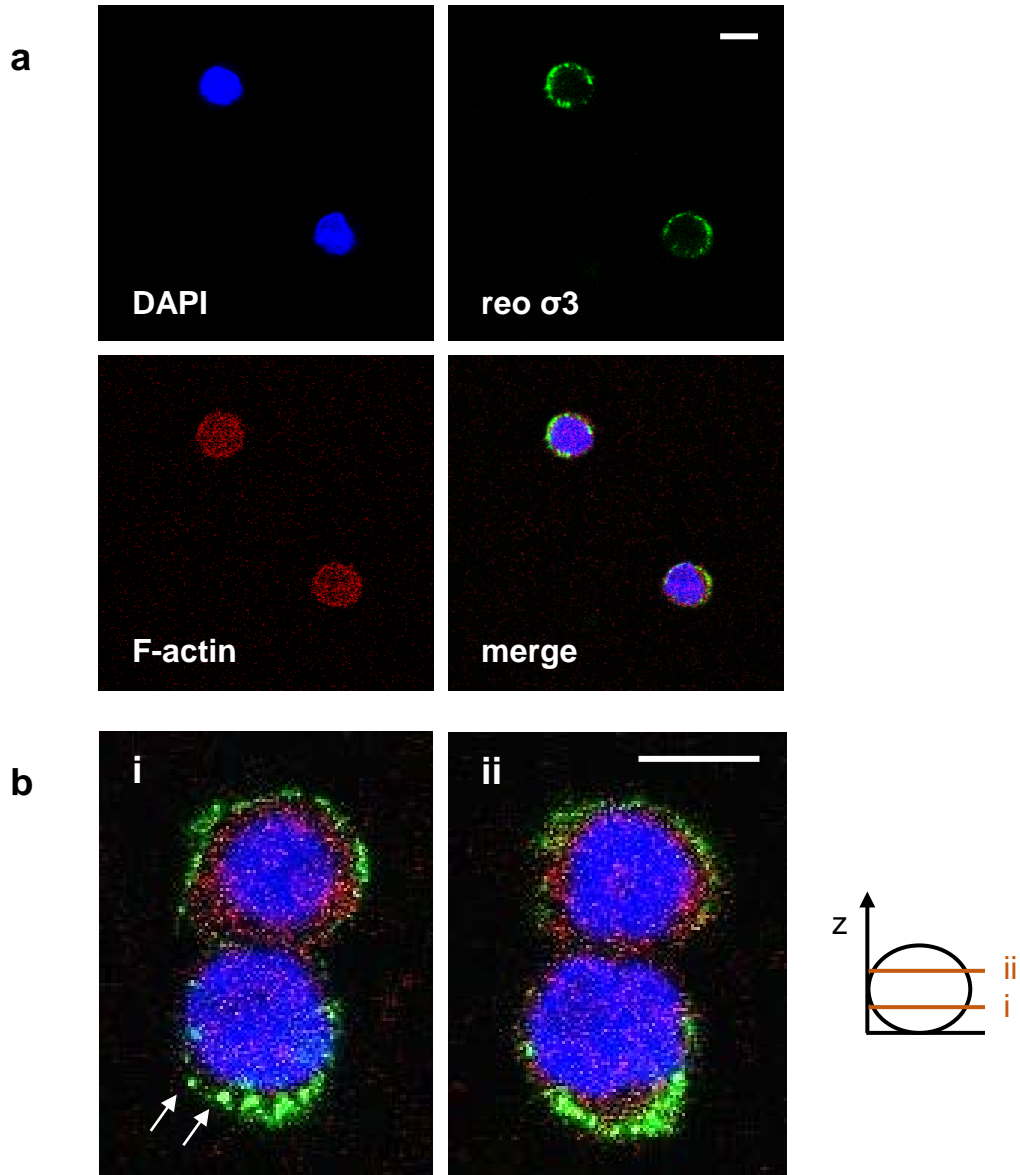
of virus with monocytes obtained by positive selection of CD14<sup>+</sup> cells were compromised by cellular uptake of the magnetic beads used for their isolation – consistent with their phagocytic nature – which interfered with the identification of virus particles (data not shown). Consequently, cells used for EM were obtained by negative selection from PBMC, generating a cell population of 91.5% purity for the pan-myeloid marker CD11b (data not shown).

After selection, as for flow cytometry, these cells were treated with reo-NAb (MOI 50) or an equivalent dose of NAb or reovirus alone. After washing, cells were rested at RT for 5 minutes to allow internalisation, then fixed with PFA and GA. Cells were pelleted, positively stained using osmium tetroxide, embedded, and ultra-thin sections (80 nm) cut for transmission electron microscopy. Representative images of monocytes treated with reovirus (a,b) or reo-NAb (c,d) are shown in Figure 6.2.3.

Evidence of reovirus entry was found with both treatments. Intact viral particles were identifiable by the electron-dense staining of the genome within the viral core (Figure 6.2.3b, arrows); a substantial proportion of empty capsids were also seen (arrowheads). In reovirus-treated cells, viral structures were observed in large endosome-like inclusions, with considerable virus still present at the cell surface. In cells treated with reo-NAb, similar viral inclusions were noted, with the number of viruses found within cells appearing markedly lower (not quantified). In contrast to the sharply delineated borders of free reovirus particles (Figure 6.2.3b), evidence of the presence of NAb upon the viral capsid within inclusions could be observed as a furry ring around its perimeter (Figure 6.2.3d).

To confirm that the structures found were indeed reovirus particles, cells were treated as before and processed using an immunogold labelling protocol, with 70 nm sections cut. Cells were stained using a mouse primary antibody against reovirus  $\sigma$ 3 (or isotype control), followed by an anti-mouse secondary antibody, then 10 nm gold particles conjugated to protein A, and finally contrasted with uranyl acetate. In mock-treated cells, no gold labelling was observed, demonstrating the specificity of labelling (Figure 6.2.4a). By comparison to reovirus-treated, isotype-stained cells (Figure 6.2.4b), gold particles can be found in reovirus-treated,  $\sigma$ 3-stained cells (Figure 6.2.4c). Gold labelling is also observed in reo-NAb treated,  $\sigma$ 3-stained cells (Figure 6.2.4d). The degree of labelling in reo-NAb treated cells appears substantially lower than with the free virus, even taking into account the higher viral load with reovirus.

Having demonstrated the ability of free and antibody-neutralised reovirus to bind and enter monocytes using various modes of imaging, subsequent assays were performed in order to investigate the mechanisms by which reo-NAb enters, persists within, and is released from monocytes in the hand-off paradigm.

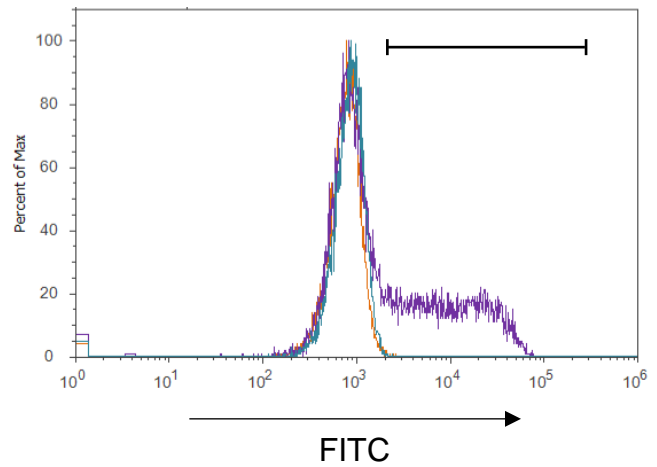


**Figure 6.2.1 Immunofluorescence analysis of reovirus-treated monocytes**

Following CD14-selection, monocytes were plated on coverslips and treated with reovirus (MOI 2,000, 4°C for 1 hour) and incubated for 2 hours at 37°C, then washed and fixed. Cells were then permeabilised, and stained with DAPI (blue), Alexa Fluor 647 phalloidin (red) or mouse anti-reovirus  $\sigma$ 3 antibody (4F2) and Alexa Fluor 488 anti-mouse secondary antibody (green) prior to confocal microscopy analysis. Representative single channel (a) and merged (b) images are shown. Arrows indicate apparent 'pockets' of possibly internalised virus. Scale bars = 10  $\mu$ m.

**a reovirus  $\sigma 3$** 

— NAb	0.03%
— reo	28.09%
— reo-NAb	0.17%

**b human IgG**

— NAb	0.99%
— reo	0.37%
— reo-NAb	10.09%

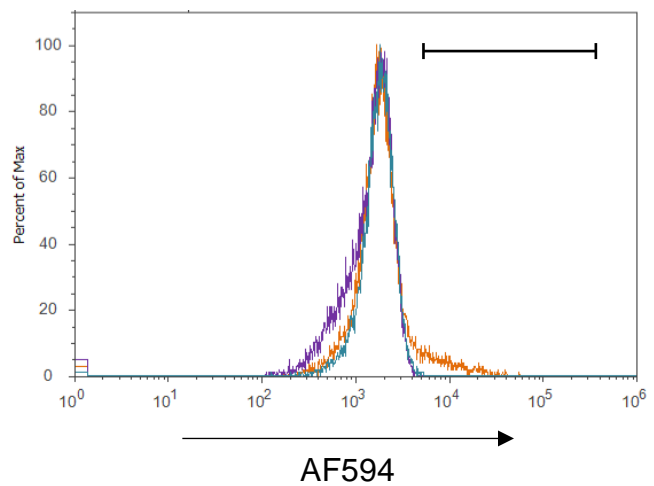


**Figure 6.2.2 Flow cytometry analysis of binding of reovirus or reo-NAb to monocytes**

Healthy donor monocytes were treated with NAb, reovirus (MOI 50) or reo-NAb, washed, and stained for (a) reovirus  $\sigma 3$  protein (FITC) or (b) human IgG (Alexa Fluor 594). The legend indicates the percentage of viable cells showing positive staining.

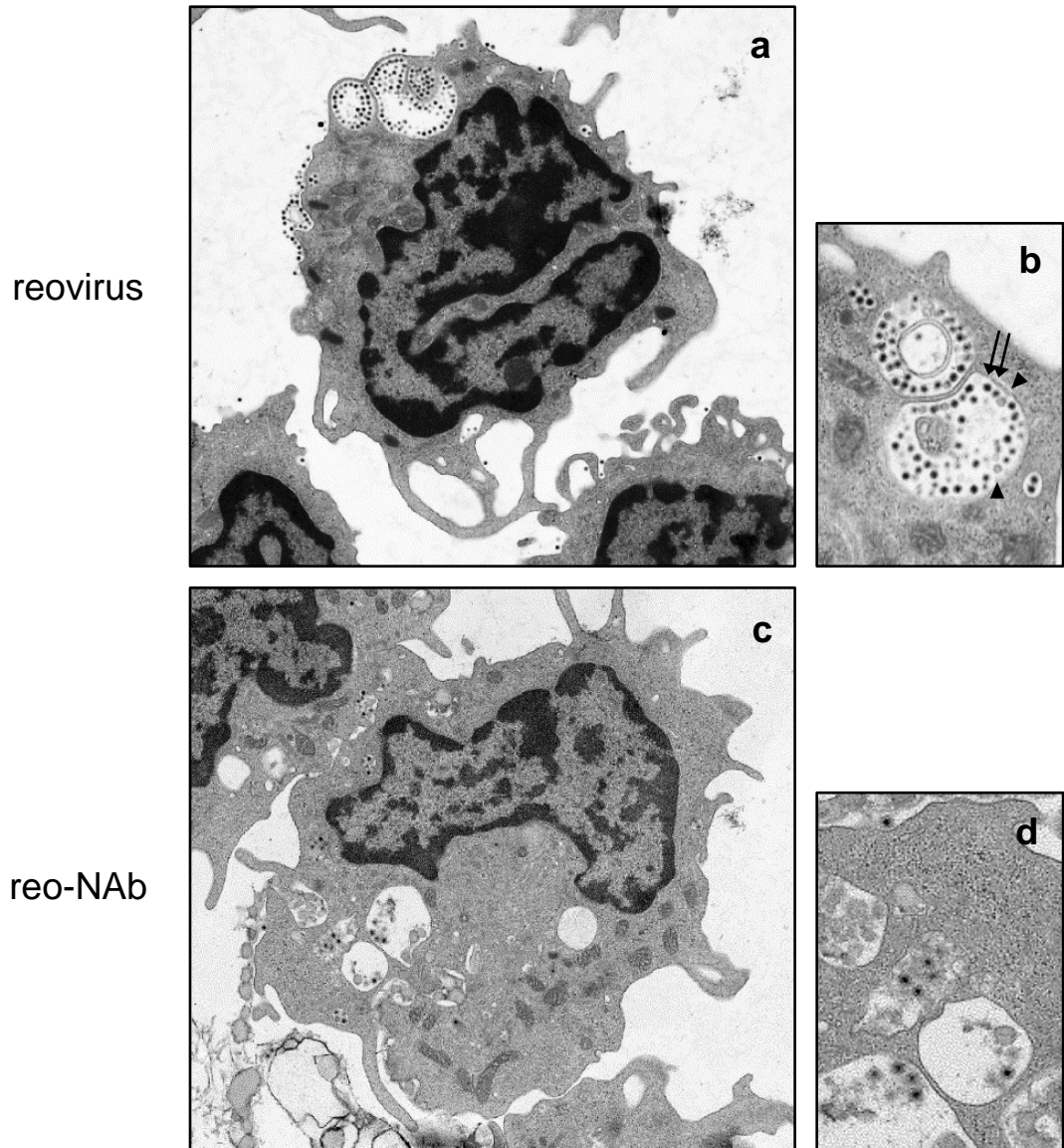


**Figure 6.2.3 Positive staining of reovirus or reo-NAb treated monocytes**

Healthy donor monocytes were treated with reovirus (a,b) or reo-NAb (c,d) (MOI 50) and washed. Virus was allowed to internalise at RT for 10 min. prior to fixation and pelleting. Samples were post-fixed with osmium tetroxide, dehydrated, and infiltrated with resin. Sections were cut and visualised by TEM. Representative low-resolution (a,c) and high-resolution (b,d) images are shown. Scale bars were not available for these images.

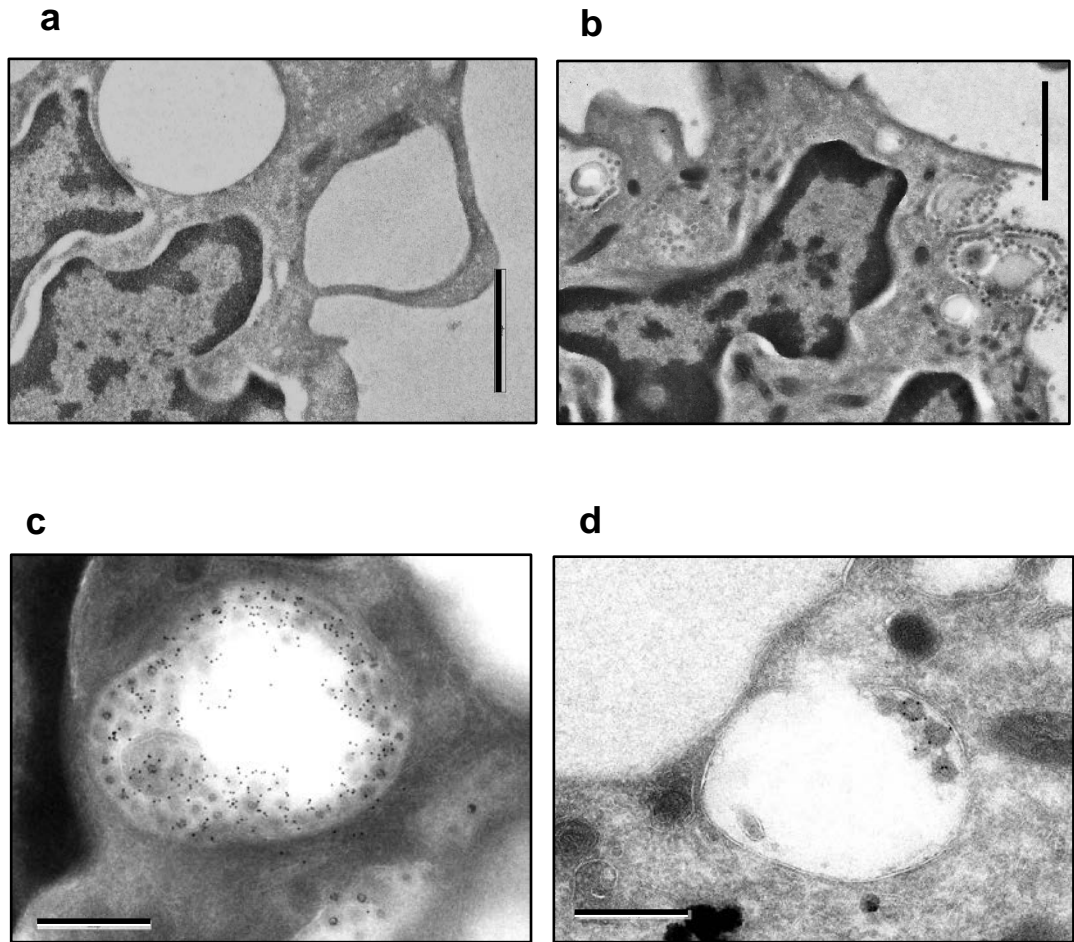


**Figure 6.2.4 Immunogold labelling of reovirus or reo-NAb treated monocytes for  $\sigma 3$  protein**

Healthy donor monocytes were untreated, or treated with reovirus or reo-NAb (MOI 50), and washed. Virus was allowed to internalise at RT for 10 min. prior to fixation, pelleting and sectioning. Sections were stained with primary antibody against reovirus  $\sigma 3$  (4F2) or isotype control, followed by mouse secondary antibody, then protein A-conjugated 10 nm gold. Samples were contrasted with uranyl acetate prior to transmission electron microscopy. Scale bars = 1  $\mu\text{m}$  (a,b) or 300 nm (c,d).

Representative images are shown:

- (a) – mock;  $\sigma 3$  staining
- (b) – reovirus; isotype control
- (c) – reovirus;  $\sigma 3$  staining
- (d) – reo-NAb;  $\sigma 3$  staining

### 6.3 Mechanism of reo-NAb entry

Two cell surface molecules are key in the classical mechanism of reovirus entry. First, low-affinity interactions occur between sialic acid and the virus  $\sigma 1$  protein; these are followed by high-affinity viral attachment to the aforementioned JAM-A protein (Barton et al., 2001). Both molecules are central to viral persistence *in vivo* (Antar et al., 2009; Barton et al., 2003). In the context of human leukocytes, the role of sialic acid appears to predominate in virus attachment *in vitro* (Ilett et al., 2011).

A fully opsonised pathogen presents a subtly different challenge to one that is untouched by humoral effectors. Antibody binding not only limits the free interaction of viral mediators of attachment and fusion to the target cell, but also provides a route by which opsonised virus can be cleared, termed *antibody-dependent cellular phagocytosis* (ADCP). ADCP is reliant on the recognition of pathogen-bound antibody Fc regions by Fc receptors on phagocytes, leading to uptake and ultimately degradation.

It is perhaps unsurprising, given the continual arms race between pathogen and host, that viruses can co-opt this clearance pathway for their benefit – in limited circumstances. The role that antibodies can play in promoting infection at the cellular level – ADE – is a paradoxical one. The enhancing effect of antibodies in ADE operates at the point of entry to a phagocytic cell, whereby receptors for virus-bound antibody or complement can facilitate infection and/or subsequent virus amplification – leading to more severe disease *in vivo* (Halstead et al., 1973). Following its initial description in the context of dengue virus, this phenomenon has been extended to other viruses, both oncolytic and non-oncolytic (reviewed in Taylor et al., 2015).

Circulating human monocytes are principal targets of viral infection, in both the classical setting and in the context of ADE (Hou et al., 2012; Kou et al., 2008; Sun et al., 2011; Tsai et al., 2014; Wang et al., 2010). Reovirus, which infects and replicates in human monocytic cells (Thirukkumaran et al., 2003), has been the subject of two studies in which antiviral antibodies have been employed to promote infection. Virus-immune sera were found to enhance infection of mouse macrophages (Burstin et al., 1983). More recently, the artificial endowment of otherwise non-permissive cells with the expression of Fc receptors was sufficient to permit reovirus infection in the presence of neutralising antibodies (Danthi et al., 2006).

Before investigating the function of specific receptors, the theory that the presence of neutralising antibodies could promote reovirus infection of myeloid cells was addressed. Whole blood was taken from healthy donors in anti-coagulant tubes, and supplemented or not with patient-derived serum as a source of NAb. Reovirus was then added at an approximate MOI of 10 with respect to PBMC count, and incubated for 30 minutes at 37°C. The CD14-selected and -depleted populations were obtained from PBMC as before by magnetic selection, and virus titre analysed by plaque assay (Figure 6.3.1). Although the total virus load on CD14<sup>+</sup> cells was decreased following the addition of patient serum, CD14<sup>+</sup> cells did carry a significantly increased load as a proportion of the total cell-associated virus ( $p = 0.049$  by Student's t-test). This suggests that patient serum does favour the routing of reovirus to the myeloid population in the context of whole blood.

It was therefore hypothesised that the previously observed carriage of reo-NAb (section 6.2) was reliant upon the interaction of virus-bound antibody with monocyte Fc receptors. The expression of the four major surface-expressed Fc receptor isoforms was first established. CD14-selected monocytes were stained with antibodies (Table 8) against CD64 (FcγR I), CD32 (FcγR II), CD16 (FcγR III) and CD89 (FcαR) and fluorescence analysed by flow cytometry (Figure 6.3.2). CD32, CD64 and CD89 were present on the entire cell population; CD32 was most highly expressed, followed by CD64 and CD89. In contrast, CD16 was found to be present on a limited sub-population of approximately 13%. These observations are consistent with monocyte Fc receptor expression at the RNA and protein level, and the existence of multiple monocyte subsets in blood, between which CD16 is a key discriminator (Cros et al., 2010; Wong et al., 2011; Ziegler-Heitbrock and Hofer, 2013).

To prove a role for Fc receptors in the carriage of reo-NAb, monoclonal antibodies or F(ab')<sub>2</sub> fragments were used to functionally block receptors prior to the addition of cargo during the hand-off assay (section 5.3). Whole monoclonal antibodies were used as isotype control or used to block CD89; the anti-CD89 REA234 clone (see Table 4) binds the same epitope as the function-blocking MIP8a clone (Zhang et al., 2000). CD64, CD32 and CD16 were targeted using F(ab')<sub>2</sub> fragments with documented blocking activity (Laborde et al., 2007). Cells were incubated with blocking agents for 45 minutes at 4°C prior to the addition of reo-NAb at MOI 10, and further incubation for 2-3 hours at 4°C. Monocytes were washed in PBS, resuspended in RPMI-10 and added to targets for 72 hours as described previously (section 3.4.1.4).

Figure 6.3.3 describes the effect of Fc receptor blockade on the ability of monocytes to convey neutralised reovirus to kill Mel-624 target cells. Only the blockade of monocyte FcγR III (CD16) with the higher dose of the well-characterised antibody clone 3G8 (Chauhan et al., 2015) was sufficient to yield a significant decrease in endpoint Mel-624 death ( $p = 0.0089$  vs isotype by Student's t-test). All other manipulations failed to generate any significant change in Mel-624 death. Similarly, subsequent experiments blocking the neonatal Fc receptor (FcRn) with three concentrations of an inhibitor peptide SYN1436 (Mezo et al., 2008) indicated no role for this receptor in monocyte loading with reo-NAb (data not shown).

In the same experiments, samples of monocytes were also obtained immediately after loading, and were segregated for analysis of virus titre. These samples were subjected to three freeze-thaw cycles and vortexed (to release any rapidly internalised virus) prior to standard plaque assay. The resulting pattern of virus loading (Figure 6.3.4) is extremely similar to that of Mel-624 cell death: only a high dose of F(ab')<sub>2</sub> fragments against FcγR III generates a significant decrease in loading of reo-NAb treated monocytes ( $p = 0.031$  vs isotype by Student's t-test). Consequently, it can be summarised that blockade of FcγR III leads to a significant decrease in target cell killing via a reduction in the virus cargo carried.

To further substantiate a role for monocyte FcγR III in the interaction and carriage of reo-NAb, two monocyte sub-populations were studied: the larger classical monocyte subset (CD14<sup>++</sup> CD16<sup>-</sup>) and the non-classical subset (CD14<sup>+</sup> CD16<sup>+</sup>). It was hypothesised that the non-classical subset would form superior mediators of reo-NAb hand-off, on account of their expression of FcγR III.

Both cell populations were selected from PBMC using magnetic beads, each by a two-step sorting process, to generate populations expressing the appropriate markers (data not shown). They were rested overnight in order to permit the dissociation of selection beads from functional surface receptors such as FcγR III itself. Subsequently these CD16<sup>+</sup> and CD16<sup>-</sup> populations were tested for their ability to hand off reo-NAb as described previously. As shown in Figure 6.3.5, CD16<sup>+</sup> monocytes carrying reo-NAb do yield a significantly higher degree of cell death than their CD16<sup>-</sup> counterparts ( $p = 0.0072$  by Student's t-test). This effect cannot be attributed to a non-specific effect of co-culture with this population, as CD16<sup>+</sup> monocytes are not otherwise toxic to Mel-624 cells. Similarly, no significant difference could be found in the ability of CD16<sup>+</sup> and CD16<sup>-</sup> cells to

mediate killing via free reovirus, suggesting that only antibody-bound virus is subject to differential carriage by these populations.

Together, these results indicate that FcγR III is at least partly responsible for facilitating reo-NAb carriage by monocyte cells. These results substantiate evidence from a murine model, in which Fc receptors were found to be necessary for reo-NAb mediated killing via immune cells (Ilett et al., 2014).

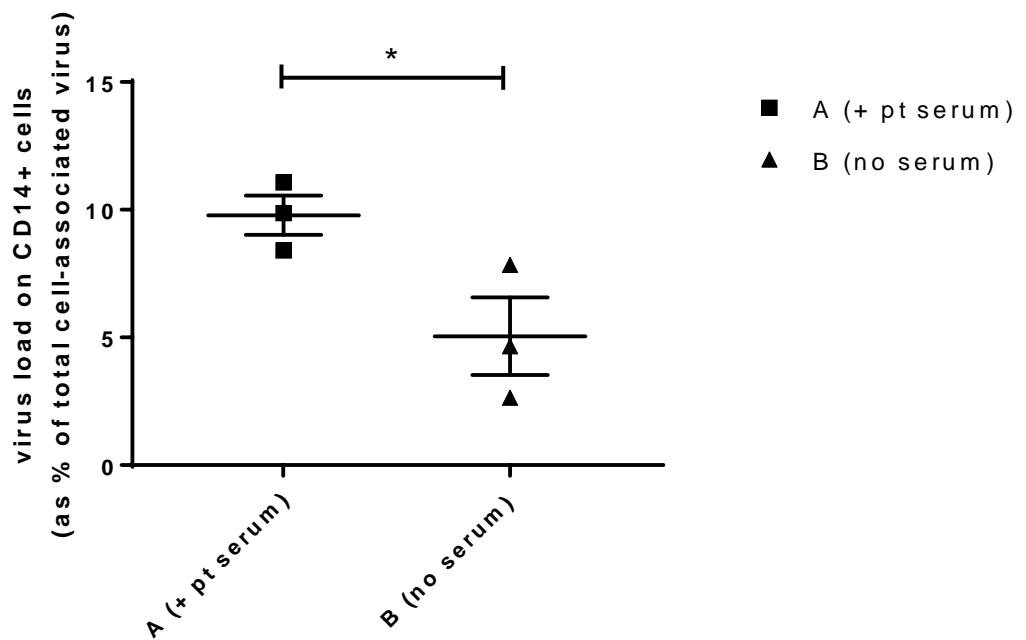


**Figure 6.3.1 Neutralising patient antibodies favour routing of virus to CD14<sup>+</sup> cells in whole blood**

Whole blood from healthy donors was combined with patient-derived serum and incubated with reovirus for 30 min. at 37°C. The CD14<sup>+</sup> and CD14<sup>-</sup> populations were then selected and virus titre determined by plaque assay. The virus load on the CD14<sup>+</sup> population is displayed, as a percentage of the total cell-associated virus load.

Data ± SEM from three individual donors are shown. \* $p < 0.05$  by Student's t-test.

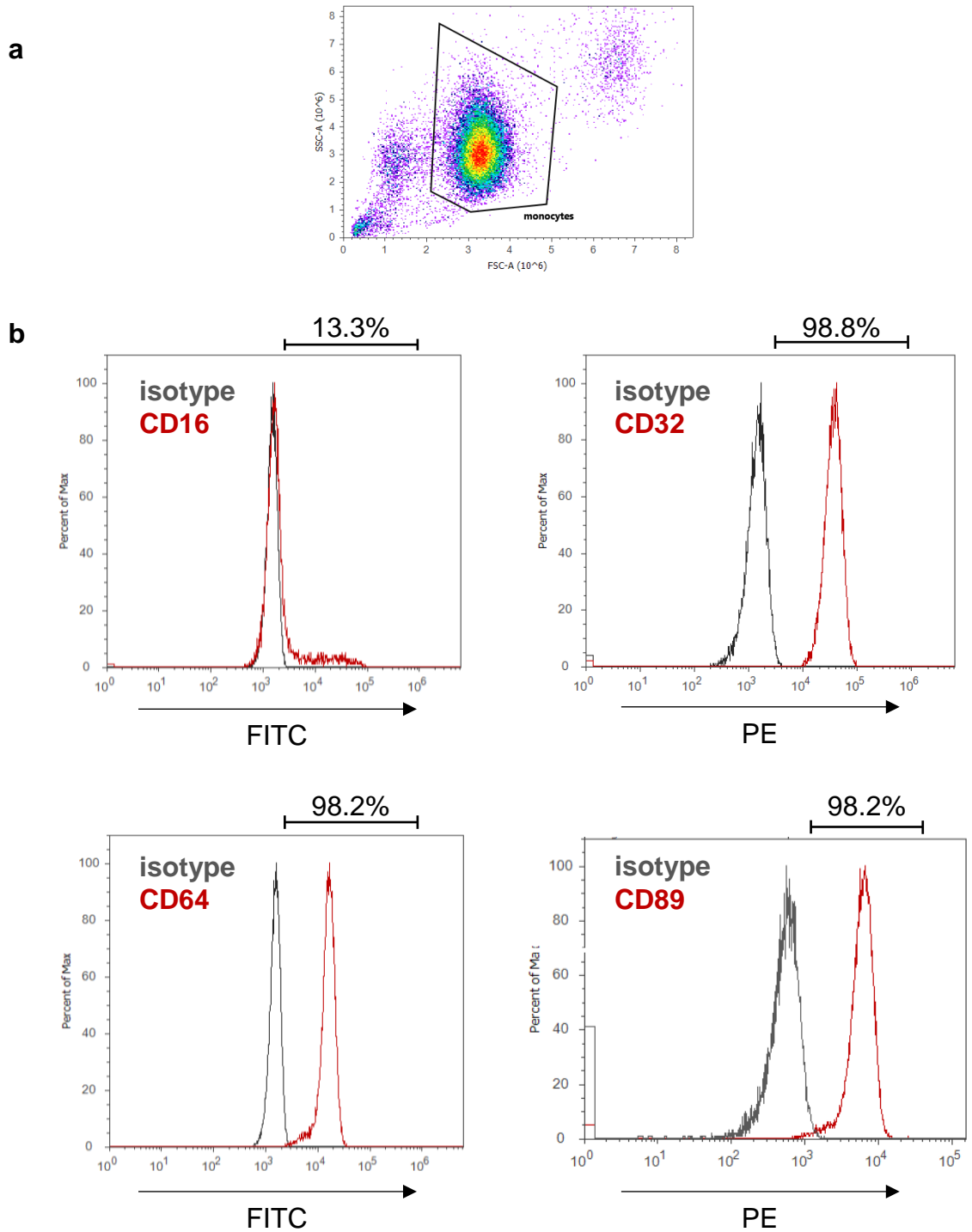


**Figure 6.3.2 Expression of Fc receptors on primary human monocytes**

Following CD14 selection, monocytes were stained with fluorophore-conjugated antibodies against specific Fc receptors (red), or isotype control (grey). Monocytes were gated as in (a) and surface expression of protein was determined by FITC or PE staining respectively (b). The percentage staining positively for each marker is indicated. Plots are representative of two donors.

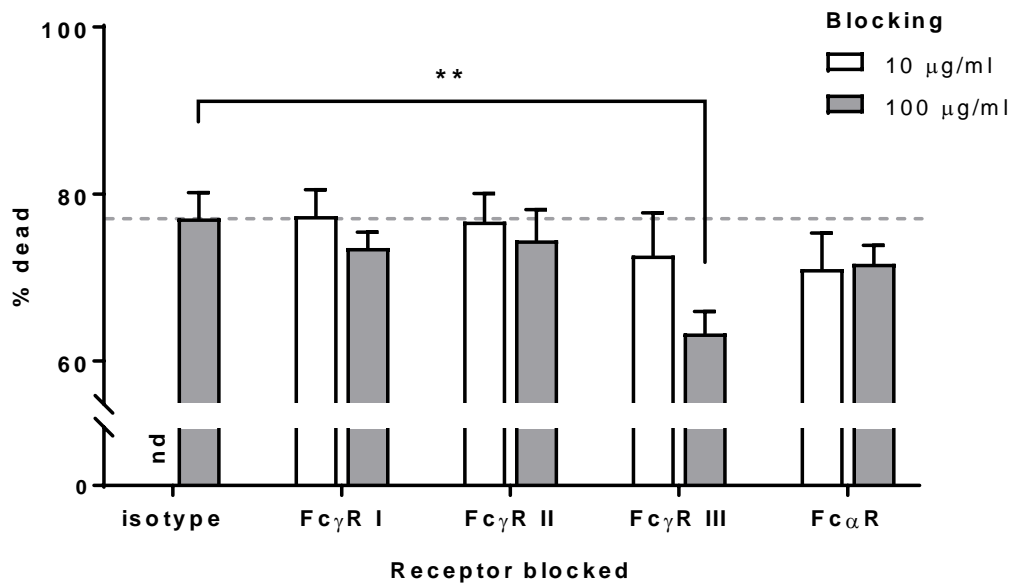


**Figure 6.3.3 Effect of monocyte Fc receptor blockade upon Mel-624 killing via reo-NAb hand-off**

CD14-selected monocytes from healthy donors were treated with Fc receptor-blocking monoclonal antibodies or F(ab')<sub>2</sub> fragments, or isotype control, at two concentrations (10 or 100 μg/ml) for 45 minutes at 4°C. Monocytes were then loaded with reo-NAb (MOI 10), washed and added to Mel-624 targets. Target cell death was assessed by flow cytometry after 72 hours in co-culture.

Mean values ± SEM from four donors are shown. \*\* $p < 0.01$  by Student's t-test (multiple comparisons with Holm-Šidák correction). *nd* = not determined.

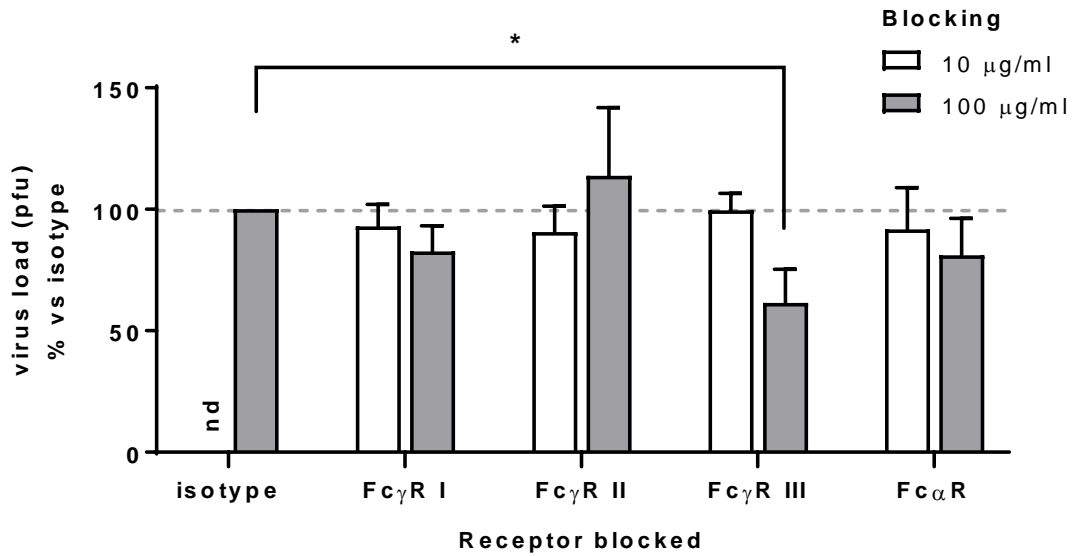


**Figure 6.3.4 Effect of monocyte Fc receptor blockade upon virus loading**

CD14-selected monocytes from healthy donors were treated with Fc receptor-blocking monoclonal antibodies or F(ab')<sub>2</sub> fragments, or isotype control, at two concentrations (10 or 100 µg/ml) for 45 minutes at 4°C. Monocytes were then loaded with reo-NAb (MOI 10) and washed. Virus load was determined by plaque assay.

Data ± SEM from four donors are shown. \* $p < 0.05$  by Student's t-test (multiple comparisons with Holm-Šidák correction). *nd* = not determined.

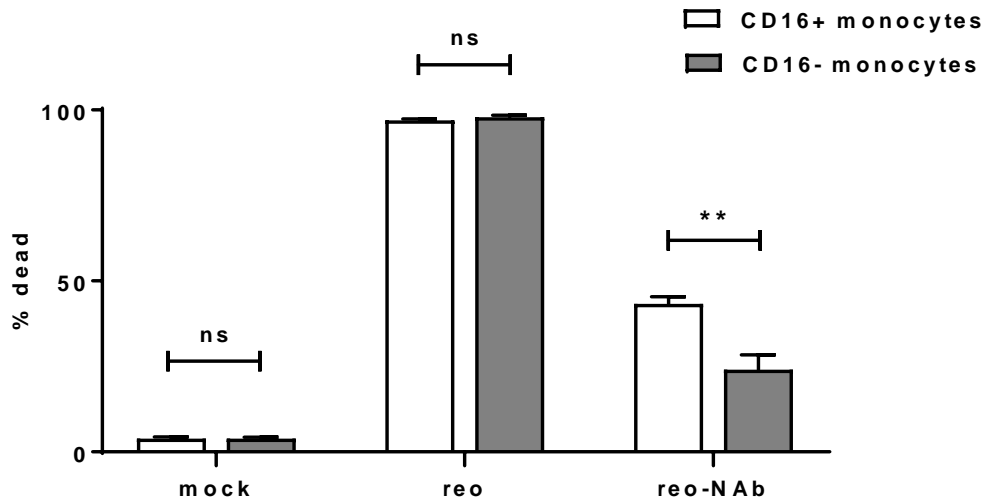


**Figure 6.3.5 CD16<sup>+</sup> monocytes are superior mediators of reo-NAb hand-off**

CD16<sup>+</sup> or CD16<sup>-</sup> monocytes were selected from PBMC, and rested overnight. Cells were then resuspended and pulsed with reo or reo-NAb (MOI 5), washed and added to Mel-624 targets for 72 hours. The proportion of dead Mel-624 cells was determined by flow cytometry.

Mean values  $\pm$  SEM from four donors are shown. \*\* $p < 0.01$  by Student's t-test (multiple comparisons with Holm-Šidák correction).

## 6.4 Monocytes as replication factories?

The process by which antiviral antibody can promote the binding and entry of virus to phagocytes is termed the 'cell-extrinsic' mechanism of ADE. A second, 'cell-intrinsic' mechanism refers to intracellular signalling processes which result in an increased viral load being released from infected cells (Halstead et al., 2010). This increase is a relative one compared to the often abortive or highly restricted degree of virus replication permitted by myeloid cells (Byrd et al., 2014; Jenne et al., 2000; Royo et al., 2014), ostensibly as an immunogenic strategy (Yewdell and Brooke, 2012). In the context of dengue virus *in vitro*, Fc receptor-mediated entry suppresses antiviral cascades, such as by stimulating negative regulators of the pivotal antiviral axis controlled by RIG-I and MDA5, and enhances replication (Chareonsirisuthigul et al., 2007; Ubol et al., 2010). This phenomenon is also observed *in vivo*: compared to primary dengue infection, the presence of antiviral antibody upon secondary infection leads to an elevated viraemia, and often precipitates the more severe clinical syndrome of dengue haemorrhagic fever (Cohen and Halstead, 1966; Green et al., 1999).

Reovirus type 3 Dearing does not appear capable of significant amplification in the heterogenous human PBMC population (Douville et al., 2008). However, given that primary human monocytes appear to permit infection by free reovirus and reo-NAb, it was postulated that monocytes alone may be capable of amplifying virus titres during transit, and that the parameters of viral persistence or replication in the presence of reo-NAb may be different to those in the face of free reovirus. In order to examine this system, the requirement for virus replication in the hand-off assay was first examined.

After the addition of reovirus- or reo-NAb loaded monocytes, or viral cargo alone, to target cells, all supernatant and cells were harvested from wells either immediately (0 hour 'input') or at the same endpoint used for analysis of cell viability (72 hours) and virus titre determined by plaque assay. As was predicted based on the viability data (Figures 5.3.4 and 5.3.5), significant viral replication is observed after 72 hours following treatment of Mel-624 cells with either reovirus, reovirus-pulsed monocytes or reo-NAb pulsed monocytes (Figure 6.4.1). The titre resulting from reo-NAb pulsed monocytes is no less than – and in fact exceeds – that resulting from conditions involving free reovirus; a statistically significant six-log increase over the 'input' titre ( $p = 2.58 \times 10^{-6}$  by Student's t-test). By contrast, the direct addition of reo-NAb to Mel-624 cells yields no significant increase in virus titre, consistent with the absence of cell

death observed previously. Consequently it can be considered that while virus in the form of an immune complex (reo-NAb) is fully neutralised, monocytes are capable of carrying and liberating virus in a form which is either already amplified, or is capable of rapid amplification.

The importance of viral replication was further investigated using reovirus which had been rendered incapable of replicating by UV irradiation. This virus ('UVreo') was subjected to a two-minute dose of UV-C, the equivalent of 500 mJ, and proven to be non-replicative by plaque assay (data not shown). UVreo was then compared to free reovirus in its ability to generate cell death via the monocyte hand-off assay. Three modes of virus application to Mel-624 cells were again considered, at equal input doses: direct addition of virus; monocytes pulsed with free virus; and monocytes pulsed with reo-NAb complexes. As before, populations were harvested from co-culture wells after 72 hours and analysed for viability by flow cytometry.

Examining first the direct addition of virus to target cells (clear bars), UVreo is equally capable of generating melanoma cell death as compared to replicating virus (Figure 6.4.2). This observation is likely a consequence of the high virus dose used, in that it appears sufficient to engender cytopathic effect (CPE), a rapid, non-lytic mode of cell death independent of virus replication. When conveyed by monocytes, free UVreo remains able to kill over 50% of target cells after 72 hours (light grey bars), albeit significantly fewer than when using replicating virus ( $p = 5.90 \times 10^{-4}$  by Student's t-test). It could be considered that a higher dose may be able to entirely eliminate the Mel-624 population by CPE. Lastly, when carried by monocytes, UVreo-NAb does not generate any target cell death above baseline, unlike with the use of the replicating virus ( $p = 2.45 \times 10^{-7}$  by Student's t-test). This indicates that the dose of virus delivered here is considerably lower than by other routes, such that the killing of melanoma target cells is entirely reliant on replication within them.

However, this assay does not address the question of whether monocytes act as amplifiers of virus, or mere carriers. Thus the permissivity of monocytes to reovirus, either free or antibody-neutralised, was examined by the detection of viral genomes and plaque-forming units respectively. Monocytes were pulsed with reovirus or reo-NAb as before, washed, and cultured on their own in RPMI-10 for 48 hours. After 2, 16 or 48 hours, cells and supernatants were harvested, and either processed to obtain RNA for qPCR, or analysed by plaque assay.

RNA from infected monocytes was extracted and converted to cDNA with an unbiased method based on random hexamer primers. The comparative  $C_T$

method of qPCR analysis was subsequently used to quantify the number of copies of the reovirus *S4* gene present relative to the cellular gene for  $\beta$ -actin, assuming equal primer efficiency. As shown in Figure 6.4.3, after treatment with reovirus, monocytes exhibit a peak in reovirus gene expression after 16 hours which is approximately 100-fold higher than that at the 2-hour baseline. This peak is largely diminished after 48 hours, indicating that a wave of viral transcription occurs within one day of infection that is subsequently suppressed.

Unfortunately, the number of reovirus genomes present in reo-NAb treated monocytes was insufficient to reach the limit of detection in this qPCR assay. Consequently, in lieu of data regarding nucleic acids, the plaque assay method was employed to obtain data on the titre of replicating virus particles (pfu) present over time in both the cells and supernatant (Figure 6.4.4a). In the cell fraction, in comparison to the 100-fold increase in genomes detected by qPCR, the 16-hour peak in pfu is very limited – within a 2-fold increase, for both reovirus- and reo-NAb treated monocytes. For reovirus-treated cells, this titre then drops sharply after 48 hours, while the decline is more gradual for reo-NAb treated cells.

A decline in pfu within cells can either indicate degradation, or virus release into the supernatant. In the context of both virus inputs, titre in the supernatant is already substantial within 2 hours of loading, Particularly in the context of reo-NAb, where the 2-hour supernatant titre is already at its highest, this suggests that the processing and release of virus occurs rapidly. Supernatant titres do however remain stable, indicating that there may be a low degree of ongoing virus release over the following time points.

These data can also be examined as a percentage of the total virus titre in both cells and supernatants (Figure 6.4.4b). For reovirus, the proportion of virus in the cell fraction drops over time, from 66% to 32%. Given that the increase in supernatant titre is minimal, this is suggestive of degradation rather than virus release. By contrast, in reo-NAb treated monocytes the cell-associated fraction increases from 19% to 39%, indicating that monocytes are perhaps more permissive to low level virus replication following internalisation of antibody-coated (as compared to free) virus.

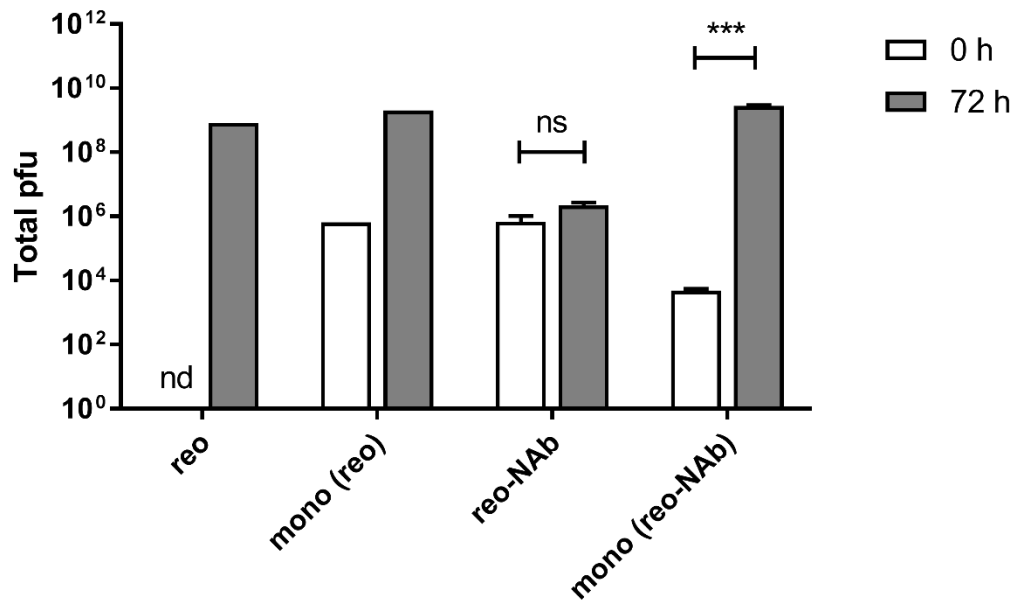


**Figure 6.4.1 Reovirus amplification following reo-NAb hand-off by monocytes**

Following addition of reovirus/reo-NAb or monocytes pulsed with reovirus/reo-NAb (MOI 10), Mel-624 cultures were harvested either immediately (0 h) or after 72 hours. Titre of replicating virus was determined by plaque assay. For conditions where neat reovirus was used, data from one representative experiment is shown; for reo-NAb conditions, data represent mean values  $\pm$  SEM from at least five independent experiments. *ns* = not significant; \*\*\* $p < 0.001$  by Student's t-test (multiple comparisons with Holm-Šidák correction). *nd* = not determined.

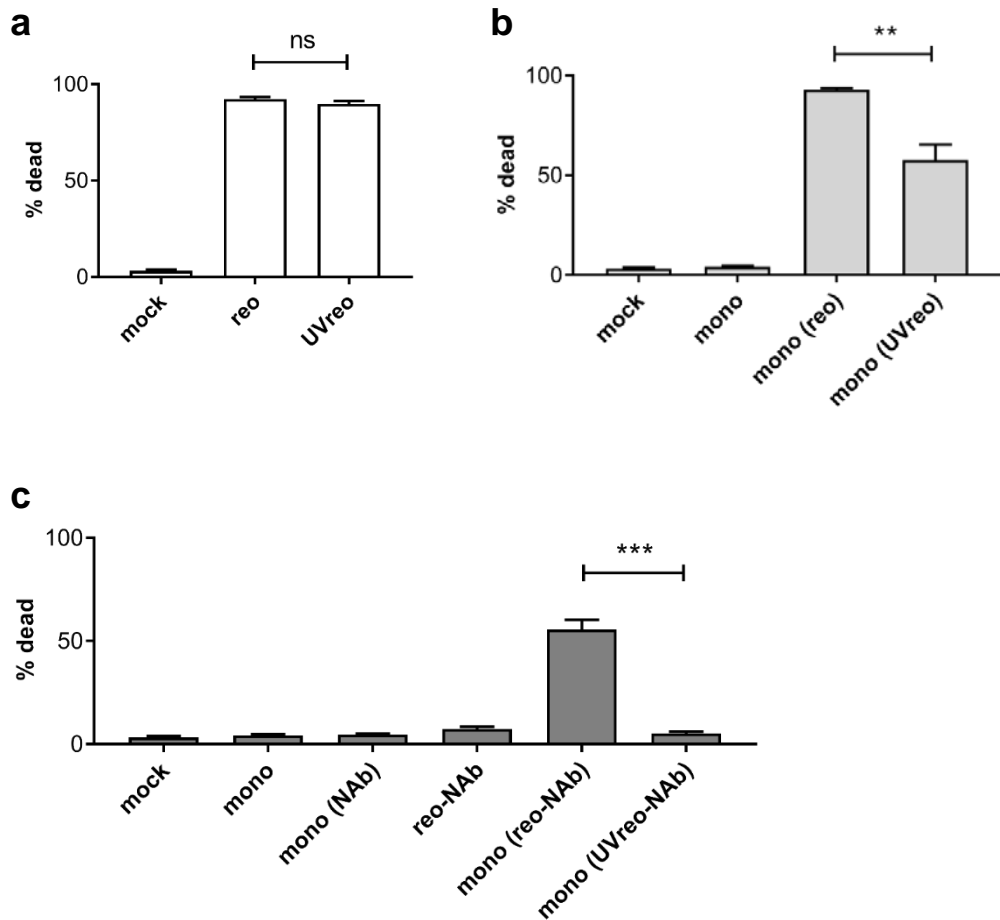


**Figure 6.4.2 Tumour cell killing via hand-off using live or UV-inactivated virus**

Data indicate the percentage of Mel-624 cells killed following 72 hours in culture with live or UV-inactivated reovirus. Virus was delivered either by (a) direct addition to Mel-624 cells, (b) monocyte hand-off of free virus, or (c) monocyte hand-off of antibody-neutralised virus. The virus dose used in all conditions was MOI 10 with respect to monocyte number.

Mean values  $\pm$  SEM from at least six independent experiments are shown. *ns* = not significant; \*\* $p < 0.01$ ; \*\*\* $p < 0.001$  by Student's t-test (multiple comparisons with Holm-Šidák correction).

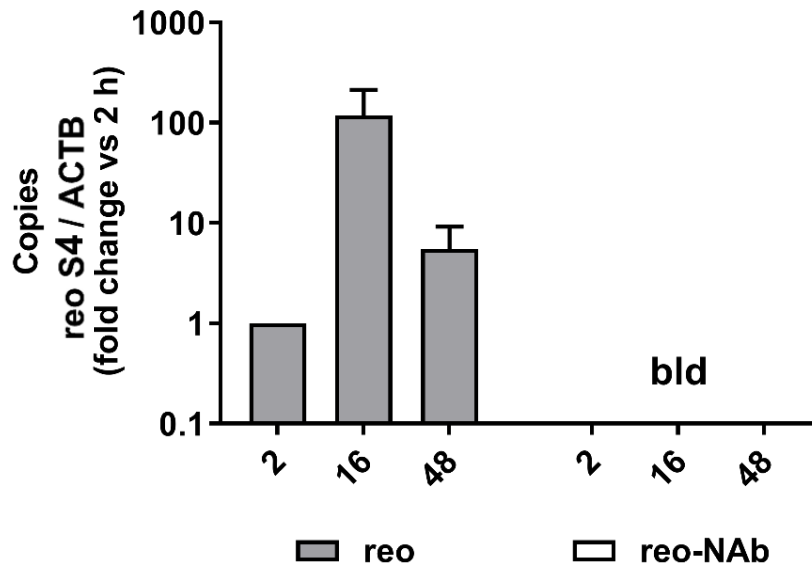


**Figure 6.4.3 Viral genomes in monocytes following reovirus or reo-NAb loading**

Monocytes were CD14-selected from PBMC and loaded with reo or reo-NAb (MOI 2.5). Cells were then washed and cultured at  $2 \times 10^6$  cells per ml for the number of hours stated on the x axis. Cells were harvested and the number of viral genomes present determined by qPCR, using reovirus *S4* as the target gene and human  $\beta$ -actin (*ACTB*) as a reference gene. Values are normalised to the 2 hour time point. Mean values  $\pm$  SEM from three donors are shown. *bld* = below limit of detection.

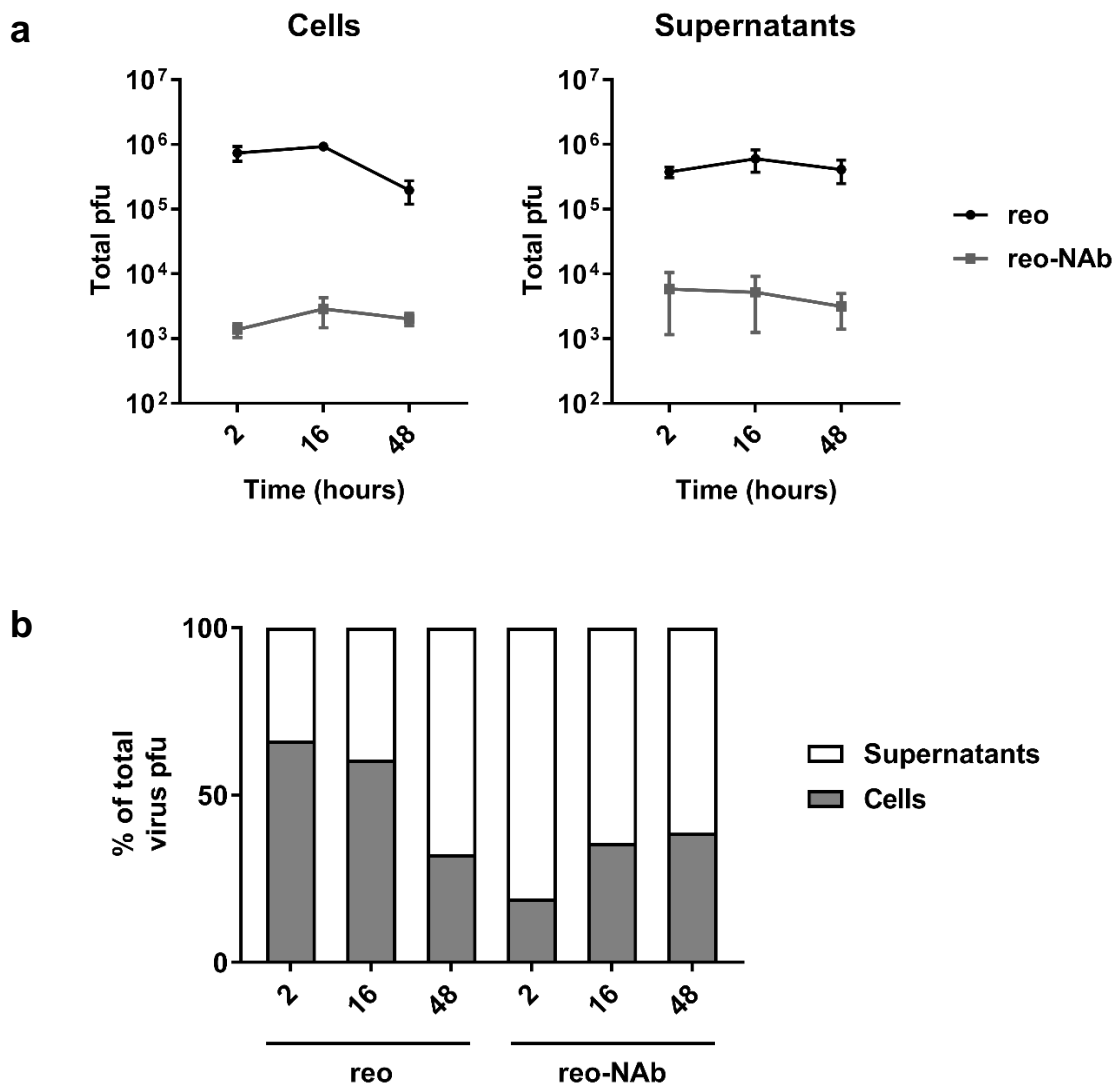


**Figure 6.4.4 Replicating virus titre in monocytes following reovirus or reo-NAb loading**

Monocytes were CD14-selected from PBMC and loaded with reo or reo-NAb (MOI 2.5). Cells were then washed and cultured at  $2 \times 10^6$  cells per ml for the times stated. Cells and cell-free supernatants were harvested and virus titre of each determined by plaque assay. Data are presented as either **(a)** the total number of pfu present or **(b)** the percentage of the total pfu present in either the cell or supernatant fraction.

Mean values  $\pm$  SEM from three donors are shown.

## 6.5 Mechanism of reovirus transfer

In terms of a purely oncolytic paradigm for cancer therapy, cellular loading of a viral cargo is worthless without its transit and effective release at the intended site. Antigen-presenting cells readily migrate from the circulation to the periphery. The trafficking of DC from the blood is pivotal to their role in T-cell stimulation during an inflammatory response (Steinman and Banchereau, 2007). Both of the major cell types deriving from monocytes (DC and macrophages) are recruited to tumours (Bingle et al., 2002); monocyte-derived macrophages in particular accumulate at the tumour site (Leek et al., 1999; Muthana et al., 2011; Peng et al., 2009). Maturation is often concomitant with extravasation, and can be facilitated by virus infection (Hou et al., 2012; Sun et al., 2011). Macrophages have thus been harnessed to deliver adenovirus and measles virus for therapy of prostate and myeloma lesions respectively (Muthana et al., 2013; Peng et al., 2009). Other cells of this lineage, such as myeloid-derived suppressor cells – which accumulate in tumours following intraperitoneal reovirus administration (Clements et al., 2015) – also represent capable OV vehicles (Eisenstein et al., 2013).

After intravenous administration, replicating reovirus can be recovered not only from patient PBMC but also from solid tumours (Adair et al., 2012). The mechanisms by which virus transfer can occur between carrier and target are myriad. Most obviously, these include a crude yet well-timed release of free virus (Muthana et al., 2013), which may nevertheless be vulnerable to subsequent neutralisation. More sophisticated mechanisms include viral transfer within exosomes or by immunological synapses, both of which may protect virus from antiviral factors in the tumour milieu (Groot et al., 2008; Kottke et al., 2006; Masciopinto et al., 2004).

The role of virus – or alternatively, other soluble factors – in Mel-624 cell killing by virus-loaded monocytes was initially examined. Monocytes were pulsed with virus and washed, and were either added directly to target cells as in the hand-off assay, or were cultured for 48 hours in order to generate cell-free conditioned medium (CM). Mel-624 cells were then treated with CM, or CM pre-filtered to remove virus (FCM), for 72 hours as in the hand-off assay. The ability of virus filters to reduce virus titre beyond detectable levels was confirmed by plaque assay on the CM and FCM of one sample of monocytes treated with reovirus (Figure 6.5.1a).

Flow cytometry was used to quantify Mel-624 viability (Figure 6.5.1b). As shown previously (Figure 5.3.5), target cells are comprehensively eliminated by monocytes loaded with free reovirus. CM from reovirus-loaded monocytes proves equally toxic, while filtration of CM significantly mitigates killing ( $p < 0.001$  by two-way ANOVA), indicating that the viral component of CM is the main mediator. This is consistent with the substantial virus titre present in supernatant from virus-treated monocytes (Figure 6.4.4).

The cytotoxic effect of reo-NAb loaded monocytes is somewhat diminished when 48-hour CM from loaded cells is used in place of the cells themselves ( $p < 0.001$  by two-way ANOVA). The remaining degree of killing can be attributed to a viral component, as target cell killing is returned to background levels upon filtration of CM ( $p < 0.05$  by two-way ANOVA). Thus although the virus present in the supernatant does appear at least partly responsible for killing, this leaves another part unaccounted for, represented by the discrepancy between CM and hand-off. This could either be attributed to the fact that CM contains virus released over 48 hours, in contrast to the 72-hour hand-off. Alternatively, another process may facilitate virus egress from monocytes in co-culture (hand-off) conditions, as compared to in culture alone.

The mechanism of virus transfer was further interrogated using two further manipulations to the hand-off assay. First, a receptor-blocking approach was taken in order to confirm the role of freely released reovirus. Prior to the addition of reovirus- or reo-NAb loaded monocytes, target cells in culture were incubated for 30 minutes with an antibody blocking JAM-A. Tumour cell viability was analysed as standard after 90 hours in co-culture (Figure 6.5.2). JAM-A blockade significantly abrogates tumour cell killing during incubation with reo-NAb loaded monocytes ( $p = 0.00082$  by Student's t-test). The same is true for reovirus-loaded monocytes ( $p = 0.00078$ ), although the effect size is smaller – perhaps due to the effective 'dose' of virus being delivered in this case being large enough to eventually out-compete the blocking antibody. Nevertheless it can be concluded that JAM-A is a key mediator of Mel-624 virus entry during hand-off by monocytes, supporting the notion that hand-off is reliant on the free release of virus.

Lastly, the effect of separating the monocyte carrier cells in suspension from the adherent target cells during hand-off was examined. Virus-loaded monocytes were added to the insert of a transwell system with a  $0.4\ \mu\text{m}$  pore size, preventing them from making direct contact with the target cells below. As previously, Mel-624 viability was assessed by flow cytometry after a 90 hour

incubation (Figure 6.5.3). While the addition of a transwell membrane did not influence killing by reovirus-loaded monocytes at this virus dose, there is a significant difference in killing between the standard and transwell conditions in the context of reo-NAb loaded monocytes ( $p = 0.0040$  by Student's t-test). This observation is somewhat unexpected, given the stated evidence for the release of free virus from monocytes, and suggests that hand-off may also involve a contact-dependent process.

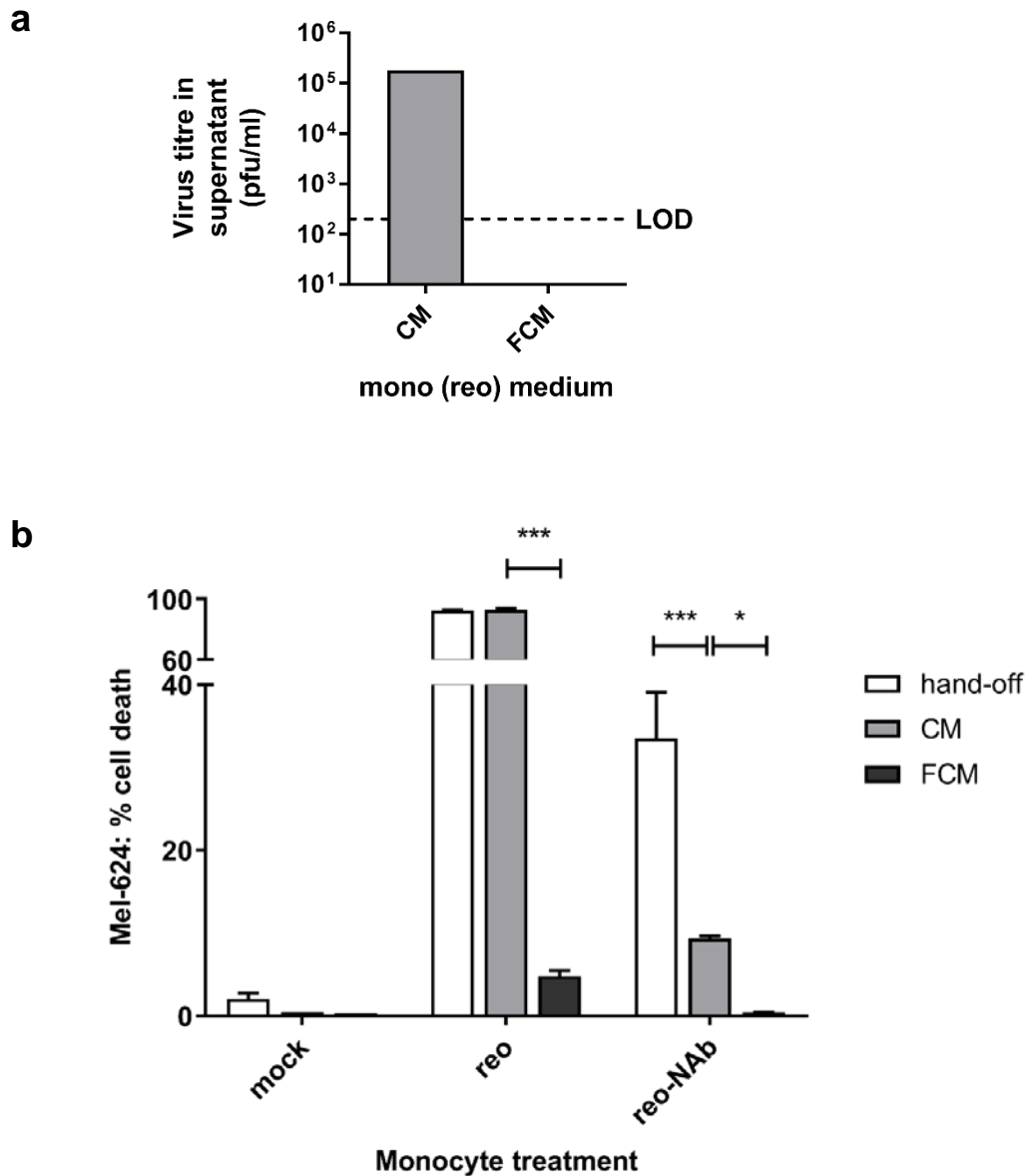


**Figure 6.5.1 Ability of conditioned medium from virus-loaded monocytes to kill tumour targets**

Monocytes were pulsed with reovirus or reo-NAb (MOI 10) and washed. Mel-624 cells were treated either with these loaded cells directly ('hand-off' condition), or with 48-hour conditioned medium from these cells, without (CM) or with (FCM) subsequent removal of virus by filtration. Proof of virus elimination is shown in (a). Mel-624 viability was assessed after 72 hours (b). Mean values  $\pm$  SEM from two independent donors are shown. \* $p < 0.05$ , \*\*\* $p < 0.001$  by two-way ANOVA (Tukey's multiple comparisons test).

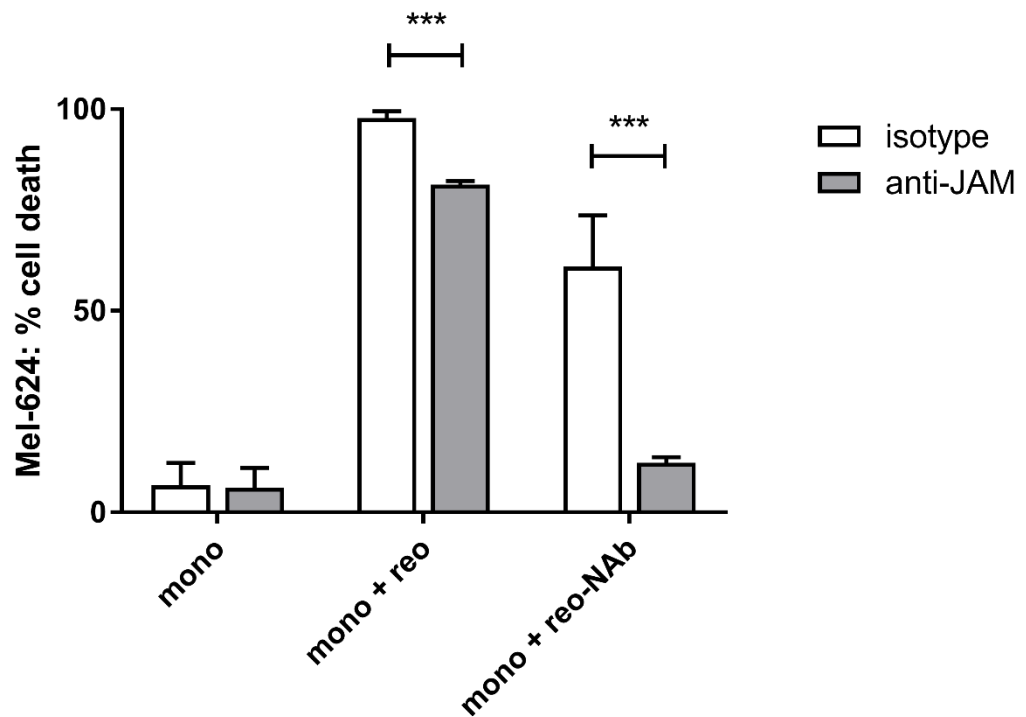


**Figure 6.5.2 Effect of tumour JAM-A blockade on tumour cell killing via hand-off**

CD14-selected monocytes were pulsed with reovirus or reo-NAb (MOI 10) and washed. Target cells were incubated with isotype control antibody (clear bars) or antibody against JAM-A (grey bars) at 10  $\mu\text{g/ml}$  for 30 minutes, prior to the addition of loaded monocytes. The percentage of Mel-624 cells killed after 90 hours is displayed.

Mean values  $\pm$  SEM from four independent donors are shown. \*\*\* $p < 0.001$  by Student's t-test (multiple comparisons with Holm-Šidák correction).

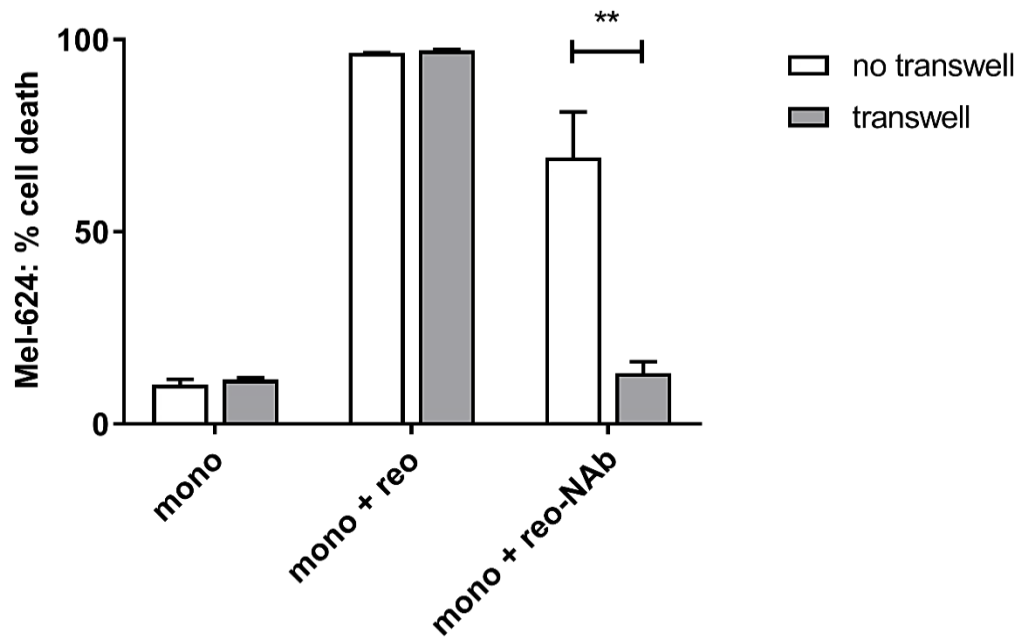


**Figure 6.5.3 Tumour cell killing via hand-off in transwell assay format**

CD14-selected monocytes were pulsed with reovirus or reo-NAb (MOI 5) and washed. Cells were either added to wells containing Mel-624 targets as usual (clear bars) or to the insert of a transwell system with pore size 0.4  $\mu\text{m}$  (grey bars). The percentage of Mel-624 cells killed after 90 hours is displayed. Mean values  $\pm$  SEM from three independent donors are shown. \*\* $p < 0.01$  by Student's t-test (multiple comparisons with Holm-Šidák correction).

## 6.6 Summary

By definition, components of the humoral immune system such as antibody and complement maintain a broad antiviral function. This study seeks to identify the potential for antiviral antibody to also function in a pro-viral capacity, based on carriage of neutralised reovirus by monocyte cells. In this chapter, the mechanisms by which reovirus, in the form of reo-NAb immune complexes, can bind to, persist within and be released from monocytes are investigated.

A variety of circulating immune populations are known sinks of virus *in vivo* (Kou et al., 2008). In the context of a non-physiological dose of OV this remains the case, in that cells readily carry virus irrespective of the presence of NAb (Adair et al., 2012; Roulstone et al., 2015). These observations are mirrored in the *in vitro* imaging and titration assays in this study, demonstrating that reovirus is able to bind to and persist within monocytes, whether presented as free virus or as reo-NAb.

The presence or absence of neutralising antibody can however considerably influence the routing of virus in circulation. 30 minutes after reovirus administration to virus-immune mice, replicating virus is absent from plasma, but in blood cells is present at significantly higher titre than in naïve mice; most of this being in the myeloid fraction (Ilett et al., 2014). The data in this study do not reproduce this absolute increase in myeloid cell loading by NAb, but do indicate that NAb may promote virus routing to this population as a proportion of the whole.

The apparent parallels between the monocyte uptake of reo-NAb complexes observed here and the existing literature documenting antibody-mediated entry of various viruses prompted an investigation of the receptors enabling myeloid cells to interact with an antibody-coated virus. The family of Fc receptors, which are heavily implicated in ADE, were therefore marked as primary candidates. Blocking studies, and the use of populations discriminated by their Fc receptor expression, strongly identified the CD16 molecule (FcγR III) as the most important mediator of reo-NAb hand-off of those tested.

Along with the transitory 'intermediate' monocyte subset, CD16 is expressed on a minor population (~ 10%) of circulating monocytes, known as the non-classical subset (Wong et al., 2011). It should be noted that although non-classical monocytes express comparatively lower levels of CD14 (Cros et al., 2010), the presence of CD16<sup>+</sup> cells indicates that they are still present in the CD14-selected monocyte population employed for hand-off in section 5.3.

The non-classical subset exhibits a 'patrolling' phenotype *in vivo*, functioning as a sensor for viruses and immune complexes (Cros et al., 2010). In a range of inflammatory conditions including viral infections, the CD16<sup>+</sup> population is expanded (Kwissa et al., 2014; Wong et al., 2012). Additionally, the ability of common polymorphisms in CD16 to predict the therapeutic response to oncolytic adenovirus may signal its relevance, not just to virus-stimulated ADCC but also potentially in antibody-dependent adenovirus infection (Hirvonen et al., 2013).

However, to date, Fc receptor-mediated virus ADE has largely been restricted to the other two Fc $\gamma$  receptors, CD64 and CD32 (reviewed in Taylor et al., 2015). Evidence for the role of CD16 in ADE is limited. However, like its better-characterised cousin CD32, CD16 is a low-affinity Fc receptor and is associated with the intracellular  $\gamma$ -chain which is crucial for both receptor assembly and signalling (Wirthmueller et al., 1992). Indeed, CD16 is capable of mediating ADE of unrelated viruses in both porcine and human cell types (Gu et al., 2015; Tóth et al., 1994). Most recently, CD16 was specifically implicated in the recognition of virus-bound IgG in the development of severe dengue disease (Wang et al., 2017). To our knowledge, the present study represents the first report of CD16-mediated OV entry in human myeloid cells.

It is notable that some degree of reo-NAb hand-off remains, both in the presence of CD16-blocking antibodies, or in the context of hand-off by CD16<sup>-</sup> monocytes. The basis for this observation is unclear. In this scenario as before (Fanger et al., 1996; Rodrigo et al., 2006) there may exist a degree of redundancy between Fc receptors, in that others such as CD64 and CD32 may also play a lesser role. It remains possible that the hand-off assay in this study is insufficiently sensitive to detect a role for these receptors, perhaps due to their incomplete saturation by blocking antibody prior to loading. It is also clear that the assay used to compare hand-off by populations differentially expressing CD16 does not take into account the potential for variable efficiency of virus delivery by these two monocyte subsets, which may confound the readout. As such although this study implicates CD16 in the uptake of reo-NAb by monocytes, a role for other receptors cannot be excluded.

Returning to the relevance of the ADE phenomenon to the hand-off paradigm, two major discrepancies are apparent. First, reovirus loading and delivery is demonstrated in the context of complete neutralisation. By contrast, ADE is almost exclusively identified in the presence of sub-neutralising concentrations of antibody, or non-neutralising antibody (Halstead and O'Rourke, 1977; Mori et

al., 2008). There are few reports of virus entry by a fully neutralised virus. These include the observation of adenovirus infection of FcγR-expressing cells despite antibody neutralisation (Leopold et al., 2006). However, to our knowledge, this study is the first to report the infection of primary human phagocytes by a fully neutralised OV.

Second – as shown by both the somewhat artificial hand-off assay and the more physiologically relevant test with whole blood – the loading and delivery of virus by monocytes is not enhanced by the presence of NAb. In fact, by assessment of viral titre and (by extension) target cell killing, the viral load of reo-NAb pulsed monocytes is consistently a factor of two logarithms below that of cells pulsed with the equivalent amount of neat virus. Given the virus is fully neutralised in reo-NAb, this suggests that antibody opsonisation is highly limiting to reovirus loading of carrier cells by the classical route which likely involves sialic acid (Ilett et al., 2011) and possibly JAM-A. Thus, although reo-NAb is reliably delivered to targets, NAb cannot be said to be remotely ‘enhancing’ in terms of monocyte virus uptake (extrinsic ADE). While not strictly ADE, reo-NAb loading of monocytes does appear to share the same mechanism: supplying an alternative route of loading, via Fc receptors. It can be speculated that in the case of a virus whose cognate receptor is not abundant on the phagocyte surface, NAb – even at fully neutralising concentrations – could expand virus tropism to include phagocytes and hence promote OV persistence *in vivo*.

Our results describing the ability of myeloid cells to enable reo-NAb complexes to exert anti-tumour activity in the context of human cell types are highly comparable to those observed in the murine setting (Ilett et al., 2014). Elevation of Fc receptor expression by GM-CSF was associated with the enhanced ability of myeloid cells to take up neutralised reovirus for hand-off to kill target cells, and also to stimulate immune-mediated cytotoxicity. The aforementioned data are consistent with this study in that they support a substantial role for Fc receptor function in reo-NAb uptake, upon which hand-off depends.

Following loading with reovirus or reo-NAb, the murine myeloid population clearly plays host to significant amplification of the virus (Ilett et al., 2014). This finding is not replicated in human monocytes – albeit in a shorter time frame – as virus titres remain relatively stable. Indeed, limited evidence was found for the relevance of intrinsic ADE to reo-NAb loaded monocytes. There is a minimal (46%) increase in cell-associated virus titre over 48 hours in the context of reo-NAb, in contrast to a considerable decrease in the context of free reovirus.

Thus, although these data provide tentative evidence for low level virus replication following treatment of monocytes with reo-NAb complexes, it is clear that in this *in vitro* system with reovirus, these cells do not host the type of explosive amplification that occurs in ADE infection with dengue. In this sense, human myeloid cells do not mirror murine DC, which do support considerable reovirus amplification *in vitro* (Ilett et al., 2009). Rather, it is likely that the bulk of virus replication in the hand-off assay occurs in target tumour cells. This is despite the observation that – at least in the context of free reovirus – there is a substantial increase in reovirus genomes within the first 24 hours of infection, which is not manifested at the protein level. Such a disparity between the RNA and protein level would suggest a somewhat abortive replication cycle, perhaps due to the uncoupling of transcription and translation, which is explored further in the next chapter.

Spatial information regarding the subcellular trafficking and fate of viral cargo would be useful in interpreting the patterns of viral persistence that were detected. Detection of the viral component of reo-NAb by antibody staining is precluded by the coating of the virus by neutralising serum antibodies. Owing to this – and to the unavailability of a reovirus construct encoding a fluorescent transgene – trafficking data could not be generated in this study. The expression of GFP in reovirus is detrimental to the stability of its RNA genome; the insertion of smaller constructs is possible but may require the replacement of endogenous genes (D. van den Wollenberg, personal communication, and van den Wollenberg et al., 2015). The semi-permanent labelling of reovirus RNA using nucleic acid stains and subsequent purification (Brandenburg et al., 2007), which has proven difficult to achieve to date, represents a promising option by which reo-NAb trafficking may be investigated in future should a labelled virus remain unavailable.

Following internalisation, free reovirus undergoes endo-lysosomal trafficking (Ehrlich et al., 2004; Mainou and Dermody, 2012a) and proteolysis (Mainou and Dermody, 2012b; Sturzenbecker et al., 1987), following which escape to the cytosol enables the formation of factory-like ‘viral inclusions’ which host replication (Becker et al., 2001; Broering et al., 2004; Silverstein and Schur, 1970). The ability of reo-NAb to access both the endosome and possibly the cytosol may therefore explain the limited ability of the virus to replicate within monocytes. It should subsequently be possible, either by the co-localisation of virus with specific endocytic GTPases (Mainou and Dermody, 2012a) or the use of trafficking inhibitor compounds such as monensin (Wang et al., 2007), to determine the process by which a degree of virus load is so promptly released.

The capability of monocytes to rapidly liberate a significant proportion of their cargo is reinforced by the finding that successful hand-off is reliant on target cell JAM-A. These observations suggest that hand-off depends on the release of free virus, likely in the form of an intact virion rather than a disassembly intermediate able to infect independent of JAM-A (Alain et al., 2007; Borsa et al., 1979). In light of this, the observation that hand-off killing is limited upon separation of carriers and targets by a transwell membrane appears incongruent: if release of free virus represents the sole mechanism leading to killing, then the transwell should have no effect. Barring artifacts such as the aberrant adhesion of virus to the membrane, these data are challenging to reconcile. Processes of viral transfer commonly involve either a virus release- or cellular contact-dependent mechanism (reviewed in Zhong et al., 2013); a more complex process requiring both appears unlikely. It is therefore speculated that hand-off occurs via release of free virus, and that decreased killing in the transwell condition simply reflects the impact of increased diffusion distance between the carrier and target cells. Further manipulations would need to be made to the hand-off assay in order to consolidate this conclusion.

However, given the critical nature of systemic anti-tumour immunity (Andtbacka et al., 2015b), perhaps of greater value to the field are the potential immunological consequences of monocyte carriage of reo-NAb. The ability of reo-NAb to influence monocyte phenotype and subsequently to stimulate the anti-tumour activity of other immune populations are therefore explored in the next chapter.

## 7. Immunological consequences of antibody-bound reovirus on immune populations

### 7.1 Introduction

Whether therapeutic or pathogenic, a virus – like other microorganisms – presents a variety of exogenous ‘danger signals’ to the host immune system. Individually known as pathogen-associated molecular patterns (PAMP), these evolutionarily conserved features of pathogens are readily detected by a range of cellular sensors collectively termed pattern recognition receptors (PRR), according to Janeway’s ‘infectious non-self model (Janeway, 1989). The initial sensing of viruses is fundamental to their potent ability to stimulate the host immune system in both a specific and non-specific manner.

While there are effective immune mechanisms that specifically target the invading pathogen – the generation of antiviral NAb being a key example – viruses also act as non-specific inflammatory devices within the immune milieu. In the context of cancer, such inflammatory properties are highly valuable as they are well suited to reversing the suppressive tumour microenvironment. Alongside the direct oncolytic traits that earned the name of OV, they add a second string to their bow: an immunostimulatory capacity, which is increasingly regarded as central to OV therapy (Prestwich et al., 2008b). The mechanisms by which OV can induce immune-mediated anti-tumour activity are manifold. Aside from direct lysis, these include the modulation of the cytokine environment and the activation of DC, which, as key linkers of innate and adaptive immunity, can elicit cytotoxic responses from both NK and T lymphocytes.

The ability of reovirus to promote these immunological processes has been well documented (Adair et al., 2013; Errington et al., 2008a; Jennings et al., 2014; Prestwich et al., 2009a). The impact of antibody neutralisation upon reovirus immunogenicity is less well understood. Therefore the ability of both free reovirus and reo-NAb complexes to modulate monocyte phenotype and subsequently to stimulate anti-tumour immunity were investigated.

## 7.2 Activation of monocyte carrier cells

During the evolution of innate pathogen surveillance mechanisms, significant functional redundancy has been generated. This comprises a host of germline-encoded PRR 'sentinels' which are most richly expressed by APC. The individual PRR classes include C-type lectin receptors (CLR) at the cell surface, toll-like receptors (TLR) at the surface and within endosomes, and NOD-like receptors (NLR) and RIG-I-like receptors (RLR) in the cytosol. This spatial segregation leaves some (such as TLR) primarily suited to sensing extracellular pathogens, and others (such as RLR) responsible for detection of intracellular ligands, usually nucleic acids (reviewed in Akira et al., 2006). By converging on a set of 'hub' transcription factors – principally interferon response factors (IRF) and NF- $\kappa$ B – in the cytosol, these sensors trigger the transcription of inflammatory genes including type I interferons (IFN), pro-inflammatory cytokines and microbial defence peptides. In immature cells such as monocytes, this antiviral response is accompanied by a concomitant elevation of co-stimulatory markers and transition to a more mature phenotype (Errington et al., 2008a; Hou et al., 2012).

The virus is an obligate intracellular parasite, entirely reliant on the host cell to replicate its DNA or RNA. Although proteinaceous viral components are readily recognised, the necessary exposure of nucleic acids is likely linked to the acute cellular sensitivity to these types of PAMP. The double-stranded RNA (dsRNA) of Class III virus genomes, and replication intermediates of some ssRNA viruses (Weber et al., 2006), are sensed by membrane-bound TLR3 and the cytosolic helicases termed retinoic acid-inducible protein I (RIG-I) and melanoma differentiation associated gene 5 (MDA5). The helicases have different ligand specifications – the 5' triphosphorylated ends of short RNA for RIG-I, longer dsRNA species for MDA5 (Hornung et al., 2006; Kato et al., 2006) – and detect different RNA viruses accordingly (Loo et al., 2008).

The downstream signal from RIG-I and MDA5 is integrated by the mitochondrial antiviral signalling (MAVS) adaptor protein (Kawai et al., 2005), while TLR3 signals via the TIR domain-containing adaptor inducing IFN- $\beta$  (TRIF) protein. Signalling cascades from MAVS and TRIF converge upon IRF3, whose phosphorylation triggers the transcription of antiviral response genes including PRR themselves (de Veer et al., 2001).

TLR3 appears dispensable for virus sensing by many cell types (Edelmann et al., 2004; López et al., 2004). Despite its predominantly endo-lysosomal

localisation there is limited evidence to suggest a role for TLR3 in sensing viruses with specific entry routes; it may instead function in a cellular context, such as in detection of dsRNA upon presentation by dying, virus-infected cells (Schulz et al., 2005). By contrast, cytosolic helicases appear less dispensable. IFN responses are amplified or abrogated upon RIG-I overexpression or knock-out respectively (Kato et al., 2005; Yoneyama et al., 2004) and knock-out of either helicase results in increased cellular susceptibility to virus (Kato et al., 2006).

Complementing the helicases RIG-I and MDA5, PKR represents an alternative dsRNA sensor in the cytosol. Following autophosphorylation, PKR responds to dsRNA ligand by phosphorylating eukaryotic initiation factor 2-alpha (eIF2 $\alpha$ ), a master regulator of translation, and thus precluding protein synthesis (Williams, 2001). Simultaneously, PKR activation leads to the stimulation of NF- $\kappa$ B signalling by releasing the inhibitory action of I $\kappa$ B- $\beta$ , yielding pro-inflammatory cytokine release (Bonnet et al., 2006; Deb et al., 2001; Williams, 1999).

In order to examine the role of virus-sensing PRR in the interaction between monocytes and reovirus, the expression of individual sensor proteins was examined by western blot, as shown in Figure 7.2.1. Freshly isolated human monocytes were treated with patient serum, free reovirus or reo-NAb complexes at a high MOI of 10, cultured for 24 hours, and cell lysates probed with antibodies against PRR or downstream effectors. Free reovirus induces the robust upregulation of PKR and RIG-I, and there is evidence to suggest limited induction of MDA5. Reo-NAb treatment results in similar changes in the synthesis of PKR and RIG-I protein, to a slightly lesser degree; this can be attributed to the viral component, as free NAb has negligible impact. No bands could be detected when probing for TLR3 (data not shown).

Looking further downstream at key transcription factors, the upregulation of IRF3 and the p50 subunit of NF- $\kappa$ B was observed upon reovirus or reo-NAb treatment, further demonstrating the induction of a global antiviral state. Investigation of the phosphorylation status of PKR or IRF3 by western blot, which would directly demonstrate their active involvement in proximal signalling, was not informative (data not shown). Consequently, while it appears likely, it cannot be concluded with certainty that cytosolic sensors are exposed to viral dsRNA following reovirus and reo-NAb treatment.

In order to gain further information on the impact of reovirus or reo-NAb carriage on human monocyte phenotype, cells were cultured for 48 hours after treatment and expression of key surface markers analysed by flow cytometry. The

isotype-corrected median fluorescence intensity was determined on the myeloid CD11b<sup>+</sup> population (Figure 7.2.2). The lipopolysaccharide receptor and immature myeloid marker CD14 is strongly downregulated by reovirus or reo-NAb ( $p = 0.0001$  and  $0.0143$  respectively by one-way ANOVA). This is mirrored by a reduction in surface CD11c protein, which does not reach significance upon reo-NAb treatment ( $p = 0.043$  and  $0.052$  respectively). Together, these markers indicate that both free and neutralised reovirus induces monocyte maturation, but not towards a conventional DC (cDC) phenotype.

Surface expression of the co-stimulatory protein CD86 is increased by over 100% versus mock-treated cells ( $p = 0.0012$  and  $0.0023$  for reovirus and reo-NAb respectively), while only free reovirus induces elevated expression of the MHC class II antigen HLA-DR ( $p = 0.0368$ ). These results suggest that virus-treated monocytes may be more readily able to stimulate T cell activation. In all cases, it should be noted that the influence of free reovirus upon the surface expression of these proteins is greater than that of reo-NAb.

During maturation and recruitment to lymphatic tissues, sites of damage or tumour lesions, monocytes must extravasate from the vasculature. The steps of endothelial adhesion and transmigration demand an increase in cellular migratory capacity. In keeping with its role in response to pathogens, migration is profoundly influenced by virus insult (reviewed in Smith and Sanderson, 1999). The migratory capacity of reovirus- and reo-NAb treated monocytes was thus investigated, in order to detect potential modulation by the presence of antiviral antibody.

Monocytes were treated with virus at MOI 5 and cultured for 16 hours, then transferred to the insert of a 5  $\mu\text{m}$  transwell system in which the lower chamber contained either medium conditioned for 48 hours by Mel-624 cells, or unconditioned medium. The number of monocytes successfully migrating into the lower chamber after 5 hours was quantified. As shown by the data from one representative donor (Figure 7.2.3), in this assay, with respect to mock-treated cells, reo-NAb treatment was associated with increased migration, while reovirus was associated with a potential decrease. As these differences appear to be independent of the chemotactic gradient established by the melanoma cells, it can be concluded that they represent changes in motility – and likely chemokinesis via an autocrine cytokine response – but not necessarily in the directional process of chemotaxis. Further investigation would thus be required to tease apart these processes, partly as a non-directional autocrine response

to monocyte-produced cytokines could interfere with the potential for chemotaxis.

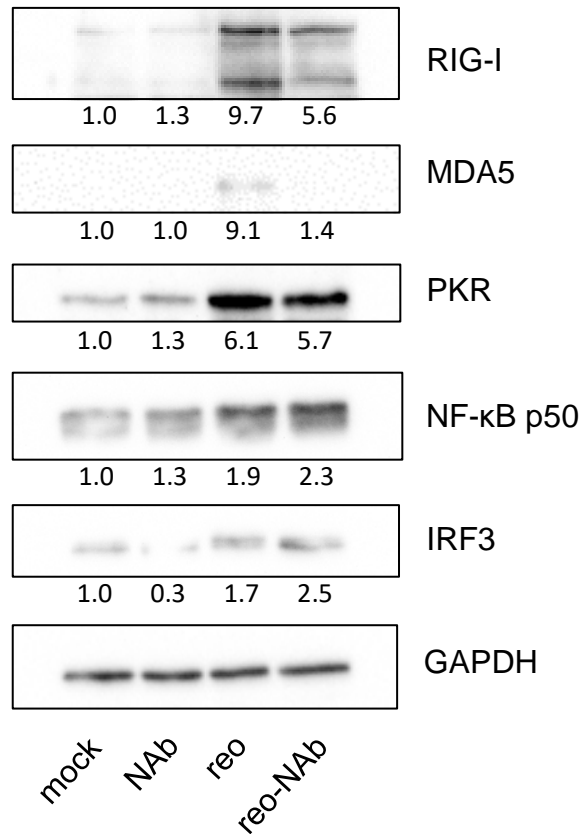


**Figure 7.2.1 Analysis of treated monocyte phenotype by western blot**

Monocytes were treated with antibody (NAb), reovirus (reo) or reo-NAb complexes at MOI 10, washed, and cultured in RPMI-10 for 24 hours. Lysates were made and probed by western blot for the indicated proteins of interest. Protein densitometry values (normalised to mock samples) are shown. Images are representative of two monocyte donors.

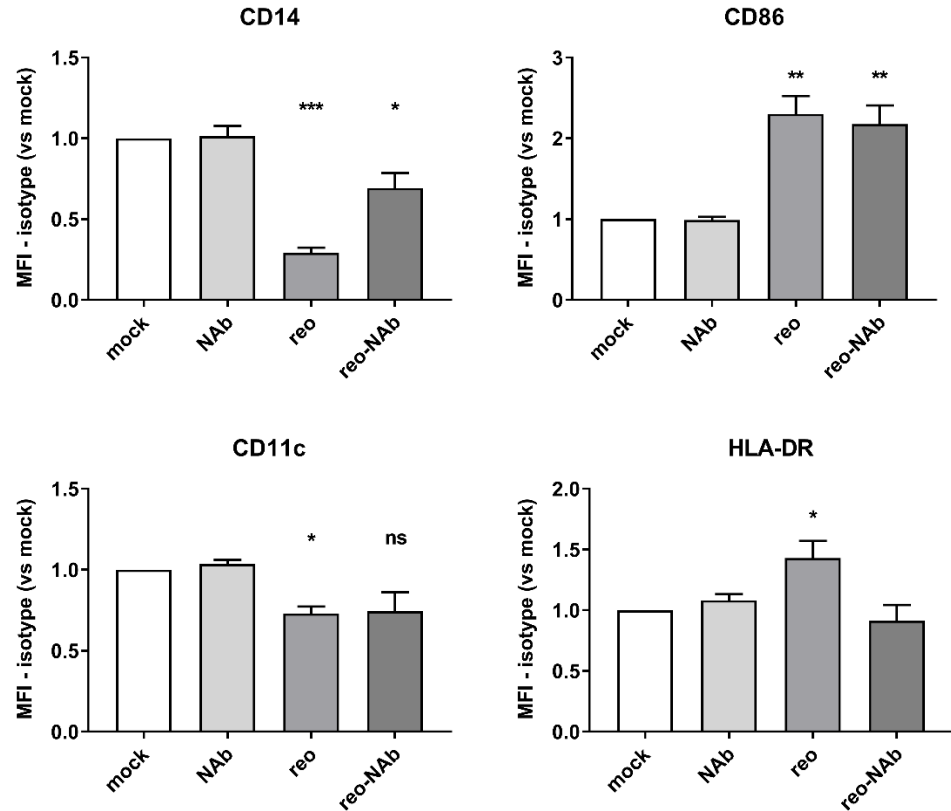


**Figure 7.2.2 Analysis of treated monocyte phenotype by flow cytometry**

Monocytes were treated with antibody (NAb), reovirus (reo) or reo-NAb complexes at MOI 10, washed, and cultured in RPMI-10 for 48 hours. Surface protein expression was assessed by flow cytometry. Isotype staining was subtracted from median fluorescence intensity (MFI) for each marker, and values normalised to mock-treated cells. Data  $\pm$  SEM from three individual donors are shown. \* $p < 0.05$ , \*\* $p < 0.01$ , \*\*\* $p < 0.001$  vs mock by one-way ANOVA (Dunnett's multiple comparisons test).

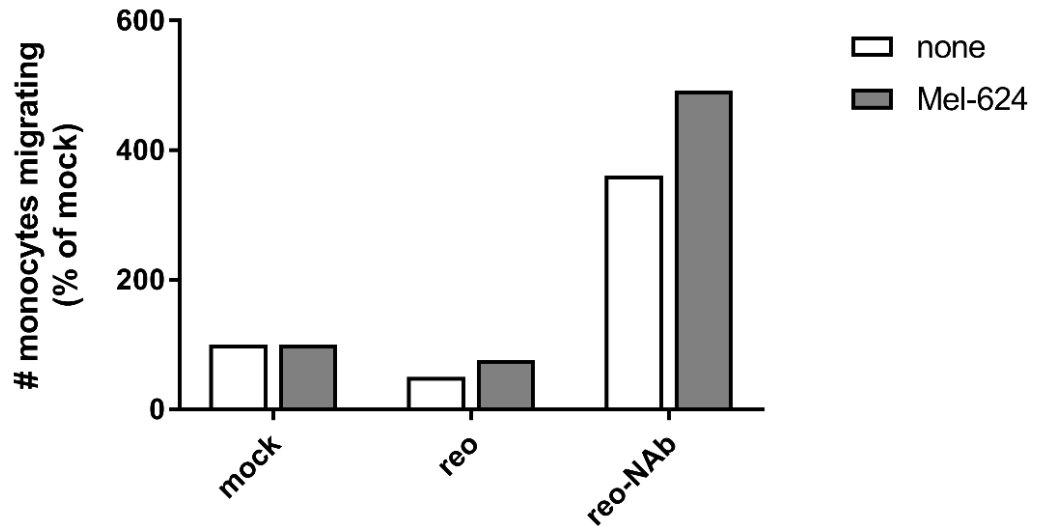


**Figure 7.2.3 Migratory capacity of treated monocytes**

Monocytes were treated with reovirus or reo-NAb (MOI 5), washed, and cultured overnight (16 hours). Cells were resuspended and  $2 \times 10^5$  added to the upper chamber of a transwell system with 5  $\mu\text{m}$  pore size. The lower chamber contained either no chemoattractant (clear bars) or medium conditioned for 48 hours by Mel-624 cells (grey bars). The number of monocytes in the lower chamber after 5 hours was assessed by flow cytometry using CD11b FITC staining. Data are presented as a percentage of mock-treated cells, and are representative of two donors.

### 7.3 Effects of carriage on transcriptional profile

From epigenetic regulation and transcription to translation and post-translational modification, transcription is perhaps the most fundamental process in regulating the creation of functional gene products. Virus infection of immune cells not only triggers the transcription of antiviral defence genes but influences other, more diverse elements of the host cell phenotype, from growth and differentiation to movement and cell death (Liew and Chow, 2006), and modulates the outcome of infection.

The nature of the transcriptional response to a free virus can to some extent be predicted, based on virus and cell type, and the expression of relevant receptor and sensor proteins. By contrast, the outcome of the more complex interaction between an antibody-opsonised virus and any given cell is less easy to foresee. This likely stems from more limited knowledge of both the mechanisms enabling cells to 'see' these immune complexes and of their downstream sequelae. While the viral component is by definition the same, the difference in response to free and antibody-bound virus can range from minimal to total (Boonnak et al., 2011; Watkinson et al., 2015).

Consequently, following the preliminary evidence for monocyte activation, the global transcriptional profile of monocytes was assessed in order to detect differential responses to free or neutralised reovirus. After treatment with antibody or virus, monocytes were cultured for 24 hours – rather than the 48 hours for protein-level changes – prior to extraction of RNA for gene expression analysis by RNAseq.

First, a number of analytical tools were employed to assess the magnitude of the response to treatment in terms of differentially expressed (DE) genes. The mean normalised gene count (expression) value was plotted against the  $\log_2$  fold-change between treatment and mock, to generate graphs termed diagnostic MA or 'volcano' plots (Figure 7.3.1). Individual data points in red represent DE genes. DE was defined as an adjusted  $p$  value ( $p_{adj}$ ) of less than 0.1. Remarkably, the addition of patient-derived serum (NAb, in the absence of virus) to human monocytes generated no DE genes whatsoever compared to mock, as indicated by a lack of deviation on the  $y$  axis (Figure 7.3.1a).

By contrast, the transcriptional response to free reovirus is extreme: of the approximately 17,300 genes analysed, over 45% (7,907) are differentially expressed versus mock (Figure 7.3.1b). Some genes exceed the  $2^6$  (64)-fold change limit in the scale shown on the  $y$  axis. At first glance, the MA plot for

reo-NAb versus mock resembles an attenuated version of that for the free virus. DE transcripts represent approximately 30% (5,109) of those tested, and the fold-change values appear reduced (Figure 7.3.1c).

Other tools enabled the transcription-level data to be harnessed in order to illustrate the scale of the transcriptional changes. For each of the three donors (A-C), the log-transformed expression data shown in Figure 7.3.1 were integrated, and samples from each of the four treatment groups (1-4) compared by clustering and principal component analysis (PCA). Heat maps resulting from clustering analysis between mock- and antibody- or virus-treated cells (1 vs 2/3/4) are shown in Figure 7.3.2a. Lighter colours indicate greater differences between individual samples. Comparing mock- and NAb-treated monocytes (1 vs 2), samples convincingly cluster by donor rather than by treatment group, indicating that the endogenous genetic variation between donors exceeds that induced by treatment. Conversely, when comparing mock- to reovirus- or reo-NAb treated monocytes (1 vs 3/4), the hierarchical clustering patterns and dark colours shared within treatment groups demonstrate that the transcriptional effects of these agents far exceed the underlying variation between donors.

A complementary mode of quantifying sample-to-sample distance, PCA reduces the dimensionality of the data by integrating sample variation into a limited number of principal components. Figure 7.3.2b shows biplots – that is, based on the top two PC only – of the six samples (1 vs 2/3/4 respectively), indicating the similarity between each. The results mirror those of the clustering analysis. Mock- and NAb-treated sample ‘nodes’ scatter according to donor, while mock- and reovirus-/reo-NAb treated nodes scatter by condition. In these plots, nodes for mock- and virus-treated samples are spatially separated along the x axis – PC1, accounting for most of the observed variation – showing that the influence of virus (whether free or neutralised) on monocyte expression profile predominates over other covariates.

The comparisons used to this point have examined individual treatment conditions against mock-treated monocytes as an expression profile baseline. Recognising the apparent qualitative similarities between the effects of reovirus and reo-NAb, in terms of surface marker expression and transcriptional profile, the finer discrepancies between the two viral groups were pursued. This comparison is a relevant one in that it is an *in vitro* representation of the differential responses of naïve and pre-immune patients to reovirus. Transcriptional differences may prove informative as to the potential for virus to yield immunogenic responses from each type of patient.

In order to obtain an overview of these potential differences, the gene expression data sets from reovirus and reo-NAb treated monocytes were initially interrogated at a global level. First, using the same tools, inter-sample variation was assessed by including mock-, reovirus- and reo-NAb treated samples in a single analysis. The resulting clustering heat map and PCA plot are shown in Figure 7.3.3a and 7.3.3b. Both plots indicate that, rather than clustering together, reovirus- and reo-NAb treated samples cluster in their two distinct groups. The PCA plot is particularly informative, identifying a minor degree of variation (PC2, 9%) that discriminates between reo-NAb nodes and mock/reovirus nodes. Indeed, these plots suggest that the free and neutralised forms of reovirus do not provoke identical transcriptional profiles.

The degree of similarity between the profiles was quantified by identifying the individual DE genes shared by, or unique to, reovirus/reo-NAb treatment (Figure 7.3.3c). Here, modified criteria were used to define DE: (i)  $p_{adj} < 0.1$ , and (ii)  $\log_2$  fold-change of  $> 1.0$  or  $< -1.0$ . A total of 6,037 DE genes were detected in either group. Of these, while 1,764 (29.2%) were common to both groups, a majority (3,992 genes, 66.1%) were unique to the reovirus group. A minor subset of 281 genes (4.7%) were found to be DE for reo-NAb but not reovirus.

This DE gene set unique to reo-NAb was of particular interest, given its potential value in identifying the putative qualitative differences in impact between free and neutralised reovirus. In order to detect a 'reo-NAb unique' gene signature, the 281-gene subset was submitted for enrichment analysis using the online multi-database tool Enrichr (<http://amp.pharm.mssm.edu/Enrichr>; Chen et al., 2013; Kuleshov et al., 2016). Within Enrichr, the Kyoto Encyclopaedia of Genes and Genomes (KEGG) and the Gene Ontology (GO) repositories were selected as databases of particular focus, given their ability to distil gene lists into information regarding over-represented cellular functions and pathways. Figure 7.3.4a shows the enriched GO terms based on the reo-NAb DE gene set, within each of the three GO categories: cellular context (CC), biological process (BP) and molecular function (MF). The enriched terms are assigned adjusted  $p$  values (corrected values from the Fisher exact test) and z-scores (a measure of the deviation from the expected rank of a term). The listed GO terms are ranked by  $p_{adj}$  values, with 'combined score' (a hybrid metric of  $p_{adj}$  values and z-scores) also provided for reference.

Figure 7.3.4a strongly suggests that upon reo-NAb treatment of monocytes, in terms of subcellular localisation (CC), genes related to the lysosomal

compartment are significantly enriched – that is, these genes represent a significantly higher proportion of the DE gene set than expected. These genes include those encoding Rab family GTPases (RAB12, RAB27A, RAB38) and cathepsin family proteases (CTSB, CSTC, CTSD, CTSK, CTSZ) which are modulators of vesicle trafficking and intravesicular degradation respectively. In the BP category, the enriched gene terms following reo-NAb treatment include inflammatory response genes, largely cytokines; as corroborated by the results in the MF category, these sets are partly composed of various chemokines implicated in binding CXCR receptors. This is consistent with the top hit generated by KEGG pathway analysis, namely ‘cytokine-cytokine receptor interaction’ (padj = 0.00114, data not shown).

Upon direct analysis of the changes in gene expression, a specific upregulation of the *FCGR3A* and *FCGR3B* genes upon reo-NAb treatment was identified, in contrast to a slight decrease upon reovirus treatment (Figure 7.3.4b). Given that *FCGR3B* expression in monocytes is negligible, this apparent increase is likely an artifact resulting from the gene’s high homology with *FCGR3A*. The changes in transcription of *FCGR3* genes by reo-NAb were not mirrored in *FCGR1* and *FCGR2* genes, which exhibited fold-change values between 1.0 and 1.9 and did not reach the threshold for differential expression (data not shown). This selective induction of genes encoding FcγR III further suggests, but does not prove, the involvement of this receptor in reo-NAb trafficking. Despite the upregulation of specific Fc receptor transcripts by reo-NAb, this did not translate into a significant enrichment of GO terms annotated under ‘FcγR-mediated phagocytosis’ in this analysis (padj = 0.442, data not shown).

In order to obtain a complete picture of the transcriptional response to each ‘type’ of virus, it was resolved that both DE gene sets, including genes common to both lists, should be compared directly. As per Figure 7.3.3c, the reovirus DE and reo-NAb DE lists – composed of 5,756 and 2,045 genes respectively as per Figure 7.3.3c – were submitted to Enrichr and analysed using the KEGG and GO databases. Figure 7.3.5 shows the degree of enrichment by padj value in numerous KEGG pathways and GO terms.

The KEGG pathways shown in Figure 7.3.5a are ordered according to padj value of the reo DE list. In the majority of cases, gene sets enriched by reovirus also appear significantly enriched by reo-NAb. In particular, pathways representing cytokine or chemokine signalling are highly significantly enriched in both conditions; other gene sets such as those representing JAK-STAT signalling are more biased towards reovirus alone. Notably, in a minority of

terms including those for the phagosome and cell adhesion molecules, higher  $p_{adj}$  values are observed following reo-NAb treatment. This suggests that reo-NAb can provoke a larger response than reovirus from certain cellular processes, and that the differences between the two are not purely quantitative.

The concept that reovirus and reo-NAb are qualitatively different in impact is reinforced when examining the enrichment of GO terms (Figure 7.3.5b). Specifically in terms of subcellular localisation, there is a substantial enrichment of genes relating to the mitochondrion in reovirus- but not reo-NAb treated monocytes. By contrast, reo-NAb appears to strongly influence the secondary lysosome, while both reovirus and reo-NAb impinge upon genes relating to the phagocytic vesicle membrane.

Looking at signalling cascades, as suggested by western blot (Figure 7.2.1), both reovirus and reo-NAb stimulate NF- $\kappa$ B, while signalling via the chemokine receptor CXCR3 is more significantly enriched upon reo-NAb treatment. Both stimuli appear to target genes involved in the restriction of viral replication, corroborating the evidence for PKR signalling by western blot (Figure 7.2.1). It can also be observed that GO terms implicated in viral transcription and host autophagy are induced much more strongly by the free virus than by the neutralised form.

Finally in this data set, there are notable disparities in IFN-related pathways. While the type I IFN signalling pathway in general appears to be more significantly enriched by reo-NAb than reovirus, actual binding of IFN receptors may be lower, and viral suppression of type I IFN may be enhanced. Thus there seem to be quite different (and potentially revealing) effects on IFN signalling between the two treatments, which are explored further below in the wider context of virus-induced cytokine production.

First, in order to have confidence in interpreting transcriptional changes at the single-gene level, the data obtained by RNAseq were validated using qPCR on a small sample gene set. This necessitated the identification of a suitable housekeeping gene (HKG) in the monocyte samples. The mean expression values of various well-studied HKG were taken from RNAseq samples and coefficient of variation ( $CV = SD/mean$ ) used to compare their deviation across treatment conditions (Figure 7.3.6a). While the expression of more 'traditional' choices such as *GADPH* and *ACTB* varied widely ( $CV$  approaching 50%), *YWHAZ* was selected as an appropriate HKG on the basis of low  $CV$  in addition to sufficient baseline expression. This gene, encoding the 14-3-3 $\zeta$  protein, has

been identified previously as a strong HKG candidate in leukocytes (Vandesompele et al., 2002).

Armed with a suitable HKG, the same RNA samples used for RNAseq from one donor (C) were submitted to qPCR analysis, in order to confirm the findings made by RNAseq. The qPCR primers used corresponded to genes of interest with either a high (*CXCL10*), intermediate (*CCL2 / MCP-1*) or low (*IL-8*) magnitude of change in expression level upon virus treatment in the RNAseq analysis. These genes were each compared to *YWHAZ* by the  $\Delta\Delta C_T$  method, corrected to mock-treated cells and converted to gene copies. As shown in Figure 7.3.6b, there appears to be consistent agreement in gene expression changes between qPCR and RNAseq. Indeed, plotting these paired values against each other yields an excellent Pearson correlation (R) of 0.992 (Figure 7.3.6c). Altogether, this evidence suggests that qPCR substantiates the quality of the outputs from RNAseq, and demonstrates that the two modes of analysis agree on both the nature and scale of the gene expression changes occurring in these monocytes.

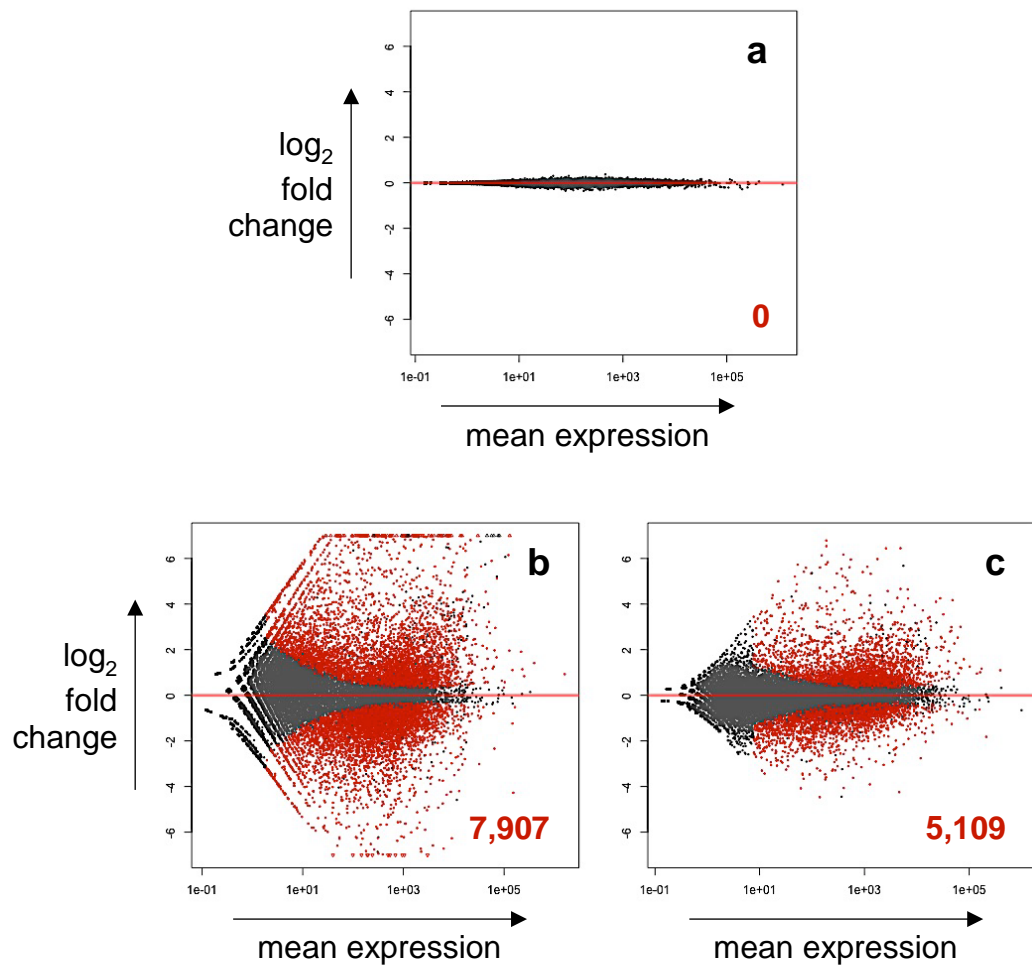


**Figure 7.3.1 Volcano plots of differential gene expression by monocytes**

Monocytes were treated with antibody (a), reovirus (b) or reo-NAb complexes (c) at MOI 10, washed and cultured for 24 hours. RNA was extracted and mRNA analysed by RNAseq. Normalised gene counts in treated samples were compared to mock-treated samples and  $\log_2$  fold change plotted on MA plots, with differentially expressed genes in red ( $p_{adj} < 0.1$ ). The mean values from three monocyte donors are reported.

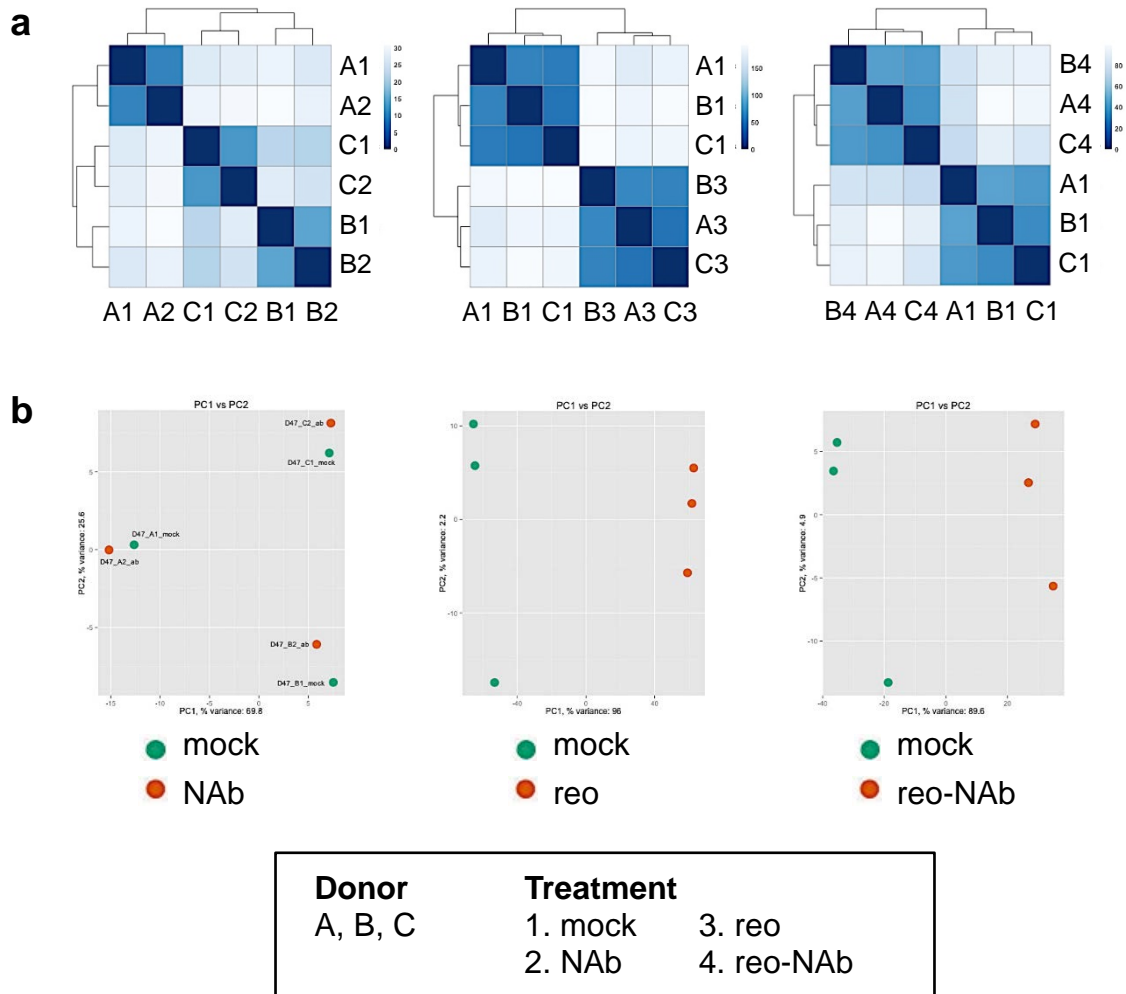


**Figure 7.3.2 Clustering and principal component analysis of the treated monocyte transcriptome**

Monocytes were treated with antibody (NAb), reovirus (reo) or reo-NAb complexes at MOI 10, washed and cultured for 24 hours. RNA was extracted and mRNA analysed by RNAseq. Similarity between normalised gene counts in mock-treated and treated samples (1-4) was assessed by (a) clustering and (b) principal component analysis.

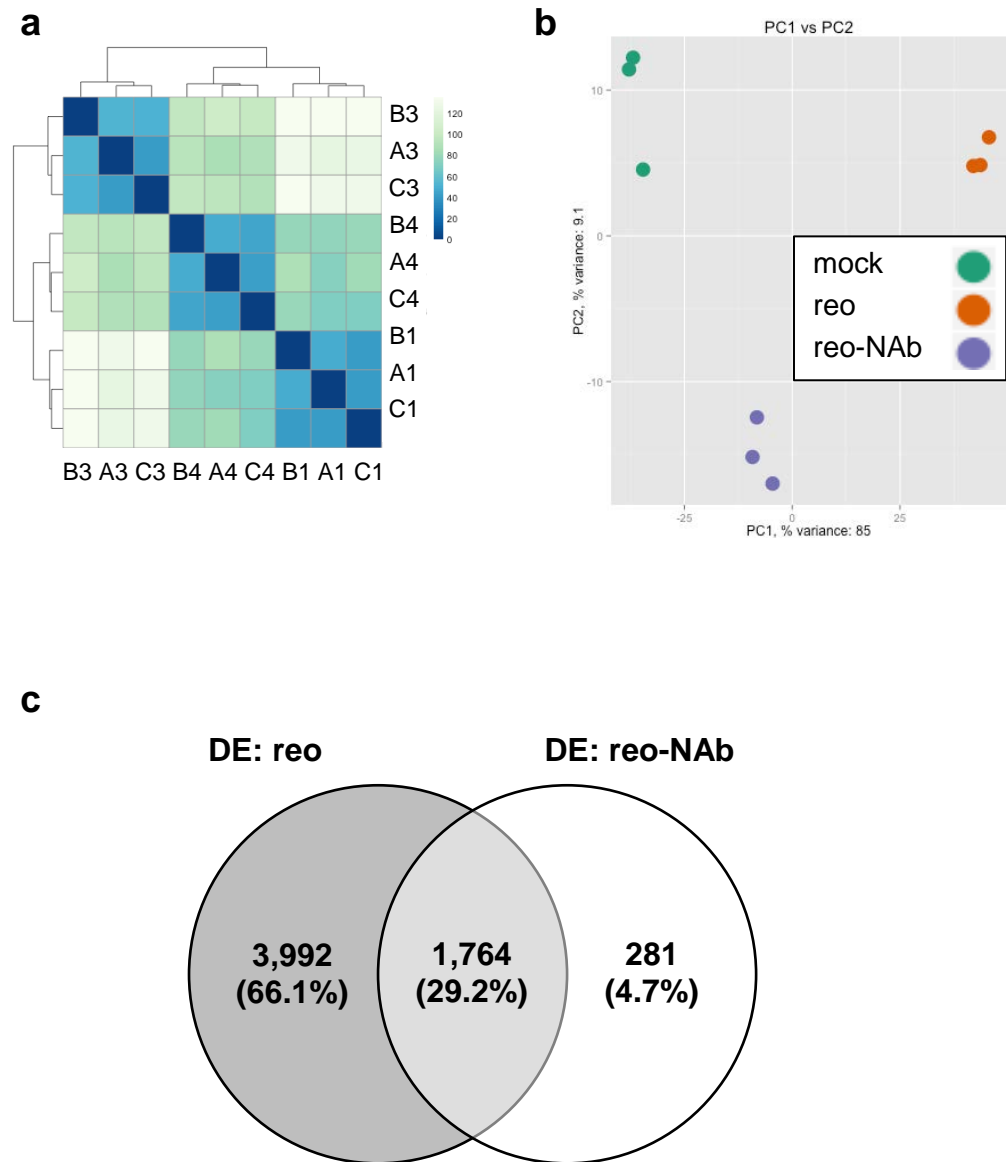


**Figure 7.3.3 Induction of a minor gene subset by reo-NAb but not reovirus**

A three-way comparison was made between the gene signatures of mock-, reovirus- and reo-NAb treated monocytes. The Euclidean distance between each of the nine samples tested is represented by (a) sample clustering and (b) principal component analysis. The number of DE genes unique to and shared by the reovirus and reo-NAb gene sets are shown in a Venn diagram (c).



**a**

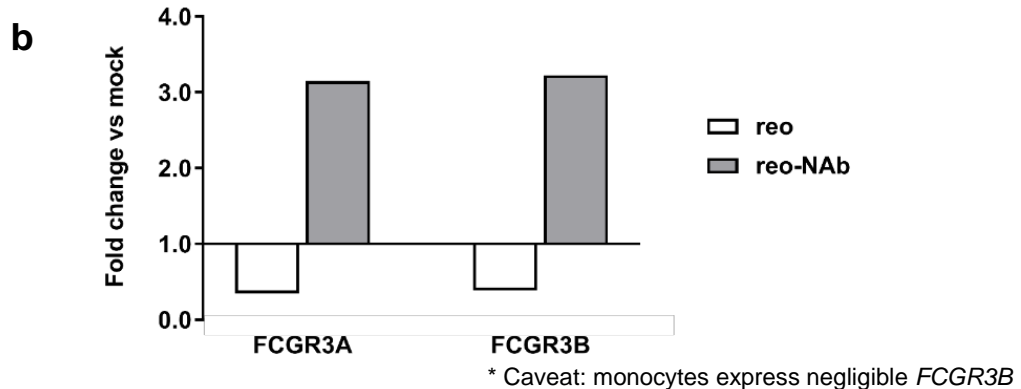
Index	Cellular component	p	padj	Z-score	Combined score
1	secondary lysosome	0.00002814	0.006227	-2.58	27.02
2	UDP-N-Ac-glucosamine-lysosomal-enzyme N-Ac-glucosaminephosphotransferase complex	0.0001367	0.006227	-2.49	22.12
3	lysosomal glycoalyx	0.0001367	0.006227	-2.47	21.96
4	primary lysosome	0.0001367	0.006227	-2.45	21.84
5	endolysosome	0.0001436	0.006227	-2.46	21.76

Index	Biological process	p	padj	Z-score	Combined score
1	chronic inflammatory response	0.0000464	0.03154	-3.71	37.03
2	acute inflammatory response	0.00004858	0.03154	-3.73	37.01
3	inflammatory response to wounding	0.0000464	0.03154	-3.71	37.01
4	inflammatory response	0.0000464	0.03154	-3.71	36.99
5	detection of lipopolysaccharide	0.00001661	0.03154	-2.72	29.97

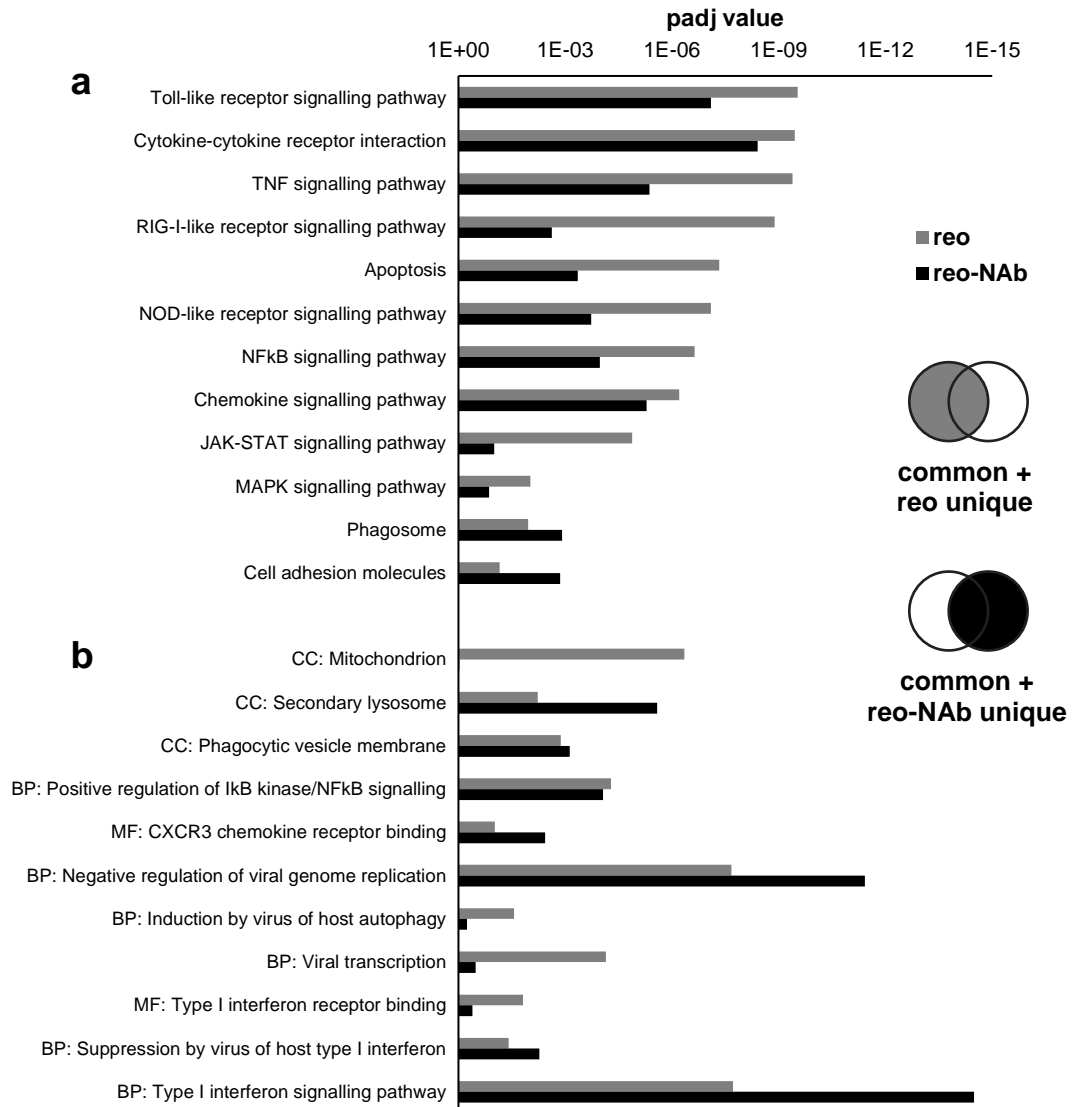
  

Index	Molecular function	p	padj	Z-score	Combined score
1	CXCR4 chemokine receptor binding	4.547E-06	0.002333	-0.72	8.88
2	CXCR6 chemokine receptor binding	4.547E-06	0.002333	-0.7	8.64
3	CXCR5 chemokine receptor binding	7.494E-06	0.002563	-0.77	9.14
4	interleukin-8 receptor binding	1.165E-05	0.002987	-0.84	9.59
5	CXCR3 chemokine receptor binding	3.417E-05	0.007012	-1.12	11.53



**Figure 7.3.4 Limited differential expression in reo-NAb treated monocytes**

The DE gene set unique to reo-NAb treatment was submitted for enrichment analysis. (a) From each GO category, the top five ontology terms ranked by padj value are shown. GO terms of particular relevance are highlighted in yellow. (b) The fold change values (vs mock) of two Fc receptor genes following reo or reo-NAb treatment are shown.

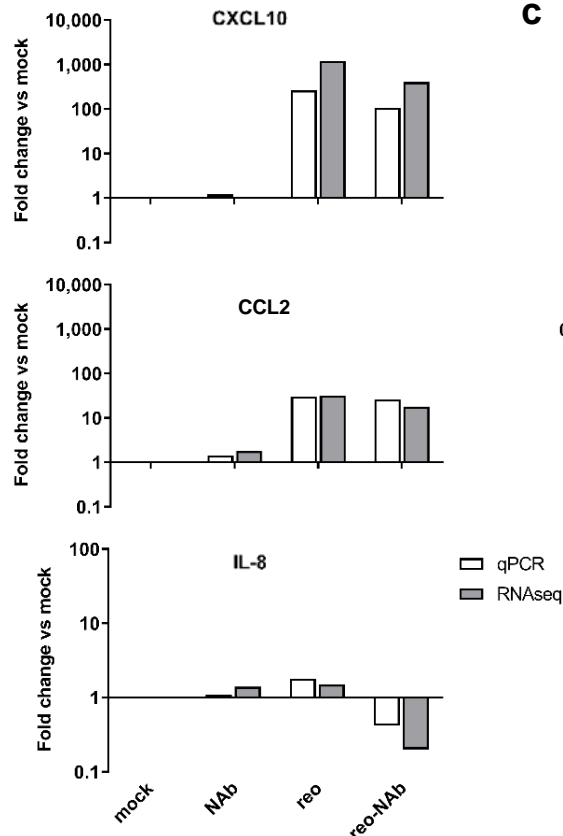
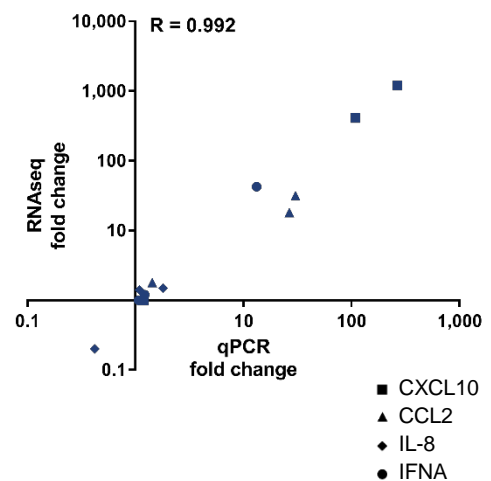


**Figure 7.3.5 Enrichment analysis of DE gene sets induced by reo or reo-NAb treatment of monocytes**

Enrichment analysis of DE gene sets identified in Figure 7.3.3, including DE genes common to both conditions. Reovirus (grey bars) and reo-NAb (black bars) are compared. Gene sets were interpreted using KEGG pathway analysis (a) and the three gene ontology (GO) categories (b). Adjusted *p* values for enrichment of selected gene sets (versus mock treatment) are shown.

**a**

Gene symbol	YWHAZ	UBC	B2M	GAPDH	RPL13A	TBP	SDHA	HPRT1	HMBS	ACTB
Mean	18,340	23,440	414,287	10,953	4,682	237	1,696	928	164	205,686
SD	1,862	8,343	167,789	5,027	2,276	22	271	233	123	80,855
CV (%) (SD/mean)	10.2	35.6	40.5	45.9	48.6	9.3	16.0	25.1	74.6	39.3

**b****c**

**Figure 7.3.6 Validation of RNAseq expression analysis by qPCR**

RNA samples used for RNAseq from one donor (C) were used for validation by qPCR. cDNA was created from RNA and subjected to qPCR. (a) *YWHAZ* was selected as an appropriate housekeeping gene, on the basis of high mean expression and low coefficient of variation (CV). (b) Three genes of interest (GOI) were compared to *YWHAZ* by the  $\Delta\Delta C_T$  method. The number of gene copies was normalised to mock-treated cells, and fold change calculated. (c) The fold change values determined by qPCR were plotted against those by RNAseq for each sample, and Pearson coefficient (R) calculated.

## 7.4 Effects of carriage on secretory profile

It is clear from whole transcriptome analysis that while there is considerable overlap in the gene signatures induced by reovirus and reo-NAb, there are also significant differences in their effects. There appears to be strong induction of pathways involved in cytokine and chemokine signalling by both stimuli (Figures 7.3.4, 7.3.5 and 7.3.6), consistent with the role of monocytes as proficient generators of soluble factors during the defence response to pathogens (Hansmann et al., 2008). As supported by the western blot data, reovirus itself is known to impinge upon PKR and NF- $\kappa$ B (Steele et al., 2011), and promotes the secretion of influential pro-inflammatory cytokines including IFN- $\alpha$  and TNF from monocyte-derived DC in a dose-dependent fashion (Errington et al., 2008a).

Interferons (IFN) in particular are the archetypal secreted factors involved in orchestrating the cellular defence process to virus. Following IFN secretion, sensing and JAK-STAT signalling, the resultant expression of IFN-stimulated genes (ISG) can mediate wholesale changes to cell growth, protein synthesis and cell fate, as part of a wider antiviral state. Many ISG encode proteins with direct activity against various aspects of the intracellular viral 'life cycle', including virus entry, replication and egress (reviewed in Schneider et al., 2014).

It is through the action of this multitude of effector proteins that IFN are capable of precipitating front-line clearance of virus. Numerous *in vivo* studies demonstrate the critical requirement for IFN signalling by antigen-presenting cells in limiting viral replication and consequently disease severity (Cervantes-Barragán et al., 2009; Lang et al., 2010). Further, in human blood, monocytes – not DC – are the main source of IFN- $\alpha$  following stimulation with poly(I:C), an analogue of viral dsRNA (Hansmann et al., 2008).

Building upon the insights made above by gene expression analysis, the same RNAseq data sets were interrogated for information on the transcriptome of secreted factors, again using the mean values across three donors. Figure 7.4.1 shows the fold change in raw count values (over mock) for transcripts of specific genes following 24-hour treatment of monocytes with reovirus or reo-NAb. The subsets of IFN genes (Figure 7.4.1a) and other cytokines and chemokines (Figure 7.4.1b) shown include the most highly expressed genes in each category in addition to some selected on the basis of relevance.

First, it is important to note that the vast majority of IFN genes scored mean of zero counts in mock-treated samples; these were ascribed an arbitrary value of 1 in order to facilitate the analysis of differences in IFN upregulation. Indeed, all of the IFN genes listed in Figure 7.4.1a scored below 10 counts in mock-treated samples, indicating a total absence of IFN signalling at baseline; for context, scores for reovirus were commonly in the thousands. Consequently, while the values shown refer to fold change, they are also typically the same or very close to the gene count values for both the reo and reo-NAb conditions.

In the context of this baseline, it can be observed that free reovirus provokes the extensive generation of various types of IFN from monocytes. Consistent with their classical role in virus resistance, genes corresponding to type I IFN isoforms are particularly strongly expressed; IFN- $\alpha$  and IFN- $\beta$  predominate, accompanied by the less well known type I subtypes IFN- $\epsilon$  and IFN- $\omega$ . A number of additional genes encoding other IFN- $\alpha$  isoforms have been omitted for brevity. Reovirus also induces the expression of members of the type III IFN family, in particular IL-29 (IFN- $\lambda$ 1), which possess antiviral activity by signalling via a separate IFN receptor. The sole type II species IFN- $\gamma$  (the *IFNG* gene) is expressed to a negligible degree.

Having revealed the apparent equivalence of the monocyte response to reo-NAb in some diverse gene sets – including those relating to cytokine and chemokine activity (Figure 7.3.5) – it is striking to note the scale of the difference in the IFN response between reovirus and reo-NAb (Figure 7.4.1a). Across all IFN isoforms, while the patterns are the same for both, reo-NAb values are 100- to 1,000-fold lower than those for free reovirus. Indeed, for reo-NAb, counts for all IFN genes were below 100, and the majority were below 10; a level at which the ‘biological relevance’ of transcripts is doubtful (R. Chauhan, personal communication).

The comparison of changes in various other cytokine and chemokine transcripts is shown in Figure 7.4.1b. Fold change values are again displayed, although unlike in Figure 7.4.1a, baseline expression was present but low. Towards the left of the graph are genes in which the increase upon reo-NAb and reovirus treatment was comparable, a group including genes encoding TRAIL (TNFSF10), the CXC-family chemokines CXCL9, 10 and 11, and CCL2, CCL8 and CCL7 (monocyte chemotactic protein (MCP)-1, 2 and 3). Other genes, including those encoding CCL3 and CCL4 (macrophage inflammatory protein (MIP)-1 $\alpha$  and 1 $\beta$ ), CCL5 (RANTES) and TNF, more closely resemble the pattern seen in IFN expression, being strongly biased towards free reovirus.

While RNAseq has the benefit of providing high volumes of gene expression data, it can only inform as to the impact of stimuli at the transcriptional level, with no guarantee that protein-coding RNA is translated into corresponding levels of protein. Consequently, the protein factors secreted by isolated monocytes were profiled in order to confirm the trends observed in RNA. First, luminex assays were used to gain a broad overview of the 'secretome'.

Monocytes were treated as previously with reovirus or reo-NAb at MOI 10, and cultured for 48 hours to permit maximal cytokine release. Supernatant was harvested, and the level of specific analytes quantified. Mean values were determined from two donors, and used to calculate the fold change in each analyte compared to supernatant from mock-treated monocytes. As for the RNAseq data, it was necessary to assign a lower limit of detection value of 5 pg/ml to the mock-treated samples for some proteins (marked with a dagger), to enable the calculation of fold change values.

The data shown in Figure 7.4.2 are ordered according to reovirus-induced fold change values. The most conspicuous result at first glance is the extreme elevation in the abundance of IFN- $\alpha$ 2, the representative type I IFN in this assay, by reovirus – in contrast to reo-NAb which appears to yield none. The luminex data are also consistent with RNA-level data in indicating the equivalence of reovirus and reo-NAb in stimulating the release of CXCL9 and CXCL10, along with CCL2 (MCP-1). The bias towards reovirus in the induction of CCL5/RANTES, TNF and MIP isoforms (CCL3/4) is also maintained at the protein level. It is notable that other specific analytes relevant to monocyte (GM-CSF, IL-10) and NK cell (IL-15) behaviour exhibit limited changes which are comparable between reovirus and reo-NAb.

Having broadly illustrated that transcriptional trends are maintained in terms of secreted proteins, a more quantitative assessment of virus-induced cytokine production was obtained by ELISA. The results obtained substantiated the luminex results, both in terms of trends between conditions, and in protein concentration (Figure 7.4.3). While substantial CXCL10 was generated by both reovirus and reo-NAb ( $p = 0.99$  between reovirus and reo-NAb by one-way ANOVA), significant elevations in IFN- $\alpha$ , TNF (both  $p < 0.0001$ ) and CCL5/RANTES ( $p < 0.01$ ) were found to be highly specific to reovirus treatment. The same pattern – albeit not significant due to variation between donors – was observed in IL-29 ( $p = 0.311$ ). As suggested by RNAseq, reovirus-induced IFN- $\gamma$  levels appear to be functionally negligible. Thus, as detected at the transcript level (by RNAseq) and the protein level (by luminex and ELISA), while many

cytokines are selectively induced by free reovirus, others are equally produced in response to reo-NAb.

One protein from each of these groups, IFN- $\alpha$  and CXCL10 respectively, was selected for further investigation. This was done primarily in order to detect a potential role in cytokine production for virus replication – at least at the genomic level, if not the protein level (Figure 6.4.3 and 6.4.4). Monocyte cells were thus analysed for the presence of *IFNA1* and *CXCL10* transcripts by qPCR; samples were taken after 2 or 16 hours of treatment with UV-inactivated or live reovirus, in the form of free virus or reo-NAb. Number of copies<sup>2</sup> from three independent donors are displayed, following normalisation by  $\Delta\Delta C_T$  to *YWHAZ* and comparison to mock (Figure 7.4.4).

As shown by the consistency between the clear and grey bars, there is no significant difference in effect between live and UV-inactivated virus on the yield of IFN- $\alpha$  ( $p = 0.37$  by two-way ANOVA) or CXCL10 ( $p = 0.95$ ). Thus, UV inactivation appears to have no impact upon the magnitude or kinetics of secretion by monocytes in response to reovirus or reo-NAb. This strongly suggests that cytokine secretion following either stimulus is independent of the replication of viral genomes or proteins, consistent with prior studies on the activation of whole PBMC or isolated DC by reovirus (Errington et al., 2008a; Parrish et al., 2015) and specifically the production of CXCL10 (Douville et al., 2008).

It can also be concluded from the data after 2 hours that CXCL10 is induced as quickly by reo-NAb as it is by free reovirus, implying that neutralisation has no detrimental effect on the kinetics of cytokine production ( $p = 0.99$ ). Unlike prior results however, the data do suggest that the magnitude of CXCL10 transcript induction may be lower in the context of reo-NAb, at least after 16 hours ( $p < 0.05$ ).

The critical role for IFN signalling in front-line antiviral defence is in part mediated by antigen-presenting cells. Cells of this type have evolved intricate and often paradoxical strategies in the ‘arms race’ against pathogens. One of these tactics involves allowing a degree of virus replication, ostensibly to boost the innate reaction or to enhance the supply of virus antigen for priming of the adaptive immune system (Honke et al., 2012). At the risk of anthropomorphism,

---

<sup>2</sup> It should be noted that the low scale of change observed in copies of *IFNA1* by qPCR is due to a retrospective baseline correction. This was required as the *IFNA1* primers detected not only the *IFNA1* sequence in cDNA, but also *IFNA1* in gDNA remaining in the sample, as the *IFNA1* gene is monocistronic.

the cell gives the viruses ‘just enough replicative rope to hang themselves with’ (Yewdell and Brooke, 2012). This limited permissivity is partly enabled by the suppression of IFN signalling, which is mediated by negative regulators of RLR-induced cascades, such as USP18 (Honke et al., 2012; Komuro et al., 2008).

A further dimension is added to this topic when considering the differential effects induced by the reo-NAb immune complex versus the free virus. There is contradictory evidence regarding the quality of the IFN response following antibody-dependent entry of virus in cells of the monocyte/macrophage lineage. While some studies report equivalent IFN responses to free and antibody-bound virus (Boonnak et al., 2011; Kou et al., 2008), others provide evidence for the robust suppression of IFN following antibody-dependent entry (Rolph et al., 2011; Tsai et al., 2014; Ubol et al., 2010). IFN repressor proteins are strongly implicated in these studies.

Consequently, observing the stark disparity in IFN production between reovirus- and reo-NAb treated monocytes, it was postulated that IFN generation in response to reo-NAb may be precluded by a specific IFN-suppressing factor. RNAseq data were therefore used to examine the expression of various factors which have been found to antagonise IFN signalling: *IRF2* (Harada et al., 1989), *SOCS1/2/3* (Piganis et al., 2011), *DAK* and *ATG5/12* (Huang et al., 2016; Ubol et al., 2010), *LGP2/DHX58* (Komuro and Horvath, 2006), *RNF125* (Arimoto et al., 2007), *OASL1* (Lee et al., 2013) and *PIAS1* (Liu et al., 2004).

It was hypothesised that, through differences in the mode of virus entry, reo-NAb may trigger the upregulation of specific protein(s) which antagonise IFN expression. In particular, as the majority of interferon-stimulated genes (ISG) induced by reovirus are also upregulated by reo-NAb (data not shown) – a puzzling finding given the absence of IFN – the focus was on factors acting upstream rather than downstream of IFN expression. However, as shown in Figure 7.4.5, no substantial differences were observed in any of the factors listed. As such, although some other cytokines are produced comparably by reovirus and reo-NAb, it cannot be concluded that the significant disparity observed in type I IFN production is due to the action of specific IFN-suppressive proteins.

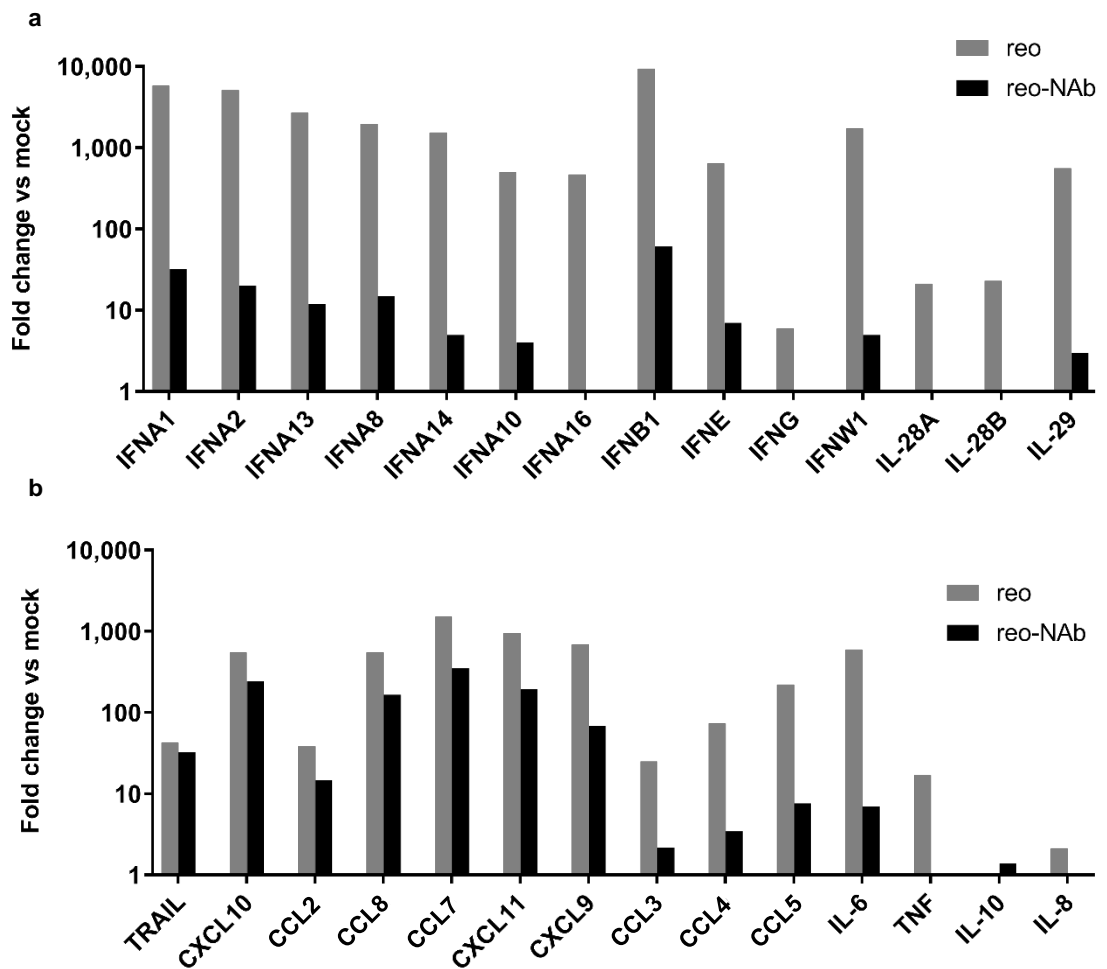


**Figure 7.4.1** Transcriptomic analysis of cytokine induction by reovirus and reo-NAb

Monocytes from 3 donors were treated with reovirus or reo-NAb (MOI 10) and cultured for 24 hours prior to gene expression analysis by RNAseq. Raw gene counts were analysed. All genes with raw counts of zero were assigned an arbitrary value of 1 to permit calculation of the fold change upon reovirus or reo-NAb treatment compared to mock-treated monocytes. Raw gene counts were determined for two groups of genes: **(a)** interferon genes and **(b)** selected cytokine genes.

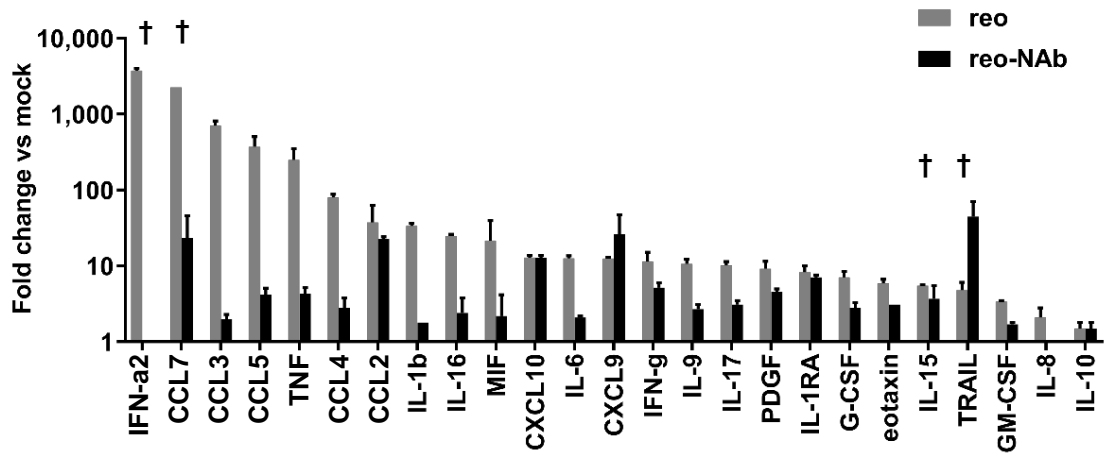


**Figure 7.4.2 Broad analysis of monocyte ‘secretome’ by luminex**

Monocytes were treated with antibody (NAb), reovirus (reo) or reo-NAb complexes at MOI 10, washed, resuspended in RPMI-10 at  $1 \times 10^6$  cells per ml and cultured for 48 hours. Supernatant was analysed using magnetic bead-based cytokine analysis kits. Analyte concentration (pg/ml) was compared to that of mock-treated monocytes and fold change following reovirus or reo-NAb treatment calculated. Data represent mean values  $\pm$  SEM from two donors. † denotes proteins assigned nominal values of 5 pg/ml as a lower limit of detection.

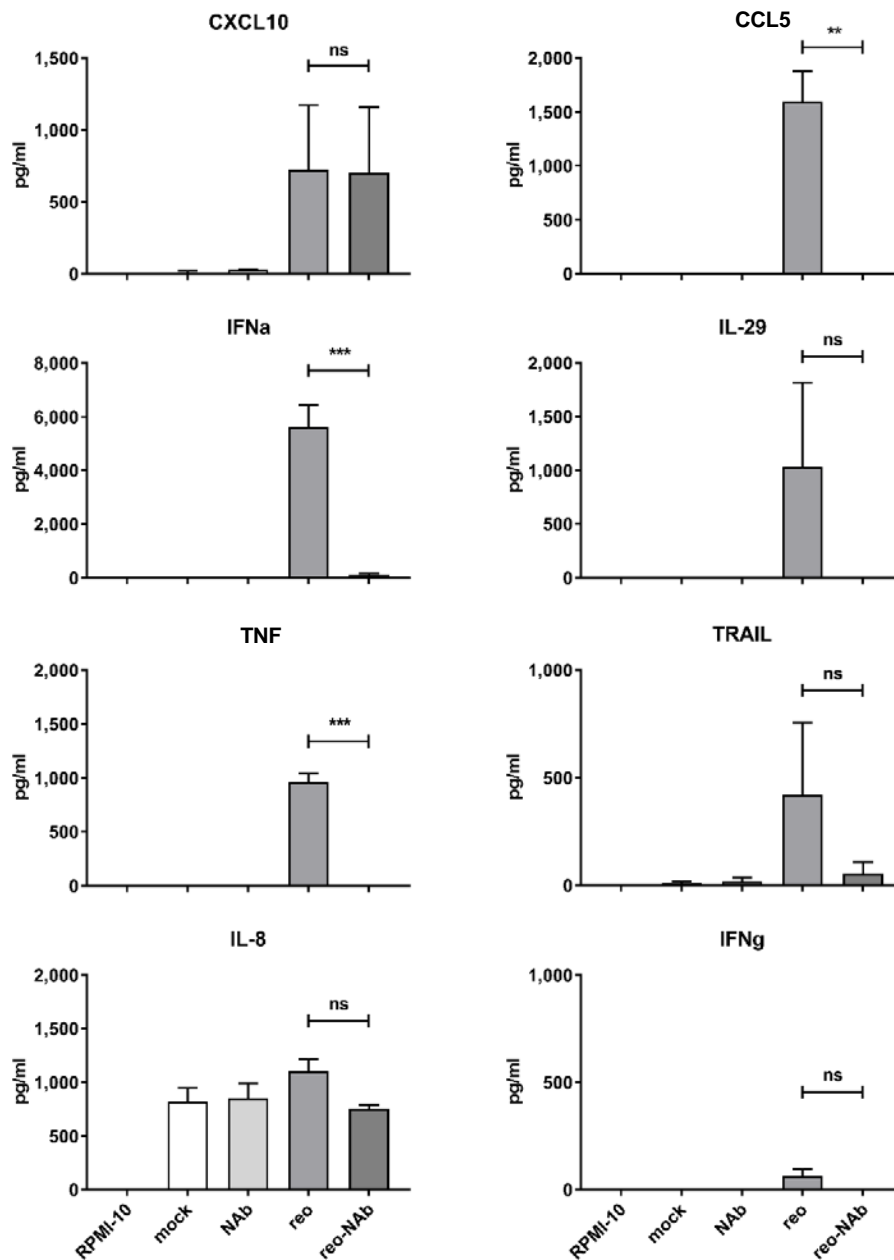


**Figure 7.4.3 Validation of monocyte-secreted factors by ELISA**

Monocytes were treated with antibody (NAb), reovirus (reo) or reo-NAb complexes at MOI 10, washed, resuspended in RPMI-10 at  $1 \times 10^6$  cells per ml and cultured for 48 hours. Cytokine concentrations (pg/ml) were determined by ELISA. Data are mean values  $\pm$  SEM from 2-3 donors. *ns* = not significant; \* $p < 0.05$ , \*\* $p < 0.01$ , \*\*\* $p < 0.001$  by one-way ANOVA (Dunnett's multiple comparisons test).

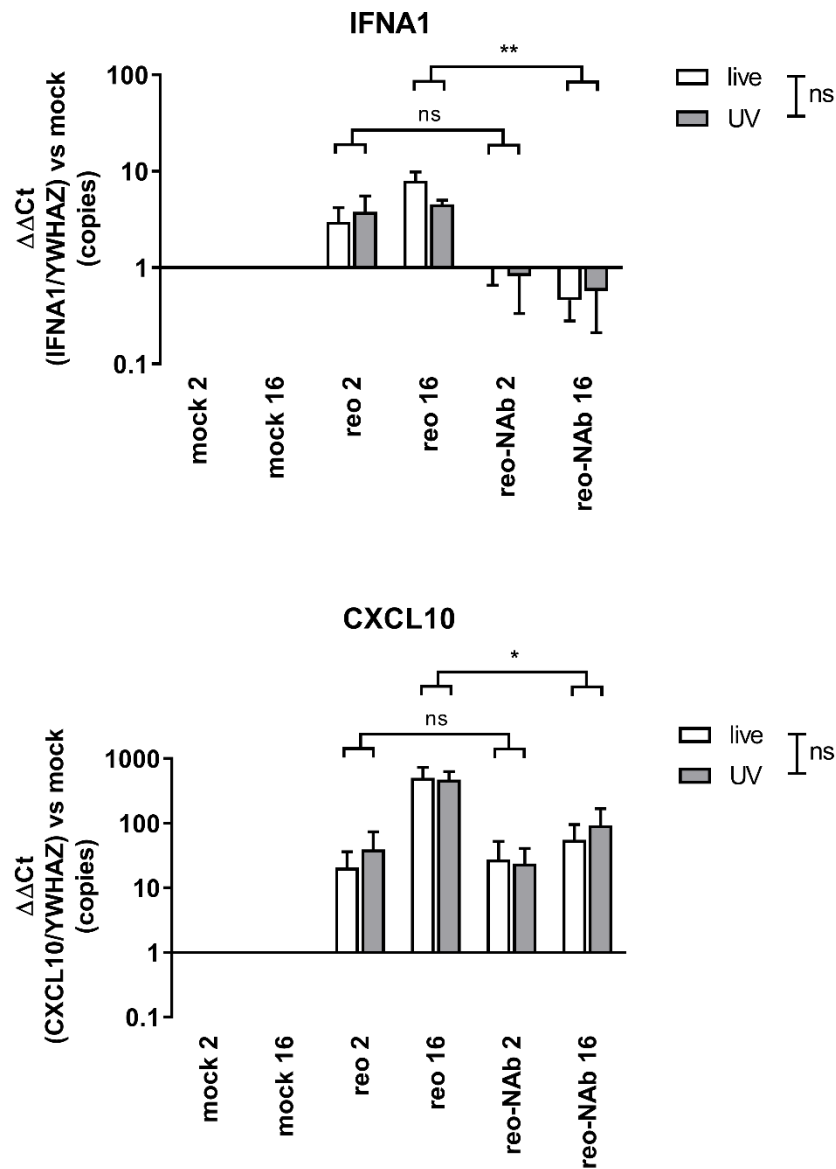


**Figure 7.4.4 Induction of cytokine secretion by live and UV-inactivated virus**

Monocytes were treated with reovirus (reo) or reo-NAb complexes at MOI 10, using live or UV-inactivated reovirus. Cells were washed, resuspended in RPMI-10 at  $1 \times 10^6$  cells per ml and cultured for 2 or 16 hours. RNA was extracted and transcript copy number evaluated by qPCR. Data are mean values  $\pm$  SEM from three donors. *ns* = not significant; \* $p < 0.05$ , \*\* $p < 0.01$ , \*\*\* $p < 0.001$  by two-way ANOVA (Tukey's multiple comparisons test).

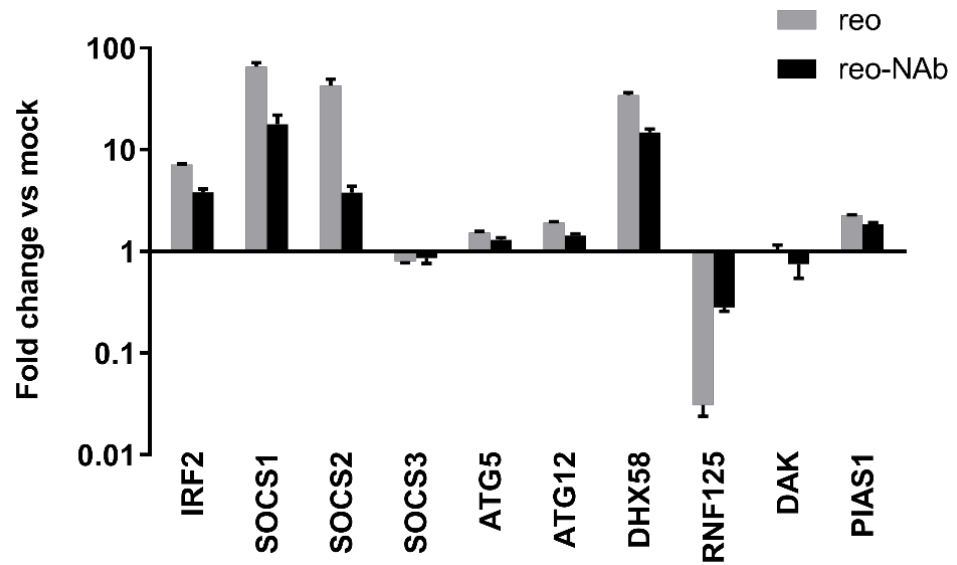


**Figure 7.4.5 Lack of evidence for an IFN-repressing factor specific to reo-NAb treated monocytes**

Human monocytes treated with MOI 10 reovirus or reo-NAb for 24 hours were analysed for the expression of the gene transcripts indicated using RNAseq. The fold change in the expression of each target with respect to mock-treated monocytes is shown. Data represent the mean fold change  $\pm$  SEM, from three individual donors.

## 7.5 Functional effects on immune effector populations

Somewhat distinct from the oncolytic properties originally thought to be key to their efficacy *in vivo*, the clinical benefit of OV is increasingly attributed to their role as immunotherapy agents. Given that viruses are generally activatory towards immune cells, this is consistent with infiltrating lymphocyte levels as a prognostic factor in the typically immunosuppressive microenvironment of solid tumours (Gooden et al., 2011). Thus OV represent one modality with the potential to either promote the infiltration of effector immune cells (when virus is present in circulation) or to provoke their pro-inflammatory capacity once there (if virus reaches the tumour bed).

The specific presence of the major adaptive and innate immune effector cells – T cells and NK cells respectively – has been associated with improved survival across multiple indications (reviewed in Fridman et al., 2012; Larsen et al., 2014). It is increasingly clear that tumour cell clearance is not only reliant on infiltration of immune cells but moreover the condition of these cells; lymphocyte dysfunctionality and exhaustion are critical roadblocks to successful immune surveillance (Zarour, 2016).

To this point, the impact of reovirus has been characterised solely in terms of the circulating monocyte population. This sub-section briefly explores the capacity of free or neutralised reovirus to influence the wider PBMC population. Like monocytes, NK cells are key to innate defence. This fraction was the subject of particular focus given its gathering importance to the therapeutic outcomes of OV, and of reovirus in particular (Gujar et al., 2011; Ilett et al., 2014; Kottke et al., 2010; Zhang et al., 2014).

In this context, the interplay between antigen-presenting cells and NK cells is highly relevant. The stimulation of NK cell anti-tumour efficacy by reovirus is facilitated by the activation of DC *in vitro* (Errington et al., 2008a; Hall et al., 2012; Prestwich et al., 2009a). Less well-characterised is the impact of NK cells upon DC. Activated NK cells are capable of stimulating the differentiation and function of monocytes and DC, through contact- and cytokine-dependent mechanisms (Holmes et al., 2014; Prestwich et al., 2009a; Zhang et al., 2007). Thus, in order to supplement the previously stated data on monocyte phenotype, the influence of NK cells towards the effect of virus on monocytes was first explored.

Positively selected monocytes were treated with serum, reovirus or reo-NAb at MOI 10, prior to 48-hour co-culture with NK cells. A 2:1 monocyte:NK ratio was

selected to best represent the proportions of these populations in peripheral blood. The phenotype of CD11b<sup>+</sup> cells was assessed by flow cytometry staining (Table 8); median fluorescence intensity was normalised to that of NAb-treated monocytes alone, as selection yielded insufficient NK cells to set up untreated control samples. Monocyte activation across three monocyte donors in the absence (clear bars) or presence (grey bars) of NK cells is shown in Figure 7.5.1.

The consistency between the paired bars demonstrates the general lack of a substantial impact when reovirus-treated monocytes are combined with NK cells in this system. The virus-mediated decrease in CD14 and increase in co-stimulatory molecules (as observed in Figure 7.2.2) were unaffected by NK cell co-culture (all pair-wise comparisons not significant by two-way ANOVA). However, while the reovirus-mediated elevation in HLA-DR is irrespective of NK cells, their presence is sufficient to increase its expression in response to either NAb or reo-NAb ( $p = 0.0012$  for NAb and  $0.012$  for reo-NAb respectively).

The ability of NK cells to upregulate HLA-DR on monocytes/DC (and accordingly enhance cross-presentation) has been reported, albeit in the context of activated NK cells (Srivastava et al., 2013; Zhang et al., 2007). The NK-derived surface proteins or secreted factors which may be responsible, or the downstream effects on the antigen-presenting ability of monocytes/DC, were not pursued.

Next, the reverse comparison was made, examining the activation of NK and T cells within PBMC upon co-culture with virus-treated monocytes. This process has been examined before, but solely in the context of free reovirus. Reovirus treatment of whole PBMC activates NK cells via a contact-independent mechanism reliant on DC-derived IFN- $\alpha$  (Parrish et al., 2015; Prestwich et al., 2009a). Indeed, NK activation can be promoted by DC treated with the TLR3 agonist poly(I:C), demonstrating the importance of viral RNA (Gerosa et al., 2005). The stimulatory effects of reovirus-treated DC can also extend to T cell activation and cytotoxicity (Errington et al., 2008a). It was therefore resolved firstly to confirm that monocytes, as DC precursors, are able to mediate the same effect, and secondly to compare the activatory potential of reovirus and reo-NAb upon NK and T cells in this context.

Monocytes were pulsed as before with NAb, reovirus or reo-NAb at MOI 10, washed, and recombined with the CD14<sup>-</sup> fraction of PBMC to permit cross-talk of monocytes with lymphocytes. After 48 hours in culture, cells were harvested and lymphocyte populations phenotyped by flow cytometry (Figure 7.5.2). The

markers examined included the canonical lymphocyte activation marker and functional regulator CD69 (Borrego et al., 1999) and the antiviral response factor CD317, or tetherin (El-Sherbiny et al., 2015), which are both linked to reovirus. Recorded on the x axis are the treatments initially given to the monocytes, rather than to the phenotyped cell population with which they were cultured.

Starting with NK cells (gated on the CD3<sup>-</sup> CD56<sup>+</sup> population), it is clear that reovirus-treated monocytes induce a significant elevation of NK CD69 expression ( $p = 0.0004$  vs mock by one-way ANOVA). There is a trend towards increased NK CD69 following co-culture with reo-NAb treated monocytes which does not reach statistical significance ( $p = 0.731$ ). The pattern of tetherin expression shows a similar trend, though again is not significant for reo-NAb ( $p = 0.0002$  and  $0.133$  respectively).

Monocytes treated with free reovirus also stimulate CD69 expression from CD4<sup>+</sup> and CD8<sup>+</sup> T cells (CD3<sup>+</sup>), although due to donor variability this does not reach significance in CD8<sup>+</sup> T cells ( $p = 0.039$  and  $0.544$  respectively). Further, there appears to be some activation of CD8<sup>+</sup> T cells by reo-NAb pulsed monocytes, although this is again highly variable ( $p = 0.620$ ). It can thus be surmised that, like DC, monocytes are in general capable of acting as the conduit for reovirus-mediated lymphocyte activation. (This is corroborated by the IFN- $\gamma$  produced in cultures containing reovirus-treated monocytes as detected by ELISA; mean without PBMC 64 pg/ml vs with PBMC 1,429 pg/ml – data not shown.) The evidence for the same effect in the context of reo-NAb is less convincing.

Gaining an understanding of the reason for this diminished effect of reo-NAb on lymphocyte activation (via monocytes) requires insight into the underlying molecular mechanism. Previous evidence suggests that type I IFN is the primary secreted factor involved (Parrish et al., 2015; Prestwich et al., 2009a). However CXCL10, here likely triggered directly by NF- $\kappa$ B signalling rather than via IFN (Brownell et al., 2014), can not only act as an NK cell chemoattractant but can also trigger NK cell activation and killing of tumour cells (Saudemont et al., 2005). As both reovirus and reo-NAb yield the generation of considerable CXCL10, the respective roles of monocyte-derived IFN- $\alpha$  and CXCL10 in NK cell activation were compared.

The cell-free supernatant from virus-treated monocytes was aspirated and added to fresh PBMC, following the optional removal of virus by filtration (F). The ability of this conditioned medium (CM) to stimulate the expression of CD69 on the CD3<sup>-</sup> CD56<sup>+</sup> population was determined by flow cytometry after 48

hours. The influence of pre-incubating target PBMC with blocking antibodies against the type I IFN receptor IFNAR2 or the CXCL10 receptor CXCR3 is shown in Figure 7.5.3. It should first be noted that filtration appears to have no effect on NK cell CD69 levels. This suggests that the virus that is rapidly released by monocytes (Figure 6.4.4) is not the responsible factor, corroborating previously published data showing that NK cells require monocytes/DC to facilitate their response to reovirus (Parrish et al., 2015).

Therefore which monocyte-secreted factor is responsible? Blocking NK cell CXCR3 does not impact CD69 modulation by the CM from virus-treated monocytes, strongly indicating that CXCL10 (along with other CXCR3 ligands) is not involved. By contrast, IFNAR2 blockade significantly diminishes NK activation in the presence of supernatant from virus-treated monocytes ( $p = 0.0123$  for reo CM and  $0.0011$  for reo FCM respectively by two-way ANOVA). Although there are non-significant trends to suggest a similar theme where reo-NAb is concerned, the degree of NK activation by CM from reo-NAb treated monocytes is too limited to allow conclusions to be drawn from only two donors.

While surface marker expression and IFN- $\gamma$  secretion by NK cells is a reasonable indicator of functional activity (Dons'koi et al., 2011), the most clinically relevant indicator of the effect of reovirus as a promoter of innate anti-tumour immunity is NK cell cytotoxicity. Activated NK cells can readily eliminate AML blasts (Hall et al., 2012) and are the main cytolytic effector cells in reovirus-treated PBMC (Adair et al., 2012). Alongside monocytes, they play an essential role in tumour cell killing in GM-CSF/reovirus therapy for murine melanoma (Ilett et al., 2014). Therefore it was important to confirm that the enhanced phenotype of NK cells is translated into cytotoxic activity.

NK cells utilise three major mechanisms to induce target cell death: (i) exocytosis of cytolytic granules containing granzymes and perforin; (ii) induction of apoptosis by the expression of Fas ligand; and (iii) generation of secretory or surface-expressed TNF-family cytokines and IFN- $\gamma$  (Lowin et al., 1995; Oshimi et al., 1996; Zamai et al., 1998). The importance of cytolytic granule release to anti-tumour NK effector function is demonstrated by the decreased tumour surveillance in perforin-deficient animals (Smyth et al., 1999; van den Broek et al., 1996).

The lysosomal-associated membrane proteins LAMP-1/-2 (CD107a/b) which at rest are associated with the granule membrane, are mobilised and ectopically expressed on the cell surface during degranulation. As surface expression of CD107a/b correlates well with cytotoxicity, it can be used as a surrogate marker

of NK cell functional activity (Alter et al., 2004; Mittendorf et al., 2005). This is a complementary assay to the traditional chromium release assay developed 50 years ago, in which the degree of  $^{51}\text{Cr}$  release from labelled target cells following NK cell co-culture represents the proportion of targets successfully killed upon degranulation (Brunner et al., 1968). Thus in evaluating cytotoxicity, one assay measures the 'cause' (degranulation), and the other measures the 'effect' (target cell lysis).

Monocytes were treated with NAb, reovirus or reo-NAb at MOI 10, washed and co-cultured with autologous NK cells at a 1:2.5 ratio; in some conditions, NK cells were cultured alone with the same treatments. After 40 hours, cells were harvested, and their level of degranulation against targets of melanoma, pancreatic or glioma cell origin was determined. Figure 7.5.4 shows the proportion of NK cells staining positively for CD107, following exposure to the stimuli indicated on the x axis and subsequent interaction with the target cells as shown.

It can be observed that the CD107 expression seen is specifically in response to tumour cell targets, as in their absence (clear bars) expression is minimal. Exposure of NK cells to NAb, or monocytes treated with NAb, remains at this baseline. By contrast, exposure of NK cells to reovirus, or to reovirus-treated monocytes, yields CD107 expression on up to 30% of NK cells. Lastly, while NK cells show no activation in response to direct application of reo-NAb, reo-NAb treated monocytes do induce some NK activity, particularly towards the U87 glioma target line.

These results are corroborated by the outcomes from the  $^{51}\text{Cr}$  release assay (Figure 7.5.5). Here, activated NK cells were supplied with U87 or SU.8686 targets at various effector:target (E:T) ratios. A 4-hour incubation is used, as this is insufficient time for viral lysis to confound the results. As for the degranulation assay, NK cell cytotoxicity appeared equivalent following stimulation with reovirus and reovirus-treated monocytes (each significant vs no treatment across all E:T ratios by two-way ANOVA). The only other condition in which NK cells generated significant target cell lysis was in the presence of reo-NAb treated monocytes, at higher E:T ratios, whereupon up to 40% of targets were lysed ( $p < 0.01$  at 20:1,  $p < 0.05$  at 10:1 respectively, for both targets).

In parallel, these two assays demonstrate that the avidity of monocytes for reovirus allows them to convey this stimulus, inducing the degranulation and resulting cytotoxicity of autologous human NK cells against a range of tumour cell targets.

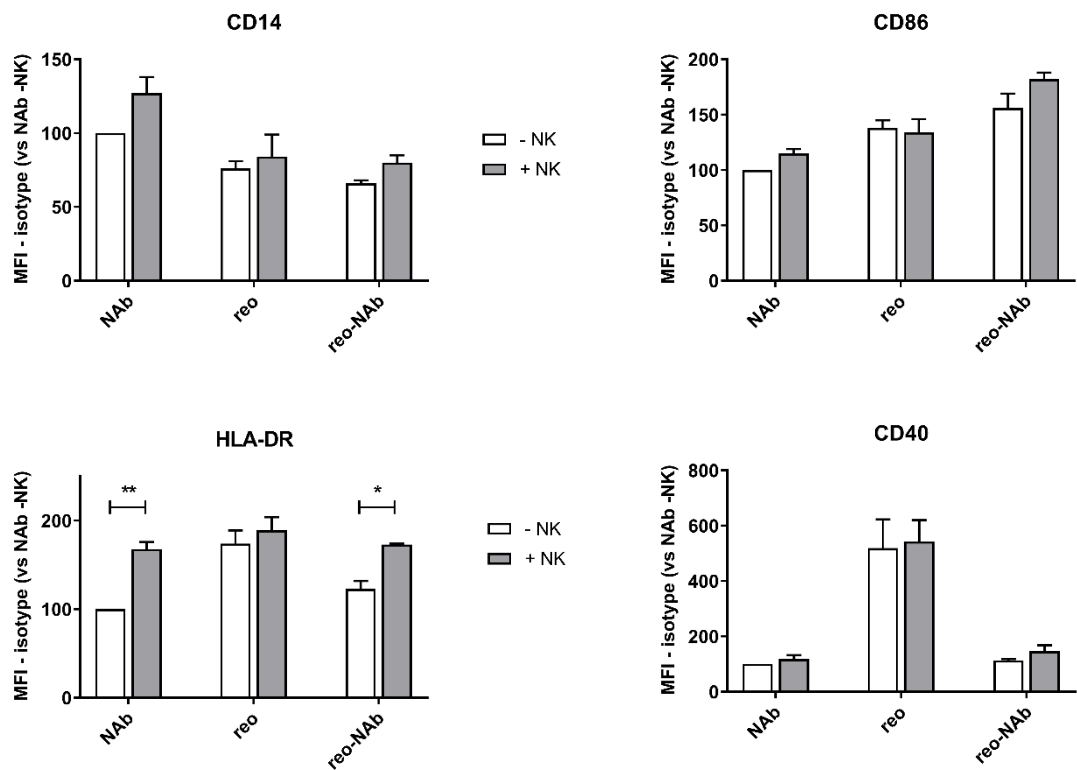


**Figure 7.5.1 Effect of NK cell co-culture on phenotype of virus-treated monocytes**

Monocytes were pulsed with NAb, reovirus or reo-NAb (MOI 10), washed and cultured with or without autologous NK cells at a 2:1 ratio for 48 hours. The surface expression of the proteins indicated was assessed by flow cytometry on the CD11b<sup>+</sup> population. Median fluorescence intensity values were isotype-corrected and normalised to 'NAb -NK', and the mean  $\pm$  SEM of three individual donors displayed. \* $p < 0.05$ , \*\* $p < 0.01$  by two-way ANOVA (Šídák's multiple comparisons test).

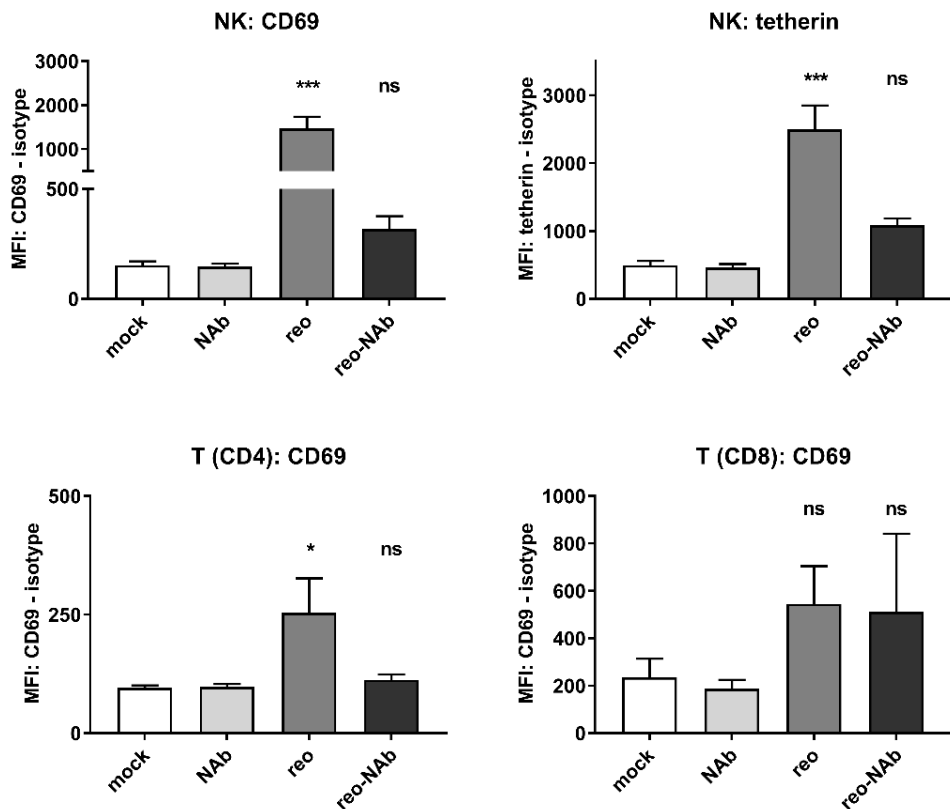


**Figure 7.5.2 Activation of immune cell populations via virus-loaded monocytes**

Monocytes pulsed with NAb, reovirus or reo-NAb (MOI 10) were washed and returned to culture with autologous PBMC for 48 hours. Cells were harvested and phenotyped for surface proteins of interest by flow cytometry on the populations indicated. Isotype-corrected median fluorescence intensity values are shown. Data are mean values  $\pm$  SEM from three donors. *ns* = not significant; \* $p < 0.05$ , \*\*\* $p < 0.001$  vs mock by one-way ANOVA (Dunnett's multiple comparisons test).

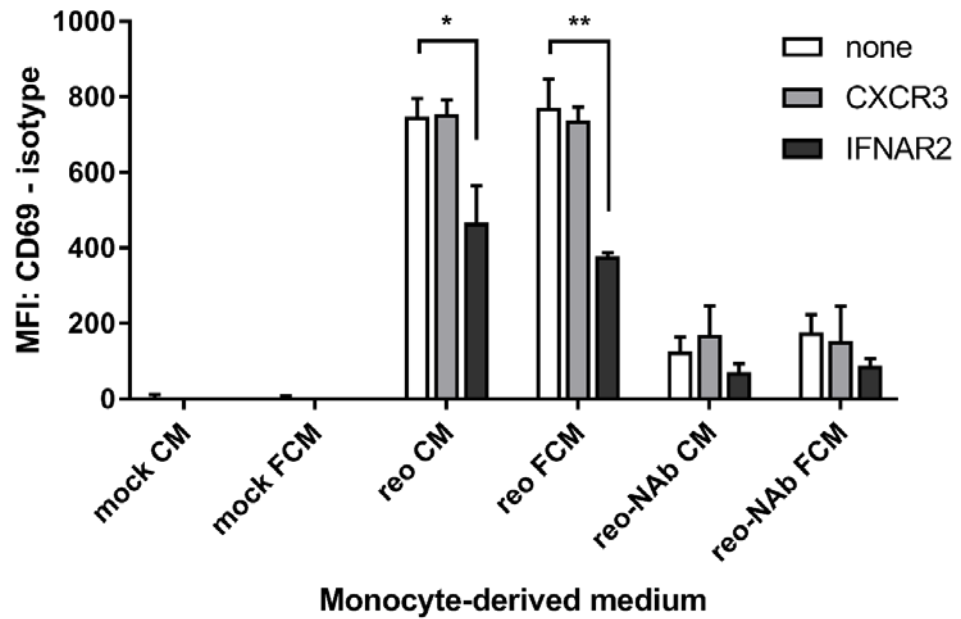


**Figure 7.5.3 Mechanism of NK cell activation by monocyte-secreted factors**

Monocytes were treated with reovirus or reo-NAb (MOI 5) and cultured overnight (16 hours). Cell-free conditioned medium (CM) was collected and virus removed using filters (FCM). CM/FCM from treated monocytes was added to fresh PBMC which had been pre-treated with blocking antibodies against CXCR3 (light grey bars), IFNAR2 (dark grey bars) or isotype control (clear bars). After 48 hours, NK cell activation was determined by CD69 PerCP staining on the CD3<sup>-</sup> CD56<sup>+</sup> population. The mean  $\pm$  SEM of the isotype-corrected median fluorescence intensity values from two donors is displayed. \* $p$  < 0.05, \*\* $p$  < 0.01 by two-way ANOVA (Tukey's multiple comparisons test).

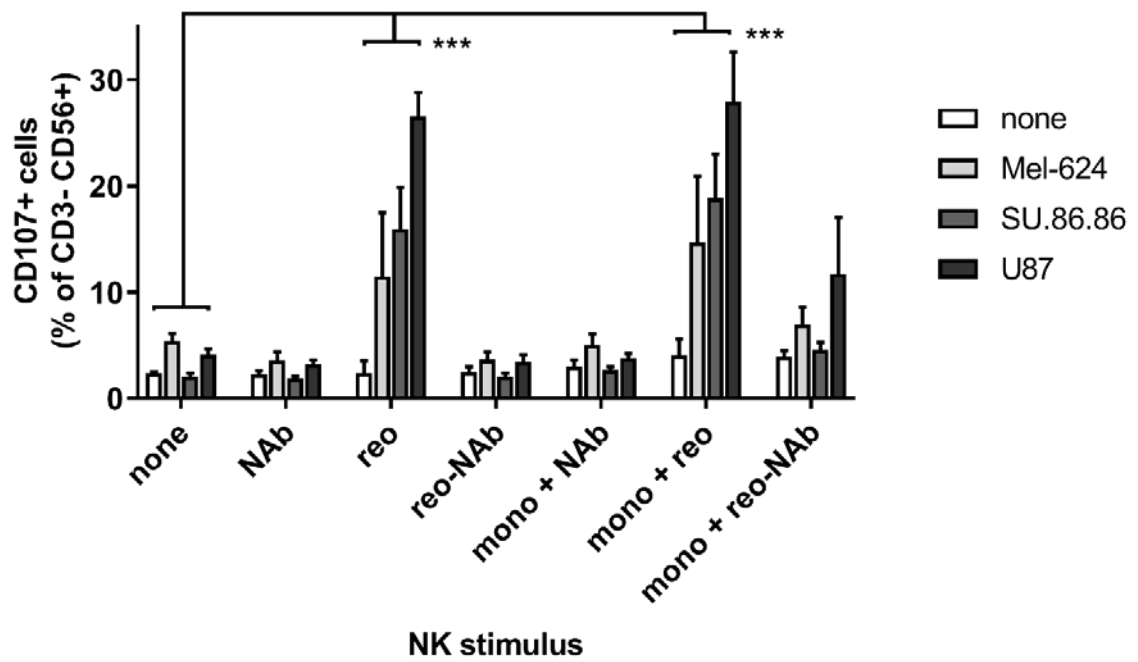


**Figure 7.5.4 Ability of treated monocytes to stimulate NK cell degranulation**

NK cells were co-cultured with monocytes treated with NAb, reovirus or reo-NAb, or were given those treatments directly, and incubated for 40 hours. Target cells (as indicated) were added for 1 hour, prior to analysis of CD107 expression % on the CD3<sup>-</sup> CD56<sup>+</sup> NK population by flow cytometry. The mean value across three individual donors  $\pm$  SEM is displayed. \*\*\* $p < 0.001$  vs untreated NK cells by two-way ANOVA (Dunnett's multiple comparisons test).

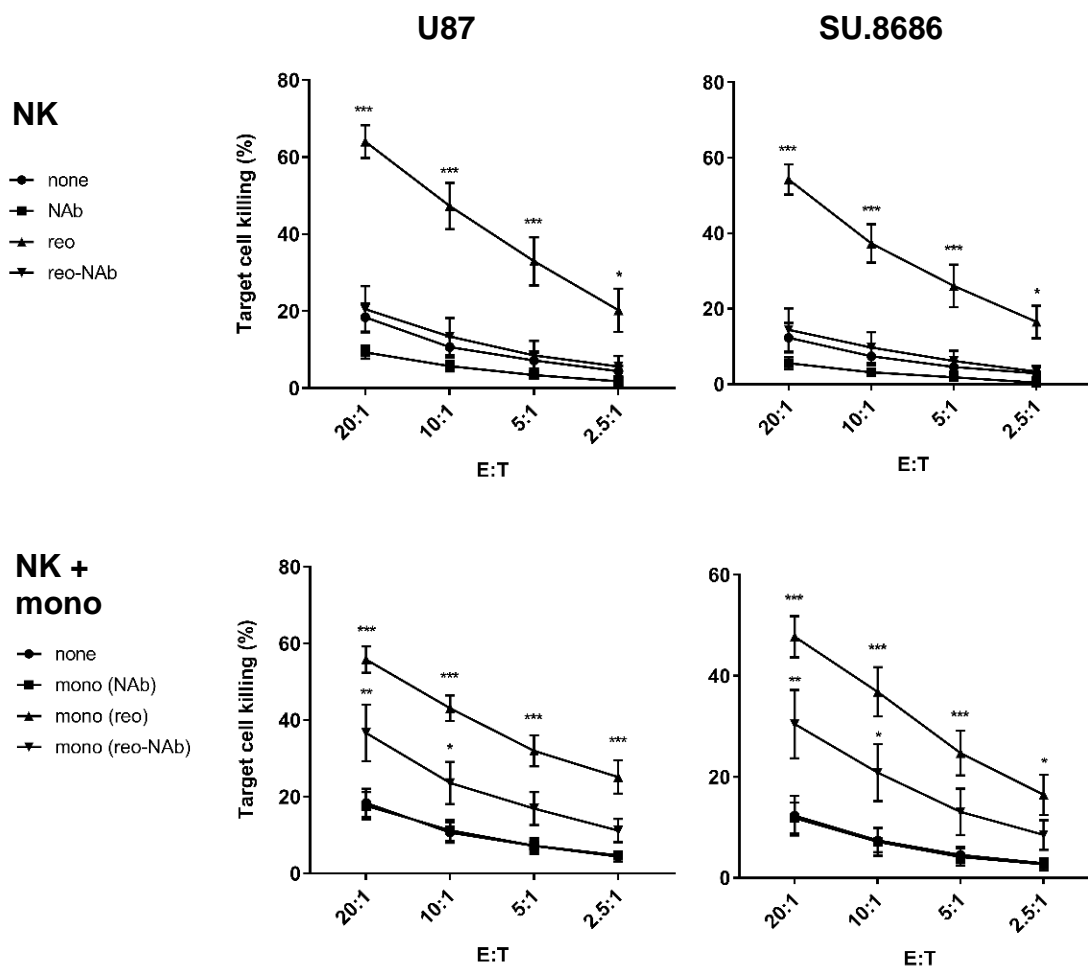


**Figure 7.5.5 Ability of treated monocytes to stimulate NK cell-mediated cytotoxicity**

NK cells were co-cultured with monocytes treated with NAb, reovirus or reo-NAb, or were given those treatments directly, and incubated for 40 hours.  $^{51}\text{Cr}$ -labelled U87 or SU.8686 target cells were added at the E:T ratios indicated for 4 hours. Supernatant was analysed for chromium release by scintillation, and converted to % killing. The mean values  $\pm$  SEM from six donors are shown. \* $p < 0.05$ , \*\* $p < 0.01$ , \*\*\* $p < 0.001$  vs NK cells alone by two-way ANOVA (Dunnett's multiple comparisons test).

## 7.6 Summary

Previous chapters have identified the human monocyte as a circulating cell type which is capable of the carriage and release of free or neutralised reovirus for the oncolytic killing of tumour cell targets *in vitro*. However, while certain OV-mediated effects are likely to be dependent on viral access to the tumour, the capacity of monocytes as hitch-hiking vehicles may prove less important than their prospective ability to impart the immunogenic effects of the virus in the *in vivo* setting. This is because in efficacy terms, lytic killing is increasingly recognised as secondary to immune activation. This is demonstrated by (i) the successful use of poorly lytic, inactivated or attenuated viruses, (ii) the need for an intact immune system in tumour purging, and (iii) the benefit of encoding various immunostimulatory molecules, such as GM-CSF, as transgenes within OV (Breitbach et al., 2011; Liu et al., 2003; Prestwich et al., 2009b; Zamarin et al., 2017). Monocytes are abundant in blood, are capable of interacting with other immune fractions, and can secrete significant quantities of functionally relevant cytokines (Boyette et al., 2017). The effects of virus carriage on monocytes, and in particular the differential effects of reovirus and reo-NAb, were therefore investigated.

Preliminary assessments of virus sensing mechanisms and phenotype were made, showing qualitative similarities between the two. Supporting the visual evidence from electron microscopy (Figure 6.2.3), activation of RIG-I suggests that the virus gains access to the cytosol, and that dsRNA may be exposed. For reo-NAb, this is consistent with evidence suggesting that antibody-opsonised virions can be uncoated for detection of viral RNA by RIG-I (McEwan et al., 2013; Watkinson et al., 2015).

The apparent induction of PKR, consistent with its role in sensing reovirus dsRNA by mouse DC (Diebold et al., 2003), is predictive of the shutdown of host cell translation, a common response to viral infection. Although no direct evidence for the restriction of monocyte translation is presented, the disparity observed between reovirus genomes and intact virions generated by infected monocytes (Figures 6.4.3 and 6.4.4) does suggest an 'uncoupling' of transcription and translation, giving rise to an abortive cycle of virus replication.

The activation of these dsRNA sensors and subsequent impingement upon key signalling hubs such as NF- $\kappa$ B suggests that carriage of virus is not phenotypically silent but induces significant changes in transcriptional programs. Indeed, RNAseq analysis (reinforced by qPCR) demonstrated

comprehensive changes in gene expression – approaching half of the genes tested – by reovirus and reo-NAb. Here, the reo-NAb set resembled an attenuated version of the reovirus set.

This study contains a number of limitations. It is important that the outputs generated from lists of ‘differentially expressed genes’ are interpreted with caution. Given the size of the data set, these gene lists were not processed further prior to enrichment analysis; the magnitude (as long as classified as DE) and directionality of the change in expression were not considered. For instance, genes upregulated 3-fold and 100-fold, as well as those significantly downregulated, were all grouped together. Secondly, although validation of transcription was performed by qPCR and correlations made with protein output, the role of post-translational modifications in virus-mediated signalling was not assessed in this study.

With this noted, the reo-NAb set did exhibit some subtle differences compared to reovirus. Although the existence of a positive feedback loop in Fc receptor expression has not been formally explored, it can be speculated that the specific upregulation of *FCGR3A* transcripts in response to reo-NAb does give further weight to the prior assays in which FcγR III (CD16) was implicated in reo-NAb entry (section 6.3). This adds to evidence from a murine model in which Fc receptor expression on myeloid cells was elevated by GM-CSF, and was associated with enhanced transfer of reo-NAb to targets (Ilett et al., 2014).

A number of the differences observed in gene expression were related to cytokine secretion or intracellular trafficking, processes which are potentially interrelated. In this study, the response to free reovirus includes the considerable generation of type I IFN and also the modulation of expression in gene ontology terms relating to mitochondria. By contrast, reo-NAb is specifically linked to the lysosomal compartment and induces negligible IFN, yet a substantial ISG response remains. No evidence for the involvement of IFN-repressing proteins in this disparity was identified. The key to this conundrum may lie in the spatial distribution of MAVS, the adaptor protein for RIG-I and MDA5, which is classically located on the mitochondrial membrane and can trigger IFN production (Seth et al., 2005).

MAVS is also present on peroxisomes; from here, MAVS signals to rapidly induce the expression of ISG – including CXCL10, NF-κB and others – in the *absence* of IFN (Dixit et al., 2010). Indeed, this signalling ‘shortcut’ may underlie the IFN-independent induction of ISG by a number of other viruses (Noyce et al., 2011, 2006; Paladino et al., 2006; Peltier et al., 2013). Based on these data,

one possibility is that the antibody opsonisation of reovirus redirects entry via FcγR III, modulating intracellular trafficking of virus from mitochondria to peroxisomes, and thus leading to the induction of an antiviral state in the absence of significant IFN. Substantiation of this hypothesis would require robust evidence for the involvement of peroxisomal MAVS, such as by blocking/knock-out assays and/or its co-localisation with reo-NAb.

A number of studies describe the potent ability of reovirus to activate NK cells within PBMC, via the induction of type I IFN (Adair et al., 2013; Parrish et al., 2015). The behaviour of reovirus-treated monocytes in this context was specifically investigated, demonstrating the convincing induction of CD69 and the corresponding generation of anti-tumour activity via degranulation. As shown by an IFN receptor-blocking assay, monocyte-derived IFN-α is at least partly responsible for the stimulatory effects of the virus.

The activation observed following direct application of the virus contradicts prior studies in which it was observed exclusively in the presence of PBMC (Adair et al., 2013; Errington et al., 2008b). Various others have however reported the converse finding, with NK activation seen in isolation (Bar-On et al., 2017; Prestwich et al., 2009a; Zhao et al., 2015), which is consistent with the recognition of the reovirus σ1 protein by NKp46. It is difficult to identify the source of this discrepancy, although it appears likely to stem from the mode of NK cell selection, which may influence cell activation, and/or the presence or absence of 'contaminating', possibly IFN-supplying PBMC in NK cell preparations. The reactivity of NK cells to free reovirus does however preclude the definitive conclusion that IFN-α is *solely* responsible for NK activation by reovirus-treated monocytes, as a degree may be due to the direct effects of the released virus.

Monocytes do appear essential to the limited generation of NK cell cytotoxicity by reo-NAb, as treatment with reo-NAb in isolation is ineffectual. Notably, although FcγR III (CD16) is the sole Fc receptor present on NK cells, they lack the phagocytic machinery to permit antibody-dependent virus entry. Thus in the case of reo-NAb, as the production of IFN-α is negligible, it is likely that the observed NK activation is owing to the ability of monocytes to 'process' reo-NAb into free infectious virus, to which NK cells can respond. In this sense, monocytes may enable antiviral NAb to be circumvented by 'recycling' the naked form of the virus.

Aside from surface CD69 expression, the effect of reovirus and reo-NAb upon T cell function was not evaluated in this study. There are however signs that

reovirus can boost not just the innate but the adaptive anti-tumour response through the enhancement of anti-tumour responses by CD8<sup>+</sup> T cells via induction of type I and II IFN (Ilett et al., 2009; Prestwich et al., 2008a; Rajani et al., 2016). Further, reo-NAb and reovirus-treated monocytes are themselves capable of priming T cell responses against tumour antigens (V. Jennings, personal communication).

In conclusion, these studies demonstrate that not only free but also fully neutralised reovirus holds significant immunogenic activity, mediated by the stimulation of the circulating monocyte population. The potential potency of reo-NAb complexes shows that pre-existing antiviral immunity may not entirely prohibit the successful use of reovirus as an immunotherapy in reovirus-immune patients.

## 8. Discussion

Melanoma inflicts a heavy burden on its victims, with the typical reduction in life expectancy approximating two decades, and its incidence is rising globally (Ferlay et al., 2015; Guy and Ekwueme, 2011; Thiam et al., 2016). However, mortality rates are decreasing. Screening and diagnosis of early-stage disease are improving, and effective therapies for advanced melanoma are emerging, shifting median survival from months to a number of years (Curiel-Lewandrowski et al., 2012; Robert et al., 2017). These trends suggest that the ‘unmet clinical need’ of melanoma is beginning to be met, with safe and effective immunotherapies playing a major role in doing so. Such progress does not mean that innovative research into new therapies and novel approaches should relent. For the majority of patients with metastatic melanoma, the prospect of a long-term ‘cure’ remains out of reach for now. Further, the ‘tumour-agnostic’ activity of some agents (Tao et al., 2018) adds to the rationale for continuing research apace, even in relatively favourable indications.

Immune checkpoint inhibitors have shifted the paradigm across tumour types. The critical question now asks how best to potentiate immunotherapies to generate long-lasting remissions in a larger proportion of patients. OV offer unique anti-neoplastic traits, such as the potential to amplify within the tumour, and an unparalleled tolerability, which addresses a major concern of today’s oncologists (Jones et al., 2015). Confidence in OV as a modality is developing, as exemplified by Merck’s recent acquisition of the company behind CVA21, Viralytics, for \$394 million ([www.viralytics.com](http://www.viralytics.com)). Such events bode well for the future use of OV as combination agents. When used in monotherapy, many OV – including reovirus – show limited efficacy (Galanis et al., 2012). The reasons for this are incompletely understood, although the neutralising capability of the humoral immune system has been heavily implicated, particularly in the context of i.v. administration (Magge et al., 2013; Tomita et al., 2012). Consequently, i.t. delivery has been favoured for some OV, such as T-VEC, with systemic anti-tumour immunity successfully elicited. However, by virtue of viraemia, i.v. infusion is theoretically better suited to global immune activation and accessing

disseminated disease. These traits appear prizes to be won, if we can find the key to unlock the efficacy of OV when given by this route.

It is increasingly clear that i.v. OV need 'help' to transition successfully from the eye of a needle to the heart of a tumour, with cellular chaperones a popular strategy (Willmon et al., 2009). Myeloid cells are natural viral sinks, and boast a number of favourable properties: virus uptake machinery (Fanger et al., 1996; Ilett et al., 2011), tumour trafficking (Clements et al., 2015; Ilett et al., 2014), and co-ordination of other immune effectors (Ilett et al., 2011; Parrish et al., 2015). In the presence of NAb, human monocyte-derived DC carry reovirus and deliver it to kill tumour cell targets *in vitro* (Ilett et al., 2011). This observation led to a murine study in which i.v. reovirus therapy for melanoma was potentiated through prior mobilisation of the myeloid compartment with GM-CSF, particularly in reovirus-immune animals (Ilett et al., 2014). The current project therefore aimed to corroborate and explore a model in which circulating monocytes convey antibody-neutralised reovirus to tumours, to initiate both oncolytic and immune-mediated cell death.

As a result of environmental exposure, seroprevalence to reovirus among the adult population is high. Thus, in an average cancer patient being considered for reovirus therapy, the first infusion of virus would occur in the context of detectable but low-level NAb. It is known that virus successfully accesses tumour beds in this scenario, even in the relatively restricted environs of the brain (Samson et al., 2018). Should subsequent therapeutic infusions be necessary, virions would encounter anamnestic NAb at high titre. In either case, the dynamic events occurring in the bloodstream immediately after viraemia is established – the recognition of virus by antibody, and the binding of cells by virus – are critical determinants of its spread and persistence.

First, the interaction between reovirus and antiviral factors in serum derived from reovirus-treated patients was explored. Electron microscopy and biochemical depletion assays were used to demonstrate the presence of highly neutralising anti-reovirus antibodies in patient serum, which bind the virion to form 'reo-NAb' immune complexes. The comparison of control- and patient-derived sera following the addition of reovirus *in vitro* provides an illustration of the difference between a first infusion and subsequent infusions. As the i.v.

administration of OV moves closer to regulatory approval, such models provide basic information with which to optimise delivery strategies.

The 100-fold increase in neutralising capacity in patients versus controls, albeit in unpaired samples, reflects the scale of the antibody response observed in previous reovirus trials (Adair et al., 2012; White et al., 2008). Characterisation of serum antibodies identified reovirus-specific IgG and IgA, with IgG in particular recognising a wide repertoire of reovirus proteins, as determined by western blot. These observations demonstrate the ability of a single i.v. infusion of reovirus to profoundly bias the serum antibody response in patients, and substantiate the hypothesis that reo-NAb complexes are formed in the circulation shortly after infusion. Our inability to isolate 'endogenous' reo-NAb, together with the absence of reovirus genomes in serum one day after infusion (Adair et al., 2012), is suggestive of a rapid process of cellular association and potentially egress from circulation.

Prior studies identified the blood monocyte as a key cell type in sequestering reovirus in circulation. Further, in mice, GM-CSF pre-conditioning prior to i.v. reovirus enhanced myeloid cell trafficking to melanoma tumours, with an associated increase in virus within the tumour (Ilett et al., 2014). Consequently the putative role of monocytes as vehicles for reovirus was investigated in the human setting, using patient-derived sera, primary human monocytes, and a human melanoma cell line. These formed elements of a novel *in vitro* 'hand-off' assay, which was used to model the loading of blood monocytes *in vivo*. The assay successfully demonstrated the ability of monocytes to deliver otherwise neutralised reovirus to kill melanoma targets by oncolysis. This study is believed to be the first to describe this interaction between human monocytes and oncolytic reovirus.

Further, this study represents a rare report of therapeutic OV carriage following antibody neutralisation. This phenomenon has been described previously using measles virus, again in the context of human monocytic cells (Iankov et al., 2007). Importantly, monocytes were also found to be capable of delivering neutralised CVA21 to tumour targets, using virus and patient-derived material from other trials. This transferability suggests that the hand-off of neutralised OV represents not a reovirus-specific quirk but a phenomenon of genuine

relevance across OV. The absence of killing with HSV1716 requires further investigation. Anti-HSV serum should be obtained to eliminate any confounding effects of using pleural fluid; other viruses may be tested to identify a role for the viral envelope in preventing hand-off by modulating antibody binding. While these are possible, the most likely explanation may lie in a poorly lytic stock of HSV1716, as shown by direct cytotoxicity assay. If monocyte-mediated hand-off is proven to be applicable across OV, this would be suggestive of an underlying immune mechanism rather than virus-specific factors.

The use of monocytes in this project not only stems from previous studies on the carriage of OV by myeloid cells, but also their abundance in circulation and their status as primary targets of viral infection (Hou et al., 2012; Kou et al., 2008). Using a number of imaging techniques, human monocytes were found to bind both free reovirus and reo-NAb complexes. The virus gains access to large intracellular compartments, likely endosomes, in which biochemical assays suggest they are rapidly stripped of any bound antibody, enabling delivery to tumour cells. This is consistent with the 'recycling' ability of myeloid cells to regurgitate intact antigen (Le Roux et al., 2012), and indicates their potentially unique capacity to liberate intact virus from its neutralising coat. Despite a transient increase in viral RNA, it does not appear that reovirus is capable of productive amplification within monocyte carriers, consistent with intact antiviral signalling identified by immunophenotyping and western blot.

It was determined using function-blocking antibodies that reo-NAb loading is at least partly dependent on monocyte Fc receptors, consistent with a hypothesis in which cellular interaction occurs via the Fc domains of virus-bound antibodies. FcγR IIIa (*FCGR3A*) was identified as the major mediator, with the superior potency of non-classical versus classical monocytes supporting this theory. However, significant functional redundancy appears to exist in this regard, suggestive of shared features between Fc receptors, as has been reported elsewhere (Fanger et al., 1996; Rodrigo et al., 2006). Interestingly, this is not the first study to demonstrate the antibody-mediated entry of reovirus: two separate studies have done so, but both as a virological model rather than in an oncolytic context, and neither in primary cells (Burstin et al., 1983; Danthi et al., 2006). The findings herein regarding FcγR IIIa involvement are consistent with

the artificial endowment of Fc receptors enabling entry (Danthi et al., 2006), and the ability of FcγR II / III blockade to abrogate the therapeutic activity of GM-CSF plus reo-NAb in murine cells (Ilett et al., 2014). The finding that reo-NAb treatment (but not reovirus treatment) upregulates the expression of this Fc receptor alone further implies its involvement, based on a putative positive feedback loop.

As discussed above, there are considerable mechanistic parallels between these data and reports of antibody-dependent enhancement (ADE) across the virological spectrum. Although ADE of infection may seem a niche mechanism lacking physiological impact, it does appear to be of genuine clinical relevance, in that by providing a pathogenic virus access to blood monocytes, antibodies can significantly exacerbate disease (Katzelnick et al., 2017). Further, in comparison to an environmental exposure, the titre of OV administered systemically is greater by many orders of magnitude, suggesting it is realistic that the impact of such a phenomenon may be equally great. Yet the process observed here is unlike ADE, in that the pathogenic amplification of virus appears to be thwarted. Most significantly, entry is not strictly *antibody-dependent*, as free virus can gain access to the monocyte interior; nor is it *enhancement*, given that the presence of serum substantially reduces monocyte viral load and consequently hand-off efficacy. Rather, the specific uptake of neutralised reovirus is better described as an *antibody-mediated* process, when the viral epitopes required for canonical entry are masked by NAb.

It is in this discrimination that the key difference in reo-NAb activity between the mouse and human settings appears to lie. In mice, the loading of myeloid cells by reovirus is roughly doubled in the presence of NAb, a difference which is amplified by the apparent ability of reovirus to replicate in these cells (Ilett et al., 2014). By contrast, although human monocytes do carry reo-NAb, the degree of loading is considerably lower than with free virus, and no appreciable increase in titre is observed over time. Thus while ADE is truly applicable to reovirus in mice, it cannot be applied wholesale to the human setting.

Human monocytes possess both Fc receptors and JAM-A and sialic acid. Theoretically, the antibody-mediated uptake of OV would have maximal impact in the context of a virus for which immune cells (particularly monocytes) do not

carry the cognate receptor, as Fc receptor access would not come at the cost of access to this receptor. This would be interesting to test as a proof of principle, but given the ubiquity of the receptors that viruses employ, few current OV meet this criterion; even the avian paramyxovirus NDV uses sialic acid (Mahon et al., 2011).

The activity of reo-NAb was further examined *in vivo* using well-characterised melanoma flank models. After i.v. administration, reovirus neutralised *ex vivo* reliably accessed tumour beds, as shown by detection of viral RNA and replication-competent viral particles, mirroring the isolation of virus from tumours in virus-immune patients (Adair et al., 2012; Samson et al., 2018). A trend towards increased tumour viral load by GM-CSF pre-conditioning provided corroborative evidence for its enhancement of reovirus therapy, as shown previously with regard to cell carriers (Ilett et al., 2014). A subsequent experiment designed to show therapeutic equivalence between reo-NAb complexes formed *ex vivo* and those formed *in vivo* (per Ilett et al., 2014) was confounded by tumour ulceration, although initial trends suggested similar effects upon tumour growth. It will be necessary to repeat this experiment with added precautions against ulceration, to gain a robust assessment of tumour burden and survival benefit; mouse group size should also be increased, as the effect size between reovirus groups may be small.

If it can be shown that *ex vivo*-formed complexes are not therapeutically inferior to those formed in virus-immune mice upon reovirus infusion, this may provide an opportunity to further examine the type of antibody mediating enhanced viral loading of monocytes. Complexes could be formed *ex vivo* using either neutralising (e.g. the anti- $\sigma$ 1 Ab G5; see Figure 5.5.3) or non-neutralising monoclonal antibodies (Tyler et al., 1993), and administered i.v. following GM-CSF pre-conditioning in naïve animals. Comparison of viral loading and therapy mediated by these artificial complexes, or free virus, would provide valuable data. They should reveal whether neutralising or non-neutralising antibodies enable Fc receptor-mediated loading, and thus underpin systemic GM-CSF/reovirus therapy as described previously (Ilett et al., 2014). Should non-neutralising antibodies be implicated – as is common in ADE of non-oncolytic viruses – a reovirus-binding, non-neutralising monoclonal antibody,

administered prior to i.v. reovirus, might represent a prospective therapeutic. A successful precedent for this strategy has already been set with VSV in mice (Eisenstein et al., 2013). The potential, then, for a paradoxical mirror image: while a protective vaccine against the pathogenic dengue virus can unintentionally deliver harm (Ferguson et al., 2016), supposedly restrictive antibodies against a helpful virus may in fact support therapy.

If the likely therapeutic impact of the hand-off process *in vivo* was simply a product of the viral titre loaded on to human monocytes, it would be expected that NAb would be limiting towards therapy, based on the hand-off assay. However, in many models, oncolysis is of secondary importance to immune-mediated killing, and is sometimes not required at all (Prestwich et al., 2009a). In the precursor study to this one, in mice, GM-CSF/reovirus therapy for melanoma was reliant upon an immune-mediated mechanism, via the activity of monocytes and NK cells (Ilett et al., 2014). Thus the monocyte 'sink' for virus was further investigated for its immunomodulatory potential, given its ability to generate a potent cytokine milieu and activate other immune effectors (Adair et al., 2013; Errington et al., 2008a; Parrish et al., 2015).

Like free reovirus, reo-NAb induced the upregulation of cellular RNA sensors, and elicited phenotypic maturation and activation of co-stimulatory molecules. Given the evidence of a robust response in these primary cells, exploratory transcriptional profiling was conducted, using a carefully selected housekeeping gene. This revealed qualitatively similar responses to free and neutralised virus, with some subtle differences suggestive of alternative trafficking, possibly resulting from the presence of virus-bound antibody. Although reo-NAb induced the release of some proteins, such as CXCL and MCP family chemokines, at similar concentrations to free virus, others such as TNF and IFN were only secreted in response to free virus. These differential secretory patterns provide further evidence that the presence of NAb modulates the monocyte response to virus. Monocyte cytokine release was not lost with UV-inactivated virus, suggesting that it is driven through PRR activation by incoming viral motifs rather than initial replication of the viral genome.

Compared to free reovirus, reo-NAb induced significantly less type I IFN at the RNA and protein level, consistent with prior reports of IFN suppression upon antibody-dependent entry of virus (Rolph et al., 2011; Tsai et al., 2014). No evidence could be found for the transcriptional activation of a specific IFN repressor by reo-NAb. Given that reo-NAb triggers monocyte ISG expression in our system, it is postulated that Fc receptor-mediated entry modulates reo-NAb trafficking and thus activation of specific PRR, which may support ISG activation in the relative absence of IFN. Based on prior studies (Dixit et al., 2010; Noyce et al., 2011; Stuart et al., 2018), the subcellular localisation of MAVS and the subsequent activation state of IRF3 should be interrogated as hallmarks of an IFN-independent ISG response.

The patients from whom serum was obtained for this study received a single infusion of i.v. reovirus prior to brain tumour resection (Samson et al., 2018). This bolus of virus induced a significant elevation in serum IFN- $\alpha$  at 48 hours post-infusion versus baseline. As data on patient NAb levels at baseline were not published, it is not clear whether IFN- $\alpha$  was generated in the context of total or partial neutralisation. It would be informative to compare IFN- $\alpha$  concentrations in serum taken after a first infusion versus after a second infusion; this would establish, with direct relevance to the *in vitro* data in this study, whether IFN- $\alpha$  is elevated in the context of complete neutralisation *in vivo*.

Reovirus-induced IFN- $\alpha$  is of functional significance, as it is necessary for virus-induced activation of NK cell cytotoxicity against human leukaemia and colorectal targets *in vitro* (Adair et al., 2013; Parrish et al., 2015). This was corroborated by the activation of NK cells by type I IFN secreted by reovirus-treated monocytes. Thus, while a relative lack of IFN- $\alpha$  in the context of reo-NAb could help to delay viral clearance *in vivo*, it may concomitantly diminish the NK-mediated element of reovirus therapy. Reovirus-mediated NK cell degranulation and cytotoxicity was indeed attenuated, but not fully abrogated, by the presence of virus-bound NAb. Monocytes were essential for the activity of reo-NAb, although it was not possible to determine whether this was a result of their ability to regenerate uncoated virus for subsequent activation, or their low-level IFN secretion.

These data are therefore indicative of human correlates for the cell populations required for systemic GM-CSF/reovirus therapy in mice: monocytes as 'first responders' to reo-NAb, and NK cells as effectors of tumour cell killing (Ilett et al., 2014). Further investigation of GM-CSF/reovirus therapy in mice has revealed that this regimen promotes homing of not only myeloid cells but also CD8<sup>+</sup> T cells into tumours, and generates a low-level T<sub>H</sub>1 response to tumour antigens, which is significantly enhanced by adding subsequent PD-1 inhibition, translating into therapeutic benefit against melanoma and glioma in syngeneic mouse models (Ilett et al., 2017; Samson et al., 2018). Indeed, emerging evidence suggests that IFN-induced PD-L1 provides a mechanism of resistance against some OV (Zamarin et al., 2018), supporting the combination of virotherapy with checkpoint inhibitors. Thus, while innate immune cells appear fundamental as early effectors in the GM-CSF/reovirus regimen, potentiating adaptive immunity may be the key to realising a truly durable benefit.

In summary, this study confirms that circulating human monocytes are capable of the uptake of reovirus, despite total neutralisation, and its release for the oncolysis of tumour targets in culture. These findings endorse a model whereby, in the bloodstream of virus-immune patients, monocytes are capable of acting as carriers for the virus, and delivering it to tumour beds for both oncolytic and immune-mediated killing. They are consistent with the presence of reovirus in widespread tumour deposits following i.v. administration in the presence of NAb, and its association with immune cells, including the myeloid population. In contrast to the aforementioned murine study, this project found no overall benefit from the presence of NAb in a human *in vitro* system: it limits monocyte loading, and appears to attenuate the IFN response, simultaneously an antiviral process and a key potential driver of innate anti-tumour activity. However, in antibody-mediated reovirus uptake, the above investigations identify a mechanism which may be necessary for the continued activity of systemically administered reovirus, and other OV, in patients with pre-existing antiviral immunity. Evidence is provided for the involvement of a mechanism which is well-defined in virology, but relatively unexplored in the context of OV.

It is critical to recognise that, for reovirus and many other therapeutic viruses, prevailing seropositivity means that even a first i.v. dose of virus encounters NAb – demanding strategies not just to manage this, but to capitalise upon it. A clinical study (NCT03282188) that aims to do so has been planned; this was designed to demonstrate the enhancement of systemic reovirus therapy by GM-CSF pre-conditioning in virus-immune melanoma patients, substantiating the cell carrier paradigm. Translational outputs from such prospective trials, in particular the correlation of monocyte virus load and phenotype with the ultimate tumour load and response, would be highly informative. They would enable a definitive conclusion on the impact of reovirus carriage in melanoma patients, and could offer ways in which the antibody response can be shaped to promote anti-tumour benefit, for reovirus and across OV.

## 9. References

- Abdel-Malek, Z.A., Kadekaro, A.L., Swope, V.B., 2010. Stepping up melanocytes to the challenge of UV exposure. *Pigment Cell Melanoma Res.* 23, 171–186. <https://doi.org/10.1111/j.1755-148X.2010.00679.x>
- Abdel-Rahman, O., 2016. PD-L1 expression and outcome of advanced melanoma patients treated with anti-PD-1/PD-L1 agents: a meta-analysis. *Immunotherapy* 8, 1081–1089. <https://doi.org/10.2217/imt-2016-0025>
- Adair, R.A., Roulstone, V., Scott, K.J., Morgan, R., Nuovo, G.J., Fuller, M., Beirne, D., West, E.J., Jennings, V.A., Rose, A., Kyula, J., Fraser, S., Dave, R., Anthoney, D.A., Merrick, A., Prestwich, R., Aldouri, A., Donnelly, O., Pandha, H., Coffey, M., Selby, P., Vile, R., Toogood, G., Harrington, K., Melcher, A.A., 2012. Cell Carriage, Delivery, and Selective Replication of an Oncolytic Virus in Tumor in Patients. *Sci. Transl. Med.* 4, 138ra77-138ra77. <https://doi.org/10.1126/scitranslmed.3003578>
- Adair, R.A., Scott, K.J., Fraser, S., Errington-Mais, F., Pandha, H., Coffey, M., Selby, P., Cook, G.P., Vile, R., Harrington, K.J., Toogood, G., Melcher, A.A., 2013. Cytotoxic and immune-mediated killing of human colorectal cancer by reovirus-loaded blood and liver mononuclear cells. *Int. J. Cancer* 132, 2327–2338. <https://doi.org/10.1002/ijc.27918>
- Agarwala, S.S., 2009. Current systemic therapy for metastatic melanoma. *Expert Rev. Anticancer Ther.* 9, 587–595. <https://doi.org/10.1586/era.09.25>
- Ahmadzadeh, M., Johnson, L.A., Heemskerk, B., Wunderlich, J.R., Dudley, M.E., White, D.E., Rosenberg, S.A., 2009. Tumor antigen-specific CD8 T cells infiltrating the tumor express high levels of PD-1 and are functionally impaired. *Blood* 114, 1537–1544. <https://doi.org/10.1182/blood-2008-12-195792>
- Ahmed, A.U., Tyler, M.A., Thaci, B., Alexiades, N.G., Han, Y., Ulasov, I.V., Lesniak, M.S., 2011. A comparative study of neural and mesenchymal stem cell-based carriers for oncolytic adenovirus in a model of malignant glioma. *Mol. Pharm.* 8, 1559–1572. <https://doi.org/10.1021/mp200161f>
- Akira, S., Uematsu, S., Takeuchi, O., 2006. Pathogen recognition and innate immunity. *Cell* 124, 783–801. <https://doi.org/10.1016/j.cell.2006.02.015>
- Alain, T., Kim, T.S., Lun, X., Liacini, A., Schiff, L.A., Senger, D.L., Forsyth, P.A., 2007. Proteolytic Disassembly Is a Critical Determinant for Reovirus Oncolysis. *Mol. Ther.* 15, 1512–1521. <https://doi.org/10.1038/sj.mt.6300207>
- Alemany, R., 2007. Cancer selective adenoviruses. *Mol. Aspects Med., Genes in the cure of cancer* 28, 42–58. <https://doi.org/10.1016/j.mam.2006.12.002>
- Alter, G., Malenfant, J.M., Altfeld, M., 2004. CD107a as a functional marker for the identification of natural killer cell activity. *J. Immunol. Methods* 294, 15–22. <https://doi.org/10.1016/j.jim.2004.08.008>
- Amigorena, S., Bonnerot, C., 1999. Fc receptor signaling and trafficking: a connection for antigen processing. *Immunol. Rev.* 172, 279–284.

- Anderson, A.C., Joller, N., Kuchroo, V.K., 2016. Lag-3, Tim-3, and TIGIT: Co-inhibitory Receptors with Specialized Functions in Immune Regulation. *Immunity* 44, 989–1004. <https://doi.org/10.1016/j.immuni.2016.05.001>
- Anderson, B.D., Nakamura, T., Russell, S.J., Peng, K.-W., 2004. High CD46 receptor density determines preferential killing of tumor cells by oncolytic measles virus. *Cancer Res.* 64, 4919–4926. <https://doi.org/10.1158/0008-5472.CAN-04-0884>
- Andreasson, K., Eriksson, M., Tegerstedt, K., Ramqvist, T., Dalianis, T., 2010. CD4+ and CD8+ T Cells Can Act Separately in Tumour Rejection after Immunization with Murine Pneumotropic Virus Chimeric Her2/neu Virus-Like Particles. *PLOS ONE* 5, e11580. <https://doi.org/10.1371/journal.pone.0011580>
- Andtbacka, R.H.I., Curti, B.D., Kaufman, H., Daniels, G.A., Nemunaitis, J.J., Spitler, L.E., Hallmeyer, S., Lutzky, J., Schultz, S.M., Whitman, E.D., Zhou, K., Karpathy, R., Weisberg, J.I., Grose, M., Shafren, D., 2015a. Final data from CALM: A phase II study of Coxsackievirus A21 (CVA21) oncolytic virus immunotherapy in patients with advanced melanoma. *J. Clin. Oncol.* 33, 9030–9030. [https://doi.org/10.1200/jco.2015.33.15\\_suppl.9030](https://doi.org/10.1200/jco.2015.33.15_suppl.9030)
- Andtbacka, R.H.I., Kaufman, H.L., Collichio, F., Amatruda, T., 2015b. Talimogene Laherparepvec Improves Durable Response Rate in Patients With Advanced Melanoma. *J. Clin. Oncol.* advanced online publication. <https://doi.org/10.1200/JCO.2014.58.3377>
- Andtbacka, R.H.I., Ross, M., Puzanov, I., Milhem, M., Collichio, F., Delman, K.A., Amatruda, T., Zager, J.S., Cranmer, L., Hsueh, E., Chen, L., Shilkrot, M., Kaufman, H.L., 2016. Patterns of Clinical Response with Talimogene Laherparepvec (T-VEC) in Patients with Melanoma Treated in the OPTiM Phase III Clinical Trial. *Ann. Surg. Oncol.* 23, 4169–4177. <https://doi.org/10.1245/s10434-016-5286-0>
- Andtbacka, R.H.I., Ross, M.I., Agarwala, S.S., Taylor, M.H., Vetto, J.T., Neves, R.I., Daud, A., Khong, H.T., Ungerleider, R.S., Tanaka, M., Grossmann, K.F., 2017. Final results of a phase II multicenter trial of HF10, a replication-competent HSV-1 oncolytic virus, and ipilimumab combination treatment in patients with stage IIIB-IV unresectable or metastatic melanoma. *J. Clin. Oncol.* 35, 9510–9510. [https://doi.org/10.1200/JCO.2017.35.15\\_suppl.9510](https://doi.org/10.1200/JCO.2017.35.15_suppl.9510)
- Antar, A.A.R., Konopka, J.L., Campbell, J.A., Henry, R.A., Perdigoto, A.L., Carter, B.D., Pozzi, A., Abel, T.W., Dermody, T.S., 2009. Junctional Adhesion Molecule-A Is Required for Hematogenous Dissemination of Reovirus. *Cell Host Microbe* 5, 59–71. <https://doi.org/10.1016/j.chom.2008.12.001>
- Antczak, J.B., Joklik, W.K., 1992. Reovirus genome segment assortment into progeny genomes studied by the use of monoclonal antibodies directed against reovirus proteins. *Virology* 187, 760–776.
- Arimoto, K., Takahashi, H., Hishiki, T., Konishi, H., Fujita, T., Shimotohno, K., 2007. Negative regulation of the RIG-I signaling by the ubiquitin ligase RNF125. *Proc. Natl. Acad. Sci. U. S. A.* 104, 7500–7505. <https://doi.org/10.1073/pnas.0611551104>
- Armstrong, B.K., Kricger, A., English, D.R., 1997. Sun exposure and skin cancer. *Australas. J. Dermatol.* 38 Suppl 1, S1-6.

- Asada, T., 1974. Treatment of human cancer with mumps virus. *Cancer* 34, 1907–1928.
- Bagga, S., Bouchard, M.J., 2014. Cell cycle regulation during viral infection. *Methods Mol. Biol.* Clifton NJ 1170, 165–227. [https://doi.org/10.1007/978-1-4939-0888-2\\_10](https://doi.org/10.1007/978-1-4939-0888-2_10)
- Balch, C.M., Gershenwald, J.E., Soong, S.-J., Thompson, J.F., Atkins, M.B., Byrd, D.R., Buzaid, A.C., Cochran, A.J., Coit, D.G., Ding, S., Eggermont, A.M., Flaherty, K.T., Gimotty, P.A., Kirkwood, J.M., McMasters, K.M., Mihm, M.C., Morton, D.L., Ross, M.I., Sober, A.J., Sondak, V.K., 2009. Final version of 2009 AJCC melanoma staging and classification. *J. Clin. Oncol. Off. J. Am. Soc. Clin. Oncol.* 27, 6199–6206. <https://doi.org/10.1200/JCO.2009.23.4799>
- Balkwill, F., Watling, D., Taylor-Papadimitriou, J., 1978. Inhibition by lymphoblastoid interferon of growth of cells derived from the human breast. *Int. J. Cancer* 22, 258–265.
- Bangari, D.S., Mittal, S.K., 2006. Current strategies and future directions for eluding adenoviral vector immunity. *Curr. Gene Ther.* 6, 215–226.
- Barber, G.N., Wambach, M., Thompson, S., Jagus, R., Katze, M.G., 1995. Mutants of the RNA-dependent protein kinase (PKR) lacking double-stranded RNA binding domain I can act as transdominant inhibitors and induce malignant transformation. *Mol. Cell. Biol.* 15, 3138–3146.
- Barkon, M.L., Haller, B.L., Virgin, H.W., 1996. Circulating immunoglobulin G can play a critical role in clearance of intestinal reovirus infection. *J. Virol.* 70, 1109–1116.
- Bar-On, Y., Charpak-Amikam, Y., Glasner, A., Isaacson, B., Duev-Cohen, A., Tsukerman, P., Varvak, A., Mandelboim, M., Mandelboim, O., 2017. NKp46 recognizes the sigma1 protein of reovirus: Implications for reovirus-based cancer therapy. *J. Virol.* JVI.01045-17. <https://doi.org/10.1128/JVI.01045-17>
- Barone, A., Hazarika, M., Theoret, M.R., Mishra-Kalyani, P., Chen, H., He, K., Sridhara, R., Subramaniam, S., Pfuma, E., Wang, Y., Li, H., Zhao, H., Zirkelbach, J.F., Keegan, P., Pazdur, R., 2017. FDA Approval Summary: Pembrolizumab for the Treatment of Patients with Unresectable or Metastatic Melanoma. *Clin. Cancer Res. Off. J. Am. Assoc. Cancer Res.* 23, 5661–5665. <https://doi.org/10.1158/1078-0432.CCR-16-0664>
- Barrow, C., Browning, J., MacGregor, D., Davis, I.D., Sturrock, S., Jungbluth, A.A., Cebon, J., 2006. Tumor Antigen Expression in Melanoma Varies According to Antigen and Stage. *Clin. Cancer Res.* 12, 764–771. <https://doi.org/10.1158/1078-0432.CCR-05-1544>
- Barton, E. S., Connolly, J.L., Forrest, J.C., Chappell, J.D., Dermody, T.S., 2001. Utilization of sialic acid as a coreceptor enhances reovirus attachment by multistep adhesion strengthening. *J. Biol. Chem.* 276, 2200–2211. <https://doi.org/10.1074/jbc.M004680200>
- Barton, E.S., Forrest, J.C., Connolly, J.L., Chappell, J.D., Liu, Y., Schnell, F.J., Nusrat, A., Parkos, C.A., Dermody, T.S., 2001. Junction adhesion molecule is a receptor for reovirus. *Cell* 104, 441–451.
- Barton, E.S., Youree, B.E., Ebert, D.H., Forrest, J.C., Connolly, J.L., Valyi-Nagy, T., Washington, K., Wetzel, J.D., Dermody, T.S., 2003. Utilization of sialic acid as a

- coreceptor is required for reovirus-induced biliary disease. *J. Clin. Invest.* 111, 1823–1833. <https://doi.org/10.1172/JCI200316303>
- Bass, D.M., Bodkin, D., Dambrauskas, R., Trier, J.S., Fields, B.N., Wolf, J.L., 1990. Intraluminal proteolytic activation plays an important role in replication of type 1 reovirus in the intestines of neonatal mice. *J. Virol.* 64, 1830–1833.
- Becker, M.M., Goral, M.I., Hazelton, P.R., Baer, G.S., Rodgers, S.E., Brown, E.G., Coombs, K.M., Dermody, T.S., 2001. Reovirus  $\zeta$ NS Protein Is Required for Nucleation of Viral Assembly Complexes and Formation of Viral Inclusions. *J. Virol.* 75, 1459–1475. <https://doi.org/10.1128/JVI.75.3.1459-1475.2001>
- Benencia, F., Courrèges, M.C., Conejo-García, J.R., Mohamed-Hadley, A., Zhang, L., Buckanovich, R.J., Carroll, R., Fraser, N., Coukos, G., 2005. HSV oncolytic therapy upregulates interferon-inducible chemokines and recruits immune effector cells in ovarian cancer. *Mol. Ther. J. Am. Soc. Gene Ther.* 12, 789–802. <https://doi.org/10.1016/j.ymthe.2005.03.026>
- Benjamini, Y., Hochberg, Y., 1995. Controlling the False Discovery Rate: A Practical and Powerful Approach to Multiple Testing. *J. R. Stat. Soc. Ser. B Methodol.* 57, 289–300. <https://doi.org/10.2307/2346101>
- Berger, A.K., Danthi, P., 2013. Reovirus activates a caspase-independent cell death pathway. *mBio* 4, e00178-00113. <https://doi.org/10.1128/mBio.00178-13>
- Berger, A.K., Hiller, B.E., Thete, D., Snyder, A.J., Perez, E., Upton, J.W., Danthi, P., 2017. Viral RNA at two stages of reovirus infection is required for the induction of necroptosis. *J. Virol.* JVI.02404-16. <https://doi.org/10.1128/JVI.02404-16>
- Berger, M.F., Hodis, E., Heffernan, T.P., Deribe, Y.L., Lawrence, M.S., Protopopov, A., Ivanova, E., Watson, I.R., Nickerson, E., Ghosh, P., Zhang, H., Zeid, R., Ren, X., Cibulskis, K., Sivachenko, A.Y., Wagle, N., Sucker, A., Sougnez, C., Onofrio, R., Ambrogio, L., Auclair, D., Fennell, T., Carter, S.L., Drier, Y., Stojanov, P., Singer, M.A., Voet, D., Jing, R., Saksena, G., Barretina, J., Ramos, A.H., Pugh, T.J., Stransky, N., Parkin, M., Winckler, W., Mahan, S., Ardlie, K., Baldwin, J., Wargo, J., Schadendorf, D., Meyerson, M., Gabriel, S.B., Golub, T.R., Wagner, S.N., Lander, E.S., Getz, G., Chin, L., Garraway, L.A., 2012. Melanoma genome sequencing reveals frequent PREX2 mutations. *Nature* 485, 502–506. <https://doi.org/10.1038/nature11071>
- Berger, R.H., Brody, J.A., 1967. Reovirus antibody patterns in Alaska. *Am. J. Epidemiol.* 86, 724–735.
- Bernstein, V., Ellard, S., Dent, S.F., Gelmon, K.A., Dhesy-Thind, S.K., Mates, M., Salim, M., Panasci, L., Song, X., Clemons, M., Tu, D., Hagerman, L.J., Seymour, L., 2017. Abstract CT131: A randomized (RCT) phase II study of oncolytic reovirus (pelareorep ) plus standard weekly paclitaxel (P) as therapy for metastatic breast cancer (mBC). *Cancer Res.* 77, CT131-CT131. <https://doi.org/10.1158/1538-7445.AM2017-CT131>
- Bhat, R., Rommelaere, J., 2013. NK-cell-dependent killing of colon carcinoma cells is mediated by natural cytotoxicity receptors (NCRs) and stimulated by parvovirus infection of target cells. *BMC Cancer* 13, 367. <https://doi.org/10.1186/1471-2407-13-367>

- Bidwell, B.N., Slaney, C.Y., Withana, N.P., Forster, S., Cao, Y., Loi, S., Andrews, D., Mikeska, T., Mangan, N.E., Samarajiva, S.A., de Weerd, N.A., Gould, J., Argani, P., Möller, A., Smyth, M.J., Anderson, R.L., Hertzog, P.J., Parker, B.S., 2012. Silencing of Irf7 pathways in breast cancer cells promotes bone metastasis through immune escape. *Nat. Med.* 18, 1224–1231. <https://doi.org/10.1038/nm.2830>
- Bierman, H.R., Crile, D.M., Dod, K.S., Kelly, K.H., Petrakis, N.L., White, L.P., Shimkin, M.B., 1953. Remissions in leukemia of childhood following acute infectious disease: staphylococcus and streptococcus, varicella, and feline panleukopenia. *Cancer* 6, 591–605.
- Bingle, L., Brown, N.J., Lewis, C.E., 2002. The role of tumour-associated macrophages in tumour progression: implications for new anticancer therapies. *J. Pathol.* 196, 254–265. <https://doi.org/10.1002/path.1027>
- Bischoff, J.R., Samuel, C.E., 1989. Mechanism of interferon action. Activation of the human p1/eIF-2 alpha protein kinase by individual reovirus s-class mRNAs: s1 mRNA is a potent activator relative to s4 mRNA. *Virology* 172, 106–115.
- Blank, C.U., Haanen, J.B., Ribas, A., Schumacher, T.N., 2016. The “cancer immunogram.” *Science* 352, 658–660. <https://doi.org/10.1126/science.aaf2834>
- Blumenthal, G.M., Pazdur, R., 2017. Approvals in 2016: the march of the checkpoint inhibitors [WWW Document]. *Nat. Rev. Clin. Oncol.* <https://doi.org/10.1038/nrclinonc.2017.15>
- Bonnet, M.C., Daurat, C., Ottone, C., Meurs, E.F., 2006. The N-terminus of PKR is responsible for the activation of the NF-kappaB signaling pathway by interacting with the IKK complex. *Cell. Signal.* 18, 1865–1875. <https://doi.org/10.1016/j.cellsig.2006.02.010>
- Boonnak, K., Dambach, K.M., Donofrio, G.C., Tassaneetrithep, B., Marovich, M.A., 2011. Cell type specificity and host genetic polymorphisms influence antibody-dependent enhancement of dengue virus infection. *J. Virol.* 85, 1671–1683. <https://doi.org/10.1128/JVI.00220-10>
- Borrego, F., Robertson, M.J., Ritz, J., Peña, J., Solana, R., 1999. CD69 is a stimulatory receptor for natural killer cell and its cytotoxic effect is blocked by CD94 inhibitory receptor. *Immunology* 97, 159–165.
- Borsa, J., Morash, B.D., Sargent, M.D., Copps, T.P., Lievaart, P.A., Szekely, J.G., 1979. Two modes of entry of reovirus particles into L cells. *J. Gen. Virol.* 45, 161–170.
- Bouziat, R., Hinterleitner, R., Brown, J.J., Stencel-Baerenwald, J.E., Ikizler, M., Mayassi, T., Meisel, M., Kim, S.M., Discepolo, V., Pruijssers, A.J., Ernest, J.D., Iskarpatyoti, J.A., Costes, L.M.M., Lawrence, I., Palanski, B.A., Varma, M., Zurenski, M.A., Khomandiak, S., McAllister, N., Aravamudhan, P., Boehme, K.W., Hu, F., Samsom, J.N., Reinecker, H.-C., Kupfer, S.S., Guandalini, S., Semrad, C.E., Abadie, V., Khosla, C., Barreiro, L.B., Xavier, R.J., Ng, A., Dermody, T.S., Jabri, B., 2017. Reovirus infection triggers inflammatory responses to dietary antigens and development of celiac disease. *Science* 356, 44–50. <https://doi.org/10.1126/science.aah5298>

- Boyette, L.B., Macedo, C., Hadi, K., Elinoff, B.D., Walters, J.T., Ramaswami, B., Chalasani, G., Taboas, J.M., Lakkis, F.G., Metes, D.M., 2017. Phenotype, function, and differentiation potential of human monocyte subsets. *PLOS ONE* 12, e0176460. <https://doi.org/10.1371/journal.pone.0176460>
- Brandenburg, B., Lee, L.Y., Lakadamyali, M., Rust, M.J., Zhuang, X., Hogle, J.M., 2007. Imaging Poliovirus Entry in Live Cells. *PLOS Biol.* 5, e183. <https://doi.org/10.1371/journal.pbio.0050183>
- Braun, D., Caramalho, I., Demengeot, J., 2002. IFN- $\alpha/\beta$  enhances BCR-dependent B cell responses. *Int. Immunol.* 14, 411–419. <https://doi.org/10.1093/intimm/14.4.411>
- Breitbach, C.J., Burke, J., Jonker, D., Stephenson, J., Haas, A.R., Chow, L.Q.M., Nieva, J., Hwang, T.-H., Moon, A., Patt, R., Pelusio, A., Le Boeuf, F., Burns, J., Evgin, L., De Silva, N., Cvancic, S., Robertson, T., Je, J.-E., Lee, Y.-S., Parato, K., Diallo, J.-S., Fenster, A., Daneshmand, M., Bell, J.C., Kirn, D.H., 2011. Intravenous delivery of a multi-mechanistic cancer-targeted oncolytic poxvirus in humans. *Nature* 477, 99–102. <https://doi.org/10.1038/nature10358>
- Brennan, A.J., Chia, J., Trapani, J.A., Voskoboinik, I., 2010. Perforin deficiency and susceptibility to cancer. *Cell Death Differ.* 17, 607. <https://doi.org/10.1038/cdd.2009.212>
- Broering, T.J., Kim, J., Miller, C.L., Piggott, C.D.S., Dinoso, J.B., Nibert, M.L., Parker, J.S.L., 2004. Reovirus nonstructural protein mu NS recruits viral core surface proteins and entering core particles to factory-like inclusions. *J. Virol.* 78, 1882–1892.
- Bronte, V., Zanovello, P., 2005. Regulation of immune responses by L-arginine metabolism. *Nat. Rev. Immunol.* 5, 641–654. <https://doi.org/10.1038/nri1668>
- Brownell, J., Bruckner, J., Wagoner, J., Thomas, E., Loo, Y.-M., Gale, M., Liang, T.J., Polyak, S.J., 2014. Direct, interferon-independent activation of the CXCL10 promoter by NF- $\kappa$ B and interferon regulatory factor 3 during hepatitis C virus infection. *J. Virol.* 88, 1582–1590. <https://doi.org/10.1128/JVI.02007-13>
- Brunner, K.T., Mael, J., Cerottini, J.C., Chapuis, B., 1968. Quantitative assay of the lytic action of immune lymphoid cells on 51-Cr-labelled allogeneic target cells in vitro; inhibition by isoantibody and by drugs. *Immunology* 14, 181–196.
- Burke, J.M., Lamm, D.L., Meng, M.V., Nemunaitis, J.J., Stephenson, J.J., Arseneau, J.C., Aimi, J., Lerner, S., Yeung, A.W., Kazarian, T., Maslyar, D.J., McKiernan, J.M., 2012. A first in human phase 1 study of CG0070, a GM-CSF expressing oncolytic adenovirus, for the treatment of nonmuscle invasive bladder cancer. *J. Urol.* 188, 2391–2397. <https://doi.org/10.1016/j.juro.2012.07.097>
- Burnet, F.M., 1970. The concept of immunological surveillance. *Prog. Exp. Tumor Res.* 13, 1–27.
- Burnet, F.M., Fenner, F., 1949. *The Production of Antibodies* (2nd Edition): 142 pp. Macmillan and Co., Ltd., Melbourne, Australia, 1949. *J. Immunol.* 66, 485–486.
- Burstin, S.J., Brandriss, M.W., Schlesinger, J.J., 1983. Infection of a macrophage-like cell line, P388D1 with reovirus; effects of immune ascitic fluids and monoclonal antibodies on neutralization and on enhancement of viral growth. *J. Immunol. Baltim. Md* 1950 130, 2915–2919.

- Byrd, D., Shepherd, N., Lan, J., Hu, N., Amet, T., Yang, K., Desai, M., Yu, Q., 2014. Primary human macrophages serve as vehicles for vaccinia virus replication and dissemination. *J. Virol.* 88, 6819–6831. <https://doi.org/10.1128/JVI.03726-13>
- Calvo, E., Gil-Martin, M., Machiels, J.-P.H., Rottey, S., Cubillo, A., Salazar, R., Mardjuadi, F.I., Geboes, K.P., Ellis, C., Beadle, J.W., Blanc, C., 2014. A first-in-class, first-in-human phase I study of enadenotucirev, an oncolytic Ad11/Ad3 chimeric group B adenovirus, administered intravenously in patients with metastatic epithelial tumors. *J. Clin. Oncol.* 32, 3103–3103. [https://doi.org/10.1200/jco.2014.32.15\\_suppl.3103](https://doi.org/10.1200/jco.2014.32.15_suppl.3103)
- Cameron, F., Whiteside, G., Perry, C., 2011. Ipilimumab: first global approval. *Drugs* 71, 1093–1104. <https://doi.org/10.2165/11594010-000000000-00000>
- Campbell, A.C., Wiernik, G., Wood, J., Hersey, P., Waller, C.A., MacLennan, I.C.M., 1976. Characteristics of the lymphopenia induced by radiotherapy. *Clin. Exp. Immunol.* 23, 200–208.
- Cashdollar, L.W., Chmelo, R.A., Wiener, J.R., Joklik, W.K., 1985. Sequences of the S1 genes of the three serotypes of reovirus. *Proc. Natl. Acad. Sci. U. S. A.* 82, 24–28.
- Cervantes-Barragán, L., Kalinke, U., Züst, R., König, M., Reizis, B., López-Macías, C., Thiel, V., Ludewig, B., 2009. Type I IFN-mediated protection of macrophages and dendritic cells secures control of murine coronavirus infection. *J. Immunol. Baltim. Md* 1950 182, 1099–1106.
- Chandran, K., Farsetta, D.L., Nibert, M.L., 2002. Strategy for nonenveloped virus entry: a hydrophobic conformer of the reovirus membrane penetration protein micro 1 mediates membrane disruption. *J. Virol.* 76, 9920–9933.
- Chandran, K., Zhang, X., Olson, N.H., Walker, S.B., Chappell, J.D., Dermody, T.S., Baker, T.S., Nibert, M.L., 2001. Complete in vitro assembly of the reovirus outer capsid produces highly infectious particles suitable for genetic studies of the receptor-binding protein. *J. Virol.* 75, 5335–5342. <https://doi.org/10.1128/JVI.75.11.5335-5342.2001>
- Chang, A.E., Karnell, L.H., Menck, H.R., 1998. The National Cancer Data Base report on cutaneous and noncutaneous melanoma: a summary of 84,836 cases from the past decade. The American College of Surgeons Commission on Cancer and the American Cancer Society. *Cancer* 83, 1664–1678.
- Chang, K.J., Senzer, N.N., Binmoeller, K., Goldsweig, H., Coffin, R., 2012. Phase I dose-escalation study of talimogene laherparepvec (T-VEC) for advanced pancreatic cancer (ca). *J. Clin. Oncol.* 30, e14546–e14546. [https://doi.org/10.1200/jco.2012.30.15\\_suppl.e14546](https://doi.org/10.1200/jco.2012.30.15_suppl.e14546)
- Chang, Y., Barrett, J.H., Bishop, D.T., Armstrong, B.K., Bataille, V., Bergman, W., Berwick, M., Bracci, P.M., Elwood, J.M., Ernstoff, M.S., Gallagher, R.P., Green, A.C., Gruis, N.A., Holly, E.A., Ingvar, C., Kanetsky, P.A., Karagas, M.R., Lee, T.K., Le Marchand, L., Mackie, R.M., Olsson, H., Østerlind, A., Rebbeck, T.R., Sasieni, P., Siskind, V., Swerdlow, A.J., Titus-Ernstoff, L., Zens, M.S., Newton-Bishop, J.A., 2009. Sun exposure and melanoma risk at different latitudes: a pooled analysis of 5700 cases and 7216 controls. *Int. J. Epidemiol.* 38, 814–830. <https://doi.org/10.1093/ije/dyp166>

- Chapman, P.B., Hauschild, A., Robert, C., Haanen, J.B., Ascierto, P., Larkin, J., Dummer, R., Garbe, C., Testori, A., Maio, M., Hogg, D., Lorigan, P., Lebbe, C., Jouary, T., Schadendorf, D., Ribas, A., O'Day, S.J., Sosman, J.A., Kirkwood, J.M., Eggermont, A.M.M., Dreno, B., Nolop, K., Li, J., Nelson, B., Hou, J., Lee, R.J., Flaherty, K.T., McArthur, G.A., BRIM-3 Study Group, 2011. Improved survival with vemurafenib in melanoma with BRAF V600E mutation. *N. Engl. J. Med.* 364, 2507–2516. <https://doi.org/10.1056/NEJMoa1103782>
- Chappell, J.D., Duong, J.L., Wright, B.W., Dermody, T.S., 2000. Identification of carbohydrate-binding domains in the attachment proteins of type 1 and type 3 reoviruses. *J. Virol.* 74, 8472–8479.
- Chareonsirisuthigul, T., Kalayanaroj, S., Ubol, S., 2007. Dengue virus (DENV) antibody-dependent enhancement of infection upregulates the production of anti-inflammatory cytokines, but suppresses anti-DENV free radical and pro-inflammatory cytokine production, in THP-1 cells. *J. Gen. Virol.* 88, 365–375. <https://doi.org/10.1099/vir.0.82537-0>
- Chauhan, A.K., Chen, C., Moore, T.L., DiPaolo, R.J., 2015. Induced Expression of FcγRIIIa (CD16a) on CD4+ T Cells Triggers Generation of IFN-γhigh Subset. *J. Biol. Chem.* 290, 5127–5140. <https://doi.org/10.1074/jbc.M114.599266>
- Chen, E.Y., Tan, C.M., Kou, Y., Duan, Q., Wang, Z., Meirelles, G.V., Clark, N.R., Ma'ayan, A., 2013. Enrichr: interactive and collaborative HTML5 gene list enrichment analysis tool. *BMC Bioinformatics* 14, 128. <https://doi.org/10.1186/1471-2105-14-128>
- Chen, W., Jin, W., Hardegen, N., Lei, K.-J., Li, L., Marinos, N., McGrady, G., Wahl, S.M., 2003. Conversion of peripheral CD4+CD25- naive T cells to CD4+CD25+ regulatory T cells by TGF-beta induction of transcription factor Foxp3. *J. Exp. Med.* 198, 1875–1886. <https://doi.org/10.1084/jem.20030152>
- Chen, Y., Yu, D.C., Charlton, D., Henderson, D.R., 2000. Pre-existent adenovirus antibody inhibits systemic toxicity and antitumor activity of CN706 in the nude mouse LNCaP xenograft model: implications and proposals for human therapy. *Hum. Gene Ther.* 11, 1553–1567. <https://doi.org/10.1089/10430340050083289>
- Chen, Y.T., Scanlan, M.J., Sahin, U., Türeci, O., Gure, A.O., Tsang, S., Williamson, B., Stockert, E., Pfreundschuh, M., Old, L.J., 1997. A testicular antigen aberrantly expressed in human cancers detected by autologous antibody screening. *Proc. Natl. Acad. Sci. U. S. A.* 94, 1914–1918.
- Chesney, J., Awasthi, S., Curti, B., Hutchins, L., Linette, G., Triozzi, P., Tan, M.C.B., Brown, R.E., Nemunaitis, J., Whitman, E., Windham, C., Lutzky, J., Downey, G.F., Batty, N., Amatruda, T., 2018. Phase IIIb safety results from an expanded-access protocol of talimogene laherparepvec for patients with unresected, stage IIIB–IVM1c melanoma. *Melanoma Res.* 28, 44. <https://doi.org/10.1097/CMR.0000000000000399>
- Chesney, J., Puzanov, I., Collichio, F., Singh, P., Milhem, M.M., Glaspy, J., Hamid, O., Ross, M., Friedlander, P., Garbe, C., Logan, T.F., Hauschild, A., Lebbé, C., Chen, L., Kim, J.J., Gansert, J., Andtbacka, R.H.I., Kaufman, H.L., 2017. Randomized, Open-Label Phase II Study Evaluating the Efficacy and Safety of Talimogene Laherparepvec in Combination With Ipilimumab Versus Ipilimumab Alone in

- Patients With Advanced, Unresectable Melanoma. *J. Clin. Oncol.* JCO.2017.73.7379. <https://doi.org/10.1200/JCO.2017.73.7379>
- Chua, K.B., Cramer, G., Hyatt, A., Yu, M., Tompang, M.R., Rosli, J., McEachern, J., Cramer, S., Kumarasamy, V., Eaton, B.T., Wang, L.-F., 2007. A previously unknown reovirus of bat origin is associated with an acute respiratory disease in humans. *Proc. Natl. Acad. Sci. U. S. A.* 104, 11424–11429. <https://doi.org/10.1073/pnas.0701372104>
- Chuk, M.K., Chang, J.T., Theoret, M.R., Sampene, E., He, K., Weis, S.L., Helms, W.S., Jin, R., Li, H., Yu, J., Zhao, H., Zhao, L., Paciga, M., Schmiel, D., Rawat, R., Keegan, P., Pazdur, R., 2017. FDA Approval Summary: Accelerated Approval of Pembrolizumab for Second-Line Treatment of Metastatic Melanoma. *Clin. Cancer Res. Off. J. Am. Assoc. Cancer Res.* 23, 5666–5670. <https://doi.org/10.1158/1078-0432.CCR-16-0663>
- Cichorek, M., Wachulska, M., Stasiewicz, A., Tymińska, A., 2013. Skin melanocytes: biology and development. *Adv. Dermatol. Allergol. Dermatol. Alergol.* 30, 30–41. <https://doi.org/10.5114/pdia.2013.33376>
- Clarke, P., Meintzer, S.M., Gibson, S., Widmann, C., Garrington, T.P., Johnson, G.L., Tyler, K.L., 2000. Reovirus-induced apoptosis is mediated by TRAIL. *J. Virol.* 74, 8135–8139.
- Clarke, P., Richardson-Burns, S.M., DeBiasi, R.L., Tyler, K.L., 2005. Mechanisms of Apoptosis During Reovirus Infection. *Curr. Top. Microbiol. Immunol.* 289, 1–24.
- Clements, D.R., Sterea, A.M., Kim, Y., Helson, E., Dean, C.A., Nunokawa, A., Coyle, K.M., Sharif, T., Marcato, P., Gujar, S.A., Lee, P.W.K., 2015. Newly recruited CD11b+, GR-1+, Ly6C(high) myeloid cells augment tumor-associated immunosuppression immediately following the therapeutic administration of oncolytic reovirus. *J. Immunol. Baltim. Md 1950* 194, 4397–4412. <https://doi.org/10.4049/jimmunol.1402132>
- Coffey, M.C., 1998. Reovirus Therapy of Tumors with Activated Ras Pathway. *Science* 282, 1332–1334. <https://doi.org/10.1126/science.282.5392.1332>
- Cohen, C., Zavala-Pompa, A., Sequeira, J.H., Shoji, M., Sexton, D.G., Cotsonis, G., Cerimele, F., Govindarajan, B., Macaron, N., Arbiser, J.L., 2002. Mitogen-activated protein kinase activation is an early event in melanoma progression. *Clin. Cancer Res. Off. J. Am. Assoc. Cancer Res.* 8, 3728–3733.
- Cohen, S.N., Halstead, S.B., 1966. Shock associated with dengue infection. I. Clinical and physiologic manifestations of dengue hemorrhagic fever in Thailand, 1964. *J. Pediatr.* 68, 448–456.
- Cohn, D.E., Sill, M.W., Walker, J.L., O'Malley, D., Nagel, C.I., Rutledge, T.L., Bradley, W., Richardson, D.L., Moxley, K.M., Aghajanian, C., 2017. Randomized phase IIB evaluation of weekly paclitaxel versus weekly paclitaxel with oncolytic reovirus (Reolysin®) in recurrent ovarian, tubal, or peritoneal cancer: An NRG Oncology/Gynecologic Oncology Group study. *Gynecol. Oncol.* 146, 477–483. <https://doi.org/10.1016/j.ygyno.2017.07.135>
- Cole, C., Qiao, J., Kottke, T., Diaz, R.M., Ahmed, A., Sanchez-Perez, L., Brunn, G., Thompson, J., Chester, J., Vile, R.G., 2005. Tumor-targeted, systemic delivery of

- therapeutic viral vectors using hitchhiking on antigen-specific T cells. *Nat. Med.* 11, 1073–1081. <https://doi.org/10.1038/nm1297>
- Coley, W.B., 1928. THE DIFFERENTIAL DIAGNOSIS OF SARCOMA OF THE LONG BONES. *JBJS* 10, 420.
- Coley, W.B., 1910. The Treatment of Inoperable Sarcoma by Bacterial Toxins (the Mixed Toxins of the *Streptococcus erysipelas* and the *Bacillus prodigiosus*). *Proc. R. Soc. Med.* 3, 1–48.
- Coley, W.B., 1891. II. Contribution to the Knowledge of Sarcoma. *Ann. Surg.* 14, 199–220.
- Comins, C., Spicer, J., Protheroe, A., Roulstone, V., Twigger, K., White, C.M., Vile, R., Melcher, A., Coffey, M.C., Mettinger, K.L., Nuovo, G., Cohn, D.E., Phelps, M., Harrington, K.J., Pandha, H.S., 2010. REO-10: a phase I study of intravenous reovirus and docetaxel in patients with advanced cancer. *Clin. Cancer Res. Off. J. Am. Assoc. Cancer Res.* 16, 5564–5572. <https://doi.org/10.1158/1078-0432.CCR-10-1233>
- Connolly, J.L., Barton, E.S., Dermody, T.S., 2001. Reovirus binding to cell surface sialic acid potentiates virus-induced apoptosis. *J. Virol.* 75, 4029–4039. <https://doi.org/10.1128/JVI.75.9.4029-4039.2001>
- Coombs, K.M., 1998. Stoichiometry of reovirus structural proteins in virus, ISVP, and core particles. *Virology* 243, 218–228. <https://doi.org/10.1006/viro.1998.9061>
- Coulie, P.G., Brichard, V., Pel, A.V., Wölfel, T., Schneider, J., Traversari, C., Mattei, S., Plaen, E.D., Lurquin, C., Szikora, J.P., Renauld, J.C., Boon, T., 1994. A new gene coding for a differentiation antigen recognized by autologous cytolytic T lymphocytes on HLA-A2 melanomas. *J. Exp. Med.* 180, 35–42. <https://doi.org/10.1084/jem.180.1.35>
- Croci, D.O., Zacarías Fluck, M.F., Rico, M.J., Matar, P., Rabinovich, G.A., Scharovsky, O.G., 2007. Dynamic cross-talk between tumor and immune cells in orchestrating the immunosuppressive network at the tumor microenvironment. *Cancer Immunol. Immunother.* CII 56, 1687–1700. <https://doi.org/10.1007/s00262-007-0343-y>
- Cros, J., Cagnard, N., Woollard, K., Patey, N., Zhang, S.-Y., Senechal, B., Puel, A., Biswas, S.K., Moshous, D., Picard, C., Jais, J.-P., D’Cruz, D., Casanova, J.-L., Trouillet, C., Geissmann, F., 2010. Human CD14<sup>dim</sup> Monocytes Patrol and Sense Nucleic Acids and Viruses via TLR7 and TLR8 Receptors. *Immunity* 33, 375–386. <https://doi.org/10.1016/j.immuni.2010.08.012>
- Crowson, A.N., Magro, C.M., Jr, M.C.M., 2006. Prognosticators of melanoma, the melanoma report, and the sentinel lymph node. *Mod. Pathol.* 19, S71. <https://doi.org/10.1038/modpathol.3800517>
- Curiel, T.J., Coukos, G., Zou, L., Alvarez, X., Cheng, P., Mottram, P., Evdemon-Hogan, M., Conejo-Garcia, J.R., Zhang, L., Burow, M., Zhu, Y., Wei, S., Kryczek, I., Daniel, B., Gordon, A., Myers, L., Lackner, A., Disis, M.L., Knutson, K.L., Chen, L., Zou, W., 2004. Specific recruitment of regulatory T cells in ovarian carcinoma fosters immune privilege and predicts reduced survival. *Nat. Med.* 10, 942–949. <https://doi.org/10.1038/nm1093>

- Curiel-Lewandrowski, C., Chen, S.C., Swetter, S.M., 2012. Screening and Prevention Measures for Melanoma: Is There a Survival Advantage? *Curr. Oncol. Rep.* 14, 458–467. <https://doi.org/10.1007/s11912-012-0256-6>
- Curti, B.D., Richards, J.M., Hallmeyer, S., Faries, M.B., Andtbacka, R.H.I., Daniels, G.A., Grose, M., Shafren, D., 2017. Activity of a novel immunotherapy combination of intralesional Coxsackievirus A21 and systemic ipilimumab in advanced melanoma patients previously treated with anti-PD1 blockade therapy. *J. Clin. Oncol.* 35, 3014–3014. [https://doi.org/10.1200/JCO.2017.35.15\\_suppl.3014](https://doi.org/10.1200/JCO.2017.35.15_suppl.3014)
- Da Costa, X.J., Brockman, M.A., Alicot, E., Ma, M., Fischer, M.B., Zhou, X., Knipe, D.M., Carroll, M.C., 1999. Humoral response to herpes simplex virus is complement-dependent. *Proc. Natl. Acad. Sci. U. S. A.* 96, 12708–12712.
- Dai, M.H., Liu, S.L., Chen, N.G., Zhang, T.P., You, L., Q Zhang, F., Chou, T.C., Szalay, A.A., Fong, Y., Zhao, Y.P., 2014. Oncolytic vaccinia virus in combination with radiation shows synergistic antitumor efficacy in pancreatic cancer. *Cancer Lett.* 344, 282–290. <https://doi.org/10.1016/j.canlet.2013.11.007>
- Danson, S., Woll, P., Edwards, J., Blyth, K., Fisher, P., Roman, J., Simpson, K., Spavin, R., Learmonth, K., Conner, J., 2017. 366P Oncolytic herpesvirus therapy for mesothelioma: A phase I/IIa trial of intrapleural administration of HSV1716 (NCT01721018). *Ann. Oncol.* 28. <https://doi.org/10.1093/annonc/mdx367.001>
- Danthi, P., Hansberger, M.W., Campbell, J.A., Forrest, J.C., Dermody, T.S., 2006. JAM-A-Independent, Antibody-Mediated Uptake of Reovirus into Cells Leads to Apoptosis. *J. Virol.* 80, 1261–1270. <https://doi.org/10.1128/JVI.80.3.1261-1270.2006>
- Davies, H., Bignell, G.R., Cox, C., Stephens, P., Edkins, S., Clegg, S., Teague, J., Woffendin, H., Garnett, M.J., Bottomley, W., Davis, N., Dicks, E., Ewing, R., Floyd, Y., Gray, K., Hall, S., Hawes, R., Hughes, J., Kosmidou, V., Menzies, A., Mould, C., Parker, A., Stevens, C., Watt, S., Hooper, S., Wilson, R., Jayatilake, H., Gusterson, B.A., Cooper, C., Shipley, J., Hargrave, D., Pritchard-Jones, K., Maitland, N., Chenevix-Trench, G., Riggins, G.J., Bigner, D.D., Palmieri, G., Cossu, A., Flanagan, A., Nicholson, A., Ho, J.W.C., Leung, S.Y., Yuen, S.T., Weber, B.L., Seigler, H.F., Darrow, T.L., Paterson, H., Marais, R., Marshall, C.J., Wooster, R., Stratton, M.R., Futreal, P.A., 2002. Mutations of the BRAF gene in human cancer. *Nature* 417, 949–954. <https://doi.org/10.1038/nature00766>
- Davis, B.D., Dulbecco, R., Eisen, H., Wood, W., 1972. Nature of viruses, in: *Microbiology*. Harper and Row, New York, pp. 1044–1053.
- Daya-Grosjean, L., Sarasin, A., 2005. The role of UV induced lesions in skin carcinogenesis: an overview of oncogene and tumor suppressor gene modifications in xeroderma pigmentosum skin tumors. *Mutat. Res.* 571, 43–56. <https://doi.org/10.1016/j.mrfmmm.2004.11.013>
- de Haro, C., Méndez, R., Santoyo, J., 1996. The eIF-2alpha kinases and the control of protein synthesis. *FASEB J. Off. Publ. Fed. Am. Soc. Exp. Biol.* 10, 1378–1387.
- De Munck, J., Binks, A., McNeish, I.A., Aerts, J.L., 2017. Oncolytic virus-induced cell death and immunity: a match made in heaven? *J. Leukoc. Biol.* 102, 631–643. <https://doi.org/10.1189/jlb.5RU0117-040R>

- de Veer, M.J., Holko, M., Frevel, M., Walker, E., Der, S., Paranjape, J.M., Silverman, R.H., Williams, B.R., 2001. Functional classification of interferon-stimulated genes identified using microarrays. *J. Leukoc. Biol.* 69, 912–920.
- Deb, A., Haque, S.J., Mogensen, T., Silverman, R.H., Williams, B.R., 2001. RNA-dependent protein kinase PKR is required for activation of NF-kappa B by IFN-gamma in a STAT1-independent pathway. *J. Immunol. Baltim. Md 1950* 166, 6170–6180.
- Decision Resources Group, 2017. Malignant Melanoma landscape and forecast.
- del Campo, A.B., Kyte, J.A., Carretero, J., Zinchencko, S., Méndez, R., González-Aseguinolaza, G., Ruiz-Cabello, F., Aamdal, S., Gaudernack, G., Garrido, F., Aptsiauri, N., 2014. Immune escape of cancer cells with beta2-microglobulin loss over the course of metastatic melanoma. *Int. J. Cancer* 134, 102–113. <https://doi.org/10.1002/ijc.28338>
- Delacroix, D.L., Dive, C., Rambaud, J.C., Vaerman, J.P., 1982. IgA subclasses in various secretions and in serum. *Immunology* 47, 383–385.
- Dennis, L.K., Vanbeek, M.J., Beane Freeman, L.E., Smith, B.J., Dawson, D.V., Coughlin, J.A., 2008. Sunburns and risk of cutaneous melanoma: does age matter? A comprehensive meta-analysis. *Ann. Epidemiol.* 18, 614–627. <https://doi.org/10.1016/j.annepidem.2008.04.006>
- DeSantis, C.E., Lin, C.C., Mariotto, A.B., Siegel, R.L., Stein, K.D., Kramer, J.L., Alteri, R., Robbins, A.S., Jemal, A., 2014. Cancer treatment and survivorship statistics, 2014. *CA. Cancer J. Clin.* 64, 252–271. <https://doi.org/10.3322/caac.21235>
- DeWeese, T.L., van der Poel, H., Li, S., Mikhak, B., Drew, R., Goemann, M., Hamper, U., DeJong, R., Detorie, N., Rodriguez, R., Haulk, T., DeMarzo, A.M., Piantadosi, S., Yu, D.C., Chen, Y., Henderson, D.R., Carducci, M.A., Nelson, W.G., Simons, J.W., 2001. A phase I trial of CV706, a replication-competent, PSA selective oncolytic adenovirus, for the treatment of locally recurrent prostate cancer following radiation therapy. *Cancer Res.* 61, 7464–7472.
- Dhomen, N., Marais, R., 2009. BRAF signaling and targeted therapies in melanoma. *Hematol. Oncol. Clin. North Am.* 23, 529–545, ix. <https://doi.org/10.1016/j.hoc.2009.04.001>
- Dias, J.D., Hemminki, O., Diaconu, I., Hirvonen, M., Bonetti, A., Guse, K., Escutenaire, S., Kanerva, A., Pesonen, S., Löskog, A., Cerullo, V., Hemminki, A., 2012. Targeted cancer immunotherapy with oncolytic adenovirus coding for a fully human monoclonal antibody specific for CTLA-4. *Gene Ther.* 19, 988–998. <https://doi.org/10.1038/gt.2011.176>
- Dias, S. da R., Salmonson, T., Zwieten-Boot, B. van, Jonsson, B., Marchetti, S., Schellens, J.H.M., Giuliani, R., Pignatti, F., 2013. The European Medicines Agency review of vemurafenib (Zelboraf®) for the treatment of adult patients with BRAF V600 mutation-positive unresectable or metastatic melanoma: Summary of the scientific assessment of the Committee for Medicinal Products for Human Use. *Eur. J. Cancer* 49, 1654–1661. <https://doi.org/10.1016/j.ejca.2013.01.015>
- Diaz, R.M., Galivo, F., Kottke, T., Wongthida, P., Qiao, J., Thompson, J., Valdes, M., Barber, G., Vile, R.G., 2007. Oncolytic immunovirotherapy for melanoma using

- vesicular stomatitis virus. *Cancer Res.* 67, 2840–2848.  
<https://doi.org/10.1158/0008-5472.CAN-06-3974>
- Diebold, S.S., Montoya, M., Unger, H., Alexopoulou, L., Roy, P., Haswell, L.E., Al-Shamkhani, A., Flavell, R., Borrow, P., Reis e Sousa, C., 2003. Viral infection switches non-plasmacytoid dendritic cells into high interferon producers. *Nature* 424, 324–328. <https://doi.org/10.1038/nature01783>
- Dispenzieri, A., Tong, C., LaPlant, B., Lacy, M.Q., Laumann, K., Dingli, D., Zhou, Y., Federspiel, M.J., Gertz, M.A., Hayman, S., Buadi, F., O'Connor, M., Lowe, V.J., Peng, K.-W., Russell, S.J., 2017. Phase I trial of systemic administration of Edmonston strain of measles virus genetically engineered to express the sodium iodide symporter in patients with recurrent or refractory multiple myeloma. *Leukemia* 31, 2791–2798. <https://doi.org/10.1038/leu.2017.120>
- Dixit, E., Boulant, S., Zhang, Y., Lee, A.S.Y., Odendall, C., Shum, B., Hacohen, N., Chen, Z.J., Whelan, S.P., Fransen, M., Nibert, M.L., Superti-Furga, G., Kagan, J.C., 2010. Peroxisomes are signaling platforms for antiviral innate immunity. *Cell* 141, 668–681. <https://doi.org/10.1016/j.cell.2010.04.018>
- Dmitriev, I., Krasnykh, V., Miller, C.R., Wang, M., Kashentseva, E., Mikheeva, G., Belousova, N., Curiel, D.T., 1998. An Adenovirus Vector with Genetically Modified Fibers Demonstrates Expanded Tropism via Utilization of a Coxsackievirus and Adenovirus Receptor-Independent Cell Entry Mechanism. *J. Virol.* 72, 9706–9713.
- Dobbelstein, M., Shenk, T., 1996. Protection against apoptosis by the vaccinia virus SPI-2 (B13R) gene product. *J. Virol.* 70, 6479–6485.
- Dock, G., 1904. The Influence Of Complicating Diseases Upon Leukæmia. \*. *Am. J. Med. Sci.* 127, 563–592.
- Dong, H., Strome, S.E., Salomao, D.R., Tamura, H., Hirano, F., Flies, D.B., Roche, P.C., Lu, J., Zhu, G., Tamada, K., Lennon, V.A., Celis, E., Chen, L., 2002. Tumor-associated B7-H1 promotes T-cell apoptosis: a potential mechanism of immune evasion. *Nat. Med.* 8, 793–800. <https://doi.org/10.1038/nm730>
- Dong, Y., Sun, Q., Zhang, X., 2016. PD-1 and its ligands are important immune checkpoints in cancer. *Oncotarget* 8, 2171–2186.  
<https://doi.org/10.18632/oncotarget.13895>
- Doniņa, S., Strēle, I., Proboka, G., Auziņš, J., Alberts, P., Jonsson, B., Venskus, D., Muceniece, A., 2015. Adapted ECHO-7 virus Rigvir immunotherapy (oncolytic virotherapy) prolongs survival in melanoma patients after surgical excision of the tumour in a retrospective study. *Melanoma Res.* 25, 421–426.  
<https://doi.org/10.1097/CMR.000000000000180>
- Dons'koi, B.V., Chernyshov, V.P., Osypchuk, D.V., 2011. Measurement of NK activity in whole blood by the CD69 up-regulation after co-incubation with K562, comparison with NK cytotoxicity assays and CD107a degranulation assay. *J. Immunol. Methods* 372, 187–195. <https://doi.org/10.1016/j.jim.2011.07.016>
- Donzé, O., Dostie, J., Sonenberg, N., 1999. Regulatable expression of the interferon-induced double-stranded RNA dependent protein kinase PKR induces apoptosis and fas receptor expression. *Virology* 256, 322–329.  
<https://doi.org/10.1006/viro.1999.9618>

- Douville, R.N., Su, R.-C., Coombs, K.M., Simons, F.E.R., HayGlass, K.T., 2008. Reovirus Serotypes Elicit Distinctive Patterns of Recall Immunity in Humans. *J. Virol.* 82, 7515–7523. <https://doi.org/10.1128/JVI.00464-08>
- Duncan, M.R., Stanish, S.M., Cox, D.C., 1978. Differential sensitivity of normal and transformed human cells to reovirus infection. *J. Virol.* 28, 444–449.
- Dunn, G.P., Koebel, C.M., Schreiber, R.D., 2006. Interferons, immunity and cancer immunoediting. *Nat. Rev. Immunol.* 6, 836–848. <https://doi.org/10.1038/nri1961>
- Durbin, A.P., Vargas, M.J., Wanionek, K., Hammond, S.N., Gordon, A., Rocha, C., Balmaseda, A., Harris, E., 2008. Phenotyping of peripheral blood mononuclear cells during acute dengue illness demonstrates infection and increased activation of monocytes in severe cases compared to classic dengue fever. *Virology* 376, 429–435. <https://doi.org/10.1016/j.virol.2008.03.028>
- Ebert, D.H., Deussing, J., Peters, C., Dermody, T.S., 2002. Cathepsin L and cathepsin B mediate reovirus disassembly in murine fibroblast cells. *J. Biol. Chem.* 277, 24609–24617. <https://doi.org/10.1074/jbc.M201107200>
- Edelmann, K.H., Richardson-Burns, S., Alexopoulou, L., Tyler, K.L., Flavell, R.A., Oldstone, M.B.A., 2004. Does Toll-like receptor 3 play a biological role in virus infections? *Virology* 322, 231–238. <https://doi.org/10.1016/j.virol.2004.01.033>
- Eggermont, A.M.M., Chiarion-Sileni, V., Grob, J.-J., Dummer, R., Wolchok, J.D., Schmidt, H., Hamid, O., Robert, C., Ascierto, P.A., Richards, J.M., Lebbé, C., Ferraresi, V., Smylie, M., Weber, J.S., Maio, M., Bastholt, L., Mortier, L., Thomas, L., Tahir, S., Hauschild, A., Hassel, J.C., Hodi, F.S., Taitt, C., de Pril, V., de Schaetzen, G., Suci, S., Testori, A., 2016. Prolonged Survival in Stage III Melanoma with Ipilimumab Adjuvant Therapy. *N. Engl. J. Med.* 375, 1845–1855. <https://doi.org/10.1056/NEJMoa1611299>
- Eggermont, A.M.M., Robert, C., 2011. New drugs in melanoma: it's a whole new world. *Eur. J. Cancer Oxf. Engl.* 1990 47, 2150–2157. <https://doi.org/10.1016/j.ejca.2011.06.052>
- Ehrlich, M., Boll, W., Van Oijen, A., Hariharan, R., Chandran, K., Nibert, M.L., Kirchhausen, T., 2004. Endocytosis by random initiation and stabilization of clathrin-coated pits. *Cell* 118, 591–605. <https://doi.org/10.1016/j.cell.2004.08.017>
- Ehrlich, P., 1909. Über den jetzigen Stand der Chemotherapie. *Berichte Dtsch. Chem. Ges.* 42, 17–47. <https://doi.org/10.1002/cber.19090420105>
- Eigentler, T.K., Caroli, U.M., Radny, P., Garbe, C., 2003. Palliative therapy of disseminated malignant melanoma: a systematic review of 41 randomised clinical trials. *Lancet Oncol.* 4, 748–759. [https://doi.org/10.1016/S1470-2045\(03\)01280-4](https://doi.org/10.1016/S1470-2045(03)01280-4)
- Eisenstein, S., Coakley, B.A., Briley-Saebo, K., Ma, G., Chen, H.-M., Meseck, M., Ward, S., Divino, C., Woo, S., Chen, S.-H., Pan, P.-Y., 2013. Myeloid-derived suppressor cells as a vehicle for tumor-specific oncolytic viral therapy. *Cancer Res.* 73, 5003–5015. <https://doi.org/10.1158/0008-5472.CAN-12-1597>
- El-Sherbiny, Y.M., Holmes, T.D., Wetherill, L.F., Black, E.V.I., Wilson, E.B., Phillips, S.L., Scott, G.B., Adair, R.A., Dave, R., Scott, K.J., Morgan, R.S.M., Coffey, M., Toogood, G.J., Melcher, A.A., Cook, G.P., 2015. Controlled infection with a

- therapeutic virus defines the activation kinetics of human natural killer cells in vivo. *Clin. Exp. Immunol.* 180, 98–107. <https://doi.org/10.1111/cei.12562>
- Elwood, J.M., Jopson, J., 1997. Melanoma and sun exposure: an overview of published studies. *Int. J. Cancer* 73, 198–203.
- Erdmann, F., Lortet-Tieulent, J., Schüz, J., Zeeb, H., Greinert, R., Breitbart, E.W., Bray, F., 2013. International trends in the incidence of malignant melanoma 1953–2008—are recent generations at higher or lower risk? *Int. J. Cancer* 132, 385–400. <https://doi.org/10.1002/ijc.27616>
- Errington, F., Steele, L., Prestwich, R., Harrington, K.J., Pandha, H.S., Vidal, L., de Bono, J., Selby, P., Coffey, M., Vile, R., Melcher, A., 2008a. Reovirus Activates Human Dendritic Cells to Promote Innate Antitumor Immunity. *J. Immunol.* 180, 6018–6026. <https://doi.org/10.4049/jimmunol.180.9.6018>
- Errington, F., White, C.L., Twigger, K.R., Rose, A., Scott, K., Steele, L., Ilett, L.J., Prestwich, R., Pandha, H.S., Coffey, M., others, 2008b. Inflammatory tumour cell killing by oncolytic reovirus for the treatment of melanoma. *Gene Ther.* 15, 1257–1270.
- Esolen, L.M., Ward, B.J., Moench, T.R., Griffin, D.E., 1993. Infection of monocytes during measles. *J. Infect. Dis.* 168, 47–52.
- Essner, R., Conforti, A., Kelley, M.C., Wanek, L., Stern, S., Glass, E., Morton, D.L., 1999. Efficacy of lymphatic mapping, sentinel lymphadenectomy, and selective complete lymph node dissection as a therapeutic procedure for early-stage melanoma. *Ann. Surg. Oncol.* 6, 442–449.
- Euvrard, S., Kanitakis, J., Claudy, A., 2003. Skin cancers after organ transplantation. *N. Engl. J. Med.* 348, 1681–1691. <https://doi.org/10.1056/NEJMra022137>
- Evgin, L., Acuna, S.A., Tanese de Souza, C., Marguerie, M., Lemay, C.G., Ilkow, C.S., Findlay, C.S., Falls, T., Parato, K.A., Hanwell, D., Goldstein, A., Lopez, R., Lafrance, S., Breitbach, C.J., Kirn, D., Atkins, H., Auer, R.C., Thurman, J.M., Stahl, G.L., Lambris, J.D., Bell, J.C., McCart, J.A., 2015. Complement Inhibition Prevents Oncolytic Vaccinia Virus Neutralization in Immune Humans and Cynomolgus Macaques. *Mol. Ther.* 23, 1066–1076. <https://doi.org/10.1038/mt.2015.49>
- Falleni, M., Savi, F., Tosi, D., Agape, E., Cerri, A., Moneghini, L., Bulfamante, G.P., 2017. M1 and M2 macrophages' clinicopathological significance in cutaneous melanoma. *Melanoma Res.* 27, 200–210. <https://doi.org/10.1097/CMR.0000000000000352>
- Fang, J., Nakamura, H., Maeda, H., 2011. The EPR effect: Unique features of tumor blood vessels for drug delivery, factors involved, and limitations and augmentation of the effect. *Adv. Drug Deliv. Rev.* 63, 136–151. <https://doi.org/10.1016/j.addr.2010.04.009>
- Fanger, N.A., Wardwell, K., Shen, L., Tedder, T.F., Guyre, P.M., 1996. Type I (CD64) and type II (CD32) Fc gamma receptor-mediated phagocytosis by human blood dendritic cells. *J. Immunol.* 157, 541–548.
- Farassati, F., Yang, A.D., Lee, P.W., 2001. Oncogenes in Ras signalling pathway dictate host-cell permissiveness to herpes simplex virus 1. *Nat. Cell Biol.* 3, 745–750. <https://doi.org/10.1038/35087061>

- Ferguson, N.M., Rodríguez-Barraquer, I., Dorigatti, I., Mier-y-Teran-Romero, L., Laydon, D.J., Cummings, D.A.T., 2016. Benefits and risks of the Sanofi-Pasteur dengue vaccine: Modeling optimal deployment. *Science* 353, 1033–1036. <https://doi.org/10.1126/science.aaf9590>
- Ferlay, J., Soerjomataram, I., Dikshit, R., Eser, S., Mathers, C., Rebelo, M., Parkin, D.M., Forman, D., Bray, F., 2015. Cancer incidence and mortality worldwide: Sources, methods and major patterns in GLOBOCAN 2012. *Int. J. Cancer* 136, E359–E386. <https://doi.org/10.1002/ijc.29210>
- Ferris, R.L., Gross, N.D., Nemunaitis, J.J., Andtbacka, R.H.I., Argiris, A., Ohr, J., Vetto, J.T., Senzer, N.N., Bedell, C., Ungerleider, R.S., Tanaka, M., Nishiyama, Y., 2014. Phase I trial of intratumoral therapy using HF10, an oncolytic HSV-1, demonstrates safety in HSV+/HSV- patients with refractory and superficial cancers. *J. Clin. Oncol.* 32, 6082–6082. [https://doi.org/10.1200/jco.2014.32.15\\_suppl.6082](https://doi.org/10.1200/jco.2014.32.15_suppl.6082)
- Fields, B.N., Raine, C.S., Baum, S.G., 1971. Temperature-sensitive mutants of reovirus type 3: defects in viral maturation as studied by immunofluorescence and electron microscopy. *Virology* 43, 569–578.
- Fisk, B., Blevins, T.L., Wharton, J.T., Ioannides, C.G., 1995. Identification of an immunodominant peptide of HER-2/neu protooncogene recognized by ovarian tumor-specific cytotoxic T lymphocyte lines. *J. Exp. Med.* 181, 2109–2117. <https://doi.org/10.1084/jem.181.6.2109>
- Flaherty, K.T., Robert, C., Hersey, P., Nathan, P., Garbe, C., Milhem, M., Demidov, L.V., Hassel, J.C., Rutkowski, P., Mohr, P., Dummer, R., Trefzer, U., Larkin, J.M.G., Utikal, J., Dreno, B., Nyakas, M., Middleton, M.R., Becker, J.C., Casey, M., Sherman, L.J., Wu, F.S., Ouellet, D., Martin, A.-M., Patel, K., Schadendorf, D., METRIC Study Group, 2012. Improved survival with MEK inhibition in BRAF-mutated melanoma. *N. Engl. J. Med.* 367, 107–114. <https://doi.org/10.1056/NEJMoa1203421>
- Forrest, J.C., Dermody, T.S., 2003. Reovirus Receptors and Pathogenesis. *J. Virol.* 77, 9109–9115. <https://doi.org/10.1128/JVI.77.17.9109-9115.2003>
- Forsyth, P., Roldán, G., George, D., Wallace, C., Palmer, C.A., Morris, D., Cairncross, G., Matthews, M.V., Markert, J., Gillespie, Y., Coffey, M., Thompson, B., Hamilton, M., 2008. A Phase I Trial of Intratumoral Administration of Reovirus in Patients With Histologically Confirmed Recurrent Malignant Gliomas. *Mol. Ther.* 16, 627–632. <https://doi.org/10.1038/sj.mt.6300403>
- Frankenberger, M., Hofer, T.P.J., Marei, A., Dayyani, F., Schewe, S., Strasser, C., Aldraihim, A., Stanzel, F., Lang, R., Hoffmann, R., Prazeres da Costa, O., Buch, T., Ziegler-Heitbrock, L., 2012. Transcript profiling of CD16-positive monocytes reveals a unique molecular fingerprint. *Eur. J. Immunol.* 42, 957–974. <https://doi.org/10.1002/eji.201141907>
- Fridman, W.H., Pagès, F., Sautès-Fridman, C., Galon, J., 2012. The immune contexture in human tumours: impact on clinical outcome. *Nat. Rev. Cancer* 12, 298–306. <https://doi.org/10.1038/nrc3245>
- Gaillard, R.K., Joklik, W.K., 1982. Quantitation of the relatedness of reovirus serotypes 1, 2, and 3 at the gene level. *Virology* 123, 152–164. [https://doi.org/10.1016/0042-6822\(82\)90302-6](https://doi.org/10.1016/0042-6822(82)90302-6)

- Galanis, E., Hartmann, L.C., Cliby, W.A., Long, H.J., Peethambaram, P.P., Barrette, B.A., Kaur, J.S., Haluska, P.J., Aderca, I., Zollman, P.J., Sloan, J.A., Keeney, G., Atherton, P.J., Podratz, K.C., Dowdy, S.C., Stanhope, C.R., Wilson, T.O., Federspiel, M.J., Kah-Whye, P., Russell, S.J., 2010. Phase I Trial of Intraperitoneal Administration of an Oncolytic Measles Virus Strain Engineered to Express Carcinoembryonic Antigen for Recurrent Ovarian Cancer. *Cancer Res.* 70, 875–882. <https://doi.org/10.1158/0008-5472.CAN-09-2762>
- Galanis, E., Markovic, S.N., Suman, V.J., Nuovo, G.J., Vile, R.G., Kottke, T.J., Nevala, W.K., Thompson, M.A., Lewis, J.E., Rumilla, K.M., Roulstone, V., Harrington, K., Linette, G.P., Maples, W.J., Coffey, M., Zwiebel, J., Kendra, K., 2012. Phase II Trial of Intravenous Administration of Reolysin® (Reovirus Serotype-3-dearing Strain) in Patients with Metastatic Melanoma. *Mol. Ther.* 20, 1998–2003. <https://doi.org/10.1038/mt.2012.146>
- Gallagher, R.P., Spinelli, J.J., Lee, T.K., 2005. Tanning beds, sunlamps, and risk of cutaneous malignant melanoma. *Cancer Epidemiol. Biomark. Prev. Publ. Am. Assoc. Cancer Res. Cosponsored Am. Soc. Prev. Oncol.* 14, 562–566. <https://doi.org/10.1158/1055-9965.EPI-04-0564>
- Ganly, I., Kirn, D., Eckhardt, G., Rodriguez, G.I., Soutar, D.S., Otto, R., Robertson, A.G., Park, O., Gulley, M.L., Heise, C., Von Hoff, D.D., Kaye, S.B., Eckhardt, S.G., 2000. A phase I study of Onyx-015, an E1B attenuated adenovirus, administered intratumorally to patients with recurrent head and neck cancer. *Clin. Cancer Res. Off. J. Am. Assoc. Cancer Res.* 6, 798–806.
- Garber, K., 2006. China approves world's first oncolytic virus therapy for cancer treatment. *J. Natl. Cancer Inst.* 98, 298–300. <https://doi.org/10.1093/jnci/djj111>
- García-Castro, J., Alemany, R., Cascalló, M., Martínez-Quintanilla, J., Arriero, M. del M., Lassaletta, A., Madero, L., Ramírez, M., 2010. Treatment of metastatic neuroblastoma with systemic oncolytic virotherapy delivered by autologous mesenchymal stem cells: an exploratory study. *Cancer Gene Ther.* 17, 476–483. <https://doi.org/10.1038/cgt.2010.4>
- Garrido, C., Paco, L., Romero, I., Berruguilla, E., Stefansky, J., Collado, A., Algarra, I., Garrido, F., Garcia-Lora, A.M., 2012. MHC class I molecules act as tumor suppressor genes regulating the cell cycle gene expression, invasion and intrinsic tumorigenicity of melanoma cells. *Carcinogenesis* 33, 687–693. <https://doi.org/10.1093/carcin/bgr318>
- Gehrke, S., Otsuka, A., Huber, R., Meier, B., Kistowska, M., Fenini, G., Cheng, P., Dummer, R., Kerl, K., Contassot, E., French, L.E., 2014. Metastatic melanoma cell lines do not secrete IL-1 $\beta$  but promote IL-1 $\beta$  production from macrophages. *J. Dermatol. Sci.* 74, 167–169. <https://doi.org/10.1016/j.jdermsci.2014.01.006>
- Geijtenbeek, T.B., Kwon, D.S., Torensma, R., van Vliet, S.J., van Duijnhoven, G.C., Middel, J., Cornelissen, I.L., Nottet, H.S., KewalRamani, V.N., Littman, D.R., Figdor, C.G., van Kooyk, Y., 2000. DC-SIGN, a dendritic cell-specific HIV-1-binding protein that enhances trans-infection of T cells. *Cell* 100, 587–597.
- Georgiades, J., Zielinski, T., Cicholska, A., Jordan, E., 1959. Research on the oncolytic effect of APC viruses in cancer of the cervix uteri; preliminary report. *Biul. Inst. Med. Morsk. Gdansk.* 10, 49–57.

- Gerosa, F., Gobbi, A., Zorzi, P., Burg, S., Briere, F., Carra, G., Trinchieri, G., 2005. The reciprocal interaction of NK cells with plasmacytoid or myeloid dendritic cells profoundly affects innate resistance functions. *J. Immunol. Baltim. Md* 1950 174, 727–734.
- Gershenwald, J.E., Scolyer, R.A., Hess, K.R., Sondak, V.K., Long, G.V., Ross, M.I., Lazar, A.J., Faries, M.B., Kirkwood, J.M., McArthur, G.A., Haydu, L.E., Eggermont, A.M.M., Flaherty, K.T., Balch, C.M., Thompson, J.F., for members of the American Joint Committee on Cancer Melanoma Expert Panel and the International Melanoma Database and Discovery Platform, 2017. Melanoma staging: Evidence-based changes in the American Joint Committee on Cancer eighth edition cancer staging manual. *CA. Cancer J. Clin.* 67, 472–492.  
<https://doi.org/10.3322/caac.21409>
- Ginhoux, F., Jung, S., 2014. Monocytes and macrophages: developmental pathways and tissue homeostasis. *Nat. Rev. Immunol.* 14, 392–404.  
<https://doi.org/10.1038/nri3671>
- Godfrey, H.P., Yashphe, D.J., Coons, A.H., 1969. Characterization of IgM and IgG antibodies produced during the anamnestic response initiated in vitro. *J. Immunol. Baltim. Md* 1950 102, 317–326.
- Golden, J.W., Schiff, L.A., 2005. Neutrophil elastase, an acid-independent serine protease, facilitates reovirus uncoating and infection in U937 promonocyte cells. *Virology* 2, 48.
- Gollamudi, R., Ghalib, M.H., Desai, K.K., Chaudhary, I., Wong, B., Einstein, M., Coffey, M., Gill, G.M., Mettinger, K., Mariadason, J.M., Mani, S., Goel, S., 2010. Intravenous administration of Reolysin, a live replication competent RNA virus is safe in patients with advanced solid tumors. *Invest. New Drugs* 28, 641–649.  
<https://doi.org/10.1007/s10637-009-9279-8>
- Gomatos, P.J., Tamm, I., 1963. THE SECONDARY STRUCTURE OF REOVIRUS RNA\*. *Proc. Natl. Acad. Sci. U. S. A.* 49, 707–714.
- Gong, J., Sachdev, E., Mita, A.C., Mita, M.M., 2016. Clinical development of reovirus for cancer therapy: An oncolytic virus with immune-mediated antitumor activity. *World J. Methodol.* 6, 25–42. <https://doi.org/10.5662/wjm.v6.i1.25>
- Gonzalez-Quintela, A., Alende, R., Gude, F., Campos, J., Rey, J., Meijide, L.M., Fernandez-Merino, C., Vidal, C., 2008. Serum levels of immunoglobulins (IgG, IgA, IgM) in a general adult population and their relationship with alcohol consumption, smoking and common metabolic abnormalities. *Clin. Exp. Immunol.* 151, 42–50.  
<https://doi.org/10.1111/j.1365-2249.2007.03545.x>
- Gooden, M.J.M., de Bock, G.H., Leffers, N., Daemen, T., Nijman, H.W., 2011. The prognostic influence of tumour-infiltrating lymphocytes in cancer: a systematic review with meta-analysis. *Br. J. Cancer* 105, 93–103.  
<https://doi.org/10.1038/bjc.2011.189>
- Green, S., Vaughn, D.W., Kalayanarooj, S., Nimmannitya, S., Suntayakorn, S., Nisalak, A., Rothman, A.L., Ennis, F.A., 1999. Elevated plasma interleukin-10 levels in acute dengue correlate with disease severity. *J. Med. Virol.* 59, 329–334.
- Greig, S.L., 2016. Talimogene Laherparepvec: First Global Approval. *Drugs* 76, 147–154. <https://doi.org/10.1007/s40265-015-0522-7>

- Groot, F., Welsch, S., Sattentau, Q.J., 2008. Efficient HIV-1 transmission from macrophages to T cells across transient virological synapses. *Blood* 111, 4660–4663. <https://doi.org/10.1182/blood-2007-12-130070>
- Gu, W., Guo, L., Yu, H., Niu, J., Huang, M., Luo, X., Li, R., Tian, Z., Feng, L., Wang, Y., 2015. Involvement of CD16 in antibody-dependent enhancement of porcine reproductive and respiratory syndrome virus infection. *J. Gen. Virol.* 96, 1712–1722. <https://doi.org/10.1099/vir.0.000118>
- Guilliams, M., Bruhns, P., Saeys, Y., Hammad, H., Lambrecht, B.N., 2014. The function of Fcγ receptors in dendritic cells and macrophages. *Nat. Rev. Immunol.* 14, 94–108. <https://doi.org/10.1038/nri3582>
- Gujar, S.A., Pan, D.A., Marcato, P., Garant, K.A., Lee, P.W.K., 2011. Oncolytic virus-initiated protective immunity against prostate cancer. *Mol. Ther. J. Am. Soc. Gene Ther.* 19, 797–804. <https://doi.org/10.1038/mt.2010.297>
- Guo, Z.S., Liu, Z., Bartlett, D.L., 2014. Oncolytic Immunotherapy: Dying the Right Way is a Key to Eliciting Potent Antitumor Immunity. *Front. Oncol.* 4. <https://doi.org/10.3389/fonc.2014.00074>
- Guo, Z.S., Parimi, V., O'Malley, M.E., Thirunavukarasu, P., Sathaiah, M., Austin, F., Bartlett, D.L., 2010. The combination of immunosuppression and carrier cells significantly enhances the efficacy of oncolytic poxvirus in the pre-immunized host. *Gene Ther.* 17, 1465–1475. <https://doi.org/10.1038/gt.2010.104>
- Guy, G.P., Ekwueme, D.U., 2011. Years of Potential Life Lost and Indirect Costs of Melanoma and Non-Melanoma Skin Cancer. *PharmacoEconomics* 29, 863–874. <https://doi.org/10.2165/11589300-000000000-00000>
- Haines, B.B., Ryu, C.J., Chang, S., Protopopov, A., Luch, A., Kang, Y.H., Draganov, D.D., Fragoso, M.F., Paik, S.G., Hong, H.J., DePinho, R.A., Chen, J., 2006. Block of T cell development in P53-deficient mice accelerates development of lymphomas with characteristic RAG-dependent cytogenetic alterations. *Cancer Cell* 9, 109–120. <https://doi.org/10.1016/j.ccr.2006.01.004>
- Hall, K., Scott, K.J., Rose, A., Desborough, M., Harrington, K., Pandha, H., Parrish, C., Vile, R., Coffey, M., Bowen, D., Errington-Mais, F., Melcher, A.A., 2012. Reovirus-mediated cytotoxicity and enhancement of innate immune responses against acute myeloid leukemia. *BioResearch Open Access* 1, 3–15. <https://doi.org/10.1089/biores.2012.0205>
- Haller Hasskamp, J., Zapas, J.L., Elias, E.G., 2005. Dendritic cell counts in the peripheral blood of healthy adults. *Am. J. Hematol.* 78, 314–315. <https://doi.org/10.1002/ajh.20296>
- Halstead, S.B., Chow, J.S., Marchette, N.J., 1973. Immunological enhancement of dengue virus replication. *Nature. New Biol.* 243, 24–26.
- Halstead, S.B., Mahalingam, P.S., Marovich, M.A., Ubol, S., Mosser, P.D.M., 2010. Intrinsic antibody-dependent enhancement of microbial infection in macrophages: disease regulation by immune complexes. *Lancet Infect. Dis.* 10, 712–722. [https://doi.org/10.1016/S1473-3099\(10\)70166-3](https://doi.org/10.1016/S1473-3099(10)70166-3)
- Halstead, S.B., O'Rourke, E.J., 1977. Dengue viruses and mononuclear phagocytes. I. Infection enhancement by non-neutralizing antibody. *J. Exp. Med.* 146, 201–217.

- Hamid, O., Gajewski, T.F., Frankel, A.E., Bauer, T.M., Olszanski, A.J., Luke, J.J., Balmanoukian, A.S., Schmidt, E.V., Sharkey, B., Maleski, J., Jones, M.J., Gangadhar, T.C., 2017. 1214OEpacadostat plus pembrolizumab in patients with advanced melanoma: Phase 1 and 2 efficacy and safety results from ECHO-202/KEYNOTE-037. *Ann. Oncol.* 28. <https://doi.org/10.1093/annonc/mdx377.001>
- Han, J., Sabbatini, P., Perez, D., Rao, L., Modha, D., White, E., 1996. The E1B 19K protein blocks apoptosis by interacting with and inhibiting the p53-inducible and death-promoting Bax protein. *Genes Dev.* 10, 461–477.
- Hanahan, D., Weinberg, R.A., 2011. Hallmarks of cancer: the next generation. *Cell* 144, 646–674. <https://doi.org/10.1016/j.cell.2011.02.013>
- Hansmann, L., Groeger, S., von Wulffen, W., Bein, G., Hackstein, H., 2008. Human monocytes represent a competitive source of interferon- $\alpha$  in peripheral blood. *Clin. Immunol.* 127, 252–264. <https://doi.org/10.1016/j.clim.2008.01.014>
- Harada, H., Fujita, T., Miyamoto, M., Kimura, Y., Maruyama, M., Furia, A., Miyata, T., Taniguchi, T., 1989. Structurally similar but functionally distinct factors, IRF-1 and IRF-2, bind to the same regulatory elements of IFN and IFN-inducible genes. *Cell* 58, 729–739.
- Harb, W.A., Cerec, V., McElwaine-Johnn, H., Champion, B., Alvis, S., Jain, N., Ellis, C., Fisher, K., Beadle, J.W., 2016. A phase I study of pembrolizumab in combination with enadenotucirev (EnAd) (SPICE) in subjects with metastatic or advanced carcinoma. *J. Clin. Oncol.* 34, TPS3112-TPS3112. [https://doi.org/10.1200/JCO.2016.34.15\\_suppl.TPS3112](https://doi.org/10.1200/JCO.2016.34.15_suppl.TPS3112)
- Hardcastle, J., Kurozumi, K., Chiocca, E.A., Kaur, B., 2007. Oncolytic viruses driven by tumor-specific promoters. *Curr. Cancer Drug Targets* 7, 181–189.
- Harrington, K.J., Andtbacka, R.H., Collichio, F., Downey, G., Chen, L., Szabo, Z., Kaufman, H.L., 2016. Efficacy and safety of talimogene laherparepvec versus granulocyte-macrophage colony-stimulating factor in patients with stage IIIB/C and IVM1a melanoma: subanalysis of the Phase III OPTiM trial. *OncoTargets Ther.* 9, 7081–7093. <https://doi.org/10.2147/OTT.S115245>
- Harrington, K.J., Hingorani, M., Tanay, M.A., Hickey, J., Bhide, S.A., Clarke, P.M., Renouf, L.C., Thway, K., Sibtain, A., McNeish, I.A., Newbold, K.L., Goldsweig, H., Coffin, R., Nutting, C.M., 2010a. Phase I/II study of oncolytic HSV GM-CSF in combination with radiotherapy and cisplatin in untreated stage III/IV squamous cell cancer of the head and neck. *Clin. Cancer Res. Off. J. Am. Assoc. Cancer Res.* 16, 4005–4015. <https://doi.org/10.1158/1078-0432.CCR-10-0196>
- Harrington, K.J., Karapanagiotou, E.M., Roulstone, V., Twigger, K.R., White, C.L., Vidal, L., Beirne, D., Prestwich, R., Newbold, K., Ahmed, M., Thway, K., Nutting, C.M., Coffey, M., Harris, D., Vile, R.G., Pandha, H.S., Debono, J.S., Melcher, A.A., 2010b. Two-stage phase I dose-escalation study of intratumoral reovirus type 3 dearing and palliative radiotherapy in patients with advanced cancers. *Clin. Cancer Res. Off. J. Am. Assoc. Cancer Res.* 16, 3067–3077. <https://doi.org/10.1158/1078-0432.CCR-10-0054>
- Harrington, K.J., Michielin, O., Malvey, J., Pezzani Grüter, I., Grove, L., Frauchiger, A.L., Dummer, R., 2017. A practical guide to the handling and administration of

- talimogene laherparepvec in Europe. *OncoTargets Ther.* 10, 3867–3880. <https://doi.org/10.2147/OTT.S133699>
- Harris, S.J., Brown, J., Lopez, J., Yap, T.A., 2016. Immuno-oncology combinations: raising the tail of the survival curve. *Cancer Biol. Med.* 13, 171–193. <https://doi.org/10.20892/j.issn.2095-3941.2016.0015>
- Hashiro, G., Loh, P.C., Yau, J.T., 1977. The preferential cytotoxicity of reovirus for certain transformed cell lines. *Arch. Virol.* 54, 307–315.
- Hasthorpe, S., Holland, K., Nink, V., Lawler, C., Hertzog, P., 1997. Mechanisms of resistance off NSCLC to interferons. *Int. J. Oncol.* 10, 933–938.
- Hauschild, A., Grob, J.-J., Demidov, L.V., Jouary, T., Gutzmer, R., Millward, M., Rutkowski, P., Blank, C.U., Miller, W.H., Kaempgen, E., Martín-Algarra, S., Karaszewska, B., Mauch, C., Chiarion-Sileni, V., Martin, A.-M., Swann, S., Haney, P., Mirakhur, B., Guckert, M.E., Goodman, V., Chapman, P.B., 2012. Dabrafenib in BRAF-mutated metastatic melanoma: a multicentre, open-label, phase 3 randomised controlled trial. *Lancet Lond. Engl.* 380, 358–365. [https://doi.org/10.1016/S0140-6736\(12\)60868-X](https://doi.org/10.1016/S0140-6736(12)60868-X)
- Heinemann, L., Simpson, G.R., Boxall, A., Kottke, T., Relph, K.L., Vile, R., Melcher, A., Prestwich, R., Harrington, K.J., Morgan, R., Pandha, H.S., 2011. Synergistic effects of oncolytic reovirus and docetaxel chemotherapy in prostate cancer. *BMC Cancer* 11, 221. <https://doi.org/10.1186/1471-2407-11-221>
- Heise, C., Sampson-Johannes, A., Williams, A., McCormick, F., Von Hoff, D.D., Kirn, D.H., 1997. ONYX-015, an E1B gene-attenuated adenovirus, causes tumor-specific cytolysis and antitumoral efficacy that can be augmented by standard chemotherapeutic agents. *Nat. Med.* 3, 639–645.
- Hemmi, H., Kaisho, T., Takeuchi, O., Sato, S., Sanjo, H., Hoshino, K., Horiuchi, T., Tomizawa, H., Takeda, K., Akira, S., 2002. Small anti-viral compounds activate immune cells via the TLR7 MyD88-dependent signaling pathway. *Nat. Immunol.* 3, 196–200. <https://doi.org/10.1038/ni758>
- Hengstschläger, M., Knöfler, M., Müllner, E.W., Ogris, E., Wintersberger, E., Wawra, E., 1994. Different regulation of thymidine kinase during the cell cycle of normal versus DNA tumor virus-transformed cells. *J. Biol. Chem.* 269, 13836–13842.
- Heo, J., Reid, T., Ruo, L., Breitbach, C.J., Rose, S., Bloomston, M., Cho, M., Lim, H.Y., Chung, H.C., Kim, C.W., Burke, J., Lencioni, R., Hickman, T., Moon, A., Lee, Y.S., Kim, M.K., Daneshmand, M., Dubois, K., Longpre, L., Ngo, M., Rooney, C., Bell, J.C., Rhee, B.-G., Patt, R., Hwang, T.-H., Kirn, D.H., 2013. Randomized dose-finding clinical trial of oncolytic immunotherapeutic vaccinia JX-594 in liver cancer. *Nat. Med.* 19, 329–336. <https://doi.org/10.1038/nm.3089>
- Hersey, P., Zhuang, L., Zhang, X.D., 2006. Current Strategies in Overcoming Resistance of Cancer Cells to Apoptosis Melanoma as a Model, in: *International Review of Cytology*. Academic Press, pp. 131–158. [https://doi.org/10.1016/S0074-7696\(06\)51004-6](https://doi.org/10.1016/S0074-7696(06)51004-6)
- Hettinger, J., Richards, D.M., Hansson, J., Barra, M.M., Joschko, A.-C., Krijgsveld, J., Feuerer, M., 2013. Origin of monocytes and macrophages in a committed progenitor. *Nat. Immunol.* 14, 821–830. <https://doi.org/10.1038/ni.2638>

- Higgins, G.K., Pack, G.T., 1951. Virus therapy in the treatment of tumors. *Bull. Hosp. Joint Dis.* 12, 379–382.
- Hino, R., Kabashima, K., Kato, Y., Yagi, H., Nakamura, M., Honjo, T., Okazaki, T., Tokura, Y., 2010. Tumor cell expression of programmed cell death-1 ligand 1 is a prognostic factor for malignant melanoma. *Cancer* 116, 1757–1766. <https://doi.org/10.1002/cncr.24899>
- Hirasawa, K., Nishikawa, S.G., Norman, K.L., Alain, T., Kossakowska, A., Lee, P.W.K., 2002. Oncolytic reovirus against ovarian and colon cancer. *Cancer Res.* 62, 1696–1701.
- Hirvonen, M., Heiskanen, R., Oksanen, M., Pesonen, S., Liikanen, I., Joensuu, T., Kanerva, A., Cerullo, V., Hemminki, A., 2013. Fc-gamma receptor polymorphisms as predictive and prognostic factors in patients receiving oncolytic adenovirus treatment. *J Transl Med* 11, 193.
- Hirvonen, M., Rajcecki, M., Kapanen, M., Parviainen, S., Rouvinen-Lagerström, N., Diaconu, I., Nokisalmi, P., Tenhunen, M., Hemminki, A., Cerullo, V., 2015. Immunological effects of a tumor necrosis factor alpha-armed oncolytic adenovirus. *Hum. Gene Ther.* 26, 134–144. <https://doi.org/10.1089/hum.2014.069>
- Hober, D., Chehadeh, W., Bouzidi, A., Wattré, P., 2001. Antibody-dependent enhancement of coxsackievirus B4 infectivity of human peripheral blood mononuclear cells results in increased interferon-alpha synthesis. *J. Infect. Dis.* 184, 1098–1108. <https://doi.org/10.1086/323801>
- Hocker, T.L., Singh, M.K., Tsao, H., 2008. Melanoma genetics and therapeutic approaches in the 21st century: moving from the benchside to the bedside. *J. Invest. Dermatol.* 128, 2575–2595. <https://doi.org/10.1038/jid.2008.226>
- Hodi, F.S., O'Day, S.J., McDermott, D.F., Weber, R.W., Sosman, J.A., Haanen, J.B., Gonzalez, R., Robert, C., Schadendorf, D., Hassel, J.C., Akerley, W., van den Eertwegh, A.J.M., Lutzky, J., Lorigan, P., Vaubel, J.M., Linette, G.P., Hogg, D., Ottensmeier, C.H., Lebbé, C., Peschel, C., Quirt, I., Clark, J.I., Wolchok, J.D., Weber, J.S., Tian, J., Yellin, M.J., Nichol, G.M., Hoos, A., Urba, W.J., 2010. Improved survival with ipilimumab in patients with metastatic melanoma. *N. Engl. J. Med.* 363, 711–723. <https://doi.org/10.1056/NEJMoa1003466>
- Holmes, T.D., Wilson, E.B., Black, E.V.I., Benest, A.V., Vaz, C., Tan, B., Tanavde, V.M., Cook, G.P., 2014. Licensed human natural killer cells aid dendritic cell maturation via TNFSF14/LIGHT. *Proc. Natl. Acad. Sci.* 111, E5688–E5696. <https://doi.org/10.1073/pnas.1411072112>
- Hölsken, O., Miller, M., Cerwenka, A., 2015. Exploiting natural killer cells for therapy of melanoma. *JDDG J. Dtsch. Dermatol. Ges.* 13, 23–28. <https://doi.org/10.1111/ddg.12557>
- Honke, N., Shaabani, N., Cadeddu, G., Sorg, U.R., Zhang, D.-E., Trilling, M., Klingel, K., Sauter, M., Kandolf, R., Gailus, N., van Rooijen, N., Burkart, C., Baldus, S.E., Grusdat, M., Löhning, M., Hengel, H., Pfeiffer, K., Tanaka, M., Häussinger, D., Recher, M., Lang, P.A., Lang, K.S., 2012. Enforced viral replication activates adaptive immunity and is essential for the control of a cytopathic virus. *Nat. Immunol.* 13, 51–57. <https://doi.org/10.1038/ni.2169>

- Hoption Cann, S.A., van Netten, J.P., van Netten, C., Glover, D.W., 2002. Spontaneous regression: a hidden treasure buried in time. *Med. Hypotheses* 58, 115–119. <https://doi.org/10.1054/mehy.2001.1469>
- Hornung, V., Ellegast, J., Kim, S., Brzózka, K., Jung, A., Kato, H., Poeck, H., Akira, S., Conzelmann, K.-K., Schlee, M., Endres, S., Hartmann, G., 2006. 5'-Triphosphate RNA is the ligand for RIG-I. *Science* 314, 994–997. <https://doi.org/10.1126/science.1132505>
- Hoster, H.A., Zanes, R.P., Von Haam, E., 1949. Studies in Hodgkin's syndrome; the association of viral hepatitis and Hodgkin's disease; a preliminary report. *Cancer Res.* 9, 473–480.
- Hou, W., Gibbs, J.S., Lu, X., Brooke, C.B., Roy, D., Modlin, R.L., Bennink, J.R., Yewdell, J.W., 2012. Viral infection triggers rapid differentiation of human blood monocytes into dendritic cells. *Blood* 119, 3128–3131. <https://doi.org/10.1182/blood-2011-09-379479>
- Hu, J.C.C., Coffin, R.S., Davis, C.J., Graham, N.J., Groves, N., Guest, P.J., Harrington, K.J., James, N.D., Love, C.A., McNeish, I., Medley, L.C., Michael, A., Nutting, C.M., Pandha, H.S., Shorrock, C.A., Simpson, J., Steiner, J., Steven, N.M., Wright, D., Coombes, R.C., 2006. A Phase I Study of OncoVEXGM-CSF, a Second-Generation Oncolytic Herpes Simplex Virus Expressing Granulocyte Macrophage Colony-Stimulating Factor. *Clin. Cancer Res.* 12, 6737–6747. <https://doi.org/10.1158/1078-0432.CCR-06-0759>
- Huang, X., Yue, Y., Li, D., Zhao, Y., Qiu, L., Chen, J., Pan, Y., Xi, J., Wang, X., Sun, Q., Li, Q., 2016. Antibody-dependent enhancement of dengue virus infection inhibits RLR-mediated Type-I IFN-independent signalling through upregulation of cellular autophagy. *Sci. Rep.* 6, srep22303. <https://doi.org/10.1038/srep22303>
- Hugo, W., Zaretsky, J.M., Sun, L., Song, C., Moreno, B.H., Hu-Lieskovan, S., Berent-Maoz, B., Pang, J., Chmielowski, B., Cherry, G., Seja, E., Lomeli, S., Kong, X., Kelley, M.C., Sosman, J.A., Johnson, D.B., Ribas, A., Lo, R.S., 2016. Genomic and Transcriptomic Features of Response to Anti-PD-1 Therapy in Metastatic Melanoma. *Cell* 165, 35–44. <https://doi.org/10.1016/j.cell.2016.02.065>
- Hurd, E.R., Giuliano, V.J., 1975. The effect of cyclophosphamide on b and t lymphocytes in patients with connective tissue diseases. *Arthritis Rheum.* 18, 67–75. <https://doi.org/10.1002/art.1780180113>
- Hwang, T.-H., Moon, A., Burke, J., Ribas, A., Stephenson, J., Breitbach, C.J., Daneshmand, M., De Silva, N., Parato, K., Diallo, J.-S., Lee, Y.-S., Liu, T.-C., Bell, J.C., Kirn, D.H., 2011. A mechanistic proof-of-concept clinical trial with JX-594, a targeted multi-mechanistic oncolytic poxvirus, in patients with metastatic melanoma. *Mol. Ther. J. Am. Soc. Gene Ther.* 19, 1913–1922. <https://doi.org/10.1038/mt.2011.132>
- Iankov, I.D., Blechacz, B., Liu, C., Schmeckpeper, J.D., Tarara, J.E., Federspiel, M.J., Caplice, N., Russell, S.J., 2007. Infected Cell Carriers: A New Strategy for Systemic Delivery of Oncolytic Measles Viruses in Cancer Virotherapy. *Mol. Ther.* 15, 114–122. <https://doi.org/10.1038/sj.mt.6300020>
- Iannacone, M.R., Youlden, D.R., Baade, P.D., Aitken, J.F., Green, A.C., 2015. Melanoma incidence trends and survival in adolescents and young adults in

- Queensland, Australia. *Int. J. Cancer* 136, 603–609.  
<https://doi.org/10.1002/ijc.28956>
- Iannello, A., Debbeche, O., Martin, E., Attalah, L.H., Samarani, S., Ahmad, A., 2006. Viral strategies for evading antiviral cellular immune responses of the host. *J. Leukoc. Biol.* 79, 16–35. <https://doi.org/10.1189/jlb.0705397>
- Ikeda, K., Ichikawa, T., Wakimoto, H., Silver, J.S., Deisboeck, T.S., Finkelstein, D., Harsh, G.R., Louis, D.N., Bartus, R.T., Hochberg, F.H., Chiocca, E.A., 1999. Oncolytic virus therapy of multiple tumors in the brain requires suppression of innate and elicited antiviral responses. *Nat. Med.* 5, 881–887.  
<https://doi.org/10.1038/11320>
- Ilett, E., Kottke, T., Donnelly, O., Thompson, J., Willmon, C., Diaz, R., Zaidi, S., Coffey, M., Selby, P., Harrington, K., Pandha, H., Melcher, A., Vile, R., 2014. Cytokine Conditioning Enhances Systemic Delivery and Therapy of an Oncolytic Virus. *Mol. Ther.* 22, 1851–1863. <https://doi.org/10.1038/mt.2014.118>
- Ilett, E., Kottke, T., Thompson, J., Rajani, K., Zaidi, S., Evgin, L., Coffey, M., Ralph, C., Diaz, R., Pandha, H., Harrington, K., Selby, P., Bram, R., Melcher, A., Vile, R., 2017. Prime-boost using separate oncolytic viruses in combination with checkpoint blockade improves anti-tumour therapy. *Gene Ther.* 24, 21–30.  
<https://doi.org/10.1038/gt.2016.70>
- Ilett, E.J., Barcena, M., Errington-Mais, F., Griffin, S., Harrington, K.J., Pandha, H.S., Coffey, M., Selby, P.J., Limpens, R.W.A.L., Mommaas, M., Hoeben, R.C., Vile, R.G., Melcher, A.A., 2011. Internalization of Oncolytic Reovirus by Human Dendritic Cell Carriers Protects the Virus from Neutralization. *Clin. Cancer Res.* 17, 2767–2776. <https://doi.org/10.1158/1078-0432.CCR-10-3266>
- Ilett, E.J., Prestwich, R.J., Kottke, T., Errington, F., Thompson, J.M., Harrington, K.J., Pandha, H.S., Coffey, M., Selby, P.J., Vile, R.G., Melcher, A.A., 2009. Dendritic cells and T cells deliver oncolytic reovirus for tumour killing despite pre-existing anti-viral immunity. *Gene Ther.* 16, 689–699. <https://doi.org/10.1038/gt.2009.29>
- Imani, F., Jacobs, B.L., 1988. Inhibitory activity for the interferon-induced protein kinase is associated with the reovirus serotype 1 sigma 3 protein. *Proc. Natl. Acad. Sci. U. S. A.* 85, 7887–7891.
- Ives, N.J., Stowe, R.L., Lorigan, P., Wheatley, K., 2007. Chemotherapy compared with biochemotherapy for the treatment of metastatic melanoma: a meta-analysis of 18 trials involving 2,621 patients. *J. Clin. Oncol. Off. J. Am. Soc. Clin. Oncol.* 25, 5426–5434. <https://doi.org/10.1200/JCO.2007.12.0253>
- Jackson, R., 1974. Saint Peregrine, O.S.M.--the patron saint of cancer patients. *Can. Med. Assoc. J.* 111, 824, 827.
- Jamieson, N.B., Maker, A.V., 2017. Gene expression profiling to predict responsiveness to immunotherapy. *Cancer Gene Ther.* 24, 134–140.  
<https://doi.org/10.1038/cgt.2016.63>
- Janeway, C.A., 1989. Approaching the asymptote? Evolution and revolution in immunology. *Cold Spring Harb. Symp. Quant. Biol.* 54 Pt 1, 1–13.

- Jeeninga, R.E., Jan, B., van den Berg, H., Berkhout, B., 2006. Construction of doxycycline-dependent mini-HIV-1 variants for the development of a virotherapy against leukemias. *Retrovirology* 3, 64. <https://doi.org/10.1186/1742-4690-3-64>
- Jenne, L., Hauser, C., Arrighi, J.F., Saurat, J.H., Hügin, A.W., 2000. Poxvirus as a vector to transduce human dendritic cells for immunotherapy: abortive infection but reduced APC function. *Gene Ther.* 7, 1575–1583. <https://doi.org/10.1038/sj.gt.3301287>
- Jennings, V.A., Ilett, E.J., Scott, K.J., West, E.J., Vile, R., Pandha, H., Harrington, K., Young, A., Hall, G.D., Coffey, M., Selby, P., Errington-Mais, F., Melcher, A.A., 2014. Lymphokine-activated killer and dendritic cell carriage enhances oncolytic reovirus therapy for ovarian cancer by overcoming antibody neutralization in ascites: LAKDC are effective carriers for reovirus. *Int. J. Cancer* 134, 1091–1101. <https://doi.org/10.1002/ijc.28450>
- Jessy, T., 2011. Immunity over inability: The spontaneous regression of cancer. *J. Nat. Sci. Biol. Med.* 2, 43–49. <https://doi.org/10.4103/0976-9668.82318>
- Jia, H., Kling, J., 2006. China offers alternative gateway for experimental drugs. *Nat. Biotechnol.* 24, 117–118. <https://doi.org/10.1038/nbt0206-117>
- Jones, C., Clapton, G., Zhao, Z., Barber, B., Saltman, D., Corrie, P., 2015. Unmet clinical needs in the management of advanced melanoma: findings from a survey of oncologists. *Eur. J. Cancer Care (Engl.)* 24, 867–872. <https://doi.org/10.1111/ecc.12359>
- Kadosawa, T., Watabe, A., 2015. The effects of surgery-induced immunosuppression and angiogenesis on tumour growth. *Vet. J. Lond. Engl.* 1997 205, 175–179. <https://doi.org/10.1016/j.tvjl.2015.04.009>
- Kaneno, R., Shurin, G.V., Kaneno, F.M., Naiditch, H., Luo, J., Shurin, M.R., 2011. Chemotherapeutic agents in low noncytotoxic concentrations increase immunogenicity of human colon cancer cells. *Cell. Oncol. Dordr.* 34, 97–106. <https://doi.org/10.1007/s13402-010-0005-5>
- Kanerva, A., Nokisalmi, P., Diaconu, I., Koski, A., Cerullo, V., Liikanen, I., Tähtinen, S., Oksanen, M., Heiskanen, R., Pesonen, Saila, Joensuu, T., Alanko, T., Partanen, K., Laasonen, L., Kairemo, K., Pesonen, Sari, Kangasniemi, L., Hemminki, A., 2013. Antiviral and antitumor T-cell immunity in patients treated with GM-CSF-coding oncolytic adenovirus. *Clin. Cancer Res. Off. J. Am. Assoc. Cancer Res.* 19, 2734–2744. <https://doi.org/10.1158/1078-0432.CCR-12-2546>
- Karapanagiotou, E.M., Roulstone, V., Twigger, K., Ball, M., Tanay, M., Nutting, C., Newbold, K., Gore, M.E., Larkin, J., Syrigos, K.N., Coffey, M., Thompson, B., Mettinger, K., Vile, R.G., Pandha, H.S., Hall, G.D., Melcher, A.A., Chester, J., Harrington, K.J., 2012. Phase I/II trial of carboplatin and paclitaxel chemotherapy in combination with intravenous oncolytic reovirus in patients with advanced malignancies. *Clin. Cancer Res. Off. J. Am. Assoc. Cancer Res.* 18, 2080–2089. <https://doi.org/10.1158/1078-0432.CCR-11-2181>
- Karnad, A.B., Haigentz, M., Miley, T., Coffey, M., Gill, G., Mita, M., 2011. Abstract C22: A phase II study of intravenous wild-type reovirus (Reolysin®) in combination with paclitaxel plus carboplatin in patients with platinum refractory metastatic and/or

- recurrent squamous cell carcinoma of the head and neck. *Mol. Cancer Ther.* 10, C22–C22. <https://doi.org/10.1158/1535-7163.TARG-11-C22>
- Kato, H., Sato, S., Yoneyama, M., Yamamoto, M., Uematsu, S., Matsui, K., Tsujimura, T., Takeda, K., Fujita, T., Takeuchi, O., Akira, S., 2005. Cell Type-Specific Involvement of RIG-I in Antiviral Response. *Immunity* 23, 19–28. <https://doi.org/10.1016/j.immuni.2005.04.010>
- Kato, H., Takeuchi, O., Sato, S., Yoneyama, M., Yamamoto, M., Matsui, K., Uematsu, S., Jung, A., Kawai, T., Ishii, K.J., Yamaguchi, O., Otsu, K., Tsujimura, T., Koh, C.-S., Reis e Sousa, C., Matsuura, Y., Fujita, T., Akira, S., 2006. Differential roles of MDA5 and RIG-I helicases in the recognition of RNA viruses. *Nature* 441, 101–105. <https://doi.org/10.1038/nature04734>
- Katzelnick, L.C., Gresh, L., Halloran, M.E., Mercado, J.C., Kuan, G., Gordon, A., Balmaseda, A., Harris, E., 2017. Antibody-dependent enhancement of severe dengue disease in humans. *Science* eaan6836. <https://doi.org/10.1126/science.aan6836>
- Kawai, T., Takahashi, K., Sato, S., Coban, C., Kumar, H., Kato, H., Ishii, K.J., Takeuchi, O., Akira, S., 2005. IPS-1, an adaptor triggering RIG-I- and Mda5-mediated type I interferon induction. *Nat. Immunol.* 6, 981–988. <https://doi.org/10.1038/ni1243>
- Kawakami, Y., Eliyahu, S., Sakaguchi, K., Robbins, P.F., Rivoltini, L., Yannelli, J.R., Appella, E., Rosenberg, S.A., 1994. Identification of the immunodominant peptides of the MART-1 human melanoma antigen recognized by the majority of HLA-A2-restricted tumor infiltrating lymphocytes. *J. Exp. Med.* 180, 347–352. <https://doi.org/10.1084/jem.180.1.347>
- Kelly, E., Russell, S.J., 2007. History of oncolytic viruses: genesis to genetic engineering. *Mol. Ther. J. Am. Soc. Gene Ther.* 15, 651–659. <https://doi.org/10.1038/sj.mt.6300108>
- Kelly, K.R., Espitia, C.M., Zhao, W., Wu, K., Visconte, V., Anwer, F., Calton, C.M., Carew, J.S., Nawrocki, S.T., 2018. Oncolytic reovirus sensitizes multiple myeloma cells to anti-PD-L1 therapy. *Leukemia* 32, 230–233. <https://doi.org/10.1038/leu.2017.272>
- Kemp, V., Hoeben, R.C., Wollenberg, D.J.M. van den, 2016. Exploring Reovirus Plasticity for Improving Its Use as Oncolytic Virus. *Viruses* 8. <https://doi.org/10.3390/v8010004>
- Khuri, F.R., Nemunaitis, J., Ganly, I., Arseneau, J., Tannock, I.F., Romel, L., Gore, M., Ironside, J., MacDougall, R.H., Heise, C., Randlev, B., Gillenwater, A.M., Bruso, P., Kaye, S.B., Hong, W.K., Kirn, D.H., 2000. a controlled trial of intratumoral ONYX-015, a selectively-replicating adenovirus, in combination with cisplatin and 5-fluorouracil in patients with recurrent head and neck cancer. *Nat. Med.* 6, 879–885. <https://doi.org/10.1038/78638>
- Kim, G., McKee, A.E., Ning, Y.-M., Hazarika, M., Theoret, M., Johnson, J.R., Xu, Q.C., Tang, S., Sridhara, R., Jiang, X., He, K., Roscoe, D., McGuinn, W.D., Helms, W.S., Russell, A.M., Miksinski, S.P., Zirkelbach, J.F., Earp, J., Liu, Q., Ibrahim, A., Justice, R., Pazdur, R., 2014. FDA approval summary: vemurafenib for treatment of unresectable or metastatic melanoma with the BRAFV600E mutation. *Clin.*

- Cancer Res. Off. J. Am. Assoc. Cancer Res. 20, 4994–5000.  
<https://doi.org/10.1158/1078-0432.CCR-14-0776>
- Kim, J., Hayton, W.L., Robinson, J.M., Anderson, C.L., 2007. Kinetics of FcRn-mediated recycling of IgG and albumin in human: pathophysiology and therapeutic implications using a simplified mechanism-based model. *Clin. Immunol. Orlando Fla* 122, 146–155. <https://doi.org/10.1016/j.clim.2006.09.001>
- Kim, M., Egan, C., Alain, T., Urbanski, S.J., Lee, P.W., Forsyth, P.A., Johnston, R.N., 2007. Acquired resistance to reoviral oncolysis in Ras-transformed fibrosarcoma cells. *Oncogene* 26, 4124–4134. <https://doi.org/10.1038/sj.onc.1210189>
- Kim, T.S., Braciale, T.J., 2009. Respiratory dendritic cell subsets differ in their capacity to support the induction of virus-specific cytotoxic CD8+ T cell responses. *PLoS One* 4, e4204. <https://doi.org/10.1371/journal.pone.0004204>
- Kirn, D., 2001. Clinical research results with dl1520 (Onyx-015), a replication-selective adenovirus for the treatment of cancer: what have we learned? *Gene Ther.* 8, 89–98. <https://doi.org/10.1038/sj.gt.3301377>
- Kirn, D.H., Thorne, S.H., 2009. Targeted and armed oncolytic poxviruses: a novel multi-mechanistic therapeutic class for cancer. *Nat. Rev. Cancer* 9, 64–71. <https://doi.org/10.1038/nrc2545>
- Klinac, D., Gray, E.S., Millward, M., Ziman, M., 2013. Advances in personalized targeted treatment of metastatic melanoma and non-invasive tumor monitoring. *Front. Oncol.* 3, 54. <https://doi.org/10.3389/fonc.2013.00054>
- Knocke, S., Fleischmann-Mundt, B., Saborowski, M., Manns, M.P., Kühnel, F., Wirth, T.C., Woller, N., 2016. Tailored Tumor Immunogenicity Reveals Regulation of CD4 and CD8 T Cell Responses against Cancer. *Cell Rep.* 17, 2234–2246. <https://doi.org/10.1016/j.celrep.2016.10.086>
- Knol, A.C., Nguyen, J.M., Quéreux, G., Brocard, A., Khammari, A., Dréno, B., 2011. Prognostic value of tumor-infiltrating Foxp3+ T-cell subpopulations in metastatic melanoma. *Exp. Dermatol.* 20, 430–434. <https://doi.org/10.1111/j.1600-0625.2011.01260.x>
- Knowlton, J.J., Dermody, T.S., Holm, G.H., 2012. Apoptosis induced by mammalian reovirus is beta interferon (IFN) independent and enhanced by IFN regulatory factor 3- and NF-κB-dependent expression of Noxa. *J. Virol.* 86, 1650–1660. <https://doi.org/10.1128/JVI.05924-11>
- Kobayashi, T., Chappell, J.D., Danthi, P., Dermody, T.S., 2006. Gene-Specific Inhibition of Reovirus Replication by RNA Interference. *J. Virol.* 80, 9053–9063. <https://doi.org/10.1128/JVI.00276-06>
- Kominsky, D.J., Bickel, R.J., Tyler, K.L., 2002. Reovirus-induced apoptosis requires both death receptor- and mitochondrial-mediated caspase-dependent pathways of cell death. *Cell Death Differ.* 9, 926–933. <https://doi.org/10.1038/sj.cdd.4401045>
- Komuro, A., Bamming, D., Horvath, C.M., 2008. Negative Regulation of Cytoplasmic RNA-Mediated Antiviral Signaling. *Cytokine* 43, 350–358. <https://doi.org/10.1016/j.cyto.2008.07.011>

- Komuro, A., Horvath, C.M., 2006. RNA- and virus-independent inhibition of antiviral signaling by RNA helicase LGP2. *J. Virol.* 80, 12332–12342. <https://doi.org/10.1128/JVI.01325-06>
- Kopf, M., Abel, B., Gallimore, A., Carroll, M., Bachmann, M.F., 2002. Complement component C3 promotes T-cell priming and lung migration to control acute influenza virus infection. *Nat. Med.* 8, 373–378. <https://doi.org/10.1038/nm0402-373>
- Kottke, T., Chester, J., Ilett, E., Thompson, J., Diaz, R., Coffey, M., Selby, P., Nuovo, G., Pulido, J., Mukhopadhyay, D., Pandha, H., Harrington, K., Melcher, A., Vile, R., 2011a. Precise scheduling of chemotherapy primes VEGF-producing tumors for successful systemic oncolytic virotherapy. *Mol. Ther. J. Am. Soc. Gene Ther.* 19, 1802–1812. <https://doi.org/10.1038/mt.2011.147>
- Kottke, T., Diaz, R.M., Kaluza, K., Pulido, J., Galivo, F., Wongthida, P., Thompson, J., Willmon, C., Barber, G.N., Chester, J., Selby, P., Strome, S., Harrington, K., Melcher, A., Vile, R.G., 2008. Use of biological therapy to enhance both virotherapy and adoptive T-cell therapy for cancer. *Mol. Ther. J. Am. Soc. Gene Ther.* 16, 1910–1918. <https://doi.org/10.1038/mt.2008.212>
- Kottke, T., Errington, F., Pulido, J., Galivo, F., Thompson, J., Wongthida, P., Diaz, R.M., Chong, H., Ilett, E., Chester, J., Pandha, H., Harrington, K., Selby, P., Melcher, A., Vile, R., 2011b. Broad antigenic coverage induced by vaccination with virus-based cDNA libraries cures established tumors. *Nat. Med.* 17, 854–859. <https://doi.org/10.1038/nm.2390>
- Kottke, T., Hall, G., Pulido, J., Diaz, R.M., Thompson, J., Chong, H., Selby, P., Coffey, M., Pandha, H., Chester, J., Melcher, A., Harrington, K., Vile, R., 2010. Antiangiogenic cancer therapy combined with oncolytic virotherapy leads to regression of established tumors in mice. *J. Clin. Invest.* 120, 1551–1560. <https://doi.org/10.1172/JCI41431>
- Kottke, T., Qiao, J., Diaz, R.M., Ahmed, A., Vroman, B., Thompson, J., Sanchez-Perez, L., Vile, R., 2006. The perforin-dependent immunological synapse allows T-cell activation-dependent tumor targeting by MLV vector particles. *Gene Ther.* 13, 1166–1177. <https://doi.org/10.1038/sj.gt.3302722>
- Kou, Z., Quinn, M., Chen, H., Rodrigo, W.W.S.I., Rose, R.C., Schlesinger, J.J., Jin, X., 2008. Monocytes, but not T or B cells, are the principal target cells for dengue virus (DV) infection among human peripheral blood mononuclear cells. *J. Med. Virol.* 80, 134–146. <https://doi.org/10.1002/jmv.21051>
- Kozak, R.A., Hattin, L., Biondi, M.J., Corredor, J.C., Walsh, S., Xue-Zhong, M., Manuel, J., McGilvray, I.D., Morgenstern, J., Lusty, E., Cherepanov, V., McBey, B.-A., Leishman, D., Feld, J.J., Bridle, B., Nagy, É., 2017. Replication and Oncolytic Activity of an Avian Orthoreovirus in Human Hepatocellular Carcinoma Cells. *Viruses* 9. <https://doi.org/10.3390/v9040090>
- Kuleshov, M.V., Jones, M.R., Rouillard, A.D., Fernandez, N.F., Duan, Q., Wang, Z., Koplev, S., Jenkins, S.L., Jagodnik, K.M., Lachmann, A., McDermott, M.G., Monteiro, C.D., Gundersen, G.W., Ma'ayan, A., 2016. Enrichr: a comprehensive gene set enrichment analysis web server 2016 update. *Nucleic Acids Res.* 44, W90-97. <https://doi.org/10.1093/nar/gkw377>

- Kumar, M.S., Lu, J., Mercer, K.L., Golub, T.R., Jacks, T., 2007. Impaired microRNA processing enhances cellular transformation and tumorigenesis. *Nat. Genet.* 39, 673–677. <https://doi.org/10.1038/ng2003>
- Kwissa, M., Nakaya, H.I., Onlamoon, N., Wrammert, J., Villinger, F., Perng, G.C., Yoksan, S., Pattanapanyasat, K., Chokephaibulkit, K., Ahmed, R., Pulendran, B., 2014. Dengue Virus Infection Induces Expansion of a CD14+CD16+ Monocyte Population that Stimulates Plasmablast Differentiation. *Cell Host Microbe* 16, 115–127. <https://doi.org/10.1016/j.chom.2014.06.001>
- Laborde, E.A., Vanzulli, S., Beigier-Bompadre, M., Isturiz, M.A., Ruggiero, R.A., Fourcade, M.G., Pellet, A.C.C., Sozzani, S., Vulcano, M., 2007. Immune Complexes Inhibit Differentiation, Maturation, and Function of Human Monocyte-Derived Dendritic Cells. *J. Immunol.* 179, 673–681. <https://doi.org/10.4049/jimmunol.179.1.673>
- Lafferty, K.J., Cunningham, A.J., 1975. A new analysis of allogeneic interactions. *Aust. J. Exp. Biol. Med. Sci.* 53, 27–42.
- Lai, C.M., Mainou, B.A., Kim, K.S., Dermody, T.S., 2013. Directional Release of Reovirus from the Apical Surface of Polarized Endothelial Cells. *mBio* 4, e00049-13. <https://doi.org/10.1128/mBio.00049-13>
- Lal, S., Raffel, C., 2017. Using Cystine Knot Proteins as a Novel Approach to Retarget Oncolytic Measles Virus. *Mol. Ther. Oncolytics* 7, 57–66. <https://doi.org/10.1016/j.omto.2017.09.005>
- Lang, P.A., Recher, M., Honke, N., Scheu, S., Borkens, S., Gailus, N., Krings, C., Meryk, A., Kulawik, A., Cervantes-Barragan, L., Van Rooijen, N., Kalinke, U., Ludewig, B., Hengartner, H., Harris, N., Häussinger, D., Ohashi, P.S., Zinkernagel, R.M., Lang, K.S., 2010. Tissue macrophages suppress viral replication and prevent severe immunopathology in an interferon-I-dependent manner in mice. *Hepatology* 52, 25–32. <https://doi.org/10.1002/hep.23640>
- Larkin, J., Ascierto, P.A., Dréno, B., Atkinson, V., Liskay, G., Maio, M., Mandalà, M., Demidov, L., Stroyakovskiy, D., Thomas, L., de la Cruz-Merino, L., Dutriaux, C., Garbe, C., Sovak, M.A., Chang, I., Choong, N., Hack, S.P., McArthur, G.A., Ribas, A., 2014. Combined vemurafenib and cobimetinib in BRAF-mutated melanoma. *N. Engl. J. Med.* 371, 1867–1876. <https://doi.org/10.1056/NEJMoa1408868>
- Larkin, J., Chiarion-Sileni, V., Gonzalez, R., Grob, J.J., Cowey, C.L., Lao, C.D., Schadendorf, D., Dummer, R., Smylie, M., Rutkowski, P., Ferrucci, P.F., Hill, A., Wagstaff, J., Carlino, M.S., Haanen, J.B., Maio, M., Marquez-Rodas, I., McArthur, G.A., Ascierto, P.A., Long, G.V., Callahan, M.K., Postow, M.A., Grossmann, K., Sznol, M., Dreno, B., Bastholt, L., Yang, A., Rollin, L.M., Horak, C., Hodi, F.S., Wolchok, J.D., 2015a. Combined Nivolumab and Ipilimumab or Monotherapy in Untreated Melanoma. *N. Engl. J. Med.* 373, 23–34. <https://doi.org/10.1056/NEJMoa1504030>
- Larkin, J., Lao, C.D., Urba, W.J., McDermott, D.F., Horak, C., Jiang, J., Wolchok, J.D., 2015b. Efficacy and Safety of Nivolumab in Patients With BRAF V600 Mutant and BRAF Wild-Type Advanced Melanoma: A Pooled Analysis of 4 Clinical Trials. *JAMA Oncol.* 1, 433–440. <https://doi.org/10.1001/jamaoncol.2015.1184>

- LaRocca, C.J., Han, J., Salzwedel, A.O., Davydova, J., Herzberg, M.C., Gopalakrishnan, R., Yamamoto, M., 2016. Oncolytic adenoviruses targeted to Human Papilloma Virus-positive head and neck squamous cell carcinomas. *Oral Oncol.* 56, 25–31. <https://doi.org/10.1016/j.oraloncology.2016.02.014>
- Larsen, S.K., Gao, Y., Basse, P.H., 2014. NK Cells in the Tumor Microenvironment. *Crit. Rev. Oncog.* 19, 91–105.
- Larson, C., Oronsky, B., Scicinski, J., Fanger, G.R., Stirn, M., Oronsky, A., Reid, T.R., 2015. Going viral: a review of replication-selective oncolytic adenoviruses. *Oncotarget* 6, 19976–19989.
- Lawson, D.H., Lee, S.J., Tarhini, A.A., Margolin, K.A., Ernstoff, M.S., Kirkwood, J.M., 2010. E4697: Phase III cooperative group study of yeast-derived granulocyte macrophage colony-stimulating factor (GM-CSF) versus placebo as adjuvant treatment of patients with completely resected stage III-IV melanoma. *J. Clin. Oncol.* 28, 8504–8504. [https://doi.org/10.1200/jco.2010.28.15\\_suppl.8504](https://doi.org/10.1200/jco.2010.28.15_suppl.8504)
- Le, D.T., Uram, J.N., Wang, H., Bartlett, B.R., Kemberling, H., Eyring, A.D., Skora, A.D., Luber, B.S., Azad, N.S., Laheru, D., Biedrzycki, B., Donehower, R.C., Zaheer, A., Fisher, G.A., Crocenzi, T.S., Lee, J.J., Duffy, S.M., Goldberg, R.M., de la Chapelle, A., Koshiji, M., Bhaijee, F., Huebner, T., Hruban, R.H., Wood, L.D., Cuka, N., Pardoll, D.M., Papadopoulos, N., Kinzler, K.W., Zhou, S., Cornish, T.C., Taube, J.M., Anders, R.A., Eshleman, J.R., Vogelstein, B., Diaz, L.A., 2015. PD-1 Blockade in Tumors with Mismatch-Repair Deficiency. *N. Engl. J. Med.* 372, 2509–2520. <https://doi.org/10.1056/NEJMoa1500596>
- Le Roux, D., Le Bon, A., Dumas, A., Taleb, K., Sachse, M., Sikora, R., Julithe, M., Benmerah, A., Bismuth, G., Niedergang, F., 2012. Antigen stored in dendritic cells after macropinocytosis is released unprocessed from late endosomes to target B cells. *Blood* 119, 95–105. <https://doi.org/10.1182/blood-2011-02-336123>
- Lech, P.J., Pappoe, R., Nakamura, T., Russell, S.J., 2014. Antibody neutralization of retargeted measles viruses. *Virology* 454, 237–246. <https://doi.org/10.1016/j.virol.2014.01.027>
- Lee, H.K., Jeong, Y.S., 2004. Comparison of Total Culturable Virus Assay and Multiplex Integrated Cell Culture-PCR for Reliability of Waterborne Virus Detection. *Appl. Environ. Microbiol.* 70, 3632–3636. <https://doi.org/10.1128/AEM.70.6.3632-3636.2004>
- Lee, M.S., Kim, B., Oh, G.T., Kim, Y.-J., 2013. OASL1 inhibits translation of the type I interferon-regulating transcription factor IRF7. *Nat. Immunol.* 14, 346–355. <https://doi.org/10.1038/ni.2535>
- Leek, R.D., Landers, R.J., Harris, A.L., Lewis, C.E., 1999. Necrosis correlates with high vascular density and focal macrophage infiltration in invasive carcinoma of the breast. *Br. J. Cancer* 79, 991–995. <https://doi.org/10.1038/sj.bjc.6690158>
- Leers, W.D., Rozee, K.R., 1966. A survey of reovirus antibodies in sera of urban children. *Can. Med. Assoc. J.* 94, 1040–1042.
- Lehrman, S., 1999. Virus treatment questioned after gene therapy death [WWW Document]. *Nature*. <https://doi.org/10.1038/43977>

- Lelli, D., Beato, M.S., Cavicchio, L., Lavazza, A., Chiapponi, C., Leopardi, S., Baioni, L., De Benedictis, P., Moreno, A., 2016. First identification of mammalian orthoreovirus type 3 in diarrheic pigs in Europe. *Viol. J.* 13, 139. <https://doi.org/10.1186/s12985-016-0593-4>
- Lennerz, V., Fatho, M., Gentilini, C., Frye, R.A., Lifke, A., Ferel, D., Wölfel, C., Huber, C., Wölfel, T., 2005. The response of autologous T cells to a human melanoma is dominated by mutated neoantigens. *Proc. Natl. Acad. Sci. U. S. A.* 102, 16013–16018. <https://doi.org/10.1073/pnas.0500090102>
- Leopold, P.L., Wendland, R.L., Vincent, T., Crystal, R.G., 2006. Neutralized adenovirus-immune complexes can mediate effective gene transfer via an Fc receptor-dependent infection pathway. *J. Virol.* 80, 10237–10247. <https://doi.org/10.1128/JVI.00512-06>
- Lerner, A.M., Cherry, J.D., Klein, J.O., Finland, M., 1962. Infections with reoviruses. *N. Engl. J. Med.* 267, 947–952. <https://doi.org/10.1056/NEJM196211082671901>
- Levaditi, C., Nicolau, S., 1922. Sur le culture du virus vaccinal dans les neoplasmes epithelieux. *CR Soc Biol* 86, 928.
- Li, J.K., Scheible, P.P., Keene, J.D., Joklik, W.K., 1980. The plus strand of reovirus gene S2 is identical with its in vitro transcript. *Virology* 105, 282–286.
- Li, X., Wang, P., Li, H., Du, X., Liu, M., Huang, Q., Wang, Y., Wang, S., 2017. The Efficacy of Oncolytic Adenovirus Is Mediated by T-cell Responses against Virus and Tumor in Syrian Hamster Model. *Clin. Cancer Res. Off. J. Am. Assoc. Cancer Res.* 23, 239–249. <https://doi.org/10.1158/1078-0432.CCR-16-0477>
- Liew, K.J.L., Chow, V.T.K., 2006. Microarray and real-time RT-PCR analyses of a novel set of differentially expressed human genes in ECV304 endothelial-like cells infected with dengue virus type 2. *J. Virol. Methods* 131, 47–57. <https://doi.org/10.1016/j.jviromet.2005.07.003>
- Linard, B., Bézieau, S., Benlalam, H., Labarrière, N., Guilloux, Y., Diez, E., Jotereau, F., 2002. A ras-Mutated Peptide Targeted by CTL Infiltrating a Human Melanoma Lesion. *J. Immunol.* 168, 4802–4808. <https://doi.org/10.4049/jimmunol.168.9.4802>
- Linch, S.N., McNamara, M.J., Redmond, W.L., 2015. OX40 Agonists and Combination Immunotherapy: Putting the Pedal to the Metal. *Front. Oncol.* 5, 34. <https://doi.org/10.3389/fonc.2015.00034>
- Linette, G.P., Hamid, O., Whitman, E.D., Nemunaitis, J.J., Chesney, J., Agarwala, S.S., Starodub, A., Barrett, J.A., Marsh, A., Martell, L.A., Cho, A., Reed, T.D., Youssoufian, H., Vergara-Silva, A., 2013. A phase I open-label study of Ad-RTS-hIL-12, an adenoviral vector engineered to express hIL-12 under the control of an oral activator ligand, in subjects with unresectable stage III/IV melanoma. *J. Clin. Oncol.* 31, 3022–3022. [https://doi.org/10.1200/jco.2013.31.15\\_suppl.3022](https://doi.org/10.1200/jco.2013.31.15_suppl.3022)
- Liu, B., Mink, S., Wong, K.A., Stein, N., Getman, C., Dempsey, P.W., Wu, H., Shuai, K., 2004. PIAS1 selectively inhibits interferon-inducible genes and is important in innate immunity. *Nat. Immunol.* 5, 891–898. <https://doi.org/10.1038/ni1104>
- Liu, B.L., Robinson, M., Han, Z.-Q., Branston, R.H., English, C., Reay, P., McGrath, Y., Thomas, S.K., Thornton, M., Bullock, P., Love, C.A., Coffin, R.S., 2003. ICP34.5 deleted herpes simplex virus with enhanced oncolytic, immune stimulating, and

- anti-tumour properties. *Gene Ther.* 10, 292–303.  
<https://doi.org/10.1038/sj.gt.3301885>
- Liu, C., Russell, S.J., Peng, K.-W., 2010. Systemic therapy of disseminated myeloma in passively immunized mice using measles virus-infected cell carriers. *Mol. Ther. J. Am. Soc. Gene Ther.* 18, 1155–1164. <https://doi.org/10.1038/mt.2010.43>
- Ljunggren, H.G., Kärre, K., 1985. Host resistance directed selectively against H-2-deficient lymphoma variants. Analysis of the mechanism. *J. Exp. Med.* 162, 1745–1759.
- Lolkema, M.P., Arkenau, H.-T., Harrington, K., Roxburgh, P., Morrison, R., Roulstone, V., Twigger, K., Coffey, M., Mettinger, K., Gill, G., Evans, T.R.J., de Bono, J.S., 2011. A phase I study of the combination of intravenous reovirus type 3 Dearing and gemcitabine in patients with advanced cancer. *Clin. Cancer Res. Off. J. Am. Assoc. Cancer Res.* 17, 581–588. <https://doi.org/10.1158/1078-0432.CCR-10-2159>
- London, N.J., Farmery, S.M., Lodge, J.P.A., Will, E.J., Davidson, A.M., 1995. Risk of neoplasia in renal transplant patients. *The Lancet* 346, 403–406.  
[https://doi.org/10.1016/S0140-6736\(95\)92780-8](https://doi.org/10.1016/S0140-6736(95)92780-8)
- Long, G.V., Dummer, R., Ribas, A., Puzanov, I., VanderWalde, A., Andtbacka, R.H.I., Michielin, O., Olszanski, A.J., Malvehy, J., Cebon, J.S., Fernandez, E., Kirkwood, J.M., Gajewski, T., Gause, C.K., Chen, L., Gorski, K., Anderson, A., Kaufman, D.R., Chou, J., Hodi, F.S., 2016. Efficacy analysis of MASTERKEY-265 phase 1b study of talimogene laherparepvec (T-VEC) and pembrolizumab (pembro) for unresectable stage IIIB-IV melanoma. *J. Clin. Oncol.* 34, 9568–9568.  
[https://doi.org/10.1200/JCO.2016.34.15\\_suppl.9568](https://doi.org/10.1200/JCO.2016.34.15_suppl.9568)
- Long, G.V., Stroyakovskiy, D., Gogas, H., Levchenko, E., de Braud, F., Larkin, J., Garbe, C., Jouary, T., Hauschild, A., Grob, J.-J., Chiarion-Sileni, V., Lebbe, C., Mandalà, M., Millward, M., Arance, A., Bondarenko, I., Haanen, J.B.A.G., Hansson, J., Utikal, J., Ferraresi, V., Kovalenko, N., Mohr, P., Probachai, V., Schadendorf, D., Nathan, P., Robert, C., Ribas, A., DeMarini, D.J., Irani, J.G., Swann, S., Legos, J.J., Jin, F., Mookerjee, B., Flaherty, K., 2015. Dabrafenib and trametinib versus dabrafenib and placebo for Val600 BRAF-mutant melanoma: a multicentre, double-blind, phase 3 randomised controlled trial. *Lancet Lond. Engl.* 386, 444–451. [https://doi.org/10.1016/S0140-6736\(15\)60898-4](https://doi.org/10.1016/S0140-6736(15)60898-4)
- Loo, Y.-M., Fornek, J., Crochet, N., Bajwa, G., Perwitasari, O., Martinez-Sobrido, L., Akira, S., Gill, M.A., García-Sastre, A., Katze, M.G., Gale, M., 2008. Distinct RIG-I and MDA5 signaling by RNA viruses in innate immunity. *J. Virol.* 82, 335–345.  
<https://doi.org/10.1128/JVI.01080-07>
- López, C.B., Moltedo, B., Alexopoulou, L., Bonifaz, L., Flavell, R.A., Moran, T.M., 2004. TLR-independent induction of dendritic cell maturation and adaptive immunity by negative-strand RNA viruses. *J. Immunol. Baltim. Md 1950* 173, 6882–6889.
- Lowin, B., Peitsch, M.C., Tschopp, J., 1995. Perforin and granzymes: crucial effector molecules in cytolytic T lymphocyte and natural killer cell-mediated cytotoxicity. *Curr. Top. Microbiol. Immunol.* 198, 1–24.
- Lu, W., Zheng, S., Li, X.-F., Huang, J.-J., Zheng, X., Li, Z., 2004. Intra-tumor injection of H101, a recombinant adenovirus, in combination with chemotherapy in patients

- with advanced cancers: a pilot phase II clinical trial. *World J. Gastroenterol.* 10, 3634–3638.
- Lui, P., Cashin, R., Machado, M., Hemels, M., Corey-Lisle, P.K., Einarson, T.R., 2007. Treatments for metastatic melanoma: synthesis of evidence from randomized trials. *Cancer Treat. Rev.* 33, 665–680. <https://doi.org/10.1016/j.ctrv.2007.06.004>
- Lyons, M., Onion, D., Green, N.K., Aslan, K., Rajaratnam, R., Bazan-Peregrino, M., Phipps, S., Hale, S., Mautner, V., Seymour, L.W., Fisher, K.D., 2006. Adenovirus type 5 interactions with human blood cells may compromise systemic delivery. *Mol. Ther. J. Am. Soc. Gene Ther.* 14, 118–128. <https://doi.org/10.1016/j.ymthe.2006.01.003>
- Mackall, C.L., 1999. T-Cell Immunodeficiency Following Cytotoxic Antineoplastic Therapy: A Review. *The Oncologist* 4, 370–378.
- Mackie, R.M., Stewart, B., Brown, S.M., 2001. Intralesional injection of herpes simplex virus 1716 in metastatic melanoma. *Lancet Lond. Engl.* 357, 525–526. [https://doi.org/10.1016/S0140-6736\(00\)04048-4](https://doi.org/10.1016/S0140-6736(00)04048-4)
- Mader, E.K., Maeyama, Y., Lin, Y., Butler, G.W., Russell, H.M., Galanis, E., Russell, S.J., Dietz, A.B., Peng, K.-W., 2009. Mesenchymal stem cell carriers protect oncolytic measles viruses from antibody neutralization in an orthotopic ovarian cancer therapy model. *Clin. Cancer Res. Off. J. Am. Assoc. Cancer Res.* 15, 7246–7255. <https://doi.org/10.1158/1078-0432.CCR-09-1292>
- Magge, D., Guo, Z.S., O'Malley, M.E., Francis, L., Ravindranathan, R., Bartlett, D.L., 2013. Inhibitors of C5 complement enhance vaccinia virus oncolysis. *Cancer Gene Ther.* 20, 342–350. <https://doi.org/10.1038/cgt.2013.26>
- Maginnis, M.S., Forrest, J.C., Kopecky-Bromberg, S.A., Dickeson, S.K., Santoro, S.A., Zutter, M.M., Nemerow, G.R., Bergelson, J.M., Dermody, T.S., 2006. 1 Integrin Mediates Internalization of Mammalian Reovirus. *J. Virol.* 80, 2760–2770. <https://doi.org/10.1128/JVI.80.6.2760-2770.2006>
- Mahalingam, D., Fountzilias, C., Moseley, J., Noronha, N., Tran, H., Chakrabarty, R., Selvaggi, G., Coffey, M., Thompson, B., Sarantopoulos, J., 2017a. A phase II study of REOLYSIN® (pelareorep) in combination with carboplatin and paclitaxel for patients with advanced malignant melanoma. *Cancer Chemother. Pharmacol.* 79, 697–703. <https://doi.org/10.1007/s00280-017-3260-6>
- Mahalingam, D., Fountzilias, C., Moseley, J.L., Noronha, N., Cheetham, K., Dzugalo, A., Nuovo, G., Gutierrez, A., Arora, S.P., 2017b. A study of REOLYSIN in combination with pembrolizumab and chemotherapy in patients (pts) with relapsed metastatic adenocarcinoma of the pancreas (MAP). *J. Clin. Oncol.* 35, e15753–e15753. [https://doi.org/10.1200/JCO.2017.35.15\\_suppl.e15753](https://doi.org/10.1200/JCO.2017.35.15_suppl.e15753)
- Mahon, P.J., Mirza, A.M., Iorio, R.M., 2011. Role of the Two Sialic Acid Binding Sites on the Newcastle Disease Virus HN Protein in Triggering the Interaction with the F Protein Required for the Promotion of Fusion. *J. Virol.* 85, 12079–12082. <https://doi.org/10.1128/JVI.05679-11>
- Mainou, B.A., Dermody, T.S., Aug 2012a. Transport to late endosomes is required for efficient reovirus infection. *J. Virol.* 86, 8346–8358. <https://doi.org/10.1128/JVI.00100-12>

- Mainou, B.A., Dermody, T.S., Dec 2012b. In search of cathepsins: how reovirus enters host cells. *DNA Cell Biol.* 31, 1646–1649. <https://doi.org/10.1089/dna.2012.1868>
- Maio, M., Grob, J.-J., Aamdal, S., Bondarenko, I., Robert, C., Thomas, L., Garbe, C., Chiarion-Sileni, V., Testori, A., Chen, T.-T., Tschaika, M., Wolchok, J.D., 2015. Five-Year Survival Rates for Treatment-Naive Patients With Advanced Melanoma Who Received Ipilimumab Plus Dacarbazine in a Phase III Trial. *J. Clin. Oncol.* 33, 1191–1196. <https://doi.org/10.1200/JCO.2014.56.6018>
- Malergue, F., Galland, F., Martin, F., Mansuelle, P., Aurrand-Lions, M., Naquet, P., 1998. A novel immunoglobulin superfamily junctional molecule expressed by antigen presenting cells, endothelial cells and platelets. *Mol. Immunol.* 35, 1111–1119.
- Mandarà, M., Nortilli, R., Sava, T., Cetto, G.L., 2006. Chemotherapy for metastatic melanoma. *Expert Rev. Anticancer Ther.* 6, 121–130. <https://doi.org/10.1586/14737140.6.1.121>
- Mari, N., Hercor, M., Denanglaire, S., Leo, O., Andris, F., 2013. The capacity of Th2 lymphocytes to deliver B-cell help requires expression of the transcription factor STAT3. *Eur. J. Immunol.* 43, 1489–1498. <https://doi.org/10.1002/eji.201242938>
- Markert, J.M., Razdan, S.N., Kuo, H.-C., Cantor, A., Knoll, A., Karrasch, M., Nabors, L.B., Markiewicz, M., Agee, B.S., Coleman, J.M., Lakeman, A.D., Palmer, C.A., Parker, J.N., Whitley, R.J., Weichselbaum, R.R., Fiveash, J.B., Gillespie, G.Y., 2014. A phase 1 trial of oncolytic HSV-1, G207, given in combination with radiation for recurrent GBM demonstrates safety and radiographic responses. *Mol. Ther. J. Am. Soc. Gene Ther.* 22, 1048–1055. <https://doi.org/10.1038/mt.2014.22>
- Martuza, R.L., Malick, A., Markert, J.M., Ruffner, K.L., Coen, D.M., 1991. Experimental therapy of human glioma by means of a genetically engineered virus mutant. *Science* 252, 854–856.
- Masciopinto, F., Giovani, C., Campagnoli, S., Galli-Stampino, L., Colombatto, P., Brunetto, M., Yen, T.S.B., Houghton, M., Pileri, P., Abrignani, S., 2004. Association of hepatitis C virus envelope proteins with exosomes. *Eur. J. Immunol.* 34, 2834–2842. <https://doi.org/10.1002/eji.200424887>
- Matsuura, K., Ishikura, M., Nakayama, T., Hasegawa, S., Morita, O., Uetake, H., 1988. Ecological Studies on Reovirus Pollution of Rivers in Toyama Prefecture. *Microbiol. Immunol.* 32, 1221–1234. <https://doi.org/10.1111/j.1348-0421.1988.tb01486.x>
- Matzinger, P., 2002. The danger model: a renewed sense of self. *Science* 296, 301–305. <https://doi.org/10.1126/science.1071059>
- Matzinger, P., 1998. An innate sense of danger. *Semin. Immunol.* 10, 399–415. <https://doi.org/10.1006/smim.1998.0143>
- Matzinger, P., 1994. Tolerance, danger, and the extended family. *Annu. Rev. Immunol.* 12, 991–1045. <https://doi.org/10.1146/annurev.iy.12.040194.005015>
- Maurer, G., Tarkowski, B., Baccarini, M., 2011. Raf kinases in cancer-roles and therapeutic opportunities. *Oncogene* 30, 3477–3488. <https://doi.org/10.1038/onc.2011.160>

- McDermott, D., Haanen, J., Chen, T.-T., Lorigan, P., O'Day, S., MDX010-20 Investigators, 2013. Efficacy and safety of ipilimumab in metastatic melanoma patients surviving more than 2 years following treatment in a phase III trial (MDX010-20). *Ann. Oncol. Off. J. Eur. Soc. Med. Oncol.* 24, 2694–2698. <https://doi.org/10.1093/annonc/mdt291>
- McDermott, M.R., Brais, L.J., Eveleigh, M.J., 1990. Mucosal and systemic antiviral antibodies in mice inoculated intravaginally with herpes simplex virus type 2. *J. Gen. Virol.* 71 ( Pt 7), 1497–1504. <https://doi.org/10.1099/0022-1317-71-7-1497>
- McDonald, S.M., Patton, J.T., 2011. Assortment and packaging of the segmented rotavirus genome. *Trends Microbiol.* 19, 136–144. <https://doi.org/10.1016/j.tim.2010.12.002>
- McEwan, W.A., Tam, J.C.H., Watkinson, R.E., Bidgood, S.R., Mallery, D.L., James, L.C., 2013. Intracellular antibody-bound pathogens stimulate immune signaling via the Fc receptor TRIM21. *Nat. Immunol.* 14, 327–336. <https://doi.org/10.1038/ni.2548>
- McGranahan, N., Furness, A.J.S., Rosenthal, R., Ramskov, S., Lyngaa, R., Saini, S.K., Jamal-Hanjani, M., Wilson, G.A., Birkbak, N.J., Hiley, C.T., Watkins, T.B.K., Shafi, S., Murugaesu, N., Mitter, R., Akarca, A.U., Linares, J., Marafioti, T., Henry, J.Y., Van Allen, E.M., Miao, D., Schilling, B., Schadendorf, D., Garraway, L.A., Makarov, V., Rizvi, N.A., Snyder, A., Hellmann, M.D., Merghoub, T., Wolchok, J.D., Shukla, S.A., Wu, C.J., Peggs, K.S., Chan, T.A., Hadrup, S.R., Quezada, S.A., Swanton, C., 2016. Clonal neoantigens elicit T cell immunoreactivity and sensitivity to immune checkpoint blockade. *Science* 351, 1463–1469. <https://doi.org/10.1126/science.aaf1490>
- Medzhitov, R., Janeway, C.A., 2002. Decoding the patterns of self and nonself by the innate immune system. *Science* 296, 298–300. <https://doi.org/10.1126/science.1068883>
- Mehlen, P., Puisieux, A., 2006. Metastasis: a question of life or death. *Nat. Rev. Cancer* 6, 449–458. <https://doi.org/10.1038/nrc1886>
- Melcher, A., Parato, K., Rooney, C.M., Bell, J.C., 2011. Thunder and lightning: immunotherapy and oncolytic viruses collide. *Mol. Ther. J. Am. Soc. Gene Ther.* 19, 1008–1016. <https://doi.org/10.1038/mt.2011.65>
- Mezo, A.R., McDonnell, K.A., Hehir, C.A.T., Low, S.C., Palombella, V.J., Stattel, J.M., Kamphaus, G.D., Fraley, C., Zhang, Y., Dumont, J.A., Bitonti, A.J., 2008. Reduction of IgG in nonhuman primates by a peptide antagonist of the neonatal Fc receptor FcRn. *Proc. Natl. Acad. Sci. U. S. A.* 105, 2337–2342. <https://doi.org/10.1073/pnas.0708960105>
- Middleton, M.R., Grob, J.J., Aaronson, N., Fierlbeck, G., Tilgen, W., Seiter, S., Gore, M., Aamdal, S., Cebon, J., Coates, A., Dreno, B., Henz, M., Schadendorf, D., Kapp, A., Weiss, J., Fraass, U., Statkevich, P., Muller, M., Thatcher, N., 2000. Randomized phase III study of temozolomide versus dacarbazine in the treatment of patients with advanced metastatic malignant melanoma. *J. Clin. Oncol. Off. J. Am. Soc. Clin. Oncol.* 18, 158–166. <https://doi.org/10.1200/JCO.2000.18.1.158>
- Miest, T.S., Yaiw, K.-C., Frenzke, M., Lampe, J., Hudacek, A.W., Springfield, C., von Messling, V., Ungerechts, G., Cattaneo, R., 2011. Envelope-chimeric entry-

- targeted measles virus escapes neutralization and achieves oncolysis. *Mol. Ther. J. Am. Soc. Gene Ther.* 19, 1813–1820. <https://doi.org/10.1038/mt.2011.92>
- Miller, C.G., Fraser, N.W., 2000. Role of the immune response during neuro-attenuated herpes simplex virus-mediated tumor destruction in a murine intracranial melanoma model. *Cancer Res.* 60, 5714–5722.
- Minuk, G.Y., Paul, R.W., Lee, P.W., 1985. The prevalence of antibodies to reovirus type 3 in adults with idiopathic cholestatic liver disease. *J. Med. Virol.* 16, 55–60.
- Minuk, G.Y., Rascenin, N., Paul, R.W., Lee, P.W., Buchan, K., Kelly, J.K., 1987. Reovirus type 3 infection in patients with primary biliary cirrhosis and primary sclerosing cholangitis. *J. Hepatol.* 5, 8–13.
- Miracco, C., Mourmouras, V., Biagioli, M., Rubegni, P., Mannucci, S., Monciatti, I., Cosci, E., Tosi, P., Luzi, P., 2007. Utility of tumour-infiltrating CD25+FOXP3+ regulatory T cell evaluation in predicting local recurrence in vertical growth phase cutaneous melanoma. *Oncol. Rep.* 18, 1115–1122.
- Mita, A., Sankhala, K., Sarantopoulos, J., 2009. A phase II study of intravenous (IV) wild-type reovirus (Reolysin) in the treatment of patients with bone and soft tissue sarcomas metastatic to the lung, in: *Journal of Clinical Oncology*. Presented at the 2009 ASCO Annual Meeting, p. 15s.
- Mita, A.C., Argiris, A., Coffey, M., Gill, G., Mita, M., 2013. Abstract C70: A phase 2 study of intravenous administration of REOLYSIN® (reovirus type 3 dearing) in combination with paclitaxel (P) and carboplatin (C) in patients with squamous cell carcinoma of the lung. *Mol. Cancer Ther.* 12, C70–C70. <https://doi.org/10.1158/1535-7163.TARG-13-C70>
- Mittendorf, E.A., Storrer, C.E., Shriver, C.D., Ponniah, S., Peoples, G.E., 2005. Evaluation of the CD107 cytotoxicity assay for the detection of cytolytic CD8+ cells recognizing HER2/neu vaccine peptides. *Breast Cancer Res. Treat.* 92, 85–93. <https://doi.org/10.1007/s10549-005-0988-1>
- Mohamed, A., Johnston, R.N., Shmulevitz, M., 2015. Potential for Improving Potency and Specificity of Reovirus Oncolysis with Next-Generation Reovirus Variants. *Viruses* 7, 6251–6278. <https://doi.org/10.3390/v7122936>
- Moore, A.E., 1952. Viruses with Oncolytic Properties and Their Adaptation to Tumors. *Ann. N. Y. Acad. Sci.* 54, 945–952. <https://doi.org/10.1111/j.1749-6632.1952.tb39969.x>
- Moore, A.E., 1951. Inhibition of growth of five transplantable mouse tumors by the virus of Russian Far East encephalitis. *Cancer* 4, 375–382.
- Moore, A.E., 1949. The destructive effect of the virus of Russian Far East encephalitis on the transplantable mouse sarcoma 180. *Cancer* 2, 525–534.
- Morecki, R., Glaser, J.H., Cho, S., Balistreri, W.F., Horwitz, M.S., 1982. Biliary atresia and reovirus type 3 infection. *N. Engl. J. Med.* 307, 481–484. <https://doi.org/10.1056/NEJM198208193070806>
- Mori, S., Takeuchi, T., Kanda, T., 2008. Antibody-dependent enhancement of adeno-associated virus infection of human monocytic cell lines. *Virology* 375, 141–147. <https://doi.org/10.1016/j.virol.2008.01.033>

- Morris, D., Tu, D., Tehfe, M.A., Nicholas, G.A., Goffin, J.R., Gregg, R.W., Shepherd, F.A., Murray, N., Wierzbicki, R., Lee, C.W., Kuruvilla, S., Keith, B., Ahmed, A., Blais, N., Goss, G.D., Korpanty, G., Sederias, J., Laurie, S.A., Seymour, L., Bradbury, P.A., 2016. A Randomized Phase II study of Reolysin in Patients with Previously Treated Advanced or Metastatic Non Small Cell Lung Cancer (NSCLC) receiving Standard Salvage Chemotherapy – Canadian Cancer Trials Group IND 211. *J. Clin. Oncol.* 34, e20512–e20512. [https://doi.org/10.1200/JCO.2016.34.15\\_suppl.e20512](https://doi.org/10.1200/JCO.2016.34.15_suppl.e20512)
- Morris, D.G., Feng, X., DiFrancesco, L.M., Fonseca, K., Forsyth, P.A., Paterson, A.H., Coffey, M.C., Thompson, B., 2013. REO-001: A phase I trial of percutaneous intralesional administration of reovirus type 3 dearing (Reolysin®) in patients with advanced solid tumors. *Invest. New Drugs* 31, 696–706. <https://doi.org/10.1007/s10637-012-9865-z>
- Morse, M.A., Chaudhry, A., Gabitzsch, E.S., Hobeika, A.C., Osada, T., Clay, T.M., Amalfitano, A., Burnett, B.K., Devi, G.R., Hsu, D.S., Xu, Y., Balcitis, S., Dua, R., Nguyen, S., Balint, J.P., Jones, F.R., Lyerly, H.K., 2013. Novel adenoviral vector induces T-cell responses despite anti-adenoviral neutralizing antibodies in colorectal cancer patients. *Cancer Immunol. Immunother.* CII 62, 1293–1301. <https://doi.org/10.1007/s00262-013-1400-3>
- Mosmann, T., 1983. Rapid colorimetric assay for cellular growth and survival: application to proliferation and cytotoxicity assays. *J. Immunol. Methods* 65, 55–63.
- Muthana, M., Giannoudis, A., Scott, S.D., Fang, H.-Y., Coffelt, S.B., Morrow, F.J., Murdoch, C., Burton, J., Cross, N., Burke, B., Mistry, R., Hamdy, F., Brown, N.J., Georgopoulos, L., Hoskin, P., Essand, M., Lewis, C.E., Maitland, N.J., 2011. Use of macrophages to target therapeutic adenovirus to human prostate tumors. *Cancer Res.* 71, 1805–1815. <https://doi.org/10.1158/0008-5472.CAN-10-2349>
- Muthana, M., Rodrigues, S., Chen, Y.-Y., Welford, A., Hughes, R., Tazzyman, S., Essand, M., Morrow, F., Lewis, C.E., 2013. Macrophage delivery of an oncolytic virus abolishes tumor regrowth and metastasis after chemotherapy or irradiation. *Cancer Res.* 73, 490–495. <https://doi.org/10.1158/0008-5472.CAN-12-3056>
- National Comprehensive Cancer Network, 2017. NCCN guidelines v1. Accessed on 19 March 2018 at [https://www.nccn.org/professionals/physician\\_gls/pdf/melanoma.pdf](https://www.nccn.org/professionals/physician_gls/pdf/melanoma.pdf).
- Nemunaitis, J., Khuri, F., Ganly, I., Arseneau, J., Posner, M., Vokes, E., Kuhn, J., McCarty, T., Landers, S., Blackburn, A., Romel, L., Randlev, B., Kaye, S., Kirn, D., 2001. Phase II trial of intratumoral administration of ONYX-015, a replication-selective adenovirus, in patients with refractory head and neck cancer. *J. Clin. Oncol. Off. J. Am. Soc. Clin. Oncol.* 19, 289–298. <https://doi.org/10.1200/JCO.2001.19.2.289>
- Nibert, M.L., Odegard, A.L., Agosto, M.A., Chandran, K., Schiff, L.A., 2005. Putative autocleavage of reovirus mu1 protein in concert with outer-capsid disassembly and activation for membrane permeabilization. *J. Mol. Biol.* 345, 461–474. <https://doi.org/10.1016/j.jmb.2004.10.026>
- Nimmerjahn, F., Ravetch, J.V., 2008. Fcγ receptors as regulators of immune responses. *Nat. Rev. Immunol.* 8, 34–47. <https://doi.org/10.1038/nri2206>

- Nizar, S., Meyer, B., Galustian, C., Kumar, D., Dalgleish, A., 2010. T regulatory cells, the evolution of targeted immunotherapy. *Biochim. Biophys. Acta* 1806, 7–17. <https://doi.org/10.1016/j.bbcan.2010.02.001>
- Noonan, A.M., Farren, M.R., Geyer, S.M., Huang, Y., Tahiri, S., Ahn, D., Mikhail, S., Ciombor, K.K., Pant, S., Aparo, S., Sexton, J., Marshall, J.L., Mace, T.A., Wu, C.S., El-Rayes, B., Timmers, C.D., Zwiebel, J., Lesinski, G.B., Villalona-Calero, M.A., Bekaii-Saab, T.S., 2016. Randomized Phase 2 Trial of the Oncolytic Virus Pelareorep (Reolysin) in Upfront Treatment of Metastatic Pancreatic Adenocarcinoma. *Mol. Ther. J. Am. Soc. Gene Ther.* 24, 1150–1158. <https://doi.org/10.1038/mt.2016.66>
- Norman, K.L., Coffey, M.C., Hirasawa, K., Demetrick, D.J., Nishikawa, S.G., DiFrancesco, L.M., Strong, J.E., Lee, P.W.K., 2002. Reovirus oncolysis of human breast cancer. *Hum. Gene Ther.* 13, 641–652. <https://doi.org/10.1089/10430340252837233>
- Norman, K.L., Hirasawa, K., Yang, A.-D., Shields, M.A., Lee, P.W.K., 2004. Reovirus oncolysis: the Ras/RalGEF/p38 pathway dictates host cell permissiveness to reovirus infection. *Proc. Natl. Acad. Sci. U. S. A.* 101, 11099–11104. <https://doi.org/10.1073/pnas.0404310101>
- Noyce, R.S., Collins, S.E., Mossman, K.L., 2006. Identification of a novel pathway essential for the immediate-early, interferon-independent antiviral response to enveloped virions. *J. Virol.* 80, 226–235. <https://doi.org/10.1128/JVI.80.1.226-235.2006>
- Noyce, R.S., Taylor, K., Ciechonska, M., Collins, S.E., Duncan, R., Mossman, K.L., 2011. Membrane perturbation elicits an IRF3-dependent, interferon-independent antiviral response. *J. Virol.* 85, 10926–10931. <https://doi.org/10.1128/JVI.00862-11>
- Oba, J., Nakahara, T., Abe, T., Hagihara, A., Moroi, Y., Furue, M., 2014. Expression of programmed death receptor ligand 1 in melanoma may indicate tumor progression and poor patient survival. *J. Am. Acad. Dermatol.* 70, 954–956. <https://doi.org/10.1016/j.jaad.2014.01.880>
- Oble, D.A., Loewe, R., Yu, P., Mihm, M.C., 2009. Focus on TILs: prognostic significance of tumor infiltrating lymphocytes in human melanoma. *Cancer Immun.* 9, 3.
- O'Byrne, K.J., Gatzemeier, U., Bondarenko, I., Barrios, C., Eschbach, C., Martens, U.M., Hotko, Y., Kortsik, C., Paz-Ares, L., Pereira, J.R., von Pawel, J., Ramlau, R., Roh, J.-K., Yu, C.-T., Stroh, C., Celik, I., Schueler, A., Pirker, R., 2011. Molecular biomarkers in non-small-cell lung cancer: a retrospective analysis of data from the phase 3 FLEX study. *Lancet Oncol.* 12, 795–805. [https://doi.org/10.1016/S1470-2045\(11\)70189-9](https://doi.org/10.1016/S1470-2045(11)70189-9)
- Ocean, A.J., Bekaii-Saab, T.S., Chaudhary, I., Palmer, R., Christos, P.J., Mercado, A., Florendo, E.O., Rosales, V.A., Ruggiero, J.T., Popa, E.C., Wilson, M., Ghalib, M.H., Hou, Y., Shah, U., Rajdev, L., Elrafei, T., Gill, G.M., Coffey, M.C., Shah, M.A., Goel, S., 2013. A multicenter phase I study of intravenous administration of reolysin in combination with irinotecan/fluorouracil/leucovorin (FOLFIRI) in patients (pts) with oxaliplatin-refractory/intolerant KRAS-mutant metastatic colorectal cancer (mCRC). *J. Clin. Oncol.* 31, 450–450. [https://doi.org/10.1200/jco.2013.31.4\\_suppl.450](https://doi.org/10.1200/jco.2013.31.4_suppl.450)

- Odegard, A.L., Chandran, K., Zhang, X., Parker, J.S.L., Baker, T.S., Nibert, M.L., 2004. Putative autocleavage of outer capsid protein micro1, allowing release of myristoylated peptide micro1N during particle uncoating, is critical for cell entry by reovirus. *J. Virol.* 78, 8732–8745. <https://doi.org/10.1128/JVI.78.16.8732-8745.2004>
- Oganesyan, G., Saha, S.K., Guo, B., He, J.Q., Shahangian, A., Zarnegar, B., Perry, A., Cheng, G., 2006. Critical role of TRAF3 in the Toll-like receptor-dependent and -independent antiviral response. *Nature* 439, 208–211. <https://doi.org/10.1038/nature04374>
- Ogbomo, H., Zemp, F.J., Lun, X., Zhang, J., Stack, D., Rahman, M.M., McFadden, G., Mody, C.H., Forsyth, P.A., 2013. Myxoma virus infection promotes NK lysis of malignant gliomas in vitro and in vivo. *PLoS One* 8, e66825. <https://doi.org/10.1371/journal.pone.0066825>
- Olofsson, S., Bergström, T., 2005. Glycoconjugate glycans as viral receptors. *Ann. Med.* 37, 154–172. <https://doi.org/10.1080/07853890510007340>
- Oshimi, Y., Oda, S., Honda, Y., Nagata, S., Miyazaki, S., 1996. Involvement of Fas ligand and Fas-mediated pathway in the cytotoxicity of human natural killer cells. *J. Immunol. Baltim. Md* 157, 2909–2915.
- Ott, P.A., Hodi, F.S., 2016. Talimogene Laherparepvec for the Treatment of Advanced Melanoma. *Clin. Cancer Res. Off. J. Am. Assoc. Cancer Res.* 22, 3127–3131. <https://doi.org/10.1158/1078-0432.CCR-15-2709>
- Ouattara, L.A., Barin, F., Barthez, M.A., Bonnaud, B., Roingeard, P., Goudeau, A., Castelnau, P., Vernet, G., Paranhos-Baccalà, G., Komurian-Pradel, F., 2011. Novel human reovirus isolated from children with acute necrotizing encephalopathy. *Emerg. Infect. Dis.* 17, 1436–1444. <https://doi.org/10.3201/eid1708.101528>
- Pack, G.T., 1950. Note on the experimental use of rabies vaccine for melanomatosis. *AMA Arch. Dermatol. Syphilol.* 62, 694–695.
- Pal, S.R., Agarwal, S.C., 1968. Sero-epidemiological study of reovirus infection amongst the normal population of the Chandigarh area--northern India. *J. Hyg. (Lond.)* 66, 519–529.
- Paladino, P., Cummings, D.T., Noyce, R.S., Mossman, K.L., 2006. The IFN-independent response to virus particle entry provides a first line of antiviral defense that is independent of TLRs and retinoic acid-inducible gene I. *J. Immunol. Baltim. Md* 177, 8008–8016.
- Pandha, H.S., Heinemann, L., Simpson, G.R., Melcher, A., Prestwich, R., Errington, F., Coffey, M., Harrington, K.J., Morgan, R., 2009. Synergistic effects of oncolytic reovirus and cisplatin chemotherapy in murine malignant melanoma. *Clin. Cancer Res. Off. J. Am. Assoc. Cancer Res.* 15, 6158–6166. <https://doi.org/10.1158/1078-0432.CCR-09-0796>
- Parato, K.A., Breitbach, C.J., Le Boeuf, F., Wang, J., Storbeck, C., Ilkow, C., Diallo, J.-S., Falls, T., Burns, J., Garcia, V., Kanji, F., Evgin, L., Hu, K., Paradis, F., Knowles, S., Hwang, T.-H., Vanderhyden, B.C., Auer, R., Kirn, D.H., Bell, J.C., 2012. The oncolytic poxvirus JX-594 selectively replicates in and destroys cancer cells driven

- by genetic pathways commonly activated in cancers. *Mol. Ther. J. Am. Soc. Gene Ther.* 20, 749–758. <https://doi.org/10.1038/mt.2011.276>
- Pardoll, D.M., 2012. The blockade of immune checkpoints in cancer immunotherapy. *Nat. Rev. Cancer* 12, 252–264. <https://doi.org/10.1038/nrc3239>
- Park, B.-H., Hwang, T., Liu, T.-C., Sze, D.Y., Kim, J.-S., Kwon, H.-C., Oh, S.Y., Han, S.-Y., Yoon, J.-H., Hong, S.-H., Moon, A., Speth, K., Park, C., Ahn, Y.-J., Daneshmand, M., Rhee, B.G., Pinedo, H.M., Bell, J.C., Kirn, D.H., 2008. Use of a targeted oncolytic poxvirus, JX-594, in patients with refractory primary or metastatic liver cancer: a phase I trial. *Lancet Oncol.* 9, 533–542. [https://doi.org/10.1016/S1470-2045\(08\)70107-4](https://doi.org/10.1016/S1470-2045(08)70107-4)
- Parrish, C., Scott, G.B., Migneco, G., Scott, K.J., Steele, L.P., Ilett, E., West, E.J., Hall, K., Selby, P.J., Buchanan, D., Varghese, A., Cragg, M.S., Coffey, M., Hillmen, P., Melcher, A.A., Errington-Mais, F., 2015. Oncolytic reovirus enhances rituximab-mediated antibody-dependent cellular cytotoxicity against chronic lymphocytic leukaemia. *Leukemia.* <https://doi.org/10.1038/leu.2015.88>
- Pawlik, T.M., Sondak, V.K., 2003. Malignant melanoma: current state of primary and adjuvant treatment. *Crit. Rev. Oncol. Hematol.* 45, 245–264.
- Pearson, G., Robinson, F., Beers Gibson, T., Xu, B.E., Karandikar, M., Berman, K., Cobb, M.H., 2001. Mitogen-activated protein (MAP) kinase pathways: regulation and physiological functions. *Endocr. Rev.* 22, 153–183. <https://doi.org/10.1210/edrv.22.2.0428>
- Pelner, L., Fowler, G.A., Nauts, H.C., 1958. Effects of concurrent infections and their toxins on the course of leukemia. *Acta Med. Scand. Suppl.* 338, 1–47.
- Peltier, D.C., Lazear, H.M., Farmer, J.R., Diamond, M.S., Miller, D.J., 2013. Neurotropic arboviruses induce interferon regulatory factor 3-mediated neuronal responses that are cytoprotective, interferon independent, and inhibited by Western equine encephalitis virus capsid. *J. Virol.* 87, 1821–1833. <https://doi.org/10.1128/JVI.02858-12>
- Peng, K.-W., Dogan, A., Vrana, J., Liu, C., Ong, H.T., Kumar, S., Dispenzieri, A., Dietz, A.B., Russell, S.J., 2009. Tumor-associated macrophages infiltrate plasmacytomas and can serve as cell carriers for oncolytic measles virotherapy of disseminated myeloma. *Am. J. Hematol.* 84, 401–407. <https://doi.org/10.1002/ajh.21444>
- Peng, K.-W., Myers, R., Greenslade, A., Mader, E., Greiner, S., Federspiel, M.J., Dispenzieri, A., Russell, S.J., 2013. Using clinically approved cyclophosphamide regimens to control the humoral immune response to oncolytic viruses. *Gene Ther.* 20, 255–261. <https://doi.org/10.1038/gt.2012.31>
- Piganis, R.A.R., De Weerd, N.A., Gould, J.A., Schindler, C.W., Mansell, A., Nicholson, S.E., Hertzog, P.J., 2011. Suppressor of cytokine signaling (SOCS) 1 inhibits type I interferon (IFN) signaling via the interferon alpha receptor (IFNAR1)-associated tyrosine kinase Tyk2. *J. Biol. Chem.* 286, 33811–33818. <https://doi.org/10.1074/jbc.M111.270207>
- Platz, A., Egyhazi, S., Ringborg, U., Hansson, J., 2008. Human cutaneous melanoma; a review of NRAS and BRAF mutation frequencies in relation to histogenetic subclass and body site. *Mol. Oncol.* 1, 395–405. <https://doi.org/10.1016/j.molonc.2007.12.003>

- Pollock, P.M., Harper, U.L., Hansen, K.S., Yudt, L.M., Stark, M., Robbins, C.M., Moses, T.Y., Hostetter, G., Wagner, U., Kakareka, J., Salem, G., Pohida, T., Heenan, P., Duray, P., Kallioniemi, O., Hayward, N.K., Trent, J.M., Meltzer, P.S., 2003. High frequency of BRAF mutations in nevi. *Nat. Genet.* 33, 19–20. <https://doi.org/10.1038/ng1054>
- Poppers, J., Mulvey, M., Khoo, D., Mohr, I., 2000. Inhibition of PKR activation by the proline-rich RNA binding domain of the herpes simplex virus type 1 Us11 protein. *J. Virol.* 74, 11215–11221.
- Post, D.E., Sandberg, E.M., Kyle, M.M., Devi, N.S., Brat, D.J., Xu, Z., Tighiouart, M., Van Meir, E.G., 2007. Targeted Cancer Gene Therapy Using a Hypoxia Inducible Factor–Dependent Oncolytic Adenovirus Armed with Interleukin-4. *Cancer Res.* 67, 6872–6881. <https://doi.org/10.1158/0008-5472.CAN-06-3244>
- Postow, M.A., Chesney, J., Pavlick, A.C., Robert, C., Grossmann, K., McDermott, D., Linette, G.P., Meyer, N., Giguere, J.K., Agarwala, S.S., Shaheen, M., Ernstoff, M.S., Minor, D., Salama, A.K., Taylor, M., Ott, P.A., Rollin, L.M., Horak, C., Gagnier, P., Wolchok, J.D., Hodi, F.S., 2015. Nivolumab and ipilimumab versus ipilimumab in untreated melanoma. *N. Engl. J. Med.* 372, 2006–2017. <https://doi.org/10.1056/NEJMoa1414428>
- Power, A.T., Wang, J., Falls, T.J., Paterson, J.M., Parato, K.A., Lichty, B.D., Stojdl, D.F., Forsyth, P.A.J., Atkins, H., Bell, J.C., 2007. Carrier cell-based delivery of an oncolytic virus circumvents antiviral immunity. *Mol. Ther. J. Am. Soc. Gene Ther.* 15, 123–130. <https://doi.org/10.1038/sj.mt.6300039>
- Prestwich, R.J., Errington, F., Ilett, E.J., Morgan, R.S.M., Scott, K.J., Kottke, T., Thompson, J., Morrison, E.E., Harrington, K.J., Pandha, H.S., Selby, P.J., Vile, R.G., Melcher, A.A., 2008a. Tumor infection by oncolytic reovirus primes adaptive antitumor immunity. *Clin. Cancer Res. Off. J. Am. Assoc. Cancer Res.* 14, 7358–7366. <https://doi.org/10.1158/1078-0432.CCR-08-0831>
- Prestwich, R.J., Errington, F., Steele, L.P., Ilett, E.J., Morgan, R.S.M., Harrington, K.J., Pandha, H.S., Selby, P.J., Vile, R.G., Melcher, A.A., 2009a. Reciprocal human dendritic cell-natural killer cell interactions induce antitumor activity following tumor cell infection by oncolytic reovirus. *J. Immunol. Baltim. Md 1950* 183, 4312–4321. <https://doi.org/10.4049/jimmunol.0901074>
- Prestwich, R.J., Harrington, K.J., Pandha, H.S., Vile, R.G., Melcher, A.A., Errington, F., 2008b. Oncolytic viruses: a novel form of immunotherapy. *Expert Rev. Anticancer Ther.* 8, 1581–1588. <https://doi.org/10.1586/14737140.8.10.1581>
- Prestwich, R.J., Ilett, E.J., Errington, F., Diaz, R.M., Steele, L.P., Kottke, T., Thompson, J., Galivo, F., Harrington, K.J., Pandha, H.S., Selby, P.J., Vile, R.G., Melcher, A.A., 2009b. Immune-Mediated Antitumor Activity of Reovirus Is Required for Therapy and Is Independent of Direct Viral Oncolysis and Replication. *Clin. Cancer Res.* 15, 4374–4381. <https://doi.org/10.1158/1078-0432.CCR-09-0334>
- Printz, C., 2001. Spontaneous regression of melanoma may offer insight into cancer immunology. *J. Natl. Cancer Inst.* 93, 1047–1048.
- Prior, I.A., Lewis, P.D., Mattos, C., 2012. A comprehensive survey of Ras mutations in cancer. *Cancer Res.* 72, 2457–2467. <https://doi.org/10.1158/0008-5472.CAN-11-2612>

- Pulido, J., Kottke, T., Thompson, J., Galivo, F., Wongthida, P., Diaz, R.M., Rommelfanger, D., Ilett, E., Pease, L., Pandha, H., Harrington, K., Selby, P., Melcher, A., Vile, R., 2012. Using virally expressed melanoma cDNA libraries to identify tumor-associated antigens that cure melanoma. *Nat. Biotechnol.* 30, 337–343. <https://doi.org/10.1038/nbt.2157>
- Qiao, J., Kottke, T., Willmon, C., Galivo, F., Wongthida, P., Diaz, R.M., Thompson, J., Ryno, P., Barber, G.N., Chester, J., Selby, P., Harrington, K., Melcher, A., Vile, R.G., 2008a. Purging metastases in lymphoid organs using a combination of antigen-nonspecific adoptive T cell therapy, oncolytic virotherapy and immunotherapy. *Nat. Med.* 14, 37–44. <https://doi.org/10.1038/nm1681>
- Qiao, J., Wang, H., Kottke, T., Diaz, R.M., Willmon, C., Hudacek, A., Thompson, J., Parato, K., Bell, J., Naik, J., Chester, J., Selby, P., Harrington, K., Melcher, A., Vile, R.G., 2008c. Loading of oncolytic vesicular stomatitis virus onto antigen-specific T cells enhances the efficacy of adoptive T-cell therapy of tumors. *Gene Ther.* 15, 604–616. <https://doi.org/10.1038/sj.gt.3303098>
- Qiao, J., Wang, H., Kottke, T., White, C., Twigger, K., Diaz, R.M., Thompson, J., Selby, P., de Bono, J., Melcher, A., Pandha, H., Coffey, M., Vile, R., Harrington, K., 2008b. Cyclophosphamide facilitates antitumor efficacy against subcutaneous tumors following intravenous delivery of reovirus. *Clin. Cancer Res. Off. J. Am. Assoc. Cancer Res.* 14, 259–269. <https://doi.org/10.1158/1078-0432.CCR-07-1510>
- Rabkin, C.S., Biggar, R.J., Horm, J.W., 1991. Increasing incidence of cancers associated with the human immunodeficiency virus epidemic. *Int. J. Cancer* 47, 692–696. <https://doi.org/10.1002/ijc.2910470511>
- Rajani, K., Parrish, C., Kottke, T., Thompson, J., Zaidi, S., Ilett, L., Shim, K.G., Diaz, R.-M., Pandha, H., Harrington, K., Coffey, M., Melcher, A., Vile, R., 2016. Combination Therapy With Reovirus and Anti-PD-1 Blockade Controls Tumor Growth Through Innate and Adaptive Immune Responses. *Mol. Ther.* 24, 166–174. <https://doi.org/10.1038/mt.2015.156>
- Rajasagi, M., Shukla, S.A., Fritsch, E.F., Keskin, D.B., DeLuca, D., Carmona, E., Zhang, W., Sougnez, C., Cibulskis, K., Sidney, J., Stevenson, K., Ritz, J., Neuberg, D., Brusica, V., Gabriel, S., Lander, E.S., Getz, G., Hacohen, N., Wu, C.J., 2014. Systematic identification of personal tumor-specific neoantigens in chronic lymphocytic leukemia. *Blood* 124, 453–462. <https://doi.org/10.1182/blood-2014-04-567933>
- Ramos-Alvarez, M., Sabin, A.B., 1958. Enteropathogenic viruses and bacteria; role in summer diarrheal diseases of infancy and early childhood. *J. Am. Med. Assoc.* 167, 147–156.
- Ramos-Alvarez, M., Sabin, A.B., 1954. Characteristics of poliomyelitis and other enteric viruses recovered in tissue culture from healthy American children. *Proc. Soc. Exp. Biol. Med. Soc. Exp. Biol. Med. N. Y.* N 87, 655–661.
- Randazzo, B.P., Bhat, M.G., Kesari, S., Fraser, N.W., Brown, S.M., 1997. Treatment of experimental subcutaneous human melanoma with a replication-restricted herpes simplex virus mutant. *J. Invest. Dermatol.* 108, 933–937.

- Rees, R.C., Mian, S., 1999. Selective MHC expression in tumours modulates adaptive and innate antitumour responses. *Cancer Immunol. Immunother.* 48, 374–381. <https://doi.org/10.1007/s002620050589>
- Ribas, A., Dummer, R., Puzanov, I., VanderWalde, A., Andtbacka, R.H.I., Michielin, O., Olszanski, A.J., Malvehy, J., Cebon, J., Fernandez, E., Kirkwood, J.M., Gajewski, T.F., Chen, L., Gorski, K.S., Anderson, A.A., Diede, S.J., Lassman, M.E., Gansert, J., Hodi, F.S., Long, G.V., 2017. Oncolytic Virotherapy Promotes Intratumoral T Cell Infiltration and Improves Anti-PD-1 Immunotherapy. *Cell* 170, 1109–1119.e10. <https://doi.org/10.1016/j.cell.2017.08.027>
- Ricca, J., Merghoub, T., Wolchok, J.D., Zamarin, D., 2016. Abstract O15: Pre-existing immunity to oncolytic virus potentiates its therapeutic efficacy. *J. Immunother. Cancer* 4, 82.
- Richardson, S.C., Bishop, R.F., Smith, A.L., 1994. Reovirus serotype 3 infection in infants with extrahepatic biliary atresia or neonatal hepatitis. *J. Gastroenterol. Hepatol.* 9, 264–268.
- Rivera, J., Fierro, N.A., Olivera, A., Suzuki, R., 2008. New Insights on Mast Cell Activation via the High Affinity Receptor for IgE. *Adv. Immunol.* 98, 85–120. [https://doi.org/10.1016/S0065-2776\(08\)00403-3](https://doi.org/10.1016/S0065-2776(08)00403-3)
- Robert, C., 2017. Checkpoint Blockade Plus Oncolytic Virus: A Hot Therapeutic Cancer Strategy. *Trends Mol. Med.* 23, 983–985. <https://doi.org/10.1016/j.molmed.2017.09.008>
- Robert, C., Long, G.V., Brady, B., Dutriaux, C., Maio, M., Mortier, L., Hassel, J.C., Rutkowski, P., McNeil, C., Kalinka-Warzocha, E., Savage, K.J., Hernberg, M.M., Lebbé, C., Charles, J., Mihalciou, C., Chiarion-Sileni, V., Mauch, C., Cognetti, F., Arance, A., Schmidt, H., Schadendorf, D., Gogas, H., Lundgren-Eriksson, L., Horak, C., Sharkey, B., Waxman, I.M., Atkinson, V., Ascierto, P.A., 2015a. Nivolumab in previously untreated melanoma without BRAF mutation. *N. Engl. J. Med.* 372, 320–330. <https://doi.org/10.1056/NEJMoa1412082>
- Robert, C., Long, G.V., Schachter, J., Arance, A., Grob, J.J., Mortier, L., Daud, A., Carlino, M.S., McNeil, C.M., Lotem, M., Larkin, J.M.G., Lorigan, P., Neyns, B., Blank, C.U., Petrella, T.M., Hamid, O., Zhou, H., Homet Moreno, B., Ibrahim, N., Ribas, A., 2017. Long-term outcomes in patients (pts) with ipilimumab (ipi)-naive advanced melanoma in the phase 3 KEYNOTE-006 study who completed pembrolizumab (pembro) treatment. *J. Clin. Oncol.* 35, 9504–9504. [https://doi.org/10.1200/JCO.2017.35.15\\_suppl.9504](https://doi.org/10.1200/JCO.2017.35.15_suppl.9504)
- Robert, C., Schachter, J., Long, G.V., Arance, A., Grob, J.J., Mortier, L., Daud, A., Carlino, M.S., McNeil, C., Lotem, M., Larkin, J., Lorigan, P., Neyns, B., Blank, C.U., Hamid, O., Mateus, C., Shapira-Frommer, R., Kosh, M., Zhou, H., Ibrahim, N., Ebbinghaus, S., Ribas, A., 2015b. Pembrolizumab versus Ipilimumab in Advanced Melanoma. *N. Engl. J. Med.* 372, 2521–2532. <https://doi.org/10.1056/NEJMoa1503093>
- Rodrigo, W.W.S.I., Jin, X., Blackley, S.D., Rose, R.C., Schlesinger, J.J., 2006. Differential enhancement of dengue virus immune complex infectivity mediated by signaling-competent and signaling-incompetent human FcγRI (CD64) or FcγRIIA (CD32). *J. Virol.* 80, 10128–10138. <https://doi.org/10.1128/JVI.00792-06>

- Rohdenburg, G.L., 1918. Fluctuations in the Growth Energy of Malignant Tumors in Man, with Especial Reference to Spontaneous Recession. *J. Cancer Res.* 3, 193–225. <https://doi.org/10.1158/jcr.1918.193>
- Rolph, M.S., Zaid, A., Rulli, N.E., Mahalingam, S., 2011. Downregulation of interferon- $\beta$  in antibody-dependent enhancement of dengue viral infections of human macrophages is dependent on interleukin-6. *J. Infect. Dis.* 204, 489–491. <https://doi.org/10.1093/infdis/jir271>
- Rosen, L., Evans, H.E., Spickard, A., 1963. Reovirus infections in human volunteers. *Am. J. Hyg.* 77, 29–37.
- Rosenberg, S.A., 2014. IL-2: the first effective immunotherapy for human cancer. *J. Immunol. Baltim. Md 1950* 192, 5451–5458. <https://doi.org/10.4049/jimmunol.1490019>
- Rosenberg, S.A., Lotze, M.T., Muul, L.M., Leitman, S., Chang, A.E., Ettinghausen, S.E., Matory, Y.L., Skibber, J.M., Shiloni, E., Vetto, J.T., 1985. Observations on the systemic administration of autologous lymphokine-activated killer cells and recombinant interleukin-2 to patients with metastatic cancer. *N. Engl. J. Med.* 313, 1485–1492. <https://doi.org/10.1056/NEJM198512053132327>
- Rosenberg, S.A., Yang, J.C., Sherry, R.M., Kammula, U.S., Hughes, M.S., Phan, G.Q., Citrin, D.E., Restifo, N.P., Robbins, P.F., Wunderlich, J.R., Morton, K.E., Laurencot, C.M., Steinberg, S.M., White, D.E., Dudley, M.E., 2011. Durable Complete Responses in Heavily Pretreated Patients with Metastatic Melanoma Using T-Cell Transfer Immunotherapy. *Clin. Cancer Res.* 17, 4550–4557. <https://doi.org/10.1158/1078-0432.CCR-11-0116>
- Roulstone, V., Khan, K., Pandha, H.S., Rudman, S., Coffey, M., Gill, G.M., Melcher, A.A., Vile, R., Harrington, K.J., de Bono, J., Spicer, J., 2015. Phase I Trial of Cyclophosphamide as an Immune Modulator for Optimizing Oncolytic Reovirus Delivery to Solid Tumors. *Clin. Cancer Res.* 21, 1305–1312. <https://doi.org/10.1158/1078-0432.CCR-14-1770>
- Royo, S., Sainz, B., Hernández-Jiménez, E., Reyburn, H., López-Collazo, E., Guerra, S., 2014. Differential Induction of Apoptosis, Interferon Signaling, and Phagocytosis in Macrophages Infected with a Panel of Attenuated and Nonattenuated Poxviruses. *J. Virol.* 88, 5511–5523. <https://doi.org/10.1128/JVI.00468-14>
- Rozeman, E.A., Blank, C.U., Van Akkooi, A.C.J., Kvistborg, P., Fanchi, L., Van Thienen, J.V., Stegenga, B., Lamon, B., Haanen, J.B.A.G., Schumacher, T., 2017. Neoadjuvant ipilimumab + nivolumab (IPI+NIVO) in palpable stage III melanoma: Updated data from the OpACIN trial and first immunological analyses. *J. Clin. Oncol.* 35, 9586–9586. [https://doi.org/10.1200/JCO.2017.35.15\\_suppl.9586](https://doi.org/10.1200/JCO.2017.35.15_suppl.9586)
- Russell, S.J., Federspiel, M.J., Peng, K.-W., Tong, C., Dingli, D., Morice, W.G., Lowe, V., O'Connor, M.K., Kyle, R.A., Leung, N., Buadi, F.K., Rajkumar, S.V., Gertz, M.A., Lacy, M.Q., Dispenzieri, A., 2014. Remission of disseminated cancer after systemic oncolytic virotherapy. *Mayo Clin. Proc.* 89, 926–933. <https://doi.org/10.1016/j.mayocp.2014.04.003>
- Sabin, A.B., 1959. Reoviruses. A new group of respiratory and enteric viruses formerly classified as ECHO type 10 is described. *Science* 130, 1387–1389.

- Sakaguchi, S., Wing, K., Onishi, Y., Prieto-Martin, P., Yamaguchi, T., 2009. Regulatory T cells: how do they suppress immune responses? *Int. Immunol.* 21, 1105–1111. <https://doi.org/10.1093/intimm/dxp095>
- Samson, A., Scott, K.J., Taggart, D., West, E.J., Wilson, E., Nuovo, G.J., Thomson, S., Corns, R., Mathew, R.K., Fuller, M.J., Kottke, T.J., Thompson, J.M., Ilett, E.J., Cockle, J.V., Hille, P. van, Sivakumar, G., Polson, E.S., Turnbull, S.J., Appleton, E.S., Migneco, G., Rose, A.S., Coffey, M.C., Beirne, D.A., Collinson, F.J., Ralph, C., Anthoney, D.A., Twelves, C.J., Furness, A.J., Quezada, S.A., Wurdak, H., Errington-Mais, F., Pandha, H., Harrington, K.J., Selby, P.J., Vile, R.G., Griffin, S.D., Stead, L.F., Short, S.C., Melcher, A.A., 2018. Intravenous delivery of oncolytic reovirus to brain tumor patients immunologically primes for subsequent checkpoint blockade. *Sci. Transl. Med.* 10, eaam7577. <https://doi.org/10.1126/scitranslmed.aam7577>
- Sandru, A., Voinea, S., Panaitescu, E., Blidaru, A., 2014. Survival rates of patients with metastatic malignant melanoma. *J. Med. Life* 7, 572–576.
- Sanford, K.K., Earle, W.R., Likely, G.D., 1948. The growth in vitro of single isolated tissue cells. *J. Natl. Cancer Inst.* 9, 229–246.
- Saudemont, A., Jouy, N., Hetuin, D., Quesnel, B., 2005. NK cells that are activated by CXCL10 can kill dormant tumor cells that resist CTL-mediated lysis and can express B7-H1 that stimulates T cells. *Blood* 105, 2428–2435. <https://doi.org/10.1182/blood-2004-09-3458>
- Saunders, M., Anthoney, A., Coffey, M., Mettinger, K., Thompson, B., Melcher, A., Nutting, C.M., Harrington, K., 2009. Results of a phase II study to evaluate the biological effects of intratumoral (ITu) reolysin in combination with low dose radiotherapy (RT) in patients (Pts) with advanced cancers. *J. Clin. Oncol.* 27, e14514–e14514. [https://doi.org/10.1200/jco.2009.27.15\\_suppl.e14514](https://doi.org/10.1200/jco.2009.27.15_suppl.e14514)
- Sborov, D.W., Nuovo, G.J., Stiff, A., Mace, T., Lesinski, G.B., Benson, D.M., Efebera, Y.A., Rosko, A.E., Pichiorri, F., Grever, M.R., Hofmeister, C.C., 2014. A Phase I Trial of Single-Agent Reolysin in Patients with Relapsed Multiple Myeloma. *Clin. Cancer Res.* 20, 5946–5955. <https://doi.org/10.1158/1078-0432.CCR-14-1404>
- Schachter, J., Ribas, A., Long, G.V., Arance, A., Grob, J.-J., Mortier, L., Daud, A., Carlino, M.S., McNeil, C., Lotem, M., Larkin, J., Lorigan, P., Neyns, B., Blank, C., Petrella, T.M., Hamid, O., Zhou, H., Ebbinghaus, S., Ibrahim, N., Robert, C., 2017. Pembrolizumab versus ipilimumab for advanced melanoma: final overall survival results of a multicentre, randomised, open-label phase 3 study (KEYNOTE-006). *The Lancet* 390, 1853–1862. [https://doi.org/10.1016/S0140-6736\(17\)31601-X](https://doi.org/10.1016/S0140-6736(17)31601-X)
- Schneider, W.M., Chevillotte, M.D., Rice, C.M., 2014. Interferon-Stimulated Genes: A Complex Web of Host Defenses. *Annu. Rev. Immunol.* 32, 513–545. <https://doi.org/10.1146/annurev-immunol-032713-120231>
- Schulz, O., Diebold, S.S., Chen, M., Näslund, T.I., Nolte, M.A., Alexopoulou, L., Azuma, Y.-T., Flavell, R.A., Liljeström, P., Reis e Sousa, C., 2005. Toll-like receptor 3 promotes cross-priming to virus-infected cells. *Nature* 433, 887–892. <https://doi.org/10.1038/nature03326>
- Sei, S., Mussio, J.K., Yang, Q., Nagashima, K., Parchment, R.E., Coffey, M.C., Shoemaker, R.H., Tomaszewski, J.E., 2009. Synergistic antitumor activity of

- oncolytic reovirus and chemotherapeutic agents in non-small cell lung cancer cells. *Mol. Cancer* 8, 47. <https://doi.org/10.1186/1476-4598-8-47>
- Selb, B., Weber, B., 1994. A study of human reovirus IgG and IgA antibodies by ELISA and western blot. *J. Virol. Methods* 47, 15–25.
- Senzer, N.N., Kaufman, H.L., Amatruda, T., Nemunaitis, M., Reid, T., Daniels, G., Gonzalez, R., Glaspy, J., Whitman, E., Harrington, K., Goldsweig, H., Marshall, T., Love, C., Coffin, R., Nemunaitis, J.J., 2009. Phase II clinical trial of a granulocyte-macrophage colony-stimulating factor-encoding, second-generation oncolytic herpesvirus in patients with unresectable metastatic melanoma. *J. Clin. Oncol. Off. J. Am. Soc. Clin. Oncol.* 27, 5763–5771. <https://doi.org/10.1200/JCO.2009.24.3675>
- Seth, R.B., Sun, L., Ea, C.-K., Chen, Z.J., 2005. Identification and characterization of MAVS, a mitochondrial antiviral signaling protein that activates NF-kappaB and IRF 3. *Cell* 122, 669–682. <https://doi.org/10.1016/j.cell.2005.08.012>
- Seymour, L.W., Fisher, K.D., 2016. Oncolytic viruses: finally delivering. *Br. J. Cancer* 114, 357–361. <https://doi.org/10.1038/bjc.2015.481>
- Shafren, D.R., Au, G.G., Nguyen, T., Newcombe, N.G., Haley, E.S., Beagley, L., Johansson, E.S., Hersey, P., Barry, R.D., 2004. Systemic therapy of malignant human melanoma tumors by a common cold-producing enterovirus, coxsackievirus a21. *Clin. Cancer Res. Off. J. Am. Assoc. Cancer Res.* 10, 53–60.
- Shafren, D.R., Dorahy, D.J., Ingham, R.A., Burns, G.F., Barry, R.D., 1997. Coxsackievirus A21 binds to decay-accelerating factor but requires intercellular adhesion molecule 1 for cell entry. *J. Virol.* 71, 4736–4743.
- Shankaran, V., Ikeda, H., Bruce, A.T., White, J.M., Swanson, P.E., Old, L.J., Schreiber, R.D., 2001. IFN $\gamma$  and lymphocytes prevent primary tumour development and shape tumour immunogenicity. *Nature* 410, 1107–1111. <https://doi.org/10.1038/35074122>
- Shatkin, A.J., Sipe, J.D., Loh, P., 1968. Separation of ten reovirus genome segments by polyacrylamide gel electrophoresis. *J. Virol.* 2, 986–991.
- Sherry, B., Li, X.Y., Tyler, K.L., Cullen, J.M., Virgin, H.W., 1993. Lymphocytes protect against and are not required for reovirus-induced myocarditis. *J. Virol.* 67, 6119–6124.
- Shmulevitz, M., Gujar, S.A., Ahn, D.-G., Mohamed, A., Lee, P.W.K., 2012. Reovirus variants with mutations in genome segments S1 and L2 exhibit enhanced virion infectivity and superior oncolysis. *J. Virol.* 86, 7403–7413. <https://doi.org/10.1128/JVI.00304-12>
- Shmulevitz, M., Marcato, P., Lee, P.W.K., 2010. Activated Ras signaling significantly enhances reovirus replication and spread. *Cancer Gene Ther.* 17, 69–70. <https://doi.org/10.1038/cgt.2009.46>
- Shmulevitz, M., Marcato, P., Lee, P.W.K., 2009. Activated Ras signaling significantly enhances reovirus replication and spread. *Cancer Gene Ther.* 17, 69–70. <https://doi.org/10.1038/cgt.2009.46>

- Shmulevitz, M., Marcato, P., Lee, P.W.K., 2005. Unshackling the links between reovirus oncolysis, Ras signaling, translational control and cancer. *Oncogene* 24, 7720–7728. <https://doi.org/10.1038/sj.onc.1209041>
- Sica, A., Schioppa, T., Mantovani, A., Allavena, P., 2006. Tumour-associated macrophages are a distinct M2 polarised population promoting tumour progression: potential targets of anti-cancer therapy. *Eur. J. Cancer Oxf. Engl.* 1990 42, 717–727. <https://doi.org/10.1016/j.ejca.2006.01.003>
- Silverstein, S.C., Schur, P.H., 1970. Immunofluorescent localization of double-stranded RNA in reovirus-infected cells. *Virology* 41, 564–566.
- Smakman, N., van den Wollenberg, D.J.M., Borel Rinkes, I.H.M., Hoeben, R.C., Kranenburg, O., 2005. Sensitization to apoptosis underlies KrasD12-dependent oncolysis of murine C26 colorectal carcinoma cells by reovirus T3D. *J. Virol.* 79, 14981–14985. <https://doi.org/10.1128/JVI.79.23.14981-14985.2005>
- Smakman, N., van der Bilt, J.D.W., van den Wollenberg, D.J.M., Hoeben, R.C., Borel Rinkes, I.H.M., Kranenburg, O., 2006. Immunosuppression promotes reovirus therapy of colorectal liver metastases. *Cancer Gene Ther.* 13, 815–818. <https://doi.org/10.1038/sj.cgt.7700949>
- Small, E.J., Carducci, M.A., Burke, J.M., Rodriguez, R., Fong, L., van Ummersen, L., Yu, D.C., Aimi, J., Ando, D., Working, P., Kirn, D., Wilding, G., 2006. A Phase I Trial of Intravenous CG7870, a Replication-Selective, Prostate-Specific Antigen-Targeted Oncolytic Adenovirus, for the Treatment of Hormone-Refractory, Metastatic Prostate Cancer. *Mol. Ther.* 14, 107–117. <https://doi.org/10.1016/j.ymthe.2006.02.011>
- Smith, G.L., Sanderson, C.M., 1999. Cell motility and cell morphology: How some viruses take control. *Expert Rev. Mol. Med.* 1, 1–16. <https://doi.org/10.1017/S1462399499000629>
- Smittenaar, C.R., Petersen, K.A., Stewart, K., Moitt, N., 2016. Cancer incidence and mortality projections in the UK until 2035. *Br. J. Cancer* 115, 1147–1155. <https://doi.org/10.1038/bjc.2016.304>
- Smyth, M.J., Thia, K.Y., Cretney, E., Kelly, J.M., Snook, M.B., Forbes, C.A., Scalzo, A.A., 1999. Perforin is a major contributor to NK cell control of tumor metastasis. *J. Immunol. Baltim. Md* 1950 162, 6658–6662.
- Sobol, P.T., Boudreau, J.E., Stephenson, K., Wan, Y., Lichty, B.D., Mossman, K.L., 2011. Adaptive antiviral immunity is a determinant of the therapeutic success of oncolytic virotherapy. *Mol. Ther. J. Am. Soc. Gene Ther.* 19, 335–344. <https://doi.org/10.1038/mt.2010.264>
- Song, L., Ohnuma, T., Gelman, I.H., Holland, J.F., 2009. Reovirus infection of cancer cells is not due to activated Ras pathway. *Cancer Gene Ther.* 16, 382. <https://doi.org/10.1038/cgt.2008.84>
- Southam, C.M., 1960. Present status of oncolytic virus studies. *Trans. N. Y. Acad. Sci.* 22, 657–673.
- Southam, C.M., Moore, A.E., 1952. Clinical studies of viruses as antineoplastic agents with particular reference to Egypt 101 virus. *Cancer* 5, 1025–1034.

- Spear, G.T., Takefman, D.M., Sullivan, B.L., Landay, A.L., Jennings, M.B., Carlson, J.R., 1993. Anti-cellular Antibodies in Sera from Vaccinated Macaques Can Induce Complement-Mediated Virolysis of Human Immunodeficiency Virus and Simian Immunodeficiency Virus. *Virology* 195, 475–480.  
<https://doi.org/10.1006/viro.1993.1398>
- Specenier, P., 2016. Ipilimumab in melanoma. *Expert Rev. Anticancer Ther.* 16, 811–826. <https://doi.org/10.1080/14737140.2016.1211936>
- Spinner, M.L., Di Giovanni, G.D., 2001. Detection and identification of mammalian reoviruses in surface water by combined cell culture and reverse transcription-PCR. *Appl. Environ. Microbiol.* 67, 3016–3020.  
<https://doi.org/10.1128/AEM.67.7.3016-3020.2001>
- Spiotto, M.T., Rowley, D.A., Schreiber, H., 2004. Bystander elimination of antigen loss variants in established tumors. *Nat. Med.* 10, 294–298.  
<https://doi.org/10.1038/nm999>
- Srivastava, R.M., Lee, S.C., Filho, P.A.A., Lord, C.A., Jie, H., Davidson, H.C., López-Albaitero, A., Gibson, S.P., Gooding, W.E., Ferrone, S., Ferris, R.L., 2013. Cetuximab-activated natural killer (NK) and dendritic cells (DC) collaborate to trigger tumor antigen-specific T cell immunity in head and neck cancer patients. *Clin. Cancer Res. Off. J. Am. Assoc. Cancer Res.* 19, 1858–1872.  
<https://doi.org/10.1158/1078-0432.CCR-12-2426>
- Stamatos, N.M., Curreli, S., Zella, D., Cross, A.S., 2004. Desialylation of glycoconjugates on the surface of monocytes activates the extracellular signal-related kinases ERK 1/2 and results in enhanced production of specific cytokines. *J. Leukoc. Biol.* 75, 307–313. <https://doi.org/10.1189/jlb.0503241>
- Stanley, N.F., 1974. The reovirus murine models. *Prog. Med. Virol. Fortschritte Med. Virusforsch. Progres En Virol. Medicale* 18, 257–272.
- Stanley, N.F., 1961. Reovirus--a ubiquitous orphan. *Med. J. Aust.* 48(2), 815–818.
- Stanley, N.F., Dorman, D.C., Ponsford, J., 1954. Studies on the hepato-encephalomyelitis virus (HEV). *Aust. J. Exp. Biol. Med. Sci.* 32, 543–561.
- Stanley, N.F., Dorman, D.C., Ponsford, J., 1953. Studies on the pathogenesis of a hitherto undescribed virus (hepato-encephalomyelitis) producing unusual symptoms in suckling mice. *Aust. J. Exp. Biol. Med. Sci.* 31, 147–159.
- Staveley-O'Carroll, K., Sotomayor, E., Montgomery, J., Borrello, I., Hwang, L., Fein, S., Pardoll, D., Levitsky, H., 1998. Induction of antigen-specific T cell anergy: An early event in the course of tumor progression. *Proc. Natl. Acad. Sci. U. S. A.* 95, 1178–1183.
- Steele, L., Errington, F., Prestwich, R., Ilett, E., Harrington, K., Pandha, H., Coffey, M., Selby, P., Vile, R., Melcher, A., 2011. Pro-inflammatory cytokine/chemokine production by reovirus treated melanoma cells is PKR/NF- $\kappa$ B mediated and supports innate and adaptive anti-tumour immune priming. *Mol. Cancer* 10, 20.  
<https://doi.org/10.1186/1476-4598-10-20>
- Stehle, T., Dermody, T.S., 2004. Structural similarities in the cellular receptors used by adenovirus and reovirus. *Viral Immunol.* 17, 129–143.  
<https://doi.org/10.1089/0882824041310621>

- Steinman, R.M., Banchereau, J., 2007. Taking dendritic cells into medicine. *Nature* 449, 419–426. <https://doi.org/10.1038/nature06175>
- Steyer, A., Gutiérrez-Aguire, I., Kolenc, M., Koren, S., Kutnjak, D., Pokorn, M., Poljšak-Prijatelj, M., Racki, N., Ravnikar, M., Sagadin, M., Fratnik Steyer, A., Toplak, N., 2013. High similarity of novel orthoreovirus detected in a child hospitalized with acute gastroenteritis to mammalian orthoreoviruses found in bats in Europe. *J. Clin. Microbiol.* 51, 3818–3825. <https://doi.org/10.1128/JCM.01531-13>
- Strand, S., Hofmann, W.J., Hug, H., Müller, M., Otto, G., Strand, D., Mariani, S.M., Stremmel, W., Krammer, P.H., Galle, P.R., 1996. Lymphocyte apoptosis induced by CD95 (APO-1/Fas) ligand-expressing tumor cells--a mechanism of immune evasion? *Nat. Med.* 2, 1361–1366.
- Strong, J.E., Coffey, M.C., Tang, D., Sabinin, P., Lee, P.W., 1998. The molecular basis of viral oncolysis: usurpation of the Ras signaling pathway by reovirus. *EMBO J.* 17, 3351–3362. <https://doi.org/10.1093/emboj/17.12.3351>
- Strong, J.E., Lee, P.W., 1996. The v-erbB oncogene confers enhanced cellular susceptibility to reovirus infection. *J. Virol.* 70, 612–616.
- Strong, J.E., Tang, D., Lee, P.W., 1993. Evidence that the epidermal growth factor receptor on host cells confers reovirus infection efficiency. *Virology* 197, 405–411. <https://doi.org/10.1006/viro.1993.1602>
- Stuart, J.D., Holm, G.H., Boehme, K.W., 2018. Differential delivery of genomic dsRNA causes reovirus strain-specific differences in IRF3 activation. *J. Virol.* JVI.01947-17. <https://doi.org/10.1128/JVI.01947-17>
- Sturzenbecker, L.J., Nibert, M., Furlong, D., Fields, B.N., 1987. Intracellular digestion of reovirus particles requires a low pH and is an essential step in the viral infectious cycle. *J. Virol.* 61, 2351–2361.
- Sullivan, B.L., Takefman, D.M., Spear, G.T., 1998. Complement can neutralize HIV-1 plasma virus by a C5-independent mechanism. *Virology* 248, 173–181. <https://doi.org/10.1006/viro.1998.9289>
- Sullivan, C.S., Tremblay, J.D., Fewell, S.W., Lewis, J.A., Brodsky, J.L., Pipas, J.M., 2000. Species-specific elements in the large T-antigen J domain are required for cellular transformation and DNA replication by simian virus 40. *Mol. Cell. Biol.* 20, 5749–5757.
- Sun, P., Bauza, K., Pal, S., Liang, Z., Wu, S., Beckett, C., Burgess, T., Porter, K., 2011. Infection and activation of human peripheral blood monocytes by dengue viruses through the mechanism of antibody-dependent enhancement. *Virology* 421, 245–252. <https://doi.org/10.1016/j.virol.2011.08.026>
- Sznol, M., Ferrucci, P.F., Hogg, D., Atkins, M.B., Wolter, P., Guidoboni, M., Lebbé, C., Kirkwood, J.M., Schachter, J., Daniels, G.A., Hassel, J., Cebon, J., Gerritsen, W., Atkinson, V., Thomas, L., McCaffrey, J., Power, D., Walker, D., Bhore, R., Jiang, J., Hodi, F.S., Wolchok, J.D., 2017. Pooled Analysis Safety Profile of Nivolumab and Ipilimumab Combination Therapy in Patients With Advanced Melanoma. *J. Clin. Oncol. Off. J. Am. Soc. Clin. Oncol.* JCO2016721167. <https://doi.org/10.1200/JCO.2016.72.1167>

- Tai, J.H., Williams, J.V., Edwards, K.M., Wright, P.F., Crowe, J.E., Dermody, T.S., 2005. Prevalence of reovirus-specific antibodies in young children in Nashville, Tennessee. *J. Infect. Dis.* 191, 1221–1224. <https://doi.org/10.1086/428911>
- Takagi-Kimura, M., Yamano, T., Tamamoto, A., Okamura, N., Okamura, H., Hashimoto-Tamaoki, T., Tagawa, M., Kasahara, N., Kubo, S., 2013. Enhanced antitumor efficacy of fiber-modified, midkine promoter-regulated oncolytic adenovirus in human malignant mesothelioma. *Cancer Sci.* 104, 1433–1439. <https://doi.org/10.1111/cas.12267>
- Tanese, K., Hashimoto, Y., Berkova, Z., Wang, Y., Samaniego, F., Lee, J.E., Ekmekcioglu, S., Grimm, E.A., 2015. Cell Surface CD74-MIF Interactions Drive Melanoma Survival in Response to Interferon- $\gamma$ . *J. Invest. Dermatol.* 135, 2901. <https://doi.org/10.1038/jid.2015.259>
- Tang, D., Strong, J.E., Lee, P.W.K., 1993. Recognition of the Epidermal Growth Factor Receptor by Reovirus. *Virology* 197, 412–414. <https://doi.org/10.1006/viro.1993.1603>
- Tao, J.J., Schram, A.M., Hyman, D.M., 2018. Basket Studies: Redefining Clinical Trials in the Era of Genome-Driven Oncology. *Annu. Rev. Med.* 69, 319–331. <https://doi.org/10.1146/annurev-med-062016-050343>
- Taqi, A.M., Abdurrahman, M.B., Yakubu, A.M., Fleming, A.F., 1981. Regression of Hodgkin's disease after measles. *Lancet Lond. Engl.* 1, 1112.
- Tas, F., 2012. Metastatic behavior in melanoma: timing, pattern, survival, and influencing factors. *J. Oncol.* 2012, 647684. <https://doi.org/10.1155/2012/647684>
- Taylor, A., Foo, S.-S., Bruzzone, R., Dinh, L.V., King, N.J.C., Mahalingam, S., 2015. Fc receptors in antibody-dependent enhancement of viral infections. *Immunol. Rev.* 268, 340–364. <https://doi.org/10.1111/imr.12367>
- Terajima, M., Cruz, J., Co, M.D.T., Lee, J.-H., Kaur, K., Wilson, P.C., Ennis, F.A., 2011. Complement-Dependent Lysis of Influenza A Virus-Infected Cells by Broadly Cross-Reactive Human Monoclonal Antibodies. *J. Virol.* 85, 13463–13467. <https://doi.org/10.1128/JVI.05193-11>
- Testa, J.R., Bellacosa, A., 2001. AKT plays a central role in tumorigenesis. *Proc. Natl. Acad. Sci. U. S. A.* 98, 10983–10985. <https://doi.org/10.1073/pnas.211430998>
- Thagard, P., 2002. Curing cancer? Patrick Lee's path to the reovirus treatment. *Int. Stud. Philos. Sci.* 16, 79–93. <https://doi.org/10.1080/02698590120118846>
- Theiss, J.C., Stoner, G.D., Kniazeff, A.J., 1978. Effect of reovirus infection on pulmonary tumor response to urethan in strain A mice. *J. Natl. Cancer Inst.* 61, 131–134.
- Thiam, A., Zhao, Z., Quinn, C., Barber, B., 2016. Years of life lost due to metastatic melanoma in 12 countries. *J. Med. Econ.* 19, 259–264. <https://doi.org/10.3111/13696998.2015.1115764>
- Thiery, P., 1909. On the use of fulguration in cancer. *Bull Mem Soc Chir Paris* 35, 604.
- Thirukkumaran, C.M., Luider, J.M., Stewart, D.A., Cheng, T., Lupichuk, S.M., Nodwell, M.J., Russell, J.A., Auer, I.A., Morris, D.G., 2003. Reovirus oncolysis as a novel

- purging strategy for autologous stem cell transplantation. *Blood* 102, 377–387. <https://doi.org/10.1182/blood-2002-08-2508>
- Thirukkumaran, C.M., Nodwell, M.J., Hirasawa, K., Shi, Z.-Q., Diaz, R., Luider, J., Johnston, R.N., Forsyth, P.A., Magliocco, A.M., Lee, P., Nishikawa, S., Donnelly, B., Coffey, M., Trpkov, K., Fonseca, K., Spurrell, J., Morris, D.G., 2010. Oncolytic viral therapy for prostate cancer: efficacy of reovirus as a biological therapeutic. *Cancer Res.* 70, 2435–2444. <https://doi.org/10.1158/0008-5472.CAN-09-2408>
- Thirukkumaran, C.M., Shi, Z.Q., Luider, J., Kopciuk, K., Gao, H., Bahlis, N., Neri, P., Pho, M., Stewart, D., Mansoor, A., Morris, D.G., 2013. Reovirus modulates autophagy during oncolysis of multiple myeloma. *Autophagy* 9, 413–414. <https://doi.org/10.4161/auto.22867>
- Thirukkumaran, C.M., Shi, Z.Q., Luider, J., Kopciuk, K., Gao, H., Bahlis, N., Neri, P., Pho, M., Stewart, D., Mansoor, A., Morris, D.G., 2012. Reovirus as a viable therapeutic option for the treatment of multiple myeloma. *Clin. Cancer Res. Off. J. Am. Assoc. Cancer Res.* 18, 4962–4972. <https://doi.org/10.1158/1078-0432.CCR-11-3085>
- Thomson, B.J., 2001. Viruses and apoptosis. *Int. J. Exp. Pathol.* 82, 65–76. <https://doi.org/10.1111/j.1365-2613.2001.iep0082-0065-x>
- Thorne, S.H., Negrin, R.S., Contag, C.H., 2006. Synergistic antitumor effects of immune cell-viral biotherapy. *Science* 311, 1780–1784. <https://doi.org/10.1126/science.1121411>
- Tillotson, J.R., Lerner, A.M., 1967. Reovirus type 3 associated with fatal pneumonia. *N. Engl. J. Med.* 276, 1060–1063. <https://doi.org/10.1056/NEJM196705112761903>
- Tomczyk, T., Wróbel, G., Chaber, R., Siemieniec, I., Piasecki, E., Krzystek-Korpacka, M., Orzechowska, B.U., 2018. Immune Consequences of in vitro Infection of Human Peripheral Blood Leukocytes with Vesicular Stomatitis Virus. *J. Innate Immun.* <https://doi.org/10.1159/000485143>
- Tomita, K., Sakurai, F., Tachibana, M., Mizuguchi, H., 2012. Correlation between adenovirus-neutralizing antibody titer and adenovirus vector-mediated transduction efficiency following intratumoral injection. *Anticancer Res.* 32, 1145–1152.
- Topalian, S.L., Hodi, F.S., Brahmer, J.R., Gettinger, S.N., Smith, D.C., McDermott, D.F., Powderly, J.D., Carvajal, R.D., Sosman, J.A., Atkins, M.B., Leming, P.D., Spigel, D.R., Antonia, S.J., Horn, L., Drake, C.G., Pardoll, D.M., Chen, L., Sharfman, W.H., Anders, R.A., Taube, J.M., McMiller, T.L., Xu, H., Korman, A.J., Jure-Kunkel, M., Agrawal, S., McDonald, D., Kollia, G.D., Gupta, A., Wigginton, J.M., Sznol, M., 2012. Safety, activity, and immune correlates of anti-PD-1 antibody in cancer. *N. Engl. J. Med.* 366, 2443–2454. <https://doi.org/10.1056/NEJMoa1200690>
- Tóth, F.D., Mosborg-Petersen, P., Kiss, J., Aboagye-Mathiesen, G., Zdravkovic, M., Hager, H., Aranyosi, J., Lampé, L., Ebbesen, P., 1994. Antibody-dependent enhancement of HIV-1 infection in human term syncytiotrophoblast cells cultured in vitro. *Clin. Exp. Immunol.* 96, 389–394.
- Tsai, T.-T., Chuang, Y.-J., Lin, Y.-S., Chang, C.-P., Wan, S.-W., Lin, S.-H., Chen, C.-L., Lin, C.-F., 2014. Antibody-dependent enhancement infection facilitates dengue

- virus-regulated signaling of IL-10 production in monocytes. *PLoS Negl. Trop. Dis.* 8, e3320. <https://doi.org/10.1371/journal.pntd.0003320>
- Tsai, V., Johnson, D.E., Rahman, A., Wen, S.F., LaFace, D., Philopena, J., Nery, J., Zepeda, M., Maneval, D.C., Demers, G.W., Ralston, R., 2004. Impact of human neutralizing antibodies on antitumor efficacy of an oncolytic adenovirus in a murine model. *Clin. Cancer Res. Off. J. Am. Assoc. Cancer Res.* 10, 7199–7206. <https://doi.org/10.1158/1078-0432.CCR-04-0765>
- Tumeh, P.C., Harview, C.L., Yearley, J.H., Shintaku, I.P., Taylor, E.J.M., Robert, L., Chmielowski, B., Spasic, M., Henry, G., Ciobanu, V., West, A.N., Carmona, M., Kivork, C., Seja, E., Cherry, G., Gutierrez, A.J., Grogan, T.R., Mateus, C., Tomasic, G., Glaspy, J.A., Emerson, R.O., Robins, H., Pierce, R.H., Elashoff, D.A., Robert, C., Ribas, A., 2014. PD-1 blockade induces responses by inhibiting adaptive immune resistance. *Nature* 515, 568–571. <https://doi.org/10.1038/nature13954>
- Twigger, K., Roulstone, V., Kyula, J., Karapanagiotou, E.M., Syrigos, K.N., Morgan, R., White, C., Bhide, S., Nuovo, G., Coffey, M., others, 2012. Reovirus exerts potent oncolytic effects in head and neck cancer cell lines that are independent of signalling in the EGFR pathway. *BMC Cancer* 12, 368.
- Twigger, K., Vidal, L., White, C.L., De Bono, J.S., Bhide, S., Coffey, M., Thompson, B., Vile, R.G., Heinemann, L., Pandha, H.S., Errington, F., Melcher, A.A., Harrington, K.J., 2008. Enhanced in vitro and in vivo cytotoxicity of combined reovirus and radiotherapy. *Clin. Cancer Res. Off. J. Am. Assoc. Cancer Res.* 14, 912–923. <https://doi.org/10.1158/1078-0432.CCR-07-1400>
- Tyler, K.L., Barton, E.S., Ibach, M.L., Robinson, C., Campbell, J.A., O'Donnell, S.M., Valyi-Nagy, T., Clarke, P., Wetzel, J.D., Dermody, T.S., 2004. Isolation and molecular characterization of a novel type 3 reovirus from a child with meningitis. *J. Infect. Dis.* 189, 1664–1675. <https://doi.org/10.1086/383129>
- Tyler, K.L., Mann, M.A., Fields, B.N., Virgin, H.W., 1993. Protective anti-reovirus monoclonal antibodies and their effects on viral pathogenesis. *J. Virol.* 67, 3446–3453.
- Tyler, M.A., Ulasov, I.V., Sonabend, A.M., Nandi, S., Han, Y., Marler, S., Roth, J., Lesniak, M.S., 2009. Neural stem cells target intracranial glioma to deliver an oncolytic adenovirus in vivo. *Gene Ther.* 16, 262–278. <https://doi.org/10.1038/gt.2008.165>
- Ubol, S., Phuklia, W., Kalayanarooj, S., Modhiran, N., 2010. Mechanisms of immune evasion induced by a complex of dengue virus and preexisting enhancing antibodies. *J. Infect. Dis.* 201, 923–935. <https://doi.org/10.1086/651018>
- Van Allen, E.M., Miao, D., Schilling, B., Shukla, S.A., Blank, C., Zimmer, L., Sucker, A., Hillen, U., Foppen, M.H.G., Goldinger, S.M., Utikal, J., Hassel, J.C., Weide, B., Kaehler, K.C., Loquai, C., Mohr, P., Gutzmer, R., Dummer, R., Gabriel, S., Wu, C.J., Schadendorf, D., Garraway, L.A., 2015. Genomic correlates of response to CTLA-4 blockade in metastatic melanoma. *Science* 350, 207–211. <https://doi.org/10.1126/science.aad0095>

- van den Broek, M.E., Kägi, D., Ossendorp, F., Toes, R., Vamvakas, S., Lutz, W.K., Melief, C.J., Zinkernagel, R.M., Hengartner, H., 1996. Decreased tumor surveillance in perforin-deficient mice. *J. Exp. Med.* 184, 1781–1790.
- van den Wollenberg, D.J.M., Dautzenberg, I.J.C., Ros, W., Lipińska, A.D., van den Hengel, S.K., Hoeben, R.C., 2015. Replicating reoviruses with a transgene replacing the codons for the head domain of the viral spike. *Gene Ther.* 22, 51–63. <https://doi.org/10.1038/gt.2014.126>
- van der Bruggen, P., Traversari, C., Chomez, P., Lurquin, C., De Plaen, E., Van den Eynde, B., Knuth, A., Boon, T., 1991. A gene encoding an antigen recognized by cytolytic T lymphocytes on a human melanoma. *Science* 254, 1643–1647.
- Vandesompele, J., De Preter, K., Pattyn, F., Poppe, B., Van Roy, N., De Paepe, A., Speleman, F., 2002. Accurate normalization of real-time quantitative RT-PCR data by geometric averaging of multiple internal control genes. *Genome Biol.* 3, research0034. <https://doi.org/10.1186/gb-2002-3-7-research0034>
- Varkila, K., Hurme, M., 1983. The effect of cyclophosphamide on cytotoxic T-lymphocyte responses: inhibition of helper T-cell induction in vitro. *Immunology* 48, 433–438.
- Veerapong, J., Bickenbach, K.A., Shao, M.Y., Smith, K.D., Posner, M.C., Roizman, B., Weichselbaum, R.R., 2007. Systemic Delivery of  $\gamma$ 134.5-Deleted Herpes Simplex Virus-1 Selectively Targets and Treats Distant Human Xenograft Tumors That Express High MEK Activity. *Cancer Res.* 67, 8301–8306. <https://doi.org/10.1158/0008-5472.CAN-07-1499>
- Vidal, L., Pandha, H.S., Yap, T.A., White, C.L., Twigger, K., Vile, R.G., Melcher, A., Coffey, M., Harrington, K.J., DeBono, J.S., 2008. A Phase I Study of Intravenous Oncolytic Reovirus Type 3 Dearing in Patients with Advanced Cancer. *Clin. Cancer Res.* 14, 7127–7137. <https://doi.org/10.1158/1078-0432.CCR-08-0524>
- Villalona-Calero, M.A., Lam, E., Otterson, G.A., Zhao, W., Timmons, M., Subramaniam, D., Hade, E.M., Gill, G.M., Coffey, M., Selvaggi, G., Bertino, E., Chao, B., Knopp, M.V., 2016. Oncolytic reovirus in combination with chemotherapy in metastatic or recurrent non-small cell lung cancer patients with KRAS-activated tumors. *Cancer* 122, 875–883. <https://doi.org/10.1002/cncr.29856>
- Virgin, H.W., Tyler, K.L., 1991. Role of immune cells in protection against and control of reovirus infection in neonatal mice. *J. Virol.* 65, 5157–5164.
- Walker, L.S.K., Sansom, D.M., 2015. Confusing signals: Recent progress in CTLA-4 biology. *Trends Immunol.* 36, 63–70. <https://doi.org/10.1016/j.it.2014.12.001>
- Wang, G., Barrett, J.W., Stanford, M., Werden, S.J., Johnston, J.B., Gao, X., Sun, M., Cheng, J.Q., McFadden, G., 2006. Infection of human cancer cells with myxoma virus requires Akt activation via interaction with a viral ankyrin-repeat host range factor. *Proc. Natl. Acad. Sci. U. S. A.* 103, 4640–4645. <https://doi.org/10.1073/pnas.0509341103>
- Wang, J.-H., Janas, A.M., Olson, W.J., Wu, L., 2007. Functionally Distinct Transmission of Human Immunodeficiency Virus Type 1 Mediated by Immature and Mature Dendritic Cells. *J. Virol.* 81, 8933–8943. <https://doi.org/10.1128/JVI.00878-07>

- Wang, R.F., Robbins, P.F., Kawakami, Y., Kang, X.Q., Rosenberg, S.A., 1995. Identification of a gene encoding a melanoma tumor antigen recognized by HLA-A31-restricted tumor-infiltrating lymphocytes. *J. Exp. Med.* 181, 799–804.
- Wang, S.-M., Chen, I.-C., Su, L.-Y., Huang, K.-J., Lei, H.-Y., Liu, C.-C., 2010. Enterovirus 71 Infection of Monocytes with Antibody-Dependent Enhancement. *Clin. Vaccine Immunol.* 17, 1517–1523. <https://doi.org/10.1128/CVI.00108-10>
- Wang, T.T., Sewatanon, J., Memoli, M.J., Wrammert, J., Bournazos, S., Bhaumik, S.K., Pinsky, B.A., Chokephaibulkit, K., Onlamoon, N., Pattanapanyasat, K., Taubenberger, J.K., Ahmed, R., Ravetch, J.V., 2017. IgG antibodies to dengue enhanced for FcγRIIIA binding determine disease severity. *Science* 355, 395–398. <https://doi.org/10.1126/science.aai8128>
- Watkinson, R.E., McEwan, W.A., Tam, J.C.H., Vaysburd, M., James, L.C., 2015. TRIM21 Promotes cGAS and RIG-I Sensing of Viral Genomes during Infection by Antibody-Opsonized Virus. *PLOS Pathog.* 11, e1005253. <https://doi.org/10.1371/journal.ppat.1005253>
- Weber, F., Wagner, V., Rasmussen, S.B., Hartmann, R., Paludan, S.R., 2006. Double-Stranded RNA Is Produced by Positive-Strand RNA Viruses and DNA Viruses but Not in Detectable Amounts by Negative-Strand RNA Viruses. *J. Virol.* 80, 5059–5064. <https://doi.org/10.1128/JVI.80.10.5059-5064.2006>
- Weber, J., Mandala, M., Del Vecchio, M., Gogas, H.J., Arance, A.M., Cowey, C.L., Dalle, S., Schenker, M., Chiarion-Sileni, V., Marquez-Rodas, I., Grob, J.-J., Butler, M.O., Middleton, M.R., Maio, M., Atkinson, V., Queirolo, P., Gonzalez, R., Kudchadkar, R.R., Smylie, M., Meyer, N., Mortier, L., Atkins, M.B., Long, G.V., Bhatia, S., Lebbé, C., Rutkowski, P., Yokota, K., Yamazaki, N., Kim, T.M., de Pril, V., Sabater, J., Qureshi, A., Larkin, J., Ascierto, P.A., 2017. Adjuvant Nivolumab versus Ipilimumab in Resected Stage III or IV Melanoma. *N. Engl. J. Med.* 377, 1824–1835. <https://doi.org/10.1056/NEJMoa1709030>
- Weber, J.S., Gibney, G., Sullivan, R.J., Sosman, J.A., Slingluff, C.L., Lawrence, D.P., Logan, T.F., Schuchter, L.M., Nair, S., Fecher, L., Buchbinder, E.I., Berghorn, E., Ruisi, M., Kong, G., Jiang, J., Horak, C., Hodi, F.S., 2016. Sequential administration of nivolumab and ipilimumab with a planned switch in patients with advanced melanoma (CheckMate 064): an open-label, randomised, phase 2 trial. *Lancet Oncol.* 17, 943–955. [https://doi.org/10.1016/S1470-2045\(16\)30126-7](https://doi.org/10.1016/S1470-2045(16)30126-7)
- Weber, J.S., Kudchadkar, R.R., Yu, B., Gallenstein, D., Horak, C.E., Inzunza, H.D., Zhao, X., Martinez, A.J., Wang, W., Gibney, G., Kroeger, J., Eysmans, C., Sarnaik, A.A., Chen, Y.A., 2013. Safety, Efficacy, and Biomarkers of Nivolumab With Vaccine in Ipilimumab-Refractory or -Naive Melanoma. *J. Clin. Oncol.* 31, 4311–4318. <https://doi.org/10.1200/JCO.2013.51.4802>
- Weide, B., Martens, A., Zelba, H., Stutz, C., Derhovanessian, E., Di Giacomo, A.M., Maio, M., Sucker, A., Schilling, B., Schadendorf, D., Büttner, P., Garbe, C., Pawelec, G., 2014. Myeloid-derived suppressor cells predict survival of patients with advanced melanoma: comparison with regulatory T cells and NY-ESO-1- or melan-A-specific T cells. *Clin. Cancer Res. Off. J. Am. Assoc. Cancer Res.* 20, 1601–1609. <https://doi.org/10.1158/1078-0432.CCR-13-2508>
- Weigert, M., Binks, A., Dowson, S., Leung, E.Y.L., Athineos, D., Yu, X., Mullin, M., Walton, J.B., Orange, C., Ennis, D., Blyth, K., Tait, S.W.G., McNeish, I.A., 2017.

- RIPK3 promotes adenovirus type 5 activity. *Cell Death Dis.* 8, 3206.  
<https://doi.org/10.1038/s41419-017-0110-8>
- Weir, H.K., Marrett, L.D., Cokkinides, V., Barnholtz-Sloan, J., Patel, P., Tai, E., Jemal, A., Li, J., Kim, J., Ekwueme, D.U., 2011. Melanoma in adolescents and young adults (ages 15-39 years): United States, 1999-2006. *J. Am. Acad. Dermatol.* 65, S38–S49. <https://doi.org/10.1016/j.jaad.2011.04.038>
- Wellbrock, C., Arozarena, I., 2016. The Complexity of the ERK/MAP-Kinase Pathway and the Treatment of Melanoma Skin Cancer. *Front. Cell Dev. Biol.* 4, 33.  
<https://doi.org/10.3389/fcell.2016.00033>
- Weller, T.H., Robbins, F.C., Enders, J.F., 1949. Cultivation of poliomyelitis virus in cultures of human foreskin and embryonic tissues. *Proc. Soc. Exp. Biol. Med. Soc. Exp. Biol. Med. N. Y.* N 72, 153–155.
- White, C.L., Twigger, K.R., Vidal, L., De Bono, J.S., Coffey, M., Heinemann, L., Morgan, R., Merrick, A., Errington, F., Vile, R.G., others, 2008. Characterization of the adaptive and innate immune response to intravenous oncolytic reovirus (Dearing type 3) during a phase I clinical trial. *Gene Ther.* 15, 911–920.
- Williams, B.R., 2001. Signal integration via PKR. *Sci. STKE Signal Transduct. Knowl. Environ.* 2001, re2. <https://doi.org/10.1126/stke.2001.89.re2>
- Williams, B.R., 1999. PKR; a sentinel kinase for cellular stress. *Oncogene* 18, 6112–6120. <https://doi.org/10.1038/sj.onc.1203127>
- Willmon, C., Harrington, K., Kottke, T., Prestwich, R., Melcher, A., Vile, R., 2009. Cell Carriers for Oncolytic Viruses: Fed Ex for Cancer Therapy. *Mol. Ther.* 17, 1667–1676. <https://doi.org/10.1038/mt.2009.194>
- Wilson, G.A., Morrison, L.A., Fields, B.N., 1994. Association of the reovirus S1 gene with serotype 3-induced biliary atresia in mice. *J. Virol.* 68, 6458–6465.
- Wilson, M.A., Schuchter, L.M., 2016. Chemotherapy for Melanoma, in: *Melanoma, Cancer Treatment and Research*. Springer, Cham, pp. 209–229.  
[https://doi.org/10.1007/978-3-319-22539-5\\_8](https://doi.org/10.1007/978-3-319-22539-5_8)
- Wirthmueller, U., Kurosaki, T., Murakami, M.S., Ravetch, J.V., 1992. Signal transduction by Fc gamma RIII (CD16) is mediated through the gamma chain. *J. Exp. Med.* 175, 1381–1390.
- Wise, J., 2016. NICE approves immunotherapy combination for advanced melanoma. *BMJ* 353, i3421.
- Wolchok, J.D., Chiarion-Sileni, V., Gonzalez, R., Rutkowski, P., Grob, J.-J., Cowey, C.L., Lao, C.D., Wagstaff, J., Schadendorf, D., Ferrucci, P.F., Smylie, M., Dummer, R., Hill, A., Hogg, D., Haanen, J., Carlino, M.S., Bechter, O., Maio, M., Marquez-Rodas, I., Guidoboni, M., McArthur, G., Lebbé, C., Ascierto, P.A., Long, G.V., Cebon, J., Sosman, J., Postow, M.A., Callahan, M.K., Walker, D., Rollin, L., Bhore, R., Hodi, F.S., Larkin, J., 2017. Overall Survival with Combined Nivolumab and Ipilimumab in Advanced Melanoma. *N. Engl. J. Med.* 377, 1345–1356.  
<https://doi.org/10.1056/NEJMoa1709684>
- Wong, K.L., Tai, J.J.-Y., Wong, W.-C., Han, H., Sem, X., Yeap, W.-H., Kourilsky, P., Wong, S.-C., 2011. Gene expression profiling reveals the defining features of the

- classical, intermediate, and nonclassical human monocyte subsets. *Blood* 118, e16–e31.
- Wong, K.L., Yeap, W.H., Tai, J.J.Y., Ong, S.M., Dang, T.M., Wong, S.C., 2012. The three human monocyte subsets: implications for health and disease. *Immunol. Res.* 53, 41–57. <https://doi.org/10.1007/s12026-012-8297-3>
- Wu, J., Liang, C., Chen, M., Su, W., 2016. Association between tumor-stroma ratio and prognosis in solid tumor patients: a systematic review and meta-analysis. *Oncotarget* 7, 68954–68965. <https://doi.org/10.18632/oncotarget.12135>
- Xia, Z.-J., Chang, J.-H., Zhang, L., Jiang, W.-Q., Guan, Z.-Z., Liu, J.-W., Zhang, Y., Hu, X.-H., Wu, G.-H., Wang, H.-Q., Chen, Z.-C., Chen, J.-C., Zhou, Q.-H., Lu, J.-W., Fan, Q.-X., Huang, J.-J., Zheng, X., 2004. [Phase III randomized clinical trial of intratumoral injection of E1B gene-deleted adenovirus (H101) combined with cisplatin-based chemotherapy in treating squamous cell cancer of head and neck or esophagus]. *Ai Zheng Aizheng Chin. J. Cancer* 23, 1666–1670.
- Yang, W.Q., Lun, X., Palmer, C.A., Wilcox, M.E., Muzik, H., Shi, Z.Q., Dyck, R., Coffey, M., Thompson, B., Hamilton, M., Nishikawa, S.G., Brasher, P.M.A., Fonseca, K., George, D., Rewcastle, N.B., Johnston, R.N., Stewart, D., Lee, P.W.K., Senger, D.L., Forsyth, P.A., 2004. Efficacy and safety evaluation of human reovirus type 3 in immunocompetent animals: racine and nonhuman primates. *Clin. Cancer Res. Off. J. Am. Assoc. Cancer Res.* 10, 8561–8576. <https://doi.org/10.1158/1078-0432.CCR-04-0940>
- Yang, Z., Zhang, Q., Xu, K., Shan, J., Shen, J., Liu, L., Xu, Y., Xia, F., Bie, P., Zhang, X., Cui, Y., Bian, X.-W., Qian, C., 2012. Combined therapy with cytokine-induced killer cells and oncolytic adenovirus expressing IL-12 induce enhanced antitumor activity in liver tumor model. *PloS One* 7, e44802. <https://doi.org/10.1371/journal.pone.0044802>
- Yee, C., Thompson, J.A., Roche, P., Byrd, D.R., Lee, P.P., Piepkorn, M., Kenyon, K., Davis, M.M., Riddell, S.R., Greenberg, P.D., 2000. Melanocyte Destruction after Antigen-Specific Immunotherapy of Melanoma: Direct Evidence of T Cell-Mediated Vitiligo. *J. Exp. Med.* 192, 1637–1644. <https://doi.org/10.1084/jem.192.11.1637>
- Yewdell, J.W., Brooke, C.B., 2012. Monocytes, viruses and metaphors. *Cell Cycle* 11, 1748–1749. <https://doi.org/10.4161/cc.20311>
- Yokokawa, J., Cereda, V., Remondo, C., Gulley, J.L., Arlen, P.M., Schlom, J., Tsang, K.Y., 2008. Enhanced functionality of CD4+CD25(high)FoxP3+ regulatory T cells in the peripheral blood of patients with prostate cancer. *Clin. Cancer Res. Off. J. Am. Assoc. Cancer Res.* 14, 1032–1040. <https://doi.org/10.1158/1078-0432.CCR-07-2056>
- Yokosuka, T., Kobayashi, W., Takamatsu, M., Sakata-Sogawa, K., Zeng, H., Hashimoto-Tane, A., Yagita, H., Tokunaga, M., Saito, T., 2010. Spatiotemporal basis of CTLA-4 costimulatory molecule-mediated negative regulation of T cell activation. *Immunity* 33, 326–339. <https://doi.org/10.1016/j.immuni.2010.09.006>
- Yoneyama, M., Kikuchi, M., Natsukawa, T., Shinobu, N., Imaizumi, T., Miyagishi, M., Taira, K., Akira, S., Fujita, T., 2004. The RNA helicase RIG-I has an essential

- function in double-stranded RNA-induced innate antiviral responses. *Nat. Immunol.* 5, 730–737. <https://doi.org/10.1038/ni1087>
- You, Y.H., Lee, D.H., Yoon, J.H., Nakajima, S., Yasui, A., Pfeifer, G.P., 2001. Cyclobutane pyrimidine dimers are responsible for the vast majority of mutations induced by UVB irradiation in mammalian cells. *J. Biol. Chem.* 276, 44688–44694. <https://doi.org/10.1074/jbc.M107696200>
- Young, K., Minchom, A., Larkin, J., 2012. BRIM-1, -2 and -3 trials: improved survival with vemurafenib in metastatic melanoma patients with a BRAF(V600E) mutation. *Future Oncol. Lond. Engl.* 8, 499–507. <https://doi.org/10.2217/fon.12.43>
- Yu, Z., Chan, M.-K., O-charoenrat, P., Eisenberg, D.P., Shah, J.P., Singh, B., Fong, Y., Wong, R.J., 2005. Enhanced nectin-1 expression and herpes oncolytic sensitivity in highly migratory and invasive carcinoma. *Clin. Cancer Res. Off. J. Am. Assoc. Cancer Res.* 11, 4889–4897. <https://doi.org/10.1158/1078-0432.CCR-05-0309>
- Yue, Z., Shatkin, A.J., 1997. Double-stranded RNA-dependent protein kinase (PKR) is regulated by reovirus structural proteins. *Virology* 234, 364–371. <https://doi.org/10.1006/viro.1997.8664>
- Zamai, L., Ahmad, M., Bennett, I.M., Azzoni, L., Alnemri, E.S., Perussia, B., 1998. Natural Killer (NK) Cell-mediated Cytotoxicity: Differential Use of TRAIL and Fas Ligand by Immature and Mature Primary Human NK Cells. *J. Exp. Med.* 188, 2375–2380.
- Zamarin, D., Holmgaard, R.B., Ricca, J., Plitt, T., Palese, P., Sharma, P., Merghoub, T., Wolchok, J.D., Allison, J.P., 2017. Intratumoral modulation of the inducible co-stimulator ICOS by recombinant oncolytic virus promotes systemic anti-tumour immunity. *Nat. Commun.* 8, ncomms14340. <https://doi.org/10.1038/ncomms14340>
- Zamarin, D., Holmgaard, R.B., Subudhi, S.K., Park, J.S., Mansour, M., Palese, P., Merghoub, T., Wolchok, J.D., Allison, J.P., 2014. Localized oncolytic virotherapy overcomes systemic tumor resistance to immune checkpoint blockade immunotherapy. *Sci. Transl. Med.* 6, 226ra32. <https://doi.org/10.1126/scitranslmed.3008095>
- Zamarin, D., Ricca, J.M., Sadekova, S., Oseledchik, A., Yu, Y., Blumenschein, W.M., Wong, J., Gigoux, M., Merghoub, T., Wolchok, J.D., 2018. PD-L1 in tumor microenvironment mediates resistance to oncolytic immunotherapy. *J. Clin. Invest.* 128. <https://doi.org/10.1172/JCI98047>
- Zarour, H.M., 2016. Reversing T-cell Dysfunction and Exhaustion in Cancer. *Clin. Cancer Res. Off. J. Am. Assoc. Cancer Res.* 22, 1856–1864. <https://doi.org/10.1158/1078-0432.CCR-15-1849>
- Zhang, A.L., Colmenero, P., Purath, U., Teixeira de Matos, C., Hueber, W., Klareskog, L., Tarner, I.H., Engleman, E.G., Söderström, K., 2007. Natural killer cells trigger differentiation of monocytes into dendritic cells. *Blood* 110, 2484–2493. <https://doi.org/10.1182/blood-2007-02-076364>
- Zhang, J., Tai, L.-H., Ilkow, C.S., Alkayyal, A.A., Ananth, A.A., de Souza, C.T., Wang, J., Sahi, S., Ly, L., Lefebvre, C., Falls, T.J., Stephenson, K.B., Mahmoud, A.B., Makrigiannis, A.P., Lichty, B.D., Bell, J.C., Stojdl, D.F., Auer, R.C., 2014. Maraba MG1 virus enhances natural killer cell function via conventional dendritic cells to

- reduce postoperative metastatic disease. *Mol. Ther. J. Am. Soc. Gene Ther.* 22, 1320–1332. <https://doi.org/10.1038/mt.2014.60>
- Zhang, M., Luo, W., Huang, B., Liu, Z., Sun, L., Zhang, Q., Qiu, X., Xu, K., Wang, E., 2013. Overexpression of JAM-A in non-small cell lung cancer correlates with tumor progression. *PloS One* 8, e79173. <https://doi.org/10.1371/journal.pone.0079173>
- Zhang, W., Bi, B., Oldroyd, R.G., Lachmann, P.J., 2000. Neutrophil lactoferrin release induced by IgA immune complexes differed from that induced by cross-linking of fcalpha receptors (FcalphaR) with a monoclonal antibody, MIP8a. *Clin. Exp. Immunol.* 121, 106–111.
- Zhao, X., Rajasekaran, N., Chester, C., Yonezawa, A., Dutt, S., Coffey, M., He, Z., Kohrt, H.E., 2015. Natural Killer Cells Activated By Oncolytic Reovirus Enhance Cetuximab Mediated Antibody Dependent Cellular Cytotoxicity in an in Vitro and In Vivo Model of Colorectal Cancer. *Blood* 126, 3439–3439.
- Zhong, P., Agosto, L.M., Munro, J.B., Mothes, W., 2013. Cell-to-cell transmission of viruses. *Curr. Opin. Virol., Virus entry / Environmental virology* 3, 44–50. <https://doi.org/10.1016/j.coviro.2012.11.004>
- Ziegler-Heitbrock, L., Hofer, T.P.J., 2013. Toward a Refined Definition of Monocyte Subsets. *Front. Immunol.* 4. <https://doi.org/10.3389/fimmu.2013.00023>
- Zurakowski, R., Wodarz, D., 2007. Model-driven approaches for in vitro combination therapy using ONYX-015 replicating oncolytic adenovirus. *J. Theor. Biol.* 245, 1–8. <https://doi.org/10.1016/j.jtbi.2006.09.029>